


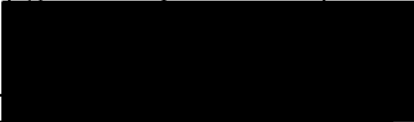

Chicago Transit Authority

5000 Series Cars

Carbody Structural Analysis Report

CDRL : DS-001

SPEC REFS : 1.09A

Responsible division:	Responsible unit:	Document type:	Confidentiality status:	Document state:
BTNA	Engineering	Bombardier Report & Analysis		Released
Prepared:	<u>Alex Polisois/Danielle Morissette/Virgilio Hilaro</u> Staff Engineer, Structure and Truck Engineering			2007-11-06
Verified:	<u>Mario Raymond</u> Manager, Structure and Truck Engineering			2007-11-06
Approved:	<u>Mathieu Perrault</u> Director, Structure and Truck Engineering			2007-11-06
Name / Title, Group		Signature	Date (YYYY-MM-DD)	
<p>This document and its contents are the property of Bombardier Inc. or its subsidiaries. This document contains confidential proprietary information. The reproduction, distribution, utilization or the communication of this document or any part thereof, without express authorisation is strictly prohibited. Offenders will be held liable for the payment of damages.</p> <p>© 2007, Bombardier Inc. or its subsidiaries. All rights reserved.</p>		Identity number:	076-BRA-0016	
		Effective date:	Revision:	Language:
		2007-11-06	0	en

Revision Log

Revision	Date YYYY-MM-DD	Description of Changes
0	2007-11-06	Initial Release

Table of Contents

Section	Subject	Page
1	Summary	5
2	Methodology	6
2.1	General	6
2.2	Symbols, Abbreviations & Nomenclature	7
2.3	Buckling Calculation of Carbon Steel and Stainless Steel Plates	8
2.4	Margin of Safety Calculation	8
2.5	Carbody Material and Allowable Stresses	9
3	Manual Calculations	10
3.1	Anticlimber:	11
3.2	End Posts:	12
3.2.1	Requirement No. 1, Collision post and connections strength, LC_14:	13
3.2.2	Requirement No. 2, Corner post bottom connections, LC_15:	18
3.2.3	Requirement No. 3, AT plate and posts top connections, LC_17:	22
3.2.4	Requirement No. 4, Roof pull down, LC_16 & LC_18:	28
3.2.5	Requirement No. 5, Posts section moduli, LC_13:	32
3.3	Roof structure:	34
3.4	Main connections, side sill to end sill, bolster to side sill and bolster to king pin:	36
3.5	Plymetal floor loads:	40
4	FEA Calculations	41
4.1	End sill:	42
4.2	Draft sill:	45
4.3	Bolster:	47
4.4	Side Sill:	52
4.5	Cross bearers:	55
4.6	Main Air Duct:	58
4.7	Side Frame:	60
4.8	Side Sheets & Side Corrugation:	63
4.9	Door Frame:	66
4.10	Belt Rail:	68
4.11	Roof Rail & AT plate:	71
4.12	Carlines, Roof Gutter and Purlines:	75

4.13 Fatigue Considerations:	79
4.14 Equipment support structures:	86
4.15 Jacking and pushing in the shop considerations:	99
4.16 Progressive Strength Distribution:	103
4.17 FEA Calculations of Natural frequencies:	104
5 Discussions and Conclusions	106
6 References	107
Appendix A: Manual Calculations References	108
A.1 Applied formulas and tables for buckling calculations	109
A.2 Corrugated roof properties calculations:	111
A.3 Corrugated side sheet properties calculations:	112
A.4 Plymetal properties calculations:	113
A.5 Sub-floor properties calculations:	115
A.6 Collision post properties calculations:	117
A.7 Corner post properties calculations:	118
A.8 Carline properties calculations:	119
A.9 Bolster properties calculations at $y = 25.5$ in:	120
Appendix B: FEA Models and Load Cases Description Plots	121
B.1 FEA modeling assumptions:	122
B.2 FEA model Plots:	122
Appendix C: FEA Displacement plots	137

1 Summary

This document presents the calculation methodology and results for the CTA 5000 carbody stress analysis. The analysis is performed according to Bombardier Transportation document 076-PLA-0012, 'Carbody Stress Analysis and Test Plan' (Ref. 1).

Based on the results of the foregoing analysis, it is concluded that the carbody structural components have sufficient strength and comply with the requirements of the CTA Specification (ref. 6). All components exhibit positive margins of safety and the minimum MS was found to be +0.01 (end sill internal web, see table below and section 4.1).

The structural integrity of the carbody will be confirmed following the Carbody static structural qualification tests as described in ref. 1.

The following table presents a summary of the minimum margins of safety for the main structural components of the carbody with respect to the most significant loading conditions. Requirements other than those presented in table 1.1 have been verified and are discussed in section 5.

COMPONENTS (MT)**	LOAD CONDITIONS								
	Vert. load @AW3(LC 02)		Comp @AW3(LC 05)		Torsion at AW0 (LC 10)		Other load cases		
	Max. Stress(ksi)	MS *	Max. Stress(ksi)	MS *	Max. Stress(ksi)	MS *	Max. Stress(ksi)	MS *	LC# ***
Anticlimber(HSLA80)							77.70	0.03	LC6, LC7
End sill (HSLA80)			71.30	0.01			76.60	0.04	LC10
Collision post (MT)								1.10	LC14
Corner post (MT)								0.03	LC15
Draft sill (HSLA 80)			55.80	0.29					
Bolster (HSLA 80)	38.30	0.04	49.40	0.45			6.00	0.60	LC3
Side sill			47.00	0.19			-3.10	0.45	LC3
Cross bearer (MT)	18.10	0.70	49.50	0.13			35.10	0.76	LC12
Main air duct (MT)	29.10	0.07	53.30	0.05			23.00	1.70	LC12
Side frame (MT)	29.40	0.05	33.00	0.70	35.90	0.72			
Side sheets (DLT)	25.60	0.21	30.90	0.80	49.70	0.01			
Door frame (MT)	23.50	0.32	48.90	0.15			-5.60	0.70	LC3
Belt rail (MT)	29.60	0.05	44.50	0.26	54.10	0.15			
Roof rail (MT)	24.10	0.28	20.70	0.70	19.80	>2			
AT plate (MT)					28.20	>2		0.54	LC17
Carlines (MT)	16.50	0.80	33.50	0.67	53.20	0.17	-43.20	0.43	LC19
Purlines (MT)					46.80	0.32			
Roof corrugation(MT)							-36.00	0.60	LC19
Equip. support HVAC							48.00	0.30	LC12
Equip. support APS							55.50	0.12	LC12
Equip. support HVB							51.10	0.21	LC12
Equip. support PCU							29.60	0.72****	LC12

NOTES: * MS = Margin of safety as calculated in section 2.4

** Material nomenclature as per table 2 of ref. 1

*** Load cases are described in table 1 of ref. 1 (Carbody Stress Analysis and Test Plan)

**** Bolted connection MS.

Table 1.1 Summary of maximum stresses and minimum margins of safety for the carbody.

2 Methodology

2.1 General

The CTA 5000 carbody stress calculations are based on manual and Finite Element Analysis (FEA) calculations. The results are presented for each main structural component by manual calculations and FEA. Calculations details are presented in appendix "A" for manual calculations and appendix "B & C" for FEA details.

The following presents a list of the structural components and related load cases as presented in the 'Carbody Stress and Test Analysis Plan' (ref.1). Load cases are identified by the prefix LC_.

Manual Calculations

- Anticlimber (LC_06, 07)
- End posts (LC_13, 14, 15, 16)
- AT plate, purline (LC_16, 17)
- Roof pull down (LC_18)
- Roof structure & corrugation (LC_19)
- Main side sill, end sill & bolster connections (LC_20)
- Plymetal floor loads(LC_02 & LC_12)

FEA Calculations (LC_1 to LC_11 excluding LC_06 & LC07 & LC_20)

- End sill
- Draft sill
- Bolster
- Side sill
- Cross bearers
- Main air duct
- Side frame
- Side sheets & side corrugation
- Door frame
- Belt rail
- Roof rail & AT plate
- Carlines, roof gutter & purlines
- Equipment support structures
- Natural frequencies

The more significant load cases are:

- LC_02, Vertical load at AW3
- LC_03, Vertical fatigue load
- LC_05, Compression load of 200 kip + the vertical load at AW3.
- LC_10, Torsion load due to re-railing jacking.

2.2 Symbols, Abbreviations & Nomenclature

This section is used to define the nomenclature & abbreviations used in the report. Table 2.2-1 can be used as a guide.

Symbol	Description
ksi	psi x 1000
E	Young's modulus (ksi)
v	Poisson's ratio
FS	Factor of safety
MS	Margin of safety
Von mises stress	Calculated equivalent stress (ksi)
σ	Axial & bending stress (ksi)
σ_1	Maximum axial + bending stress (ksi)
σ_3	Minimum axial + bending stress (ksi)
τ	Shear stress (ksi)
Stress, (XX)	Stress plots in the X direction
Stress, (YY)	Stress plots in the Y direction
Stress, (ZZ)	Stress plots in the Z direction
Stress, (P1)	Stress plots principal maximum stress
Stress, (P3)	Stress plots principal minimum stress
Displ (mag)	Stress plots maximum displacements
Displ (X)	Stress plots displacements in the 'X' direction
E_{tt}	Weld throat effective thickness
Uy	Displacement in the Y direction
Uz	Displacement in the Z direction

Table 2.2-1: Nomenclature & abbreviations table

2.3 Buckling Calculation of Carbon Steel and Stainless Steel Plates

Buckling of rectangular steel flat plates is verified with the general form of buckling equation given in Analysis and Design of Flight Vehicle Structures by Bruhn (ref. 5). The buckling strength calculation of stainless steel members is addressed using methods described in Lincoln and Watter's "Strength of Stainless Steel Structural Members as Function of Design" (ref. 4). Reference curves used for buckling calculation are provided in appendix A1. The critical stress is always limited to the yield strength of the material. The general buckling equation is:

$$\sigma = \frac{\pi^2 Kc Er}{12(1-\nu^2)} \left(\frac{t}{b}\right)^2$$

Where:	σ_{cr}	=	Critical stress in compression or bending
	τ_{cr}	=	Critical shear stress
	K	=	Buckling coefficient which depends on edge boundary conditions, and sheet aspect ratio (a/b), and the type of loading, i.e. compression (Kc), bending (Kb), or shear load (Ks) (See Appendix A.1).
	E	=	Modulus of elasticity for carbon steel.
	Er	=	Reduced modulus of elasticity from Lincoln and Watter for Stainless Steel
	t	=	Sheet thickness
	b	=	Short dimension of plate or loaded edge
	a	=	Dimension of plates unloaded edge or plates longer dimension for plates loaded in shear
	ν	=	Material Poisson's ratio.

2.4 Margin of Safety Calculation

The margin of safety will be calculated as follows:

$$MS = \frac{\text{Critical stress or Critical Load}}{\text{Calculated stress or Load}} - 1$$

The margin of safety should always be greater than 0.

2.5 Carbody Material and Allowable Stresses

The mechanical properties of the carbody materials are presented in table 2 of the carbody stress analysis and test plan (ref. 1). In summary the carbody is made of:

- HSLA 80 carbon steel material for the end underframes with a yield strength of 80 ksi and an ultimate strength of 90 ksi.
- 201 LN (1/4 hard) stainless steel material for the side sill, side frame, roof structure, central underframe, side skin corrugation, AT plate, endframe two skins and the end posts. This material has a yield strength of 75 ksi in tension and 62 ksi in compression with an ultimate strength of 120 ksi & 86 ksi in tension & compression respectively.
- 201 LN (1/16 hard, deadlight) stainless steel material for the upper part of the side skin. This material has a yield strength of 50 ksi in tension and 42 ksi in compression with an ultimate strength of 100 ksi & 82 ksi in tension & compression respectively..
- 201 LN (annealed) stainless steel material for the subfloor skin. This material has a yield strength of 45 ksi in tension and 38 ksi in compression with an ultimate strength of 95 ksi & 80 ksi in tension & compression respectively..

Weld fatigue considerations are verified for 10 million cycles as per the American Welding Society recommendations (ref. 2). Depending on the weld detail category the allowable stress range will vary from 24 ksi for a category 'A' to 4.5 ksi for a category 'E' weld (see table 3.1).

Table 3.1 – Allowable Fatigue Stresses as per AWS (ref. 2, table 2.4)

Weld Category	Weld category summary description	Allowable Stress range (ksi)
A	Base metal	24
B	Continuous CJP or built up fillet welds	16
C	Continuous fillet weld or discontinuity in CJP weld	10
E	Discontinuity in fillet weld or plug welds	4.5
F	Shear in throat of weld	8

3 Manual Calculations

The calculated stresses and margins of safety (MS) are manually calculated for the following components:

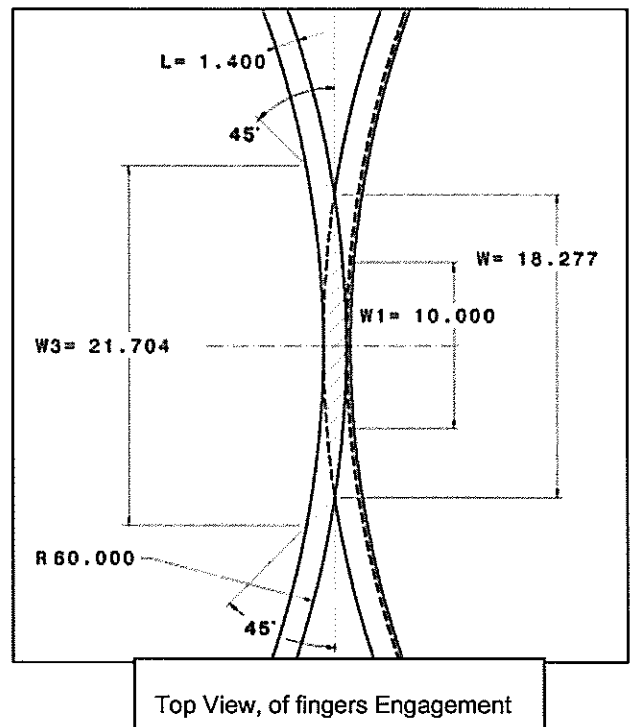
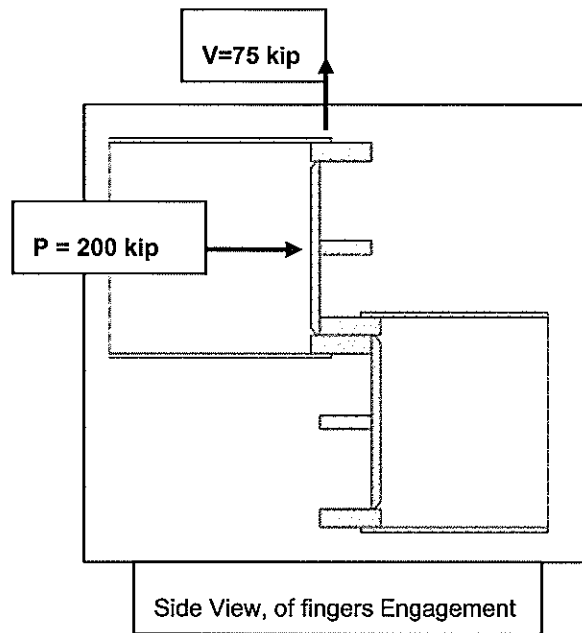
1. Anticlimber.
2. End posts, AT plate, purlines and post connections for roof pull down.
3. Roof structure.
4. Main connections, side sill to end sill and bolster to side sill.
5. Plymetal floor loads.

The complete details of the above calculations such as buckling calculations methods, section modulus calculations and of the EXCEL sheets used herein are shown in Appendix A.

3.1 Anticlimber:

The anticlimber fingers are checked for one rib engagement at 200 kip buff load + 75 kip vertical load as described in load cases LC_06 and LC_07 of ref.1 (Carbody stress and analysis plan).

The combined compression and bending load is verified for a single rib.



$$\sigma_{\text{comp}} = \frac{(P/2)}{(t)(wl)} = \frac{100}{(.5)(10)} = 20 \text{ksi}$$

$$\sigma_{\text{bending}} = \frac{(V/2)L}{S_{\text{eff}}} = \frac{(75/2)(1.4)}{(0.91)} = 57.7 \text{ksi}$$

$$\sigma_{\text{total}} = \sigma_{\text{comp}} + \sigma_{\text{bending}} = 20 + 57.7 = 77.7 \text{ksi}$$

W = width of shear contact surface.

W1 = Width of compression contact surface.

W3 = Base width of bending.

t = finger thickness = 0.5 in

L = finger length = 1.4 in

S_{eff} = Effective finger section modulus for bending = $(w3) (t)^2/6 = 0.91 \text{ in}^3$

The allowable stress for the finger (HSLA 80) for LC_06 or LC_07 is yield = 80 ksi.

The anticlimber margin of safety for LC_06 and LC_07 = $(80/77.7) - 1 = 0.03$

3.2 End Posts:

The end posts are checked for load cases LC_13 (section modulus), LC_14, LC_15 & LC_16 (post connections) as per table 1 of ref.1 (Carbody stress and analysis plan) and as per Ref. 6, CTA Specifications, section 3.02 B. A summary of these requirements is repeated below::

Requirement No. 1, Collision post, LC_14:

The two (2) end posts adjacent to the door at each end of the car shall have sufficient strength and be so attached through the entire depth of the underframe end sills that under collision conditions, the posts will develop the full strength of the end underframe if struck at any location up to six-inches (6") above the top of the underframe and at any horizontal angle up to thirty degrees (30°) to either side. The attachment of the posts to the end underframe shall be capable of resisting the torsional components resulting from the application of the loads specified above.

Requirement No. 2, Corner post, LC_15:

All other end posts shall be attached through the full depth of the underframe sill so that if struck at the top to the end underframe with an inward force at any horizontal angle up to ninety degrees (90°) from longitudinal, the sills will crush back before breaking the post connections.

Requirement No. 3, AT plate and posts top connections LC_17:

The attachment of all end posts at the top shall be by means of an anti-telescoping plate and shall be adequate to resist, without failure, the reactions of the members, either singly or in any possible combination, when assumed to be simple beams with free supports at their ends and loaded at a point eighteen-inches (18") above the connection to the underframe member to which they are attached with a load sufficient to develop the yield point of the material.

Requirement No. 4, Roof pull down, LC_16:

The vertical connections of all end posts at the underframe and at the top shall be sufficient to resist the vertical forces caused by yielding of the posts under collision conditions. The anti-telescoping plate previously mentioned shall be attached to the posts and to the roof in a manner that will develop the full vertical strength of the roof in the event of yielding of the posts.

Requirement No. 5, Posts section moduli ,LC_13:

The sum of the section moduli of all end posts at one (1) end of the car shall not be less than thirty (30) cubic inches, and the sum of the section moduli of the two (2) center posts shall be approximately seventy-five percent (75%) of the total of all end posts.

3.2.1 Requirement No. 1, Collision post and connections strength, LC_14:

This requirement applies to the strength of the collision post and its connection to the end underframe. The following calculations are organized in the following manner:

1. End Sill Load Capacity
2. Collision Post Load Capacity
3. Collision Post Connection Capacity

For this requirement, a finite element analysis (FEA) was performed with a nominal load of 100 kip applied to the post at a direction of 30° from the carbody's longitudinal axis. The load was distributed within a 6-inch depth and was centered at 6 inches from the top of the end sill.

The FEA results are complemented by manual calculations to validate the adequacy of the collision post and its connection.

End Sill Load Capacity:

The principal load path for the collision post load is the top plate of the end sill. The maximum post load that the end sill can carry is therefore limited by the buckling strength of the end sill's top plate.

Using the buckling equation and buckling coefficient curves from Appendix A1, the calculated buckling strength of the end sill's top plate is 24.46 ksi. The calculation summary and the dimensions of the end sill's top plate are shown in Figures 3.2.1.1 and 3.2.1.2.

The stress contours in the end sill top plate under the 100 kip nominal post load is shown in Figure 3.2.1.3. The compression stress inboard of the collision post ranges from -24.9 to -41.4 ksi with an average value of about -33.2 ksi.

Limiting the average stress in the end sill top plate to the calculated buckling stress of -24.46 ksi, the maximum post load that the end sill can carry is:

Maximum post load for the end sill load capacity = $(24.46 \div 33.2) \times 100 = 73.7$ kip

thickness, t =	0.13	inch
a = distance between the inboard face of the post & the rear web of the end sill =	8.90	inch
width of collision post =	4.25	inch
distance between end sill's internal ribs =	17.40	inch
b = average width for buckling calculation = $0.5 * (4.25 + 17.4) =$	10.83	inch
a / b =	0.82	
t / b =	0.01	
Kc for clamped edges condition	7.00	
E =	29000.00	ksi
critical buckling stress, σ_{cr} =	24.46	ksi

Figure 3.2.1.1, End sill top plate buckling calculation

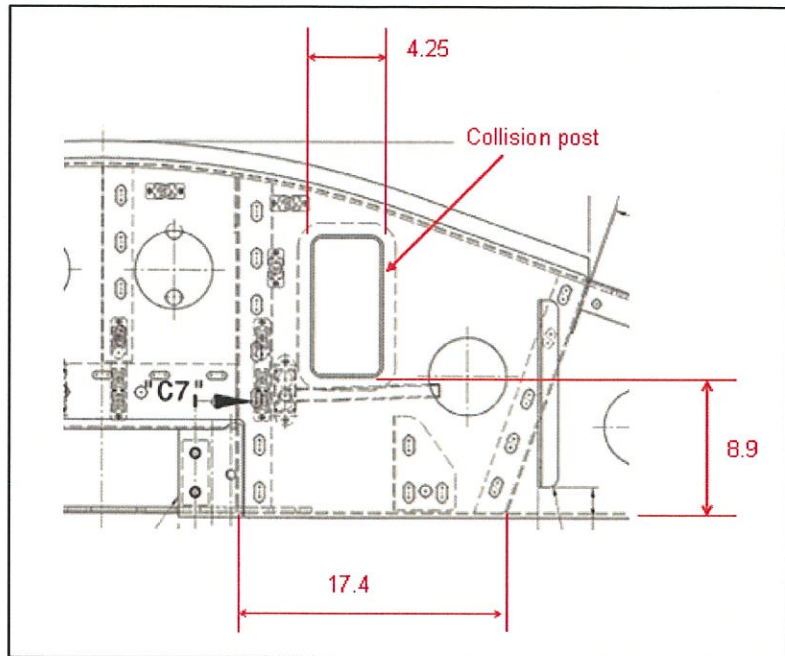


Figure A.3.2.1.2, End sill top plate dimensions for buckling calculations

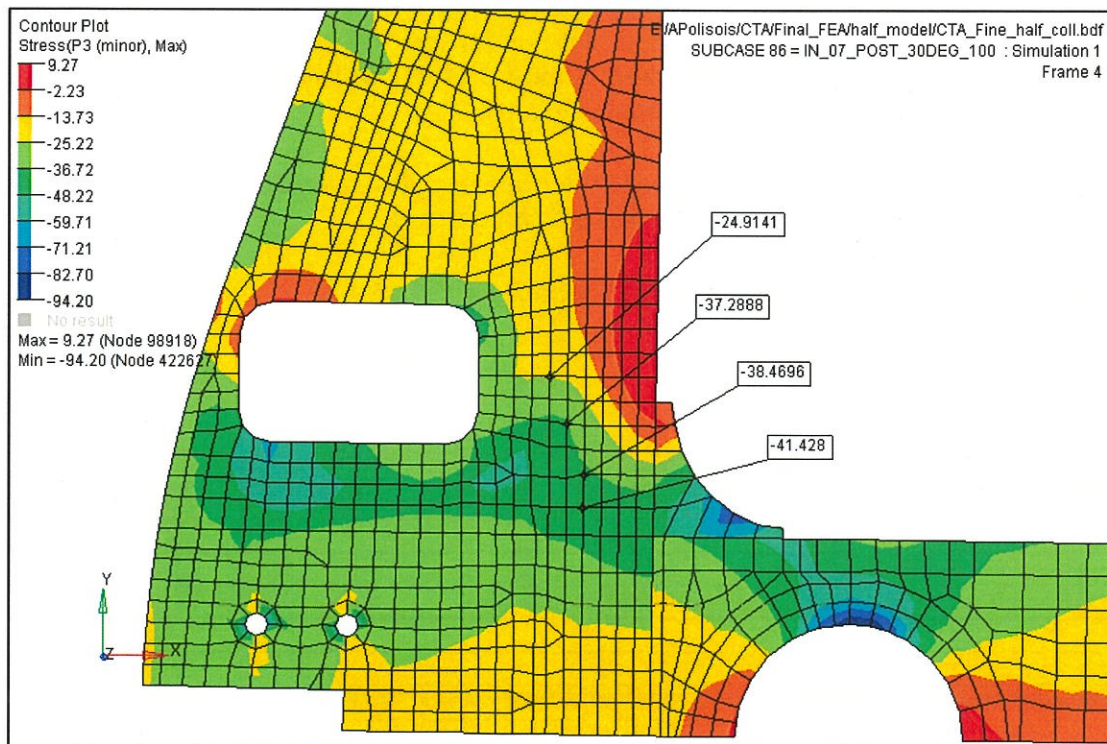


Figure 3.2.1.3, Stress contours in the end sill top plate under 100 kip load on the collision post

Collision Post Load Capacity:

The calculation of the post's load capacity is performed at 3 locations; at the top of the end sill, at 6 inches from the top of the end sill (at the center of load application) and at approximately 18 inches from the top of the end sill (where the post channel section starts). The FEA forces and moments under the 100 kip nominal post load at 30° orientation and centered at 6 inches from the top of the end sill, are used in the calculation.

The FEA stress contour in the collision post under the 100 kip nominal load is shown in Figure 3.2.1.4. The high FEA stresses in the figure are affected by local stress concentrations and are not considered in the calculation of the post's load capacity.

Buckling strength evaluation has determined that the collision post section is relatively compact; the post buckling strength is much higher than the compression & tension yield strengths of the post's stainless steel material, -62 & 75 ksi respectively, (Ref 1, Table 2, and 201LN MT). For this reason and for simplicity in analysis, the calculation of the post's load capacity is based upon the post's material yield strengths.

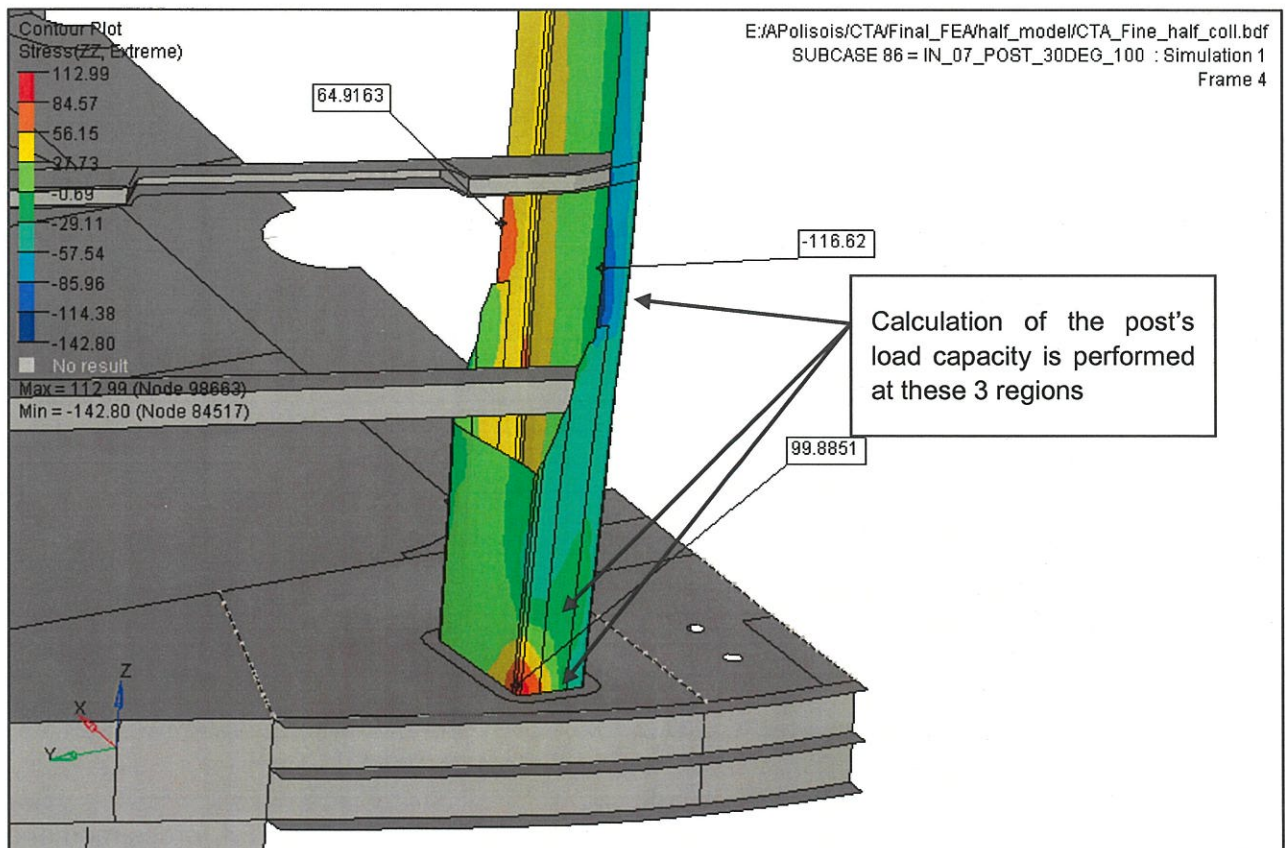


Figure 3.2.1.4, Stress contour in the collision post under 100 kip nominal load applied at 30°

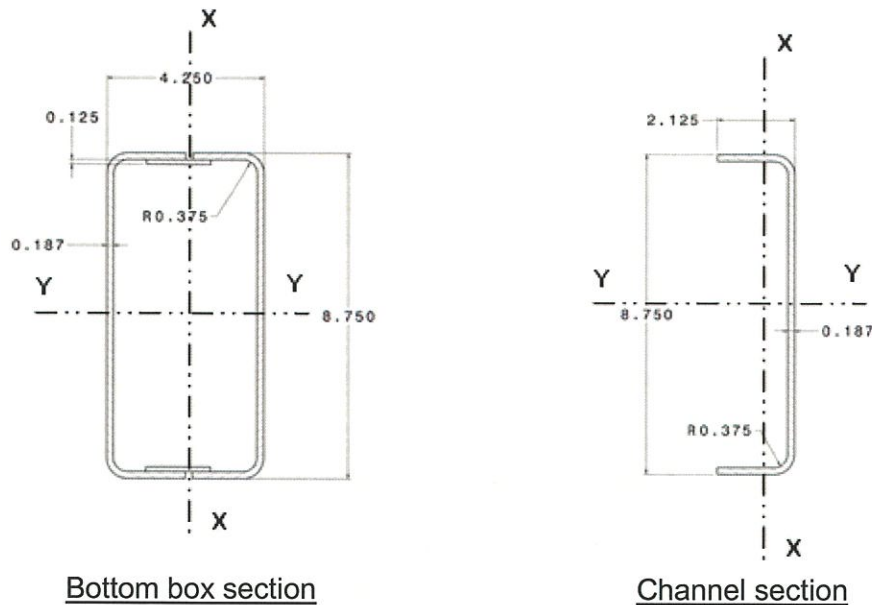


Figure 3.2.1.5 Collision post cross-sections

Calculations of the post's load capacity at the 3 post height locations are shown below:

		At the top of end sill	At 6" from top of end sill	At ~18" from top of end sill
Longitudinal shear (kip)	FX	-83.6	-25.90	4.3
Transverse shear (kip)	FY	46.2	12.70	-0.9
Moment about minor axis (kip-in)	MX	-218.3	34.20	14.6
Moment about major axis (kip-in)	MY	-151.4	302.40	295.7
Section modulus, minor axis (in ³)	SX _{max}	6.98	6.98	1.8
Section modulus, minor axis (in ³)	SX _{min}	6.98	6.98	0.46
Section modulus, major axis (in ³)	SY	11.94	11.94	5.11
Longitudinal shear area (in ²)	AX	3.28	3.28	1.64
Transverse shear area (in ²)	AY	1.59	1.59	0.80
Bending stress in compression (ksi)	Max.	-43.96	-30.23	-89.61
Bending stress in compression (ksi)	Min.	-18.60	-20.43	-49.76
Bending stress in tension (ksi)	Max.	43.96	20.43	65.98
Bending stress in tension (ksi)	Min.	18.60	30.23	26.13
Shear stress in longitudinal webs (ksi)		-25.48	-7.89	2.62
Shear stress in transverse webs (ksi)		28.99	7.97	-1.13
Equivalent "Von-Mises" stress in longitudinal web (ksi)	Max.	62.29	33.17	66.13
Equivalent "Von-Mises" stress in transverse web (ksi)	Max.	66.73	33.23	89.63

Figure 3.2.1.6 Collision post manual stress calculations based on FEA forces/moments.

From the preceding calculations in figure 3.2.1.6, the bending stresses in the post in the 3 locations are all lower than both the compression yield (-62 ksi) and the tension yield (75 ksi) of the post material. The only exception is the -89.61 ksi stress in the channel section at the 18 inches post height from the top of the end sill. This location of high stress is at the same location as the high stress of -116.62ksi shown in figure 3.2.1.4, (Note: the stress of -116.62 ksi includes the stress concentration effect in the region).

Allowing for stress re-distribution and taking the average stress in the flange:

$$\text{Average compression stress} = 0.5 \times (-89.61 - 49.76) = -69.7 \text{ ksi}$$

Considering the 100 kip load used in the above calculation and limiting the stress to a yield value of 62 ksi, the post's load capacity is estimated as:

$$\text{Post's load capacity} = (62 \div 69.7) \times 100 = 89 \text{ kip.}$$

When compared to the end sill capacity, the minimum margin of safety (MS) for Requirement no. 1 is:

$$\text{MS} = (\text{Post capacity} / \text{End sill capacity}) - 1 = (89 \div 73.7) - 1 = + 0.21$$

Collision Post Connection Capacity:

The collision post is welded to the top plate of the end sill by a 0.125 inch groove weld with reinforcing fillet weld. The weld's effective throat is 0.20 inch.

It is conservatively considered that the longitudinal welds in the connection will only carry the longitudinal shear load, and that the transverse welds will only carry the transverse shear load. The calculation of the weld shear capacity is also based upon the material's yield strength of 80 ksi, (Ref 1, Table 2, and HSLA 80 steel).

The weld lengths are 8.75 and 4.25 inches respectively in the longitudinal and transverse directions, Ref: Figure 3.2.1-5.

The load capacities in the post connection are calculated as:

$$\text{Longitudinal shear load capacity} = 2 \times 8.75 \times 0.2 \times 80 / (3)^{1/2} = 162.4 \text{ kip}$$

$$\text{Transverse shear load capacity} = 2 \times 4.25 \times 0.2 \times 80 / (3)^{1/2} = 79 \text{ kip}$$

The longitudinal and transverse shears capacity need to be oriented with respect to the 30° orientation, hence:

$$\text{Based on the longitudinal capacity; } 162.4 / (\cos 30) = 187 \text{ kip.}$$

$$\text{Based on the lateral capacity; } 79 / (\sin 30) = 158 \text{ kip.}$$

$$\text{The connection capacity (based on transverse welds)} = 158 \text{ kip.}$$

The minimum margin of safety (MS) in the post connection for Requirement no. 1 is:

$$\text{MS} = (158 \div 73.7) - 1 = + 1.1 \text{ (where 73.7 kip is the end sill top plate critical buckling load).}$$

3.2.2 Requirement No. 2, Corner post bottom connections, LC_15:

All other end posts shall be attached through the full depth of the underframe sill so that if struck at the top to the end underframe with an inward force at any horizontal angle up to ninety degrees (90°) from longitudinal, the sills will crush back before breaking the post connections.

The corner post connections are verified in the longitudinal and lateral directions.

In the longitudinal direction the post connections need to be stronger than the buckling capacity of the side sill right behind the end sill.

In the lateral direction the post connections need to be stronger than the buckling capacity of the end sill at the hole cut-out.

Side sill longitudinal load capacity:

As per Figure A.1.3, for One Edge Free (appendix A)

$$a = 9''/2 - 0.1875''/2 = 4.40625''$$

$$b = 5.313'' - 0.1875''/2 = 5.21925''$$

$$t = 0.1875''$$

$$\frac{(a+b)}{2t} = \frac{b}{t} = 25.668$$

From fig. A.1.3 (appendix A)

$$: \frac{F_{cc}}{\sqrt{F_{cy} * E}} = 0.03$$

$$F_{cy} = 62 \text{ ksi}$$

$$E = 28 \text{ 000ksi}$$

$$F_{cc} = 0.03 * \sqrt{62 * 28000} = 39.5 \text{ ksi}$$

Side sill Lower angle:

As per Figure A.1.3, for One Edge Free (appendix A)

$$a = 9''/2 - 0.1875''/2 = 4.40625''$$

$$b = 2'' - 0.1875''/2 = 1.90625''$$

$$t = 0.1875''$$

$$\frac{(a+b)}{2t} = \frac{b'}{t} = 16.83$$

$$\text{From fig A.1.3: } \frac{F_{cc}}{\sqrt{F_{cy} * E}} = 0.041$$

$$F_{cy} = 62 \text{ ksi}$$

$$E = 28\,000 \text{ ksi}$$

$$F_{cc} = 0.041 * \sqrt{62 * 28000} = 54.02 \text{ ksi}$$

$$F_{cc} = \frac{(39.5)((4.406+5.219)*0.1875) + (54.02)((4.406+1.906)*0.1875)}{((4.406+5.219)*0.1875) + ((4.406+1.906)*0.1875)} = 45.25 \text{ ksi}$$

Allowable Compression load on side sill:

$$\sigma = \frac{F}{A} \rightarrow F = \sigma * A = 45.25 * 2.89 = 130.77 \text{ kip}$$

Allowable vertical bending moment on side sill:

$$\sigma = \frac{Mc}{I_{xx}} \rightarrow M = \frac{\sigma * I_{xx}}{c} = \frac{39.5 * 32.12}{3.55} = 357.39 \text{ kip*in}$$

Side sill total longitudinal capacity:

$$\frac{P_s}{130.77} + \frac{P_s * 3.55}{357.39} = 1.0$$

$$2.73 P_s + 3.55 P_s = 357.39 \rightarrow 6.28 P_s = 357.39 \rightarrow P_s = 56.88 \text{ kip}$$

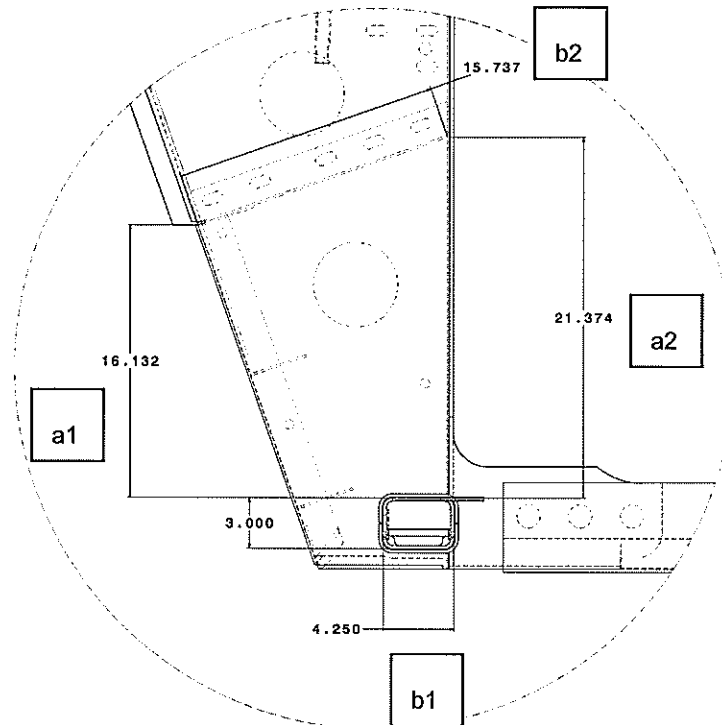
End sill lateral load capacity:

Figure 3.2.2.1, End sill buckling area for lateral load on corner post.

Where

$$a_1 = 16.132''$$

$$a_2 = 21.374''$$

$$a = 18.753''$$

$$b_1 = 4.25''$$

$$b_2 = 15.737''$$

$$b = 9.9935''$$

$$a/b = 1.8765''$$

$$K_c = 4.1 \text{ (Ref. 5, see Figure A.1.1)}$$

$$E_r = 29000 \text{ ksi}$$

$$\nu = 0.3$$

$$t = 0.125''$$

$$\sigma_{CR} = 16.8 \text{ ksi}$$

$$\text{Area} = b \cdot t = 1.25 \text{ in}^2$$

Allowable Compression load on end sill top plate:

$$\sigma = \frac{F}{A} \rightarrow F = \sigma \cdot A = 16.8 \cdot 1.25 = 21 \text{ kip}$$

$$P_s = 21 \text{ kip}$$

Corner post connection capacity:Longitudinal welds:

$$L_x = 2 * 4.25" = 8.5"$$

$$\text{Weld thickness} = 0.1875"$$

$$E_{tt} = 0.707 * 0.1875 = 0.1326"$$

$$A = L_x * E_{tt} = 1.126 \text{ in}^2$$

$$\tau_{ult} = 0.577 * 90 = 51.93 \text{ ksi}$$

$$\tau_{ult} = F_{ult} / A \rightarrow F_{ult} = \tau_{ult} * A = (51.93) * (1.126) = 58.47 \text{ kip}$$

$$\text{M.S. for the corner post longitudinal weld} = (F_{ult} / P_s) - 1 = (58.47 / 56.88) - 1 = 0.03$$

Lateral welds:

$$L_y = 2 * 3" = 6"$$

$$\text{Weld thickness} = 0.1875"$$

$$E_{tt} = 0.707 * 0.1875 = 0.1326"$$

$$A = L_y * E_{tt} = 0.795 \text{ in}^2$$

$$\tau_{ult} = 0.577 * 90 = 51.93 \text{ ksi}$$

$$\tau_{ult} = F_{ult} / A \rightarrow F_{ult} = \tau_{ult} * A = (51.93) * (0.795) = 41.28 \text{ kip}$$

$$\text{M.S. for the corner post lateral weld} = (F_{ult} / P_s) - 1 = (41.28 / 21) - 1 = 0.967$$

3.2.3 Requirement No. 3, AT plate and posts top connections, LC_17:

The attachment of all end posts at the top shall be by means of an anti-telescoping plate and shall be adequate to resist, without failure, the reactions of the members, either singly or in any possible combination, when assumed to be simple beams with free supports at their ends and loaded at a point eighteen-inches (18") above the connection to the underframe member to which they are attached with a load sufficient to develop the yield point of the material.

This requirement applies to the strength of the top connections of the collision and corner posts. The end posts arrangement is shown Figure 3.2.3.1.

The top of the collision post is connected to the AT plate and to the roof purline. The ends of the AT plate are connected to the corner posts and the corner posts are connected to the roof rails.

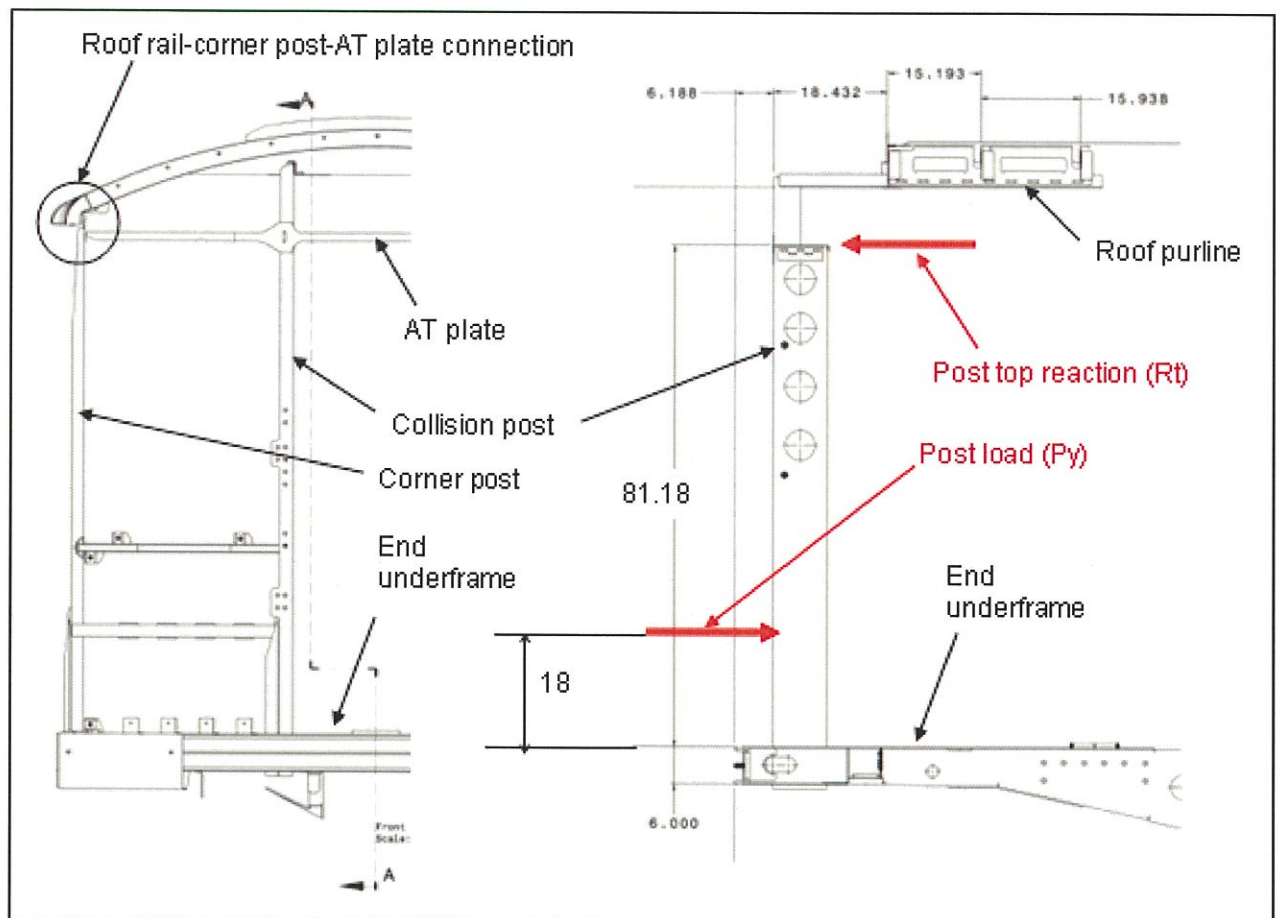


Figure 3.2.3.1, End posts arrangement & load diagram

Reaction Forces at the Post Top Connections

Treating the post as simply supported beams loaded at 18 inches from the top of the underframe, and using the load diagram in Figure 3.2.3.1, the equations for the bending moment in the post (M_y), the post yield load (P_y), and the post top reaction (R_t) are derived as:

$$R_t = (18 \div 81.18) P_y = 0.22P_y$$

$$M_y = (81.18 - 18) R_t = 63.18 \times 0.22P_y = 13.9P_y$$

Or:

$$P_y = 0.072 M_y$$

$$R_t = 0.016 M_y$$

Note: The derivation of the above equations neglects the collision post connection to the roof purline.

Requirement no. 3 stipulates that the post load shall be sufficient to develop the yield point of the post material. Thus, the maximum bending moment in the post is calculated by limiting the post stresses to the post material's yield strength. The calculation is based upon the compression yield of 62 ksi of the 201LN stainless steel post material.

The post's cross sections and section properties at 18" from the top of the underframe are shown in Figure 3.2.3.2. Limiting the post flange's bending stresses to the 62 ksi compression yield strength, the maximum bending moments in the posts are:

$$M_y \text{ for collision post} = 5.11 \times 62 = 317 \text{ kip-inch}$$

$$M_y \text{ for corner post} = 1.72 \times 62 = 107 \text{ kip-inch}$$

The post yield loads are:

$$P_y \text{ for collision post} = 0.072 \times 317 = 23 \text{ kip}$$

$$P_y \text{ for corner post} = 0.072 \times 107 = 8 \text{ kip}$$

The post top reactions are:

$$R_t \text{ for collision post} = 0.016 \times 317 = 5 \text{ kip}$$

$$R_t \text{ for corner post} = 0.016 \times 107 = 2 \text{ kip}$$

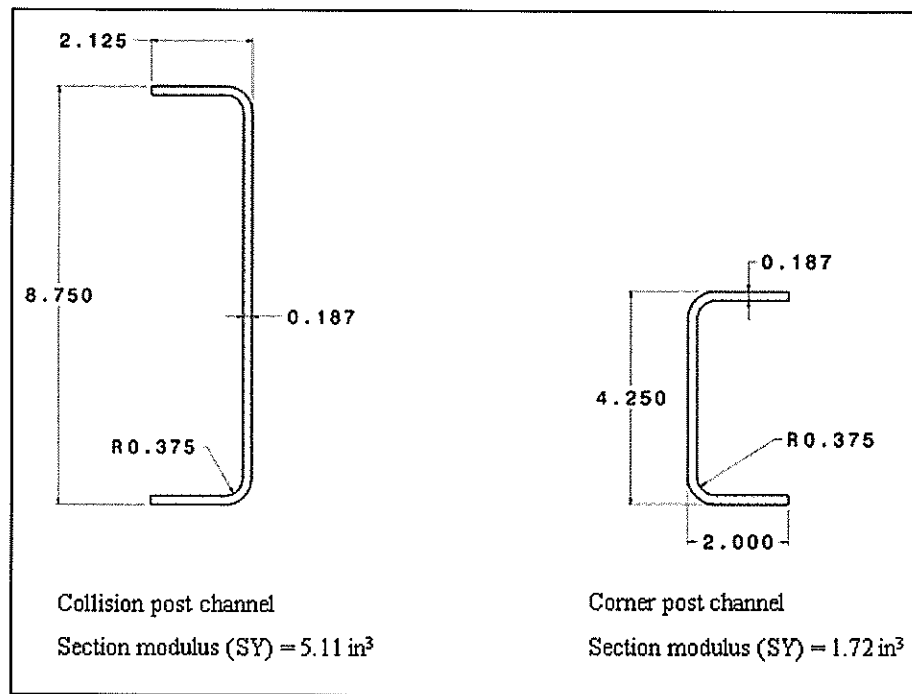


Figure 3.2.3.2, End posts cross sections & properties

Review of the Post Top Connections

The connection arrangements are shown in Figures 3.2.3.3 to 3.2.3.5. The posts are connected to the AT plate by connecting angles. The angles are spot welded to the AT plate at the collision post connection, and at the corner post, the angles are fillet welded to the AT plate. The angles are fillet welded to both the collision and corner posts. The corner posts are fillet welded to the roof rail.

Each spot weld capacity has ultimate shear strength of 3.18 kip. The ultimate shear strengths of the fillet weld's are:

- 0.075 inch size = 3.7 kip/inch
- 0.09 inch size = 4.4 kip/inch
- 0.125 inch size = 6.2 kip/inch

The calculated top reactions for the collision and corner post are only 5 & 2 kip respectively. At the corner post connection with the roof rail, the combined load is only 7 kip.

Based upon the above weld's shear strengths, all connections are passed by inspection; the connection's strengths are more than adequate.

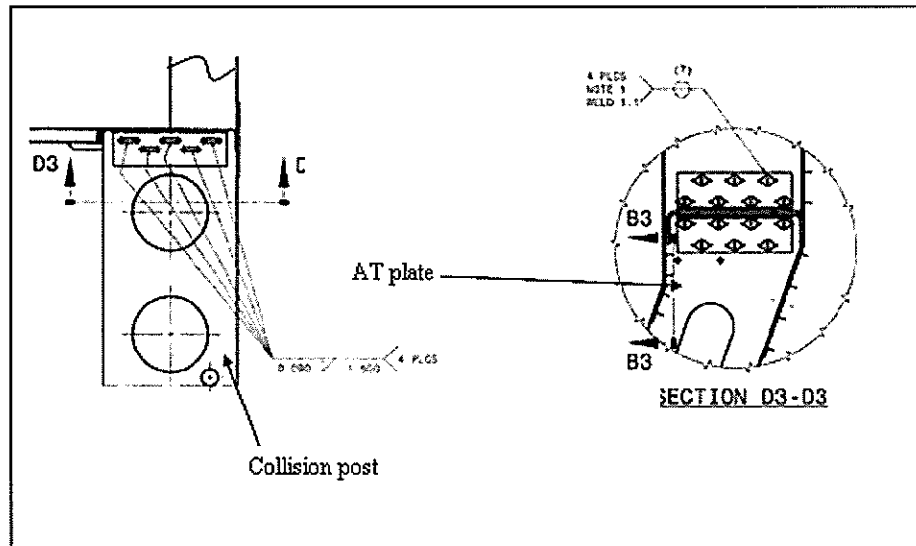


Figure 3.2.3.3, Collision post to AT plate connection

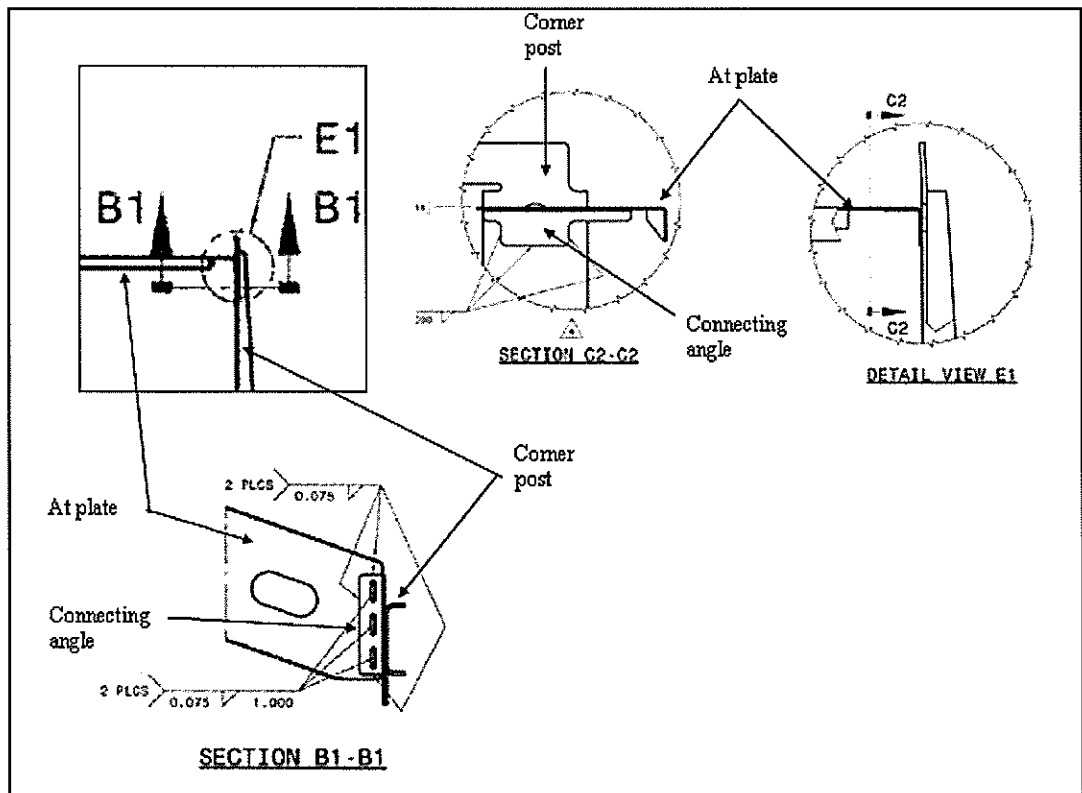


Figure 3.2.3.4, AT plate to corner post connection

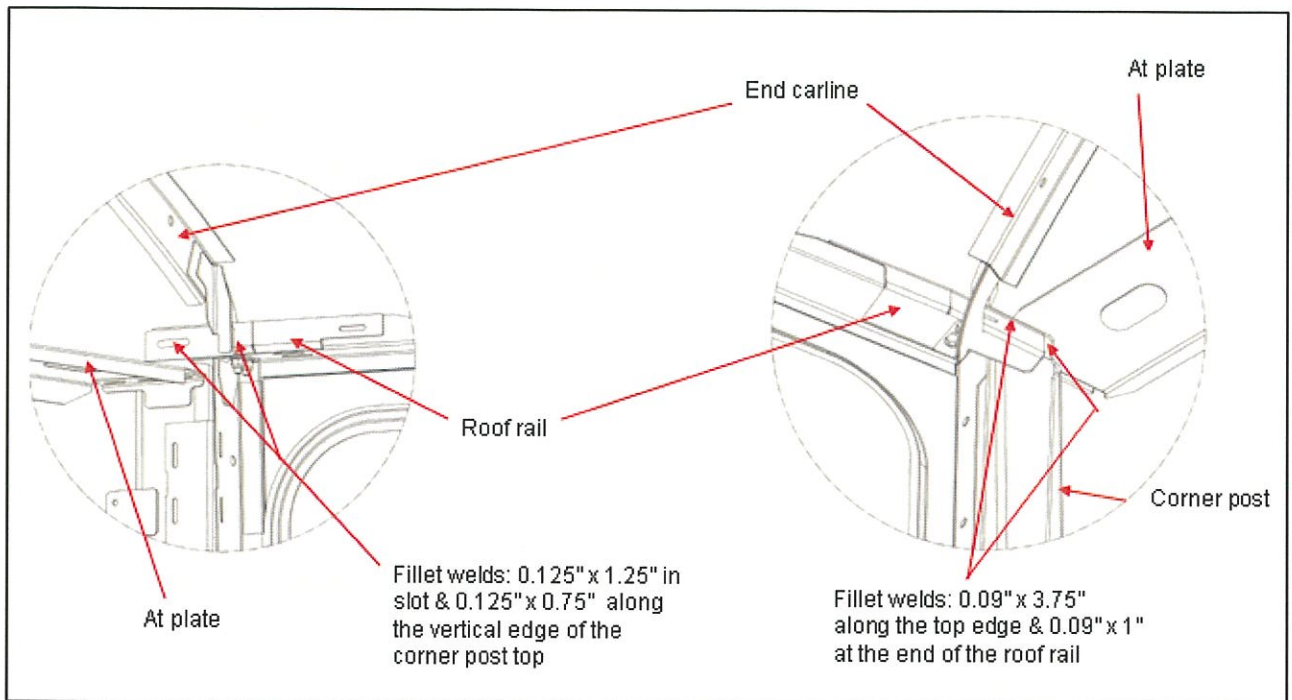


Figure 3.2.3.5, Corner post to roof rail connection

AT Plate Analysis

The AT plate loading diagram is shown in Figure 3.2.3.6. Treated as a simple beam and loaded by the 5 kip top reactions of the collision posts, the bending moment and shear load in the AT plate are:

$$MZ = 5 \times 33.80 = 169 \text{ kip-inch}$$

$$\text{Shear, } FX = 5 \text{ kip}$$

Figure 3.2.3.7 shows the AT plate's cross section just outboard of the collision post, i.e. at Section A-A.

$$\text{Section modulus, } SZ = 4.2 \text{ \& } 2.2 \text{ in}^3$$

$$\begin{aligned} \text{AT plate's bending stresses} &= 169 \div 4.2 = -40.2 \text{ ksi in the outboard flange, and} \\ &= 169 \div 2.2 = +77 \text{ ksi in the inboard flange} \end{aligned}$$

$$\text{AT plate's shear area, } Ax = 0.68 \text{ in}^2$$

$$\text{Shear stress in the AT plate} = 5 \div 0.68 = 7.4 \text{ ksi}$$

The maximum equivalent "von-mises" stress = 78 ksi

The ultimate strength of the AT plate's 201LN material = 120 ksi

$$\text{Thus, the margin of safety (MS)} = (120 \div 78) - 1 = 0.54$$

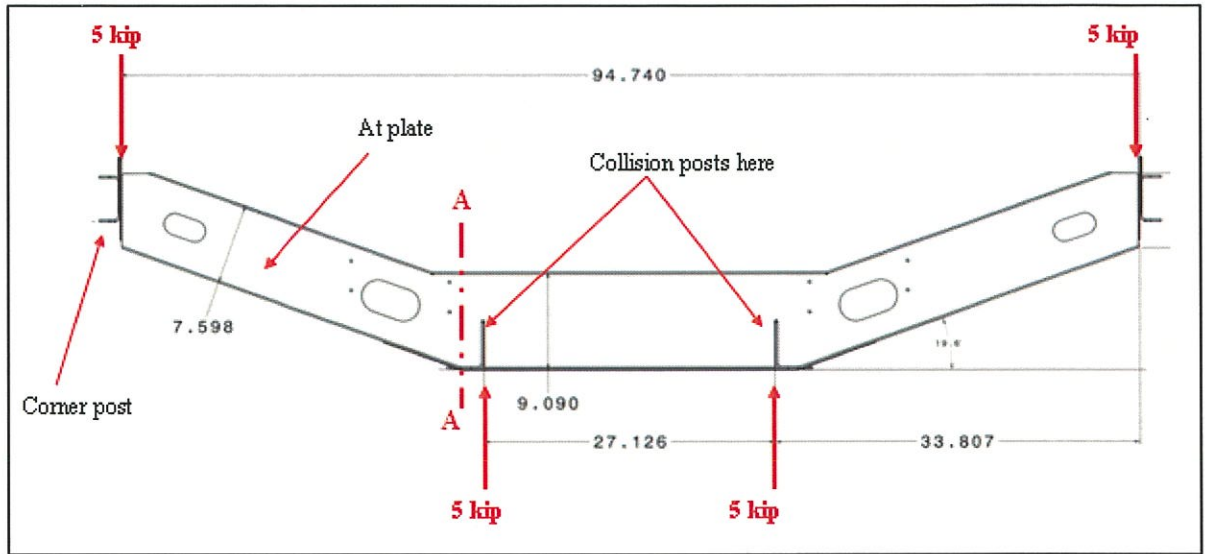


Figure 3.2.3.6, AT Plate loading diagram

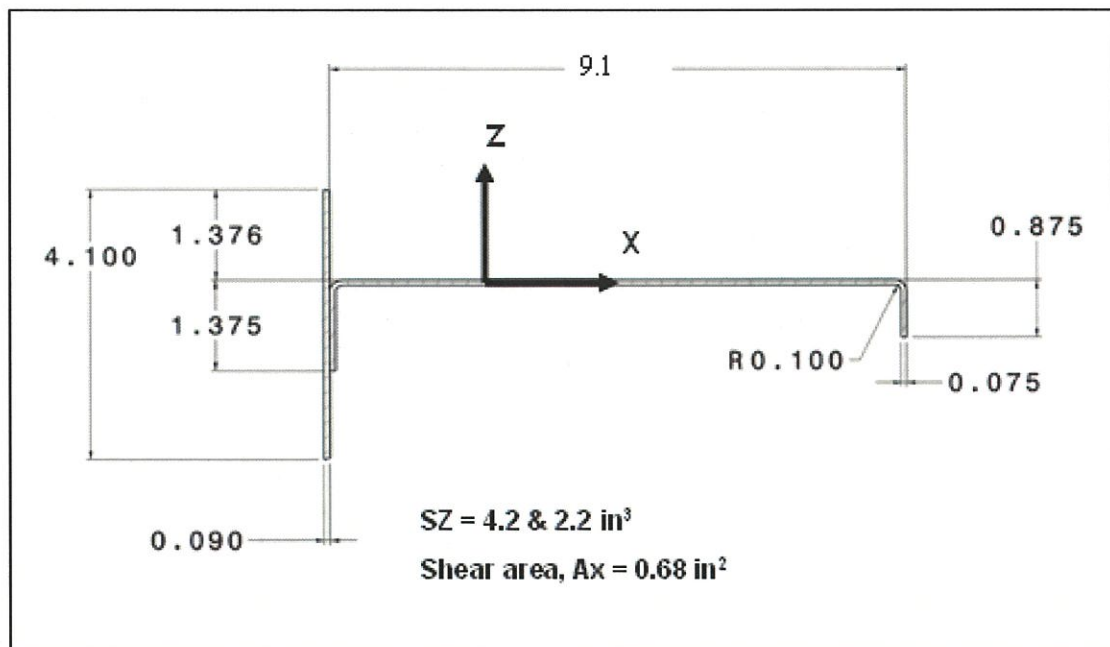


Figure 3.2.3.7, AT Plate section properties.

3.2.4 Requirement No. 4, Roof pull down, LC_16 & LC_18:

The vertical connections of all end posts at the underframe and at the top shall be sufficient to resist the vertical forces caused by yielding of the posts under collision conditions. The anti-telescoping plate previously mentioned shall be attached to the posts and to the roof in a manner that will develop the full vertical strength of the roof in the event of yielding of the posts.

Requirement no. 4 defines the vertical strength requirement of the post's connection to the roof structure.

Figure 3.2.4.1 shows the connection arrangement at end no. 1 of the carbody.

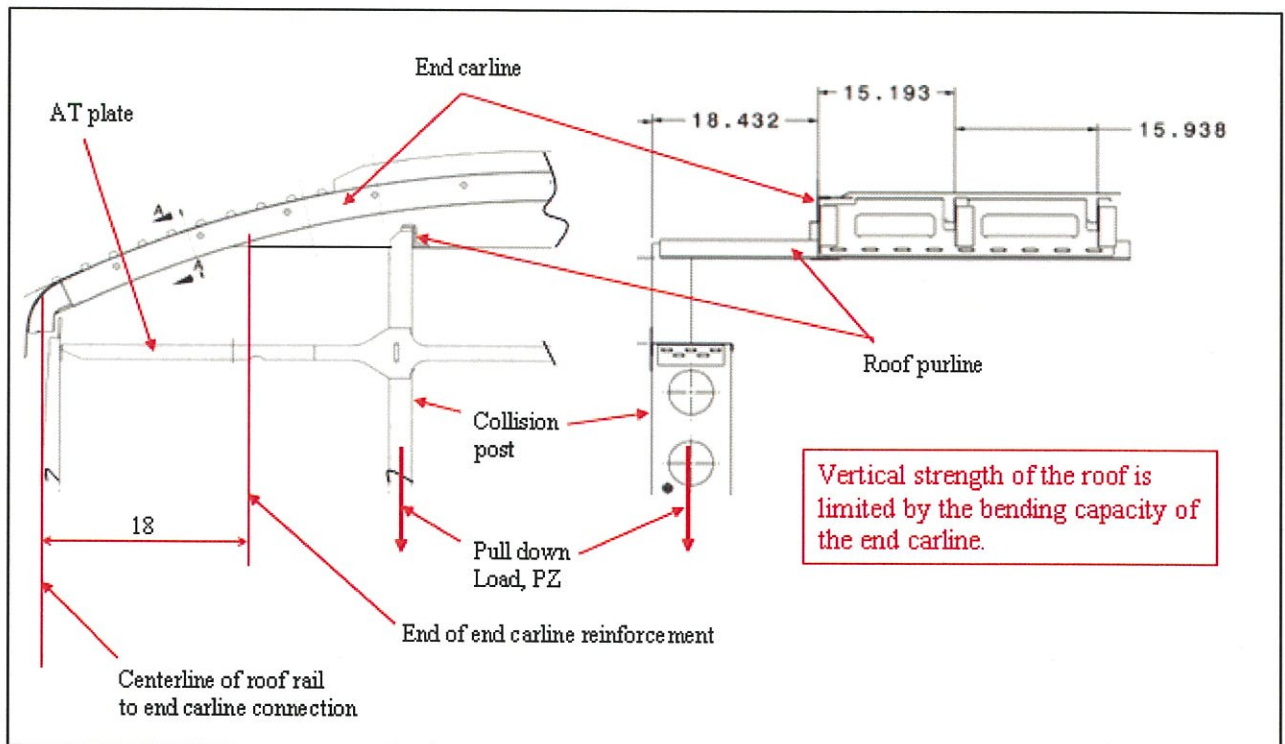


Figure 3.2.4.1, End no. 1 post to roof connection arrangement

The top end of the collision posts are connected to roof purlines which are connected to the end carline and to 2 regular carlines. Pull down loads in the event of extreme post deformation pass through the roof purline then to the roof carlines. By inspection of the above arrangement, the first line of resistance is at the end carline. The weakest region of the end carline is where the reinforcement "end bulkhead" ends, i.e. at about 18" from the centerline of the roof rail & carline connection. The cross section of the end carline at this location is shown in Figure 3.2.4.2.

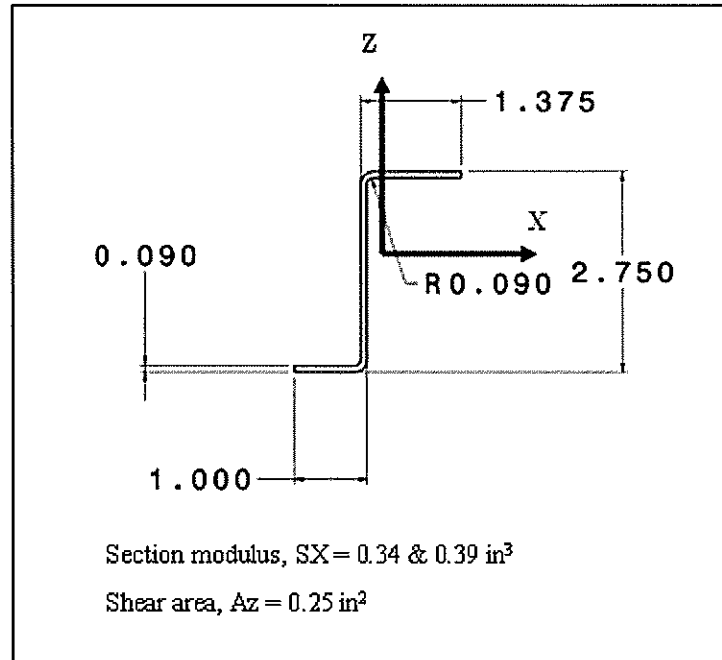


Figure 3.2.4.2, End carline section properties.

The end carline's bending capacity is limited by the -86 ksi ultimate compression strength of carline's 201LN material (ref. table 2 ref. 1). The carline's top flange is in compression and the section modulus (SX) is 0.39 inch³, thus:

$$\text{End carline's bending capacity (MX)} = 0.39 \times 86 = 33.5 \text{ kip-inch}$$

Considering pinned condition at the roof rail-end carline junction and neglecting the arch action in the carline due to the roof curvature, the maximum pull down load (PZ) that the end carline can sustain is:

$$PZ = MX \div 18 = 33.5 \div 18 = 1.9 \text{ kip}$$

In extreme loading condition and deformation, both the top end of the collision post and the roof purline can carry the load PZ by chord action, i.e. the members can function like tension cables. In this condition, the critical links are the connections of the collision post to the roof purline and the roof purline connection with the end carline. These connections are shown in Figures 3.2.4.3 & 3.2.4.4.

Collision post to roof purline connection

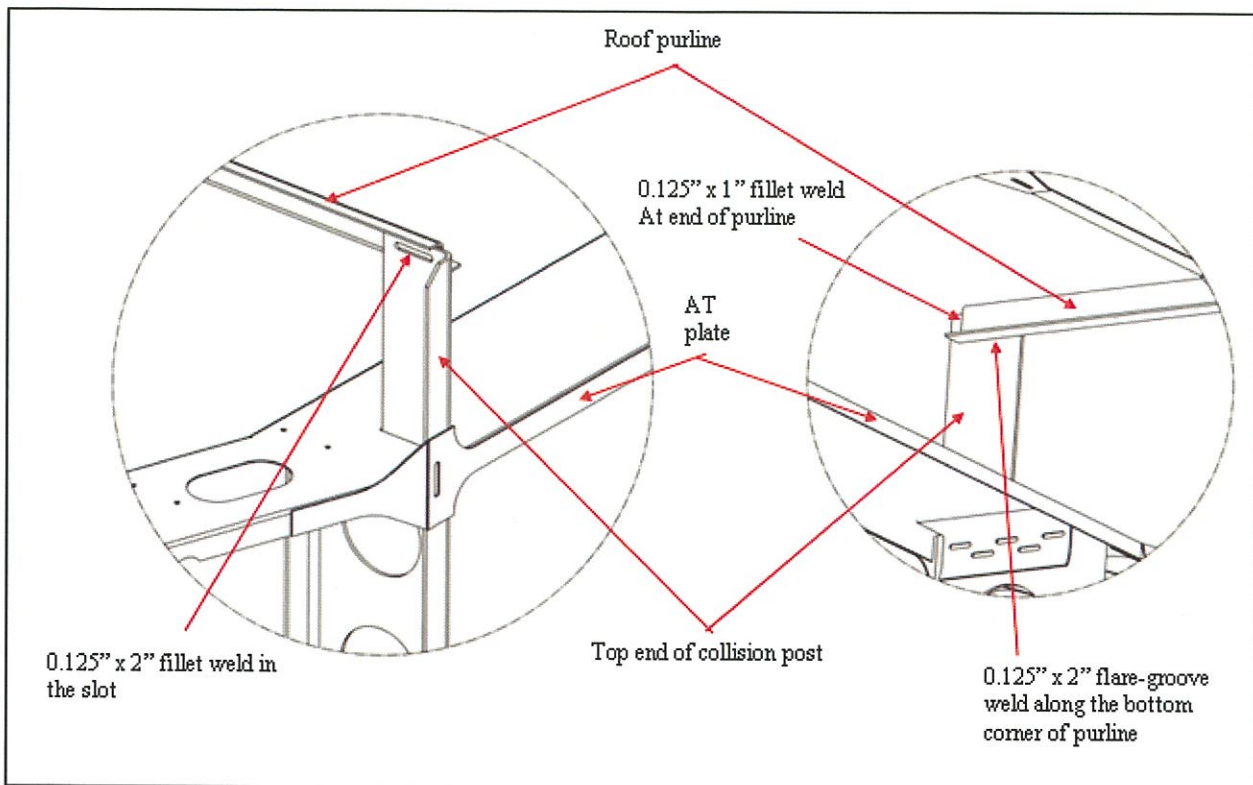


Figure 3.2.4.3, Collision post to roof purline connection

The top end of the collision is welded to the roof purline as indicated in the above figure. The ultimate shear strengths of the welds are:

- 0.125 inch flare-groove weld = 8.7 kip/inch
- 0.125 inch fillet weld = 6.2 kip/inch

Based upon the weld's shear strength, the strength of the connection of the collision post with the roof carline is much higher than the 1.9 kip vertical load capacity of the end carline.

Roof purline to end carline connection

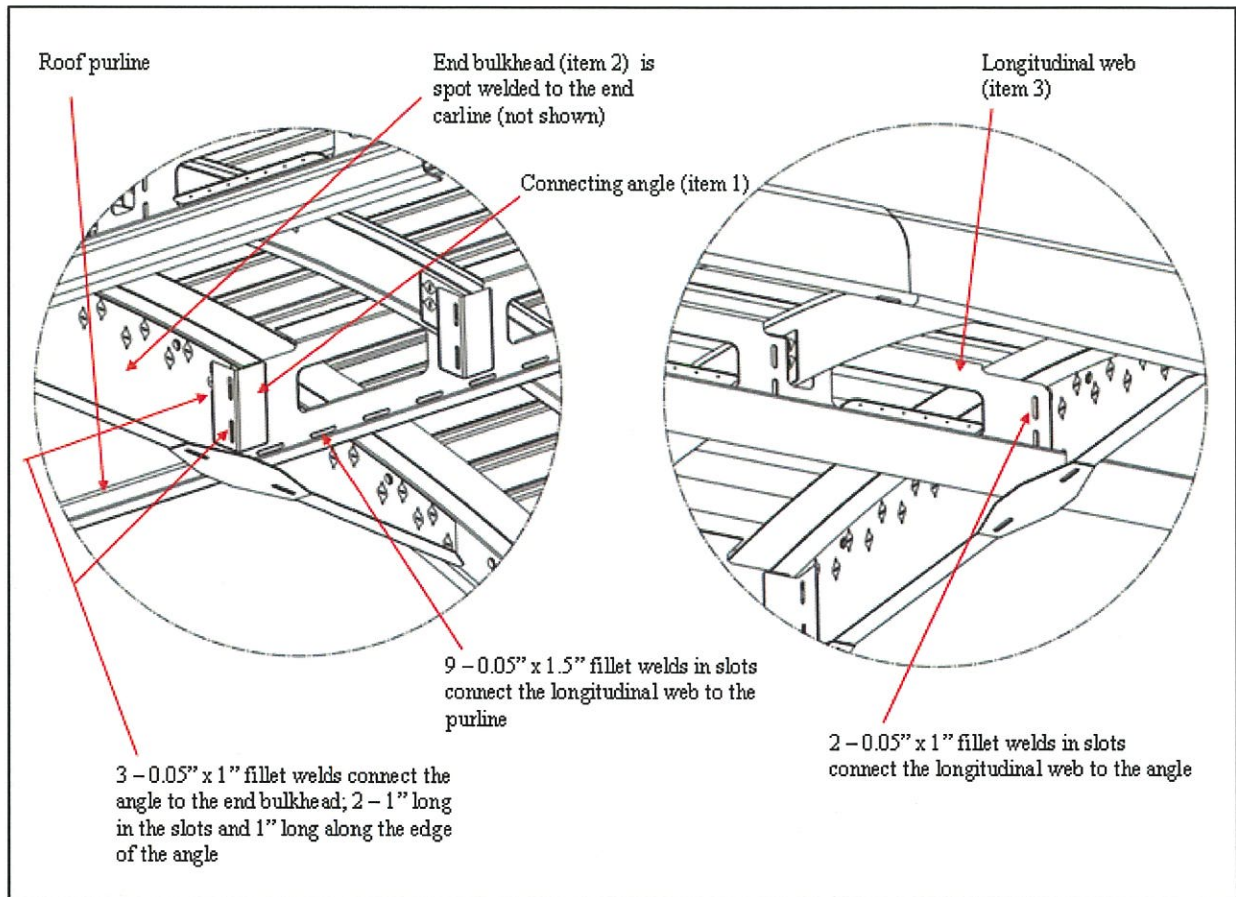


Figure 3.2.4.4, Roof purline to end carline connection

The roof purline is connected to the end carline by way of a connecting angle (item 1), a 0.05" thick end bulkhead (item 2) and a 0.05" thick longitudinal web (item 3). The end bulkhead is spot welded with the end carline. There are 37 spots in the connection and each spot weld has an ultimate strength of 1.7 kip.

The connecting angle is connected to the end bulkhead by 3 – 0.05" x 1" long fillet welds. The combined shear capacity of these 3 welds is 7.4 kip.

The longitudinal web is fillet welded to the connecting angle by 2 0.05" x 1" long welds with combined shear capacity of 4.9 kip.

Finally, the longitudinal web is connected to the roof purlines by 0.05" x 1.5" long fillet welds in 9 slots. Conservatively counting only the 1 slot as effective to carry the load (i.e. the one immediately below the connecting angle), the shear capacity is 2.5 kip.

Compared versus the calculated end carline vertical strength of 1.9 kip, the minimum margin of safety (MS) in the connection is:

$$MS = (2.5 \div 1.9) - 1 = 0.3.$$

3.2.5 Requirement No. 5, Posts section moduli, LC_13:

The sum of the section moduli of all end posts at one (1) end of the car shall not be less than thirty (30) cubic inches, and the sum of the section moduli of the two (2) center posts shall be approximately seventy-five percent (75%) of the total of all end posts.

Collision Post Section Moduli:

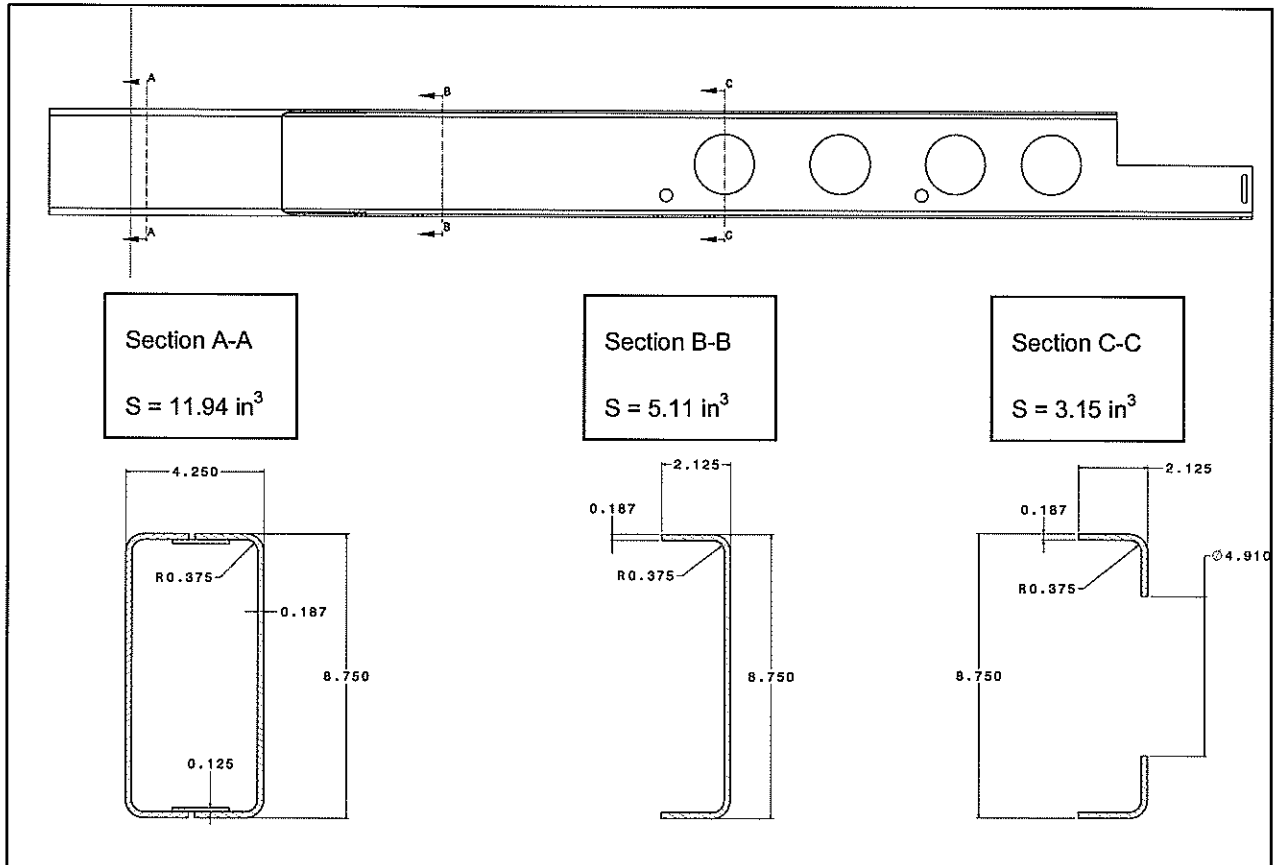


Figure 3.2.5.1, Collision post section properties.

The collision post section moduli are calculated in appendix A6.

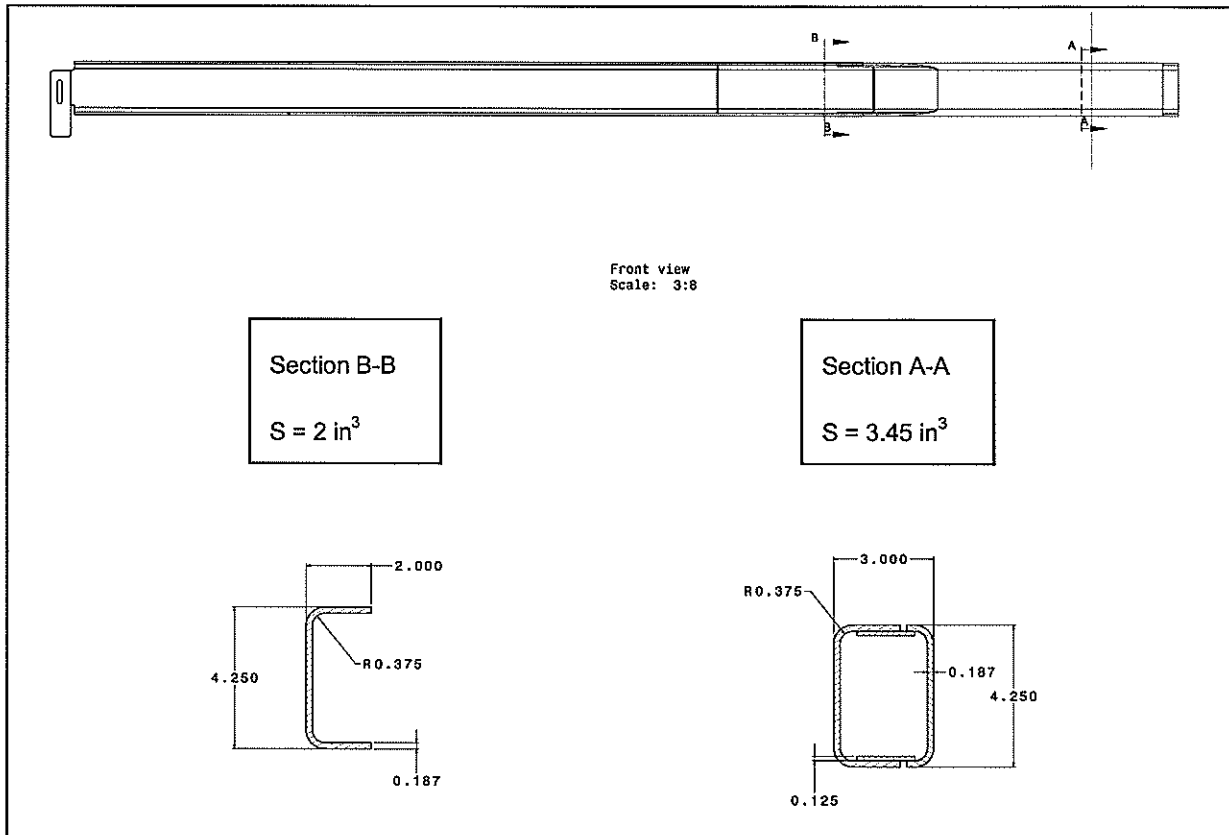
Corner Post Section Moduli:

Figure 3.2.5.2, Corner post section properties.

The corner post section moduli are calculated in appendix A7.

At section A A:

1. All end posts section modulus to be greater than 30 in^3 :

$$S_{\text{total}} = 2 \times 11.94 + 2 \times 3.45 = 30.78 \text{ in}^3 \text{ which is greater than the required } 30 \text{ in}^3$$

2. Central collision posts section modulus to be approximately 75% of the total (S_{total}):

$$S_{\text{collision posts}} = 2 \times 11.94 = 23.88 \text{ in}^3 \text{ which is greater than } (0.75 \times 30) = 22.5 \text{ in}^3$$

3.3 Roof structure:

The roof corrugation and carlines are checked for the 250 lb man loading, load case LC_19 (as per table 1 of ref.1, Carbody stress and analysis plan). The allowable stress for this load case is yield strength.

Roof corrugation:

The load of 250 lb is distributed over 1 sq. ft, $M_{\max} = 1351$ lb in.

$$\sigma_{\max} = \frac{M_{\max}(C)}{I_{xx}}$$

where:

$$C = 0.351 \text{ in (Appendix A.2)}$$

$$I_{xx} \text{ (for 3")} = 0.0033 \text{ in}^4 \text{ (Appendix A.2)}$$

$$I_{xx} \text{ (for 12")} = 0.0033 \left(\frac{12}{3}\right)^3 = 0.0132 \text{ in}^4$$

$$\sigma_{\max} = \frac{(1.351)(0.351)}{0.0132} = 36 \text{ ksi}$$

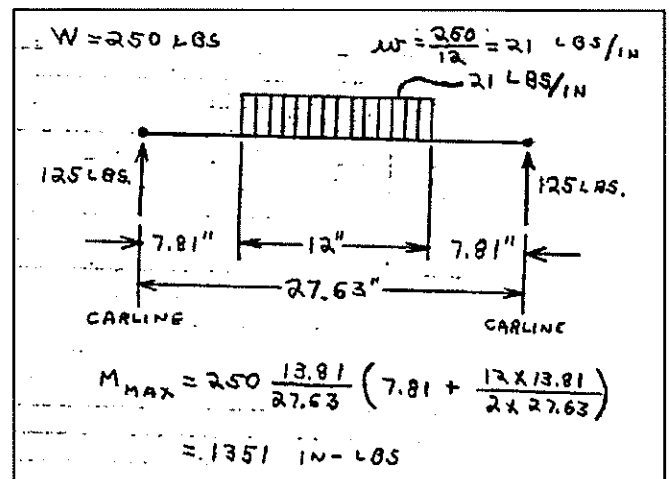


Figure 3.3.1, Roof corrugation loads.

Buckling verification for the corrugation node top plate:

$$\sigma = \frac{\pi^2 Kc Er}{12(1-\nu^2)} \left(\frac{t}{b}\right)^2$$

Where

$$a = 27.63 \text{ "}$$

$$b = 1 \text{ "}$$

$$Kc = 4 \text{ (Ref. 5, see Figure A.1.1)}$$

$$Er = 24000 \text{ ksi (as per fig. A.1.2)}$$

$$\nu = 0.3$$

$$t = 0.026 \text{ "}$$

$$\sigma_{CR} = -58.6 \text{ ksi}$$

The allowable buckling stress for the roof corrugation (201LN ¼ hard) for LC_19 = 58.6 ksi.

The roof corrugation margin of safety for LC_19 = $(58.6/36) - 1 = 0.6$.

Carline:

Punctual load of 250 lb is over 106 in, $M_{\max} = 6625$ lb in.

$$\sigma_{\max} = \frac{M_{\max}(C)}{I_{xx}}$$

where:

$C = 1.375$ in (Appendix A.6)

$I_{xx} = 0.211$ in⁴ (Appendix A.6)

$$\sigma_{\max} = \frac{(6.625)(1.375)}{0.211} = 43.2 \text{ ksi}$$

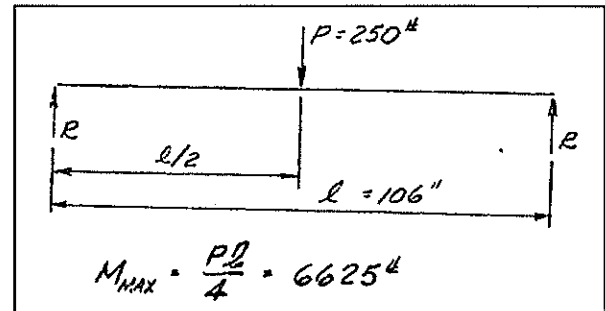


Figure 3.3.2, Carline loads.

Buckling verification for the carline top plate:

$$\sigma = \frac{\pi^2 Kc Er}{12(1-\nu^2)} \left(\frac{t}{b}\right)^2$$

Where

$a = 106$ "

$b = 1.25$ "

$Kc = 5.5$ (Ref. 5, see Figure A.1.1)

$Er = 22000$ ksi

$\nu = 0.3$

$t = 0.03$ "

$$\sigma_{CR} = -62.9 \text{ ksi} = \text{yield} = -62 \text{ ksi}$$

The allowable stress for the roof carline (201LN ¼ hard) for LC_19 is yield = 62 ksi.

The roof carline margin of safety for LC_19 = $(62 / 43.2) - 1 = 0.43$.

3.4 Main connections, side sill to end sill, bolster to side sill and bolster to king pin:

The side sill to end sill connection is verified for the compression load (LC_04)

The bolster connections with the side sill and the king pin are verified for the 50 kip vertical crash and 150 kip horizontal crash truck load (LC_20) as well as for fatigue (LC_03). The allowable stress for this load case is yield except for fatigue of course.

Side sill to end sill connection:

This connection is verified for the 200 kip compression load (LC_04).

There are 7 main round slot welds of 1.375" DIA with 0.156" fillet welds between the side sill and the end sill connecting plate (see picture below). There are also 2 smaller slot welds (blue angle) and the top long. weld which are not considered in the calculations.

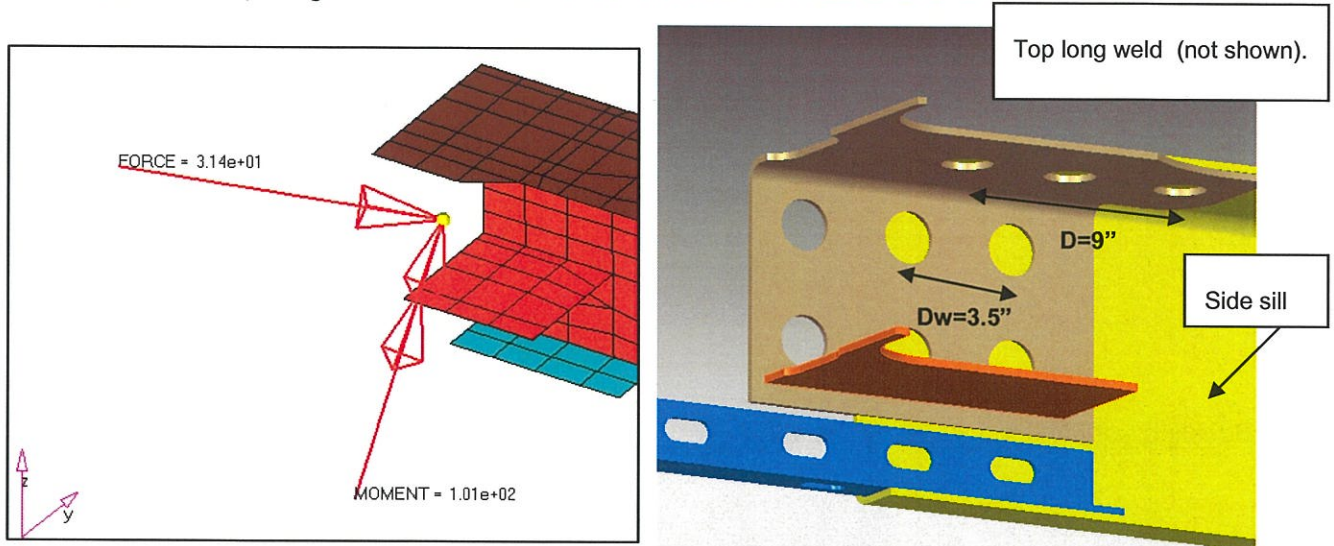


Figure 3.4.1, Side sill at end sill connection (with FEA reactions).

FEA forces & moments results for LC_04 at this connection are:

$F_x=30\text{kip}$, $F_y=10\text{kip}$, $M_y=-22\text{kipin}$, $M_z=86\text{kipin}$. (The force & moment shown are the resultants).

Resulting force for the top flange round slot = $F_x/7+F_y/3+M_z/d = (30/7)+(10/3)+(86/9) = 17.2\text{ kip}$

Resulting force for the web round slot = $F_x/7+M_y/(d_w \times 2) = (30/7)+(22/7) = 7.43\text{ kip}$

Weld capacity of one round slot (DIA = 1.375"):

$$A_w = \pi \times D \times E_{tt} = (3.14)(1.375)(0.156 \times 0.707) = 0.48\text{ in}^2$$

$$\text{Shear allowable for yield} = \text{yield} / (3)^{1/2} = 75 / (3)^{1/2} = 43.3\text{ ksi}$$

$$\text{Capacity of} = \text{Shear allowable} \times A_w = (43.3)(0.48) = 21\text{ kip}$$

$$MS = (21/17.2) - 1 = 0.22$$

This calculation is conservative since we neglected the top longitudinal weld as well as the bottom angle slot welds.

Bolster to side sill connection:

This connection is verified for the 50 kip vertical crash and 150 kip horizontal crash truck load (LC_20) as well as for fatigue (LC_03).

The connection consists of 16 vertical spots around the bolster web (8 on each side) and 16 horizontal spots main with the top flange. (see picture below).

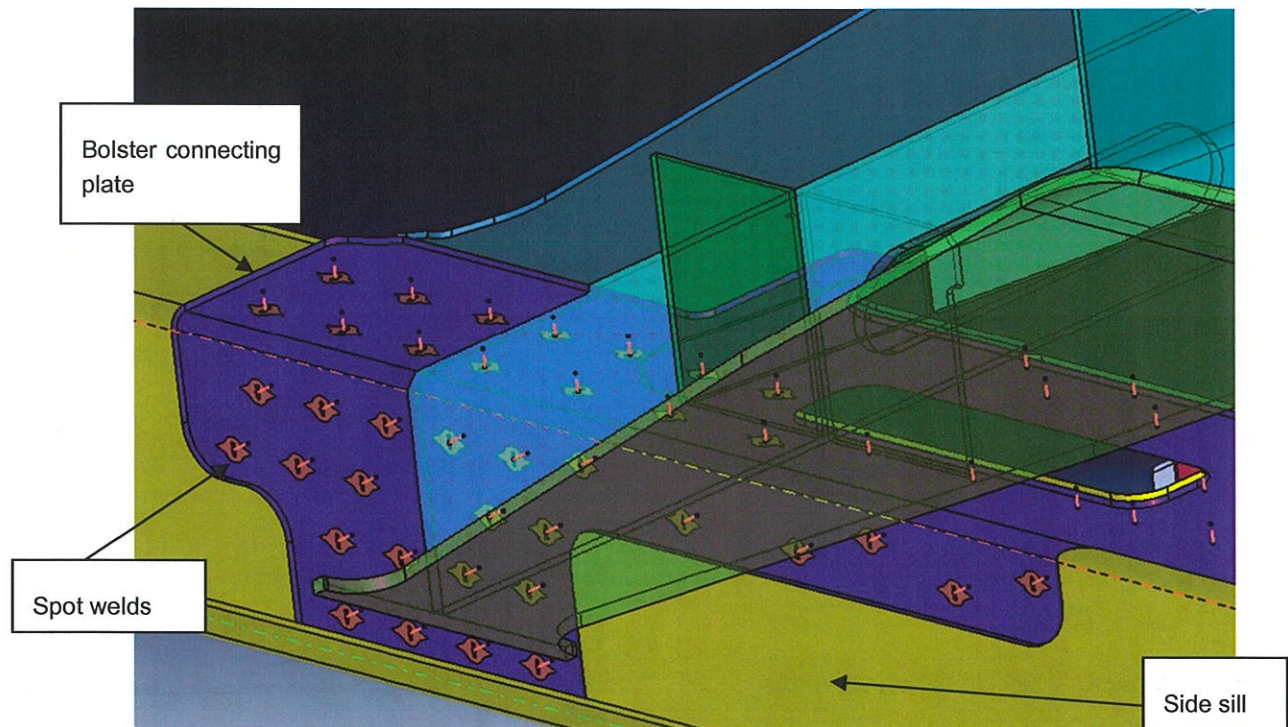


Figure 3.4.2, Side sill to bolster connecting plate (with spot welds).

Each group of spot welds (vertical and horizontal) have a shear capacity in yield of:

Each spot weld has an shear capacity in yield of $9.75 (75/120) = 6$ kip where:

- The ultimate tested capacity of a spot in shear for 0.188 thickness = 9 kip
- 75 ksi is the yield strength of 201 MT.
- 120 ksi is the ultimate strength of 201 MT.

Spot welds capacity of the vertical group = $16 \times 6 = 96$ kip

Spot welds capacity of the horizontal group = $16 \times 6 = 96$ kip

Bolster to side sill connection (cont.):LC-20, (50 kip vertical + 150 kip horizontal crash loads):Vertical spot weld group:

$$V_{\text{total}} = 25 + 35.2 \text{ (fig.3.4.4)} = 60.2 \text{ kip}$$

Capacity = 96 kip (previous page)

M.S. Vertical group for LC_20

$$\text{M.S.} = \frac{96}{60.2} - 1 = 0.59$$

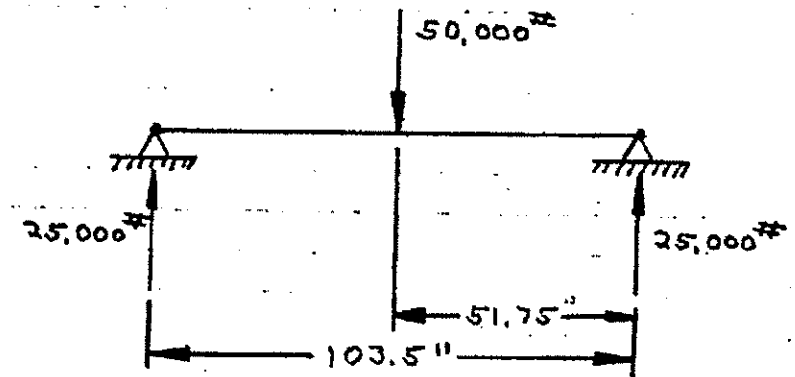


Figure 3.4.3, Bolster 50 kip vertical load.

Horizontal spot weld group:

$$V_{\text{total}} = 75 \text{ kip}$$

Capacity = 96 kip (previous page)

M.S. Horizontal group for LC_20

$$\text{M.S.} = \frac{96}{75} - 1 = 0.28$$

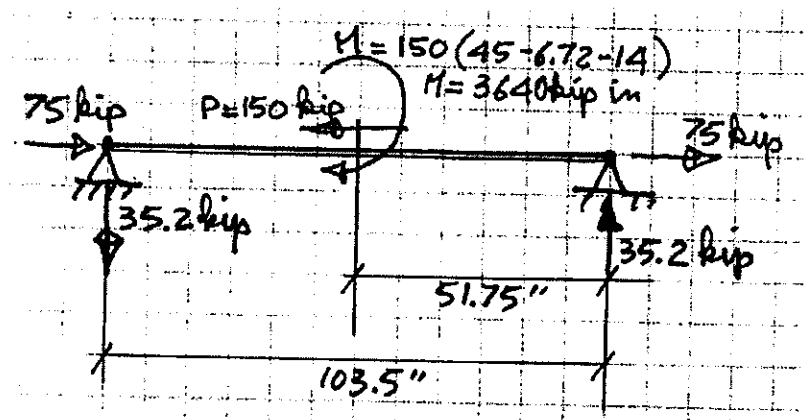


Figure 3.4.4, Bolster 150 kip lateral load.

LC-03, Vertical fatigue verification for the vertical group:Fatigue load range per vertical group for LC_03 = $(52 \times 0.3) / 4 = 4$ kipSpots in fatigue allowable range = 10% of ultimate hence, $(9.75 \times 16) \times 10\% = 15.6$ kip

$$\text{M.S. Vertical group in fatigue LC.03} = \frac{15.6}{4} - 1 = 2.9$$

Bolster to king pin connection:

This connection is verified for the 50 kip vertical crash and 150 kip horizontal crash truck load (LC_20). Allowable is yield shear stress.

Upper weld:

$$A_w = TT \times \text{Dia} \times E_{tt}$$

$$A_w = 3.14 (5.25)(0.32) = 5.3 \text{ in}^2$$

$$\text{All shear stress} = 80 / \sqrt{3} = 46 \text{ ksi}$$

$$\text{Capacity} = 46 \times 5.3 = 243 \text{ kip}$$

$$\text{M.S. upper weld} = \frac{243}{196} - 1 = 0.24$$

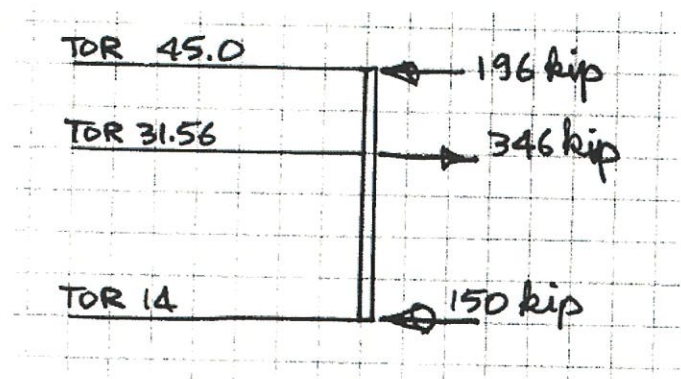


Figure 3.4.5, Bolster/king pin 150 kip shear reactions.

Lower weld:

$$A_w = TT \times \text{Dia} \times E_{tt}$$

$$A_w = 3.14 (13.25)(0.375) = 15.6 \text{ in}^2$$

$$\text{Capacity} = 46 \times 15.6 = 717 \text{ kip}$$

$$\text{M.S. lower weld} = \frac{717}{346} - 1 = 1.0$$

Vertical welds:

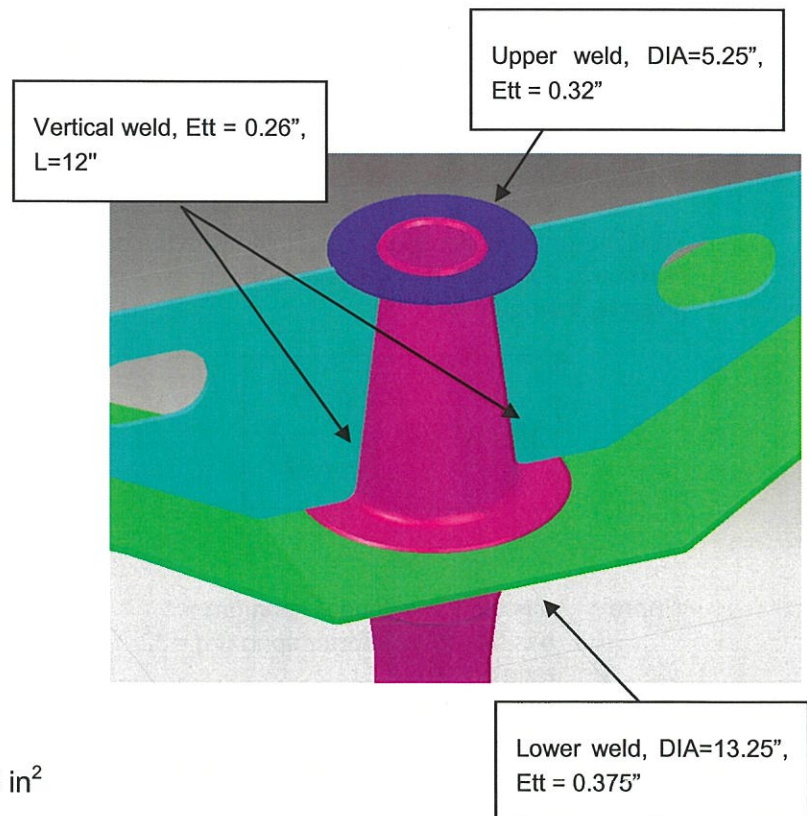
Vertical welds are reviewed for the

50 kip vertical crash load.

$$A_w = 2 \times L \times E_{tt} = (2) (12) (0.26) = 6.24 \text{ in}^2$$

$$\text{Capacity} = 46 \times 6.24 = 287 \text{ kip}$$

$$\text{M.S. vertical welds} = \frac{287}{50} - 1 = 4.7$$



3.5 Plymetal floor loads:

The plymetal deflection is verified for the AW3 passenger load (LC_02).

There is no seat pedestal load applied directly on the plymetal. In all cases there are 3/8 in tapping plates designed to take the load.

Floor passenger load:

The plymetal floor properties calculated in section A.4 are used for the following calculations:

From Technical Specification CTA 6900-4 and the available floor space for standing passengers, the pressure weight was evaluated as follow:

$$q = \frac{(W_{pass \max} - W_{seatpass})}{A_{floor}} \quad q \text{ (psi)} = 0.688$$

Where	$W_{pass \max}$ is the nominal maximum passenger weight =	23100
	$W_{seatpass}$ is the seated passenger weight =	5700
	A_{floor} is the floor surface available for standing passengers (in ²) =	25307
	q is the pressure load (psi) =	0.688

The floor panel deflection is calculated with the equation of Case 1a in table 26 of Roark's Formulas for Stress and Strain. The maximum deflection (y_{max}) is given by the equation:

$$y_{max} = \frac{\alpha q b^4}{E_{ply} d^3} \quad y_{max} \text{ (in)} = 0.054$$

Where	a is the panel longer span (in) = *	66
	b is the panel shorter span (in) = *	34.8
	ratio a/b	1.9
	Lamda varies for a ratio a/b =	0.10635
	q is the pressure load (psi) =	0.688
	E_{ply} is the equivalent Young's Modulus of the panel (psi) = **	4749333
	d is the panel thickness (in) =	0.75

* Ref: A-249-0003

** As calculated in section A.4

The plymetal maximum calculated deflection for a panel 66"x34.8" = 0.054 in which is less than 0.125 in.

4 FEA Calculations

Three FEA models are used for this analysis. Half a carbody model is used for all symmetric load cases and a full carbody is used for the torsion jacking re-railing operation LC_10. A third model without the sub-floor is used for natural frequencies analysis LC_27. A central underframe model with the detailed connections of all equipment attached is used for the analysis of the undercar equipment for LC_12.

The models are built and analyzed with MSC Nastran 2005 version 1. The FEA models are built as per the official CATIA model with Hypermesh version 8.0. The building of the FEA models is done through electronic transfers of the surfaces from CATIA to hypermesh. The model is representative of the following drawings:

- A-399-0007 Rev." " Carbody Assy "A" Car
 - A-299-0006 Rev." " Underframe Assy
 - A-319-0008 Rev." " Side Frame Assy
 - A-329-0006, Rev." " # 1 End Frame Assy
 - A-339-0005, Rev." " # Roof Assy
 - A-359-0004, Rev." " # 2 End Frame Assy

The FEA models, the applied loads and boundary conditions as well as all inherent modeling assumptions are described in appendix 'B'.

In this section, FEA results are presented by structural component. Maximum Von Mises, principal or component stresses are reviewed. FEA stresses often show stress concentrations due to modeling singularities or local application of loads. In such cases stresses at the closest node to that area will be used to evaluate nominal stresses.

This maximum stress is then compared to the allowable stress applicable to the load case and the margin of safety is calculated. The margin of safety should always be positive. Design criteria's, allowable stresses and customer specification references are described in table 1 of the 'Carbody Stress Analysis and Test Plan' (ref. 1).

When a maximum FEA stress is due to modeling singularities such as shell mid-plane intersections, holes, rigid beams supports and the discontinuity of shell element thicknesses, it is acceptable to use the closest node in order to obtain a stress which is more representative of a nominal stress in the area. This method should only be used if the FEA mesh size is adequately refined in the region.

4.1 End sill:

Von Mises stresses are reviewed for the end sill for all load cases. Results are presented for the most severe load case which is LC_05 'Compressive end load of 200 kip at AW3. The allowable stress for this load case is 90% of yield.

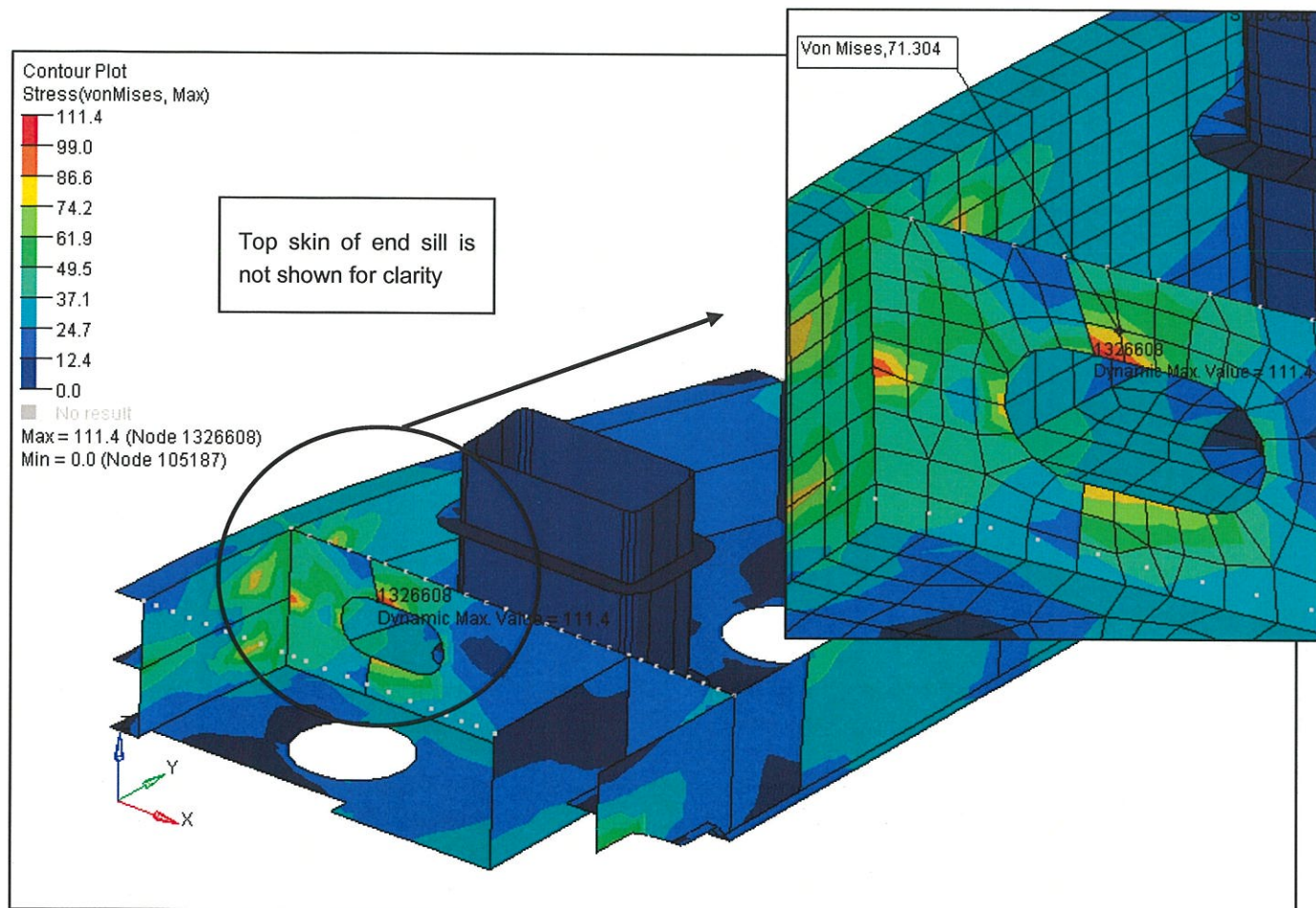


Figure 4.1.1 End sill maximum stress for LC_05 (200 kip + AW3)

- Figure 4.1.1 shows the maximum Von Mises stress concentration at the main internal rib (0.125 in thick HSLA80) right after the front doubler. The maximum stress value of 111.4 ksi is a stress concentration due to the vicinity of the much thicker element which includes the doubler (0.313 in). The next closest node stress value of 71.3 ksi shown in the close up is more representative of a nominal stress in the main web. This area is also designed for buckling during a crash (see 'Carbody Crash Analysis Report', ref. 3).

The allowable stress for the end sill (HSLA 80) for LC_05 is 90% of yield = 80 ksi x 90% = 72 ksi

The calculated FEA maximum stress (figure 4.1.1) = 71.3 ksi

The end sill main web minimum margin of safety = $(72/71.3) - 1 = 0.01$

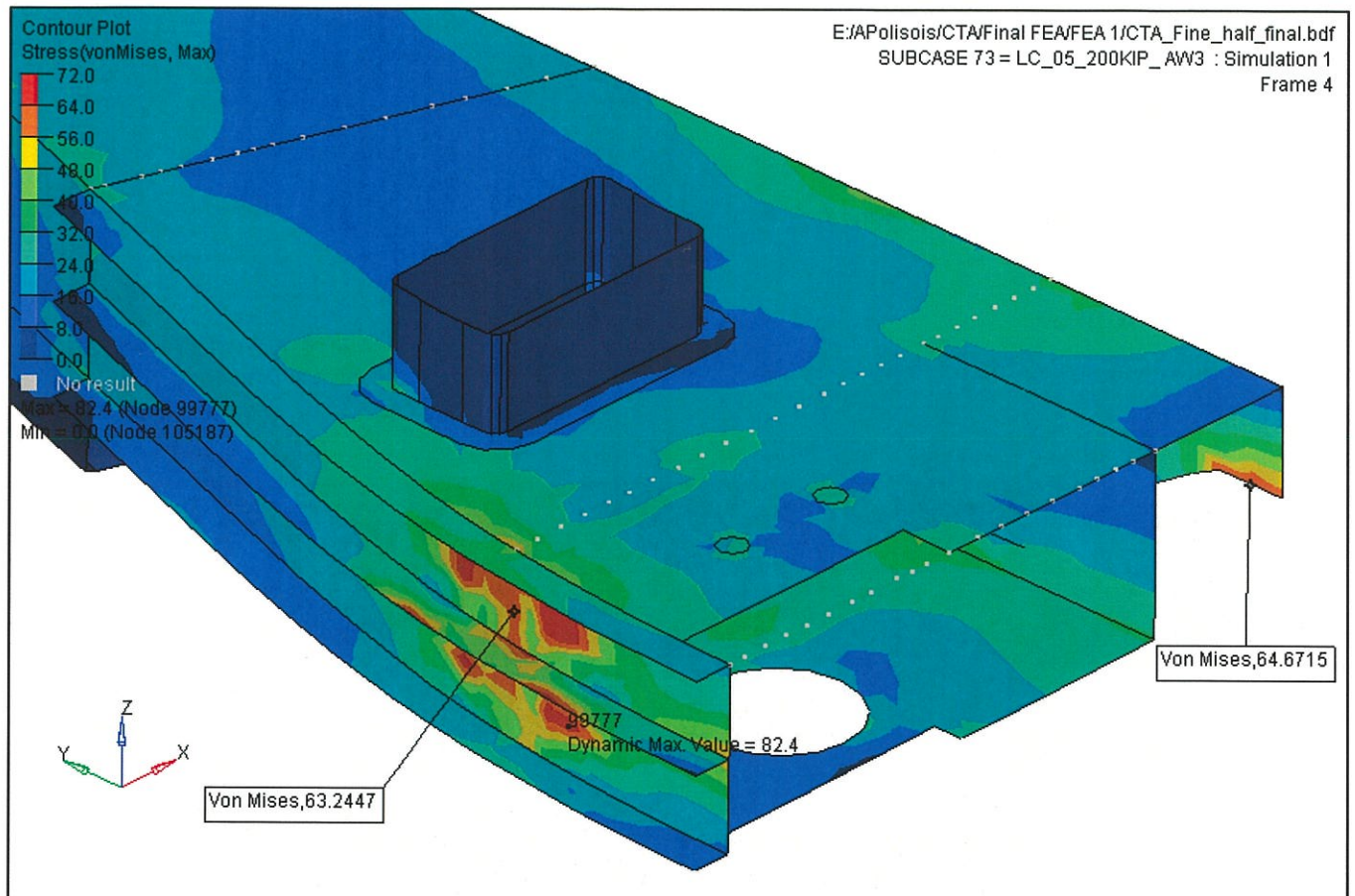


Figure 4.1.2 End sill next higher stresses

- Figure 4.1.2 shows the next maximum Von Mises stress concentrations at the anticlimber web (0.25 in thick HSAL80). The maximum stress value of 82.4 ksi is where the load is being applied which creates localized stress concentration in line with the web. The closest node has a stress value of 63.2 ksi.

The allowable stress for the end sill (HSLA 80) for LC_05 is 90% of yield = 80 ksi x 90% = 72 ksi

The calculated FEA maximum stress (figure 4.1.2) = 64.7 ksi (at the rear opening)

The end sill minimum margin of safety = $(72/64.7) - 1 = 0.1$

Buckling verification for the end sill top plate:

$$\sigma = \frac{\pi^2 Kc Er}{12(1 - \nu^2)} \left(\frac{t}{b}\right)^2$$

Where

a = 16 "

b = 14 "

Kc = 10 (Ref. 5, see Figure A.1.1)

Er = 29000 ksi

ν = 0.3

t = 0.125"

$$\sigma_{CR} = -21 \text{ ksi} \times 90\% = -19 \text{ ksi}$$

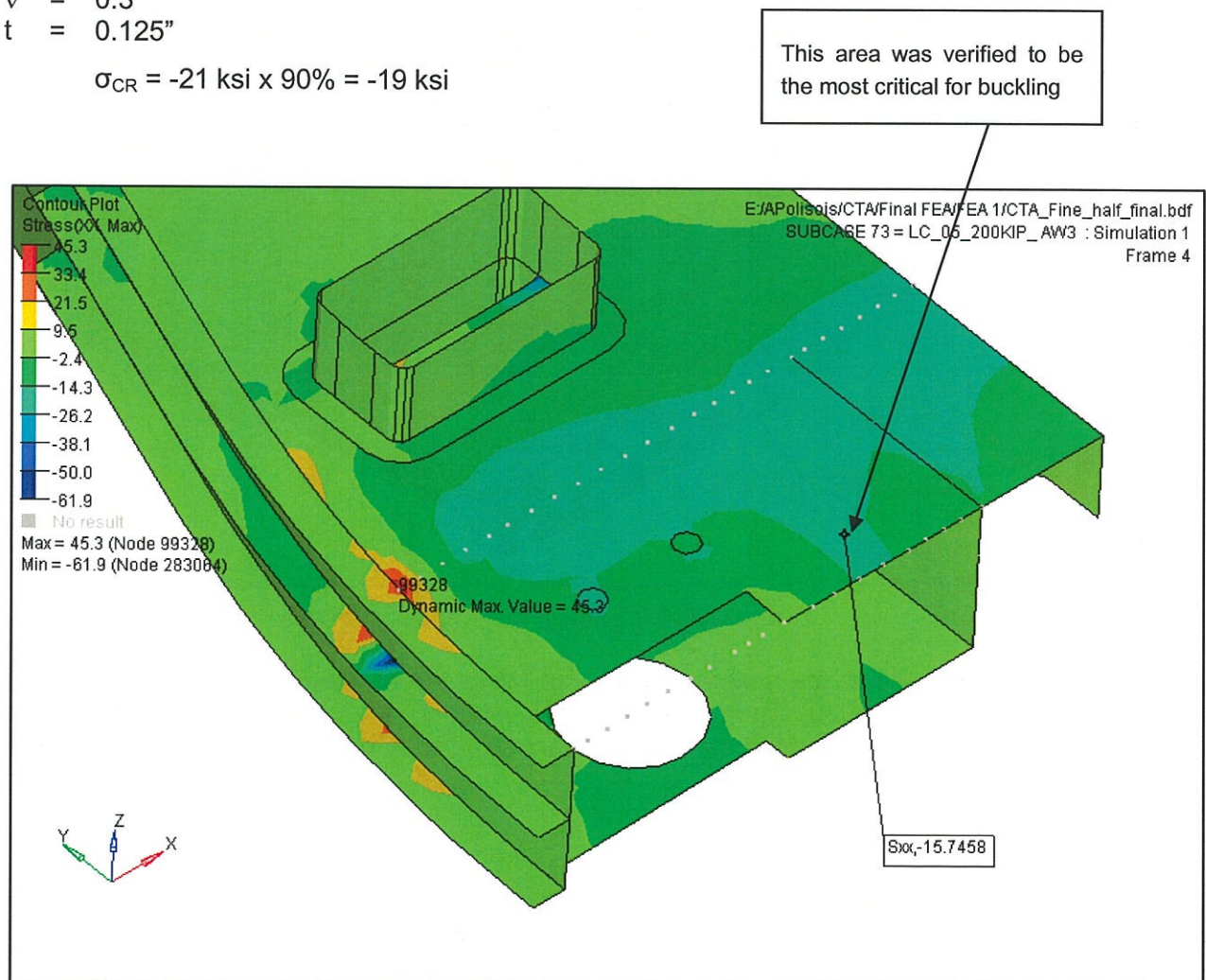


Figure 4.1.3 End sill top plate compression stress (Sxx) for LC_05 (200 kip + AW3)

$$\sigma_{CR} = -19 \text{ ksi}$$

$$\sigma_{FEA} = -15.8 \text{ ksi},$$

$$\text{The end sill buckling minimum margin of safety} = (-19 / -15.8) - 1 = 0.2$$

4.2 Draft sill:

Von Mises stresses are reviewed for the draft sill for all load cases. Results are presented for the most severe load case which is LC_05 'Compressive end load of 200 kip at AW3'. The allowable stress for this load case is 90% of yield.

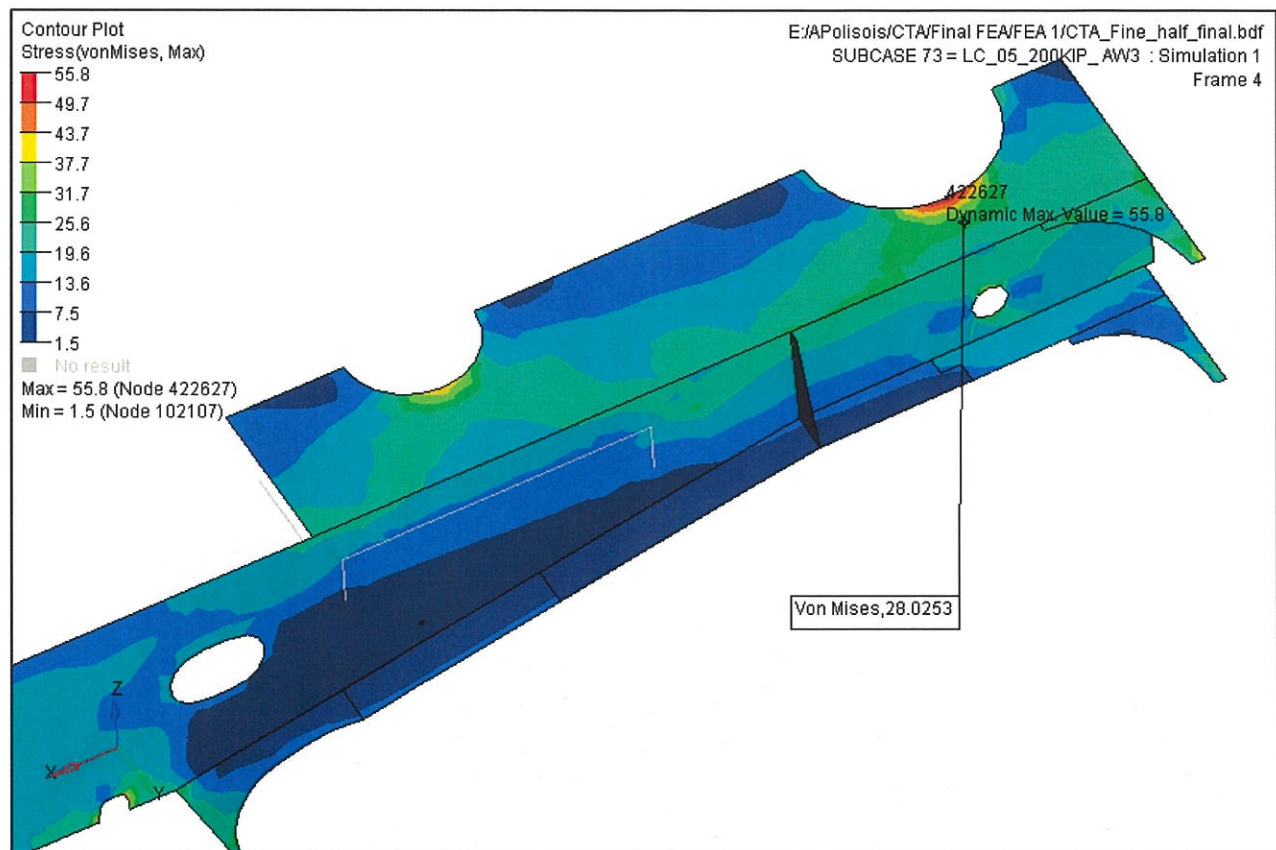


Figure 4.2.1 End sill maximum stress for LC_05 (200 kip + AW3)

- Figure 4.2.1 shows the maximum Von Mises stress at the draft sill top plate (0.188 in HSAL80) at the edge of the hole. The maximum stress value of 55.8 ksi is well below the allowable stress of 72 ksi. This area is also designed for buckling during a high speed crash (see 'Carbody Crash Analysis Report', ref. 3). The mean stress in the region is around 28 ksi.

The allowable stress for the end sill (HSLA 80) for LC_05 is 90% of yield = 80 ksi x 90% = 72 ksi

The calculated FEA maximum stress (figure 4.2.1) = 55.8 ksi

The draft sill minimum margin of safety = $(72/55.8) - 1 = 0.29$

Buckling verification for the draft sill top plate:

$$\sigma = \frac{\pi^2 Kc Er}{12(1-\nu^2)} \left(\frac{t}{b}\right)^2$$

Where

a = 20 "

b = 17 "

Kc = 8 (Ref. 5, see Figure A.1.1)

Er = 29000 ksi

ν = 0.3

t = 0.188"

$\sigma_{CR} = -26 \text{ ksi} \times 90\% = -23 \text{ ksi}$ in the draft sill largest unsupported region

$\sigma_{CR} = -80 \text{ ksi (yield)} \times 90\% = -72 \text{ ksi}$ at the draft sill hole region

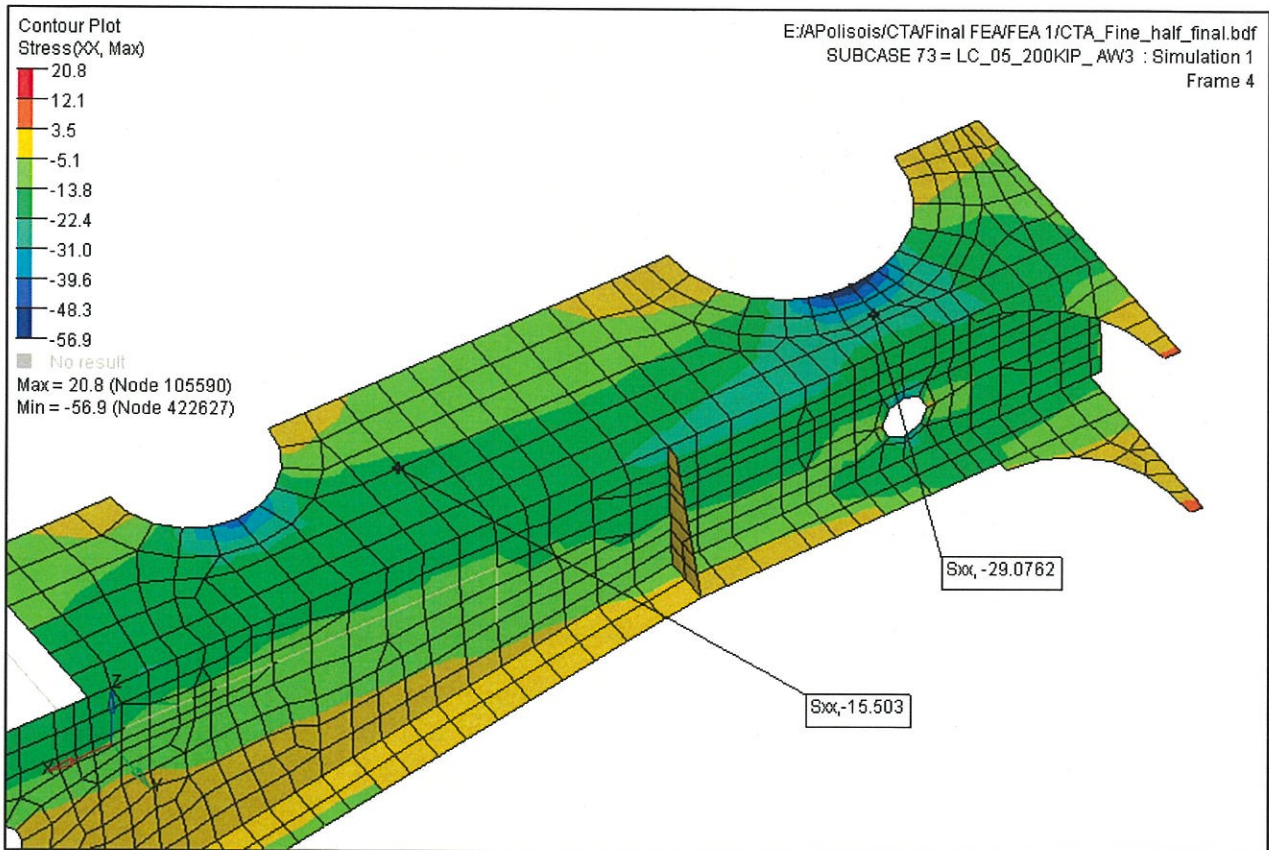


Figure 4.2.2 End sill top plate compression stress (Sxx) for LC_05 (200 kip + AW3)

$\sigma_{CR} = -23 \text{ ksi}$

$\sigma_{FEA} = -15.5 \text{ ksi,}$

The draft sill buckling minimum margin of safety = $(-23 / -15.5) - 1 = 0.48$.

4.3 Bolster:

Von Mises stresses are reviewed for the bolster for all load cases. Results are presented for LC_02 'Vertical load at AW3', LC_05 'Compressive end load of 200 kip at AW3' and LC_03, 'Vertical Fatigue'. The bolster is also verified for LC_20 'vertical (50kip) and lateral (150kip) crash loads. The allowable stresses for these load cases are 50% of yield for LC_02, 90% of yield for LC_05 and yield for LC_20. Fatigue stresses for the bolster for LC_03 will be reviewed as per AWS (ref. 3) in section 4.13.

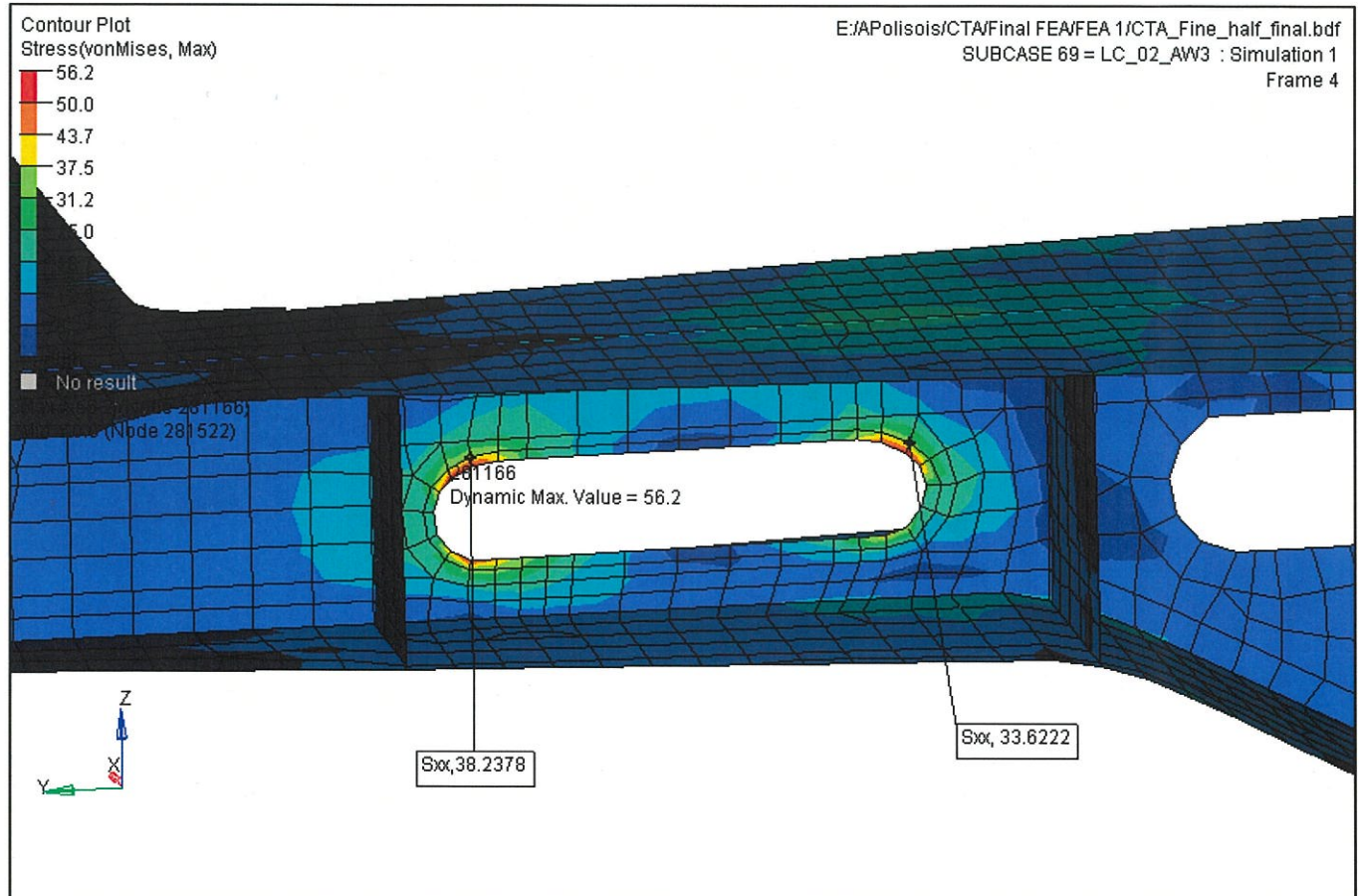


Figure 4.3.1 Bolster maximum stress for LC_02 (AW3)

- Figure 4.3.1 shows the maximum Von Mises localized stress concentration at the bolster web (0.375 in thick HSAL80) hole cut-out of 56.2 ksi, the next closest node stress value of 38.24 ksi is more representative of a nominal stress in the bolster main web.

The allowable stress for the bolster sill (HSLA 80) for LC_02 is 50% of yield = 80 ksi x 50% = 40 ksi

The calculated FEA maximum stress (figure 4.3.1) = 38.3 ksi

The bolster minimum margin of safety at the hole cut-out = $(40 / 38.3) - 1 = 0.04$

(NOTE: the bolster will be verified for fatigue in sect. 4.13 and for its main connections in sect. 4.14)

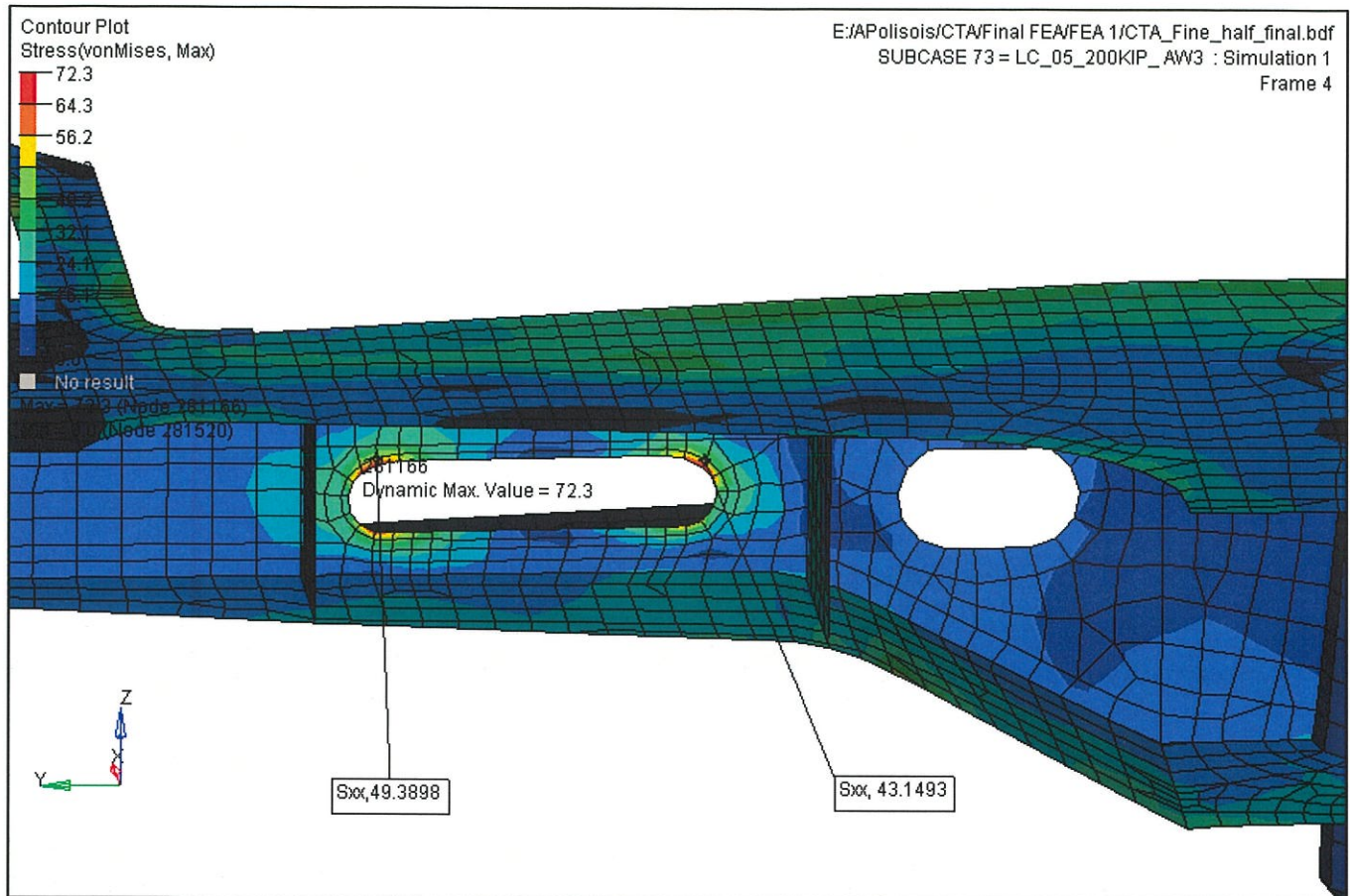


Figure 4.3.2 Bolster maximum stress for LC_05 (200 kip + AW3)

- Figure 4.3.2 shows the maximum Von Mises stress also localized as a stress concentration at the bolster web hole cut-out of 72.3 ksi, the next closest node stress value of 49.4 ksi.

The allowable stress for the bolster web (HSLA 80) for LC_02 is 90% of yield = 80 ksi x 90% = 72 ksi

The calculated FEA maximum stress (figure 4.3.2) = 49.4 ksi

The bolster margin of safety = $(72 / 49.4) - 1 = 0.45$

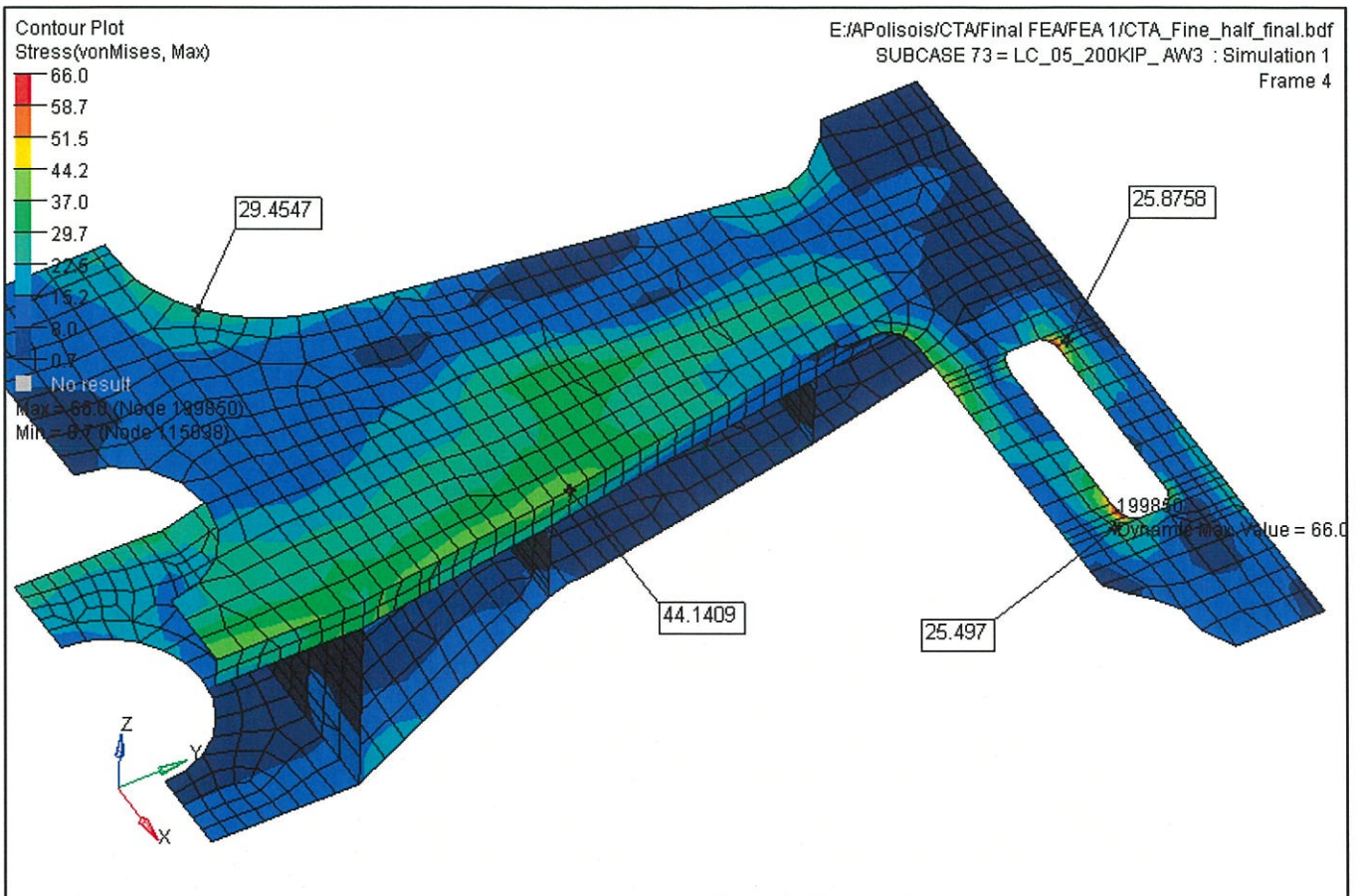


Figure 4.3.3 Bolster and its connecting plate next highest stresses for LC_05 (200 kip + AW3)

- Figure 4.3.3 shows the next higher Von Mises stresses for LC_05 which are all below the allowable stress of 72 ksi for HSLA 80. In the region of the bolster connecting plate to the side sill the allowable for stainless steel 201 ¼ hard is 56 ksi.

Buckling verification for the bolster top plate:

$$\sigma = \frac{\pi^2 Kc Er}{12(1-\nu^2)} \left(\frac{t}{b}\right)^2$$

Where

a = 10 "

b = 10 "

Kc = 1.9 (Ref. 5, see Figure A.1.1)

Er = 29000 ksi

ν = 0.3

t = 0.188"

$$\sigma_{CR} = -19.5 \text{ ksi} \times 90\% = -17.5 \text{ ksi in the bolster top plate}$$

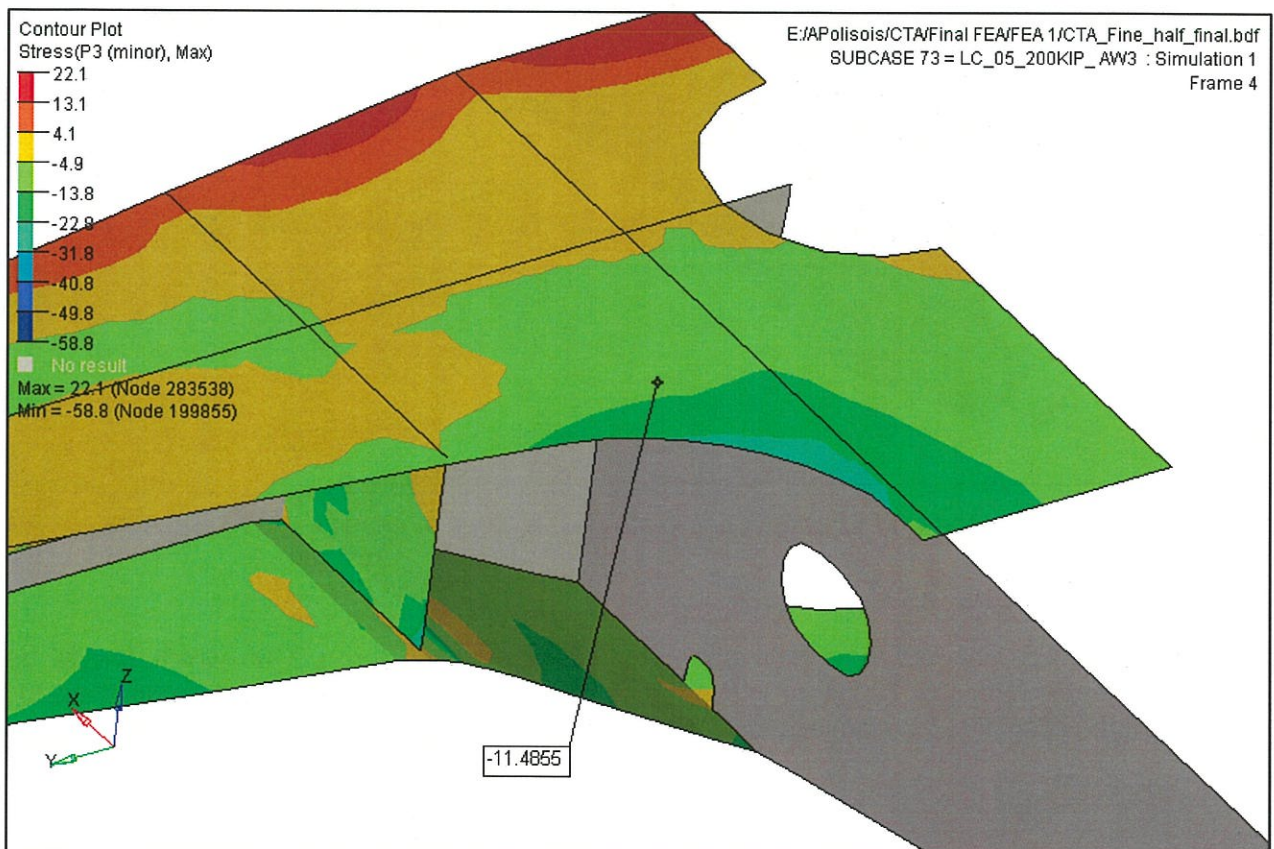


Figure 4.3.3 Bolster top plate mean compression minimum stress (P3)

$$\sigma_{CR} = -17.5 \text{ ksi}$$

$$\sigma_{FEA} = -11.5 \text{ ksi (mean stress in the buckling region of the bolster top plate).}$$

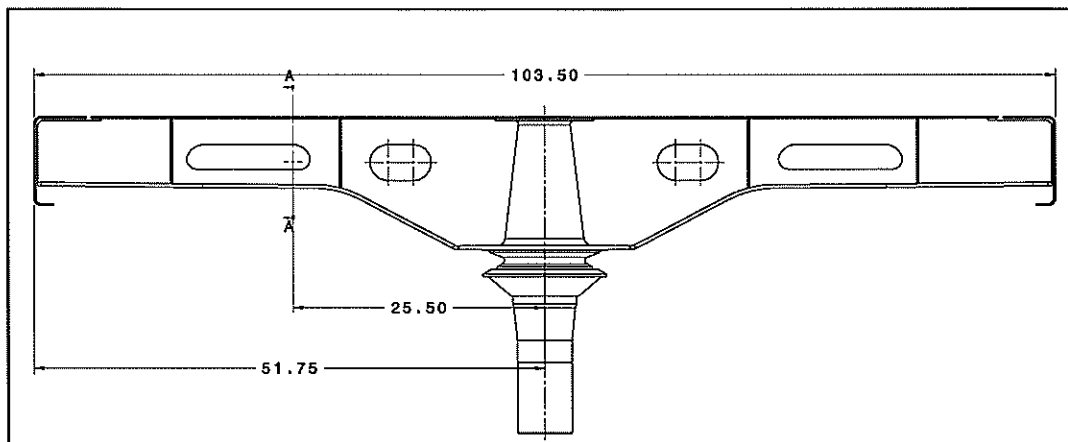
$$\text{The bolster top plate buckling minimum margin of safety} = (-17.5 / -11.5) - 1 = 0.5.$$

Bolster verification for the vertical crash load of 50 kip (LC 20):

Figure 4.3.1 shows a stress of 38.3 ksi at the bolster for a vertical load of 30 kip per bolster (AW3 = 60 kip per carbody). Hence, by extrapolating the stresses we find $(38.3 \times 50 / 30 = 64 \text{ ksi})$ which is below the yield of 80 ksi for a margin of safety = $(80/64) - 1 = 0.25$.

Bolster verification for the horizontal crash load of 150 kip (LC 20):

The horizontal 150 kip load is applied in the lateral direction at the centerline of the axle (14" from TOR). The weakest section of the bolster for the moment is at section A-A.



Moment at section A-A =, $M_{AA} = 35.2 (51.75 - 25.5) = 924 \text{ kip in.}$

$$\sigma_{\max} = \frac{M_{AA}(C)}{I_{xx}} + (F/A)$$

where:

$F = 75 \text{ kip}$

$C = 4.45 \text{ in (Appendix A.9)}$

$A = 10.7 \text{ in}^2$

$I_{xx} = 111.4 \text{ in}^4 \text{ (Appendix A.9)}$

$$\sigma_{AA} = \frac{(924)(4.45)}{111.4} = 37 \text{ ksi}$$

$$\sigma_{\max} = 37 + (75/10) = 44.5 \text{ ksi}$$

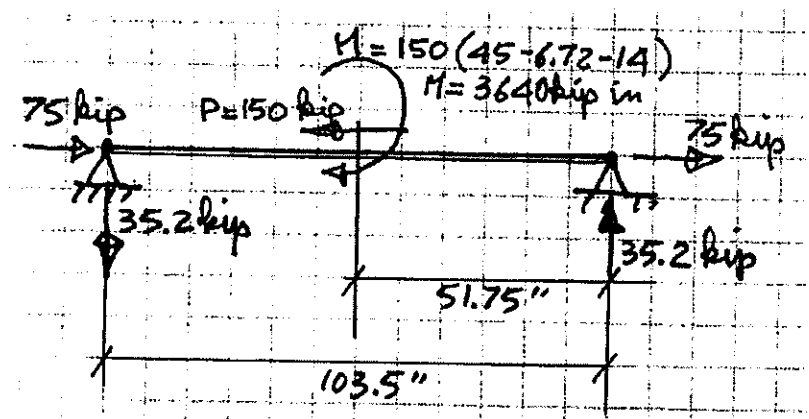


Figure 4.3.4, Bolster 150 kip lateral load.

The bolster top plate minimum margin of safety for LC_20 = $(80 / 44.5) - 1 = 0.8$.

4.4 Side Sill:

Von Mises stresses and main component stresses are reviewed for the side sill for all load cases. Results are presented for LC_02 'Vertical load at AW3', LC_05 'Compressive end load of 200 kip at AW3' and LC_03, 'Vertical Fatigue'. The allowable stresses for these load cases are 50% of yield for LC_02, and 90% of yield for LC_05,. Fatigue stresses of the side sill for LC_03 will be reviewed as per AWS (ref. 3) in section 4.13

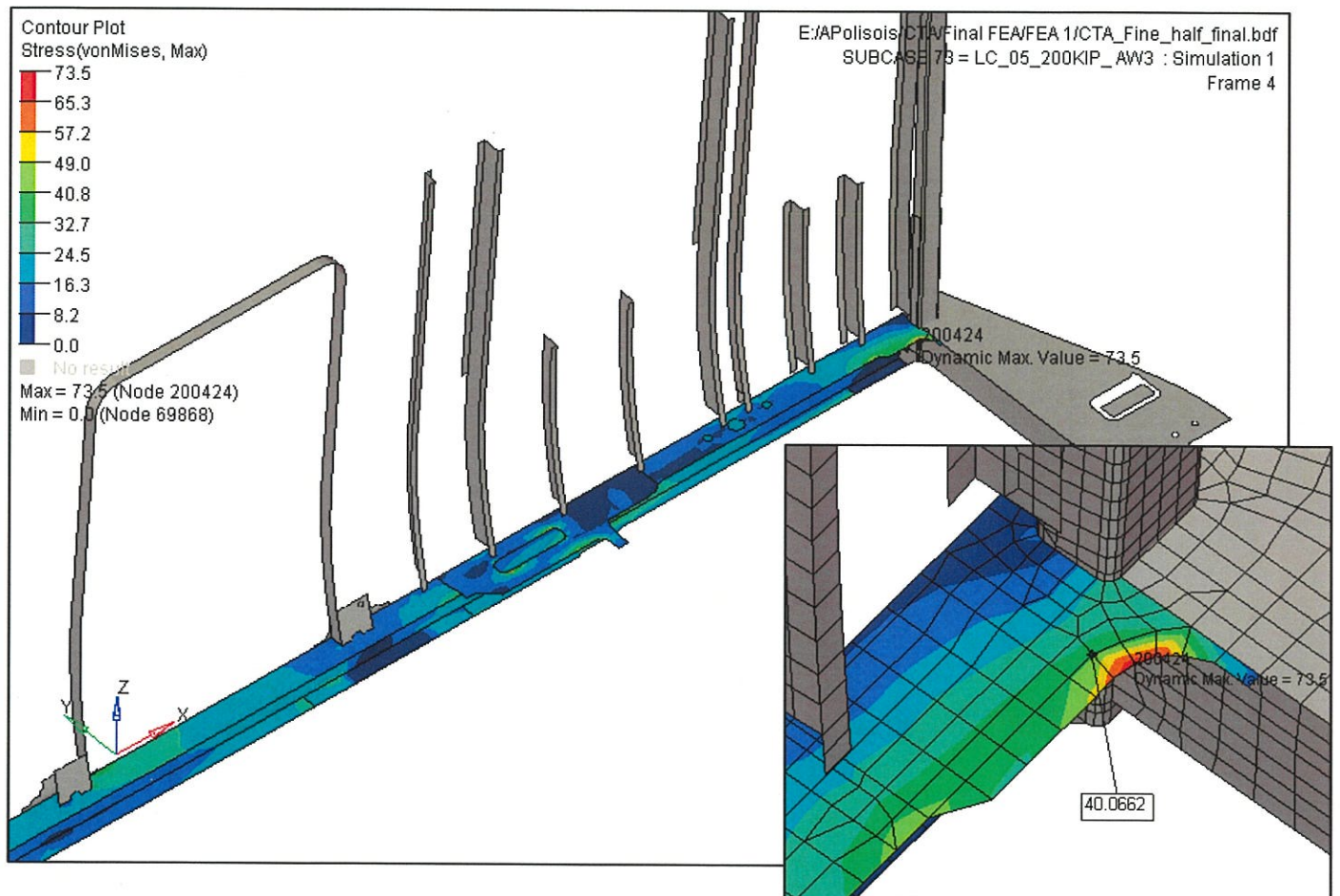


Figure 4.4.1 Side sill maximum stress for LC_05 (200 kip + AW3)

- Figure 4.4.1 shows a maximum Von Mises stress of 73.5 ksi at the side sill connecting plate to the end sill (0.188 in HSLA 80). This maximum stress is a stress concentration and the next closest node stress value of 40.1 ksi is more representative of a nominal stress in the region.

The allowable stress for the side sill connecting plate (HSLA 80) for LC_05 is 90% of yield = 80 ksi x 90% = 72 ksi

The calculated FEA maximum stress (figure 4.4.1) = 40.1 ksi

The side sill margin of safety at the end sill connection = $(72 / 40.1) - 1 = 0.79$

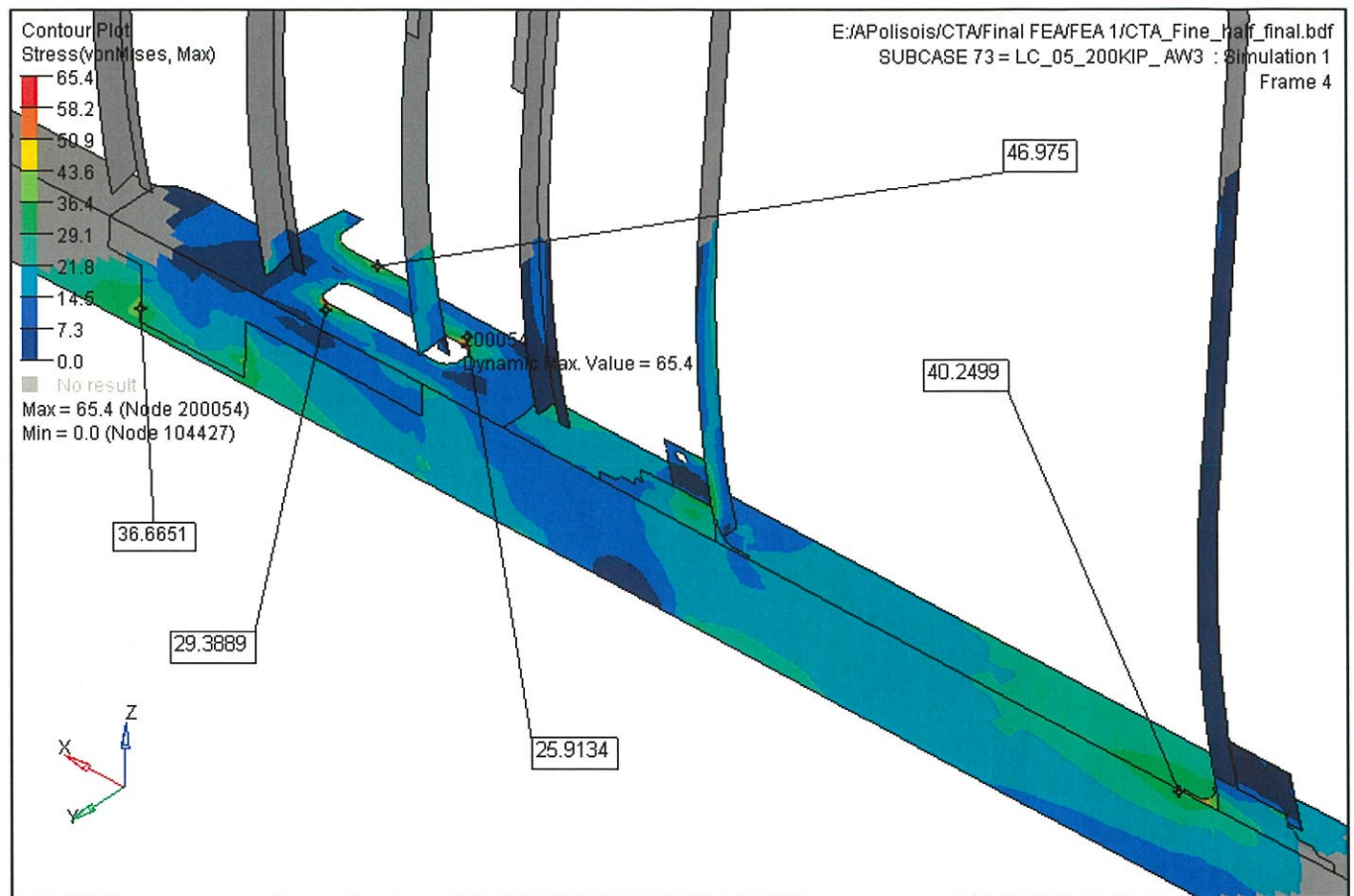


Figure 4.4.2 Side sill next highest stresses in the door region for LC_05 (200 kip + AW3)

- Figure 4.4.2 shows the next higher Von Mises stresses for LC_05 which are all below the allowable stress of 56 ksi. The highest stresses are at the bolster connecting plate (47 ksi) and at the door connection with the door mask (40.3 ksi).

The allowable stress for the end sill (201LN ¼ hard) for LC_05 is 90% of yield = 62 ksi x 90% = 56 ksi

The calculated FEA maximum stress (figure 4.4.2) = 47 ksi

The side sill minimum margin of safety at the bolster connection = $(56 / 47) - 1 = 0.19$

Buckling verification for the side sill top plate at the door region:

$$\sigma = \frac{\pi^2 Kc Er}{12(1-\nu^2)} \left(\frac{t}{b}\right)^2$$

Where

$$a = 22 \text{ "}$$

$$b = 5.2 \text{ "}$$

$$Kc = 1.2 \text{ (Ref. 5, see Figure A.1.1)}$$

$$Er = 25000 \text{ ksi (Ref. 5, see Figure A.1.2)}$$

$$\nu = 0.3$$

$$t = 0.188 \text{ "}$$

$$\sigma_{CR} = -39 \text{ ksi} \times 90\% = -35 \text{ ksi for the side sill top lip at the door region}$$

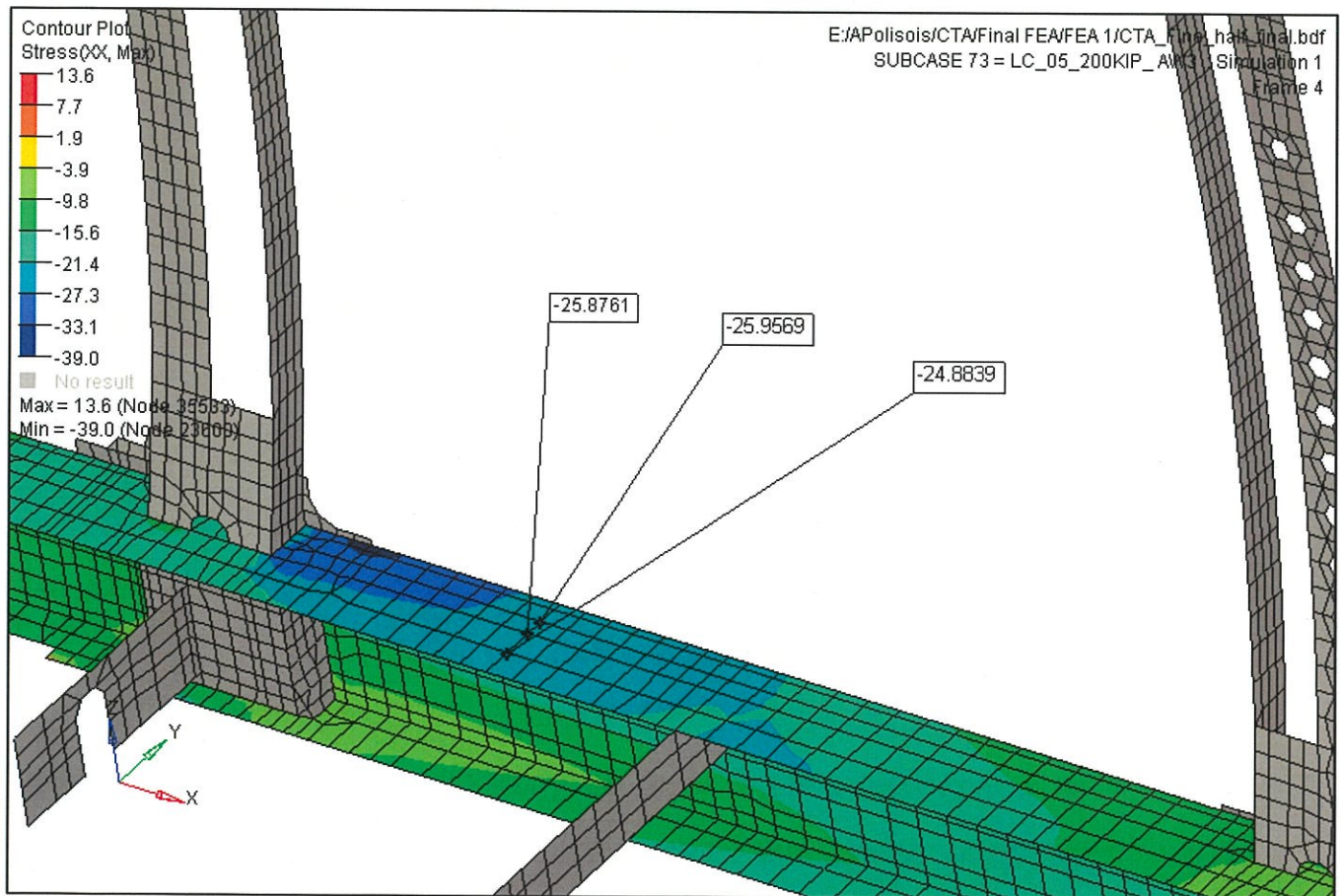


Figure 4.4.3 Side sill top plate nominal compression stress (Sxx)

$$\sigma_{CR} = -35 \text{ ksi}$$

$$\sigma_{FEA} = -26 \text{ ksi,}$$

The side sill at door buckling minimum margin of safety = $(-35 / -26) - 1 = 0.34$

4.5 Cross bearers:

The central under frame mainly consists of two major sections; the cross bearers and the main air duct. The section of the cross bearers includes the floor & equipment beams and the inter-coastal beams. Von Mises results are presented for the most critical load case which is LC_05 'Compressive end load 200 kip at AW3'. The allowable stress for this load case is 90% of the yield. Stresses and deflections are also shown for LC_02 'Vertical load at AW3'.

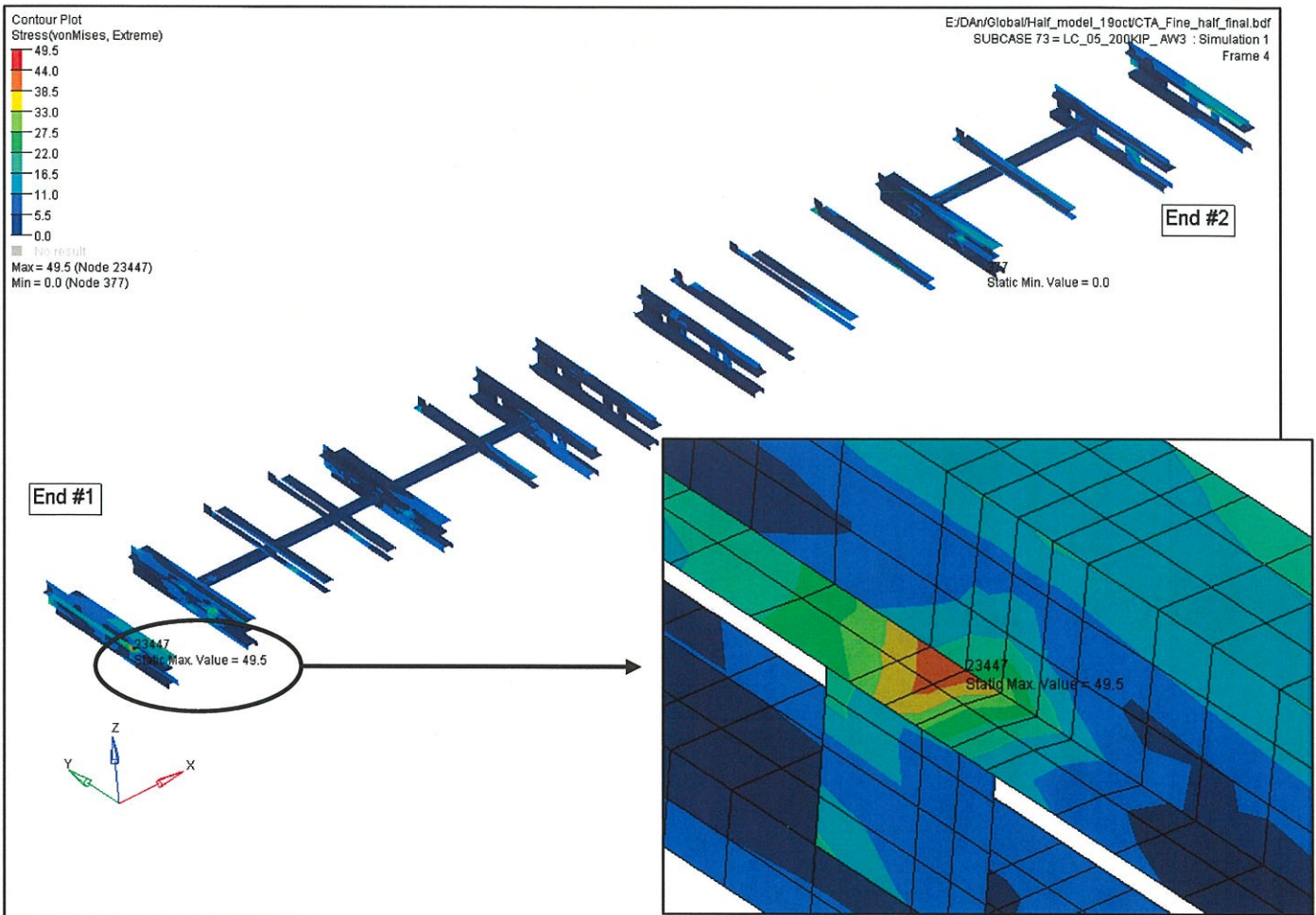


Figure 4.5.1: Cross Bearers maximum stress for LC_05 (200 kip + AW3)

Figure 4.5.1 shows the maximum Von Mises stress concentration at the first cross bearer behind the bolster. It is a very local stress of 49.5 ksi and is below the allowable of 56 ksi.

The allowable stress for the cross bearer for LC_05 is 90% of yield = 62 ksi x 90% = 56 ksi

The calculated FEA maximum stress (figure 4.5.1) = 49.5 ksi

The cross bearer minimum margin of safety = $(56 / 49.5) - 1 = 0.13$

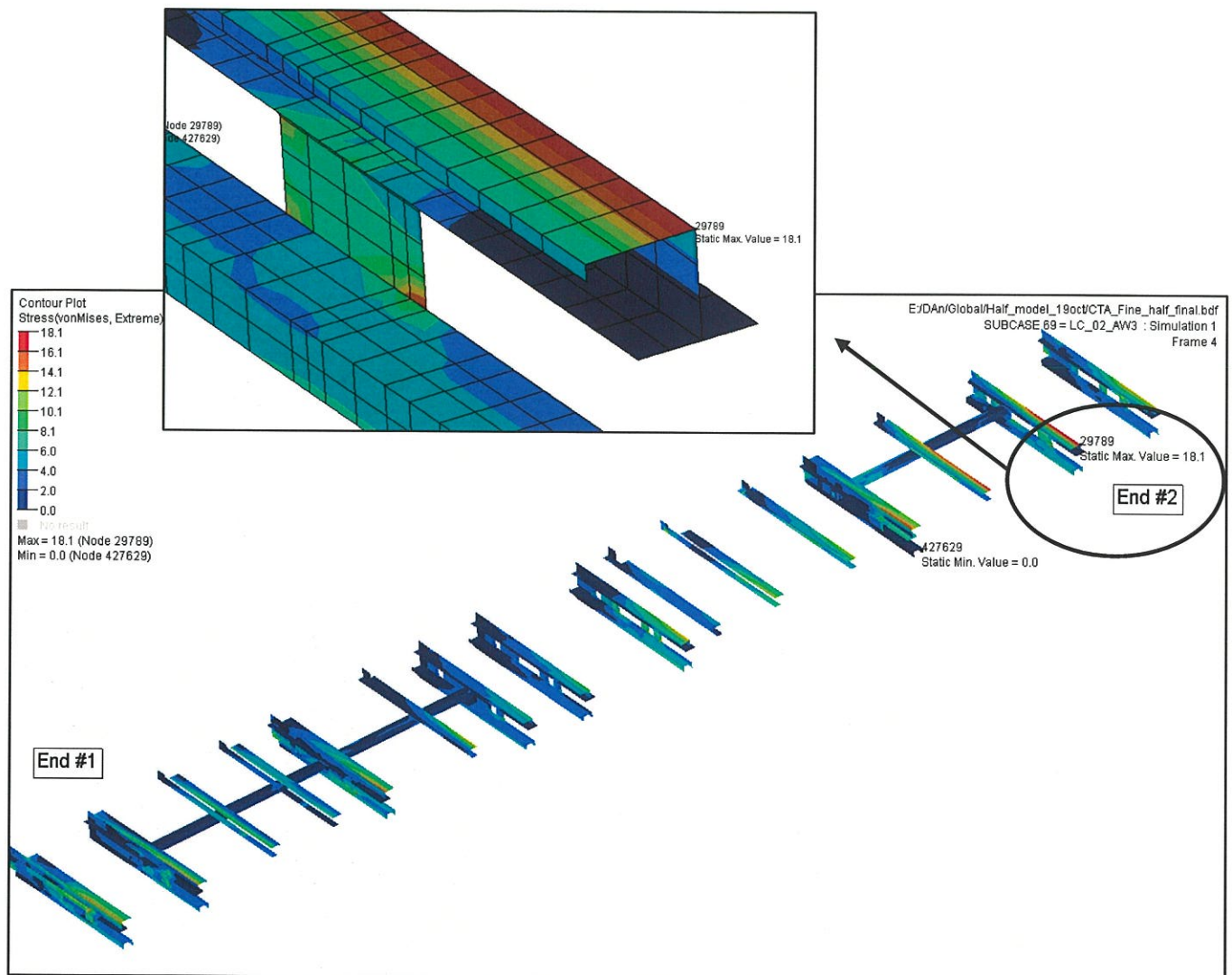


Figure 4.5.2 Cross bearer maximum stress for LC_02 (AW3)

- Figure 4.5.2 shows the nominal Von Mises stress of 18.1 ksi for the most loaded cross bearer. The calculated stress is well below the allowable of 31 ksi. From figure 4.5.2 we can see that the nominal stress in the cross-beam upper flange is only around -12 ksi, hence no buckling verification is required for such a low stress and narrow (compact) flange.

The allowable stress for the cross bearer for LC_02 is 50% of yield = 62 ksi x 50% = 31 ksi

The calculated FEA maximum stress (figure 4.5.2) = 18.1 ksi

The cross bearer minimum margin of safety = $(31 / 18.1) - 1 = 0.7$.

The Central under frame cross beam maximum deflection is verified for load case LC_02 'Maximum vertical load carbody at AW3' the criterion for the cross beam maximum deflection is equal to the beam span / 250 (ref. 1, Stress plan, table 1). As shown in Figure 4.5.3, the relative deflection of the cross bearer with respect to the side sill is calculated below:

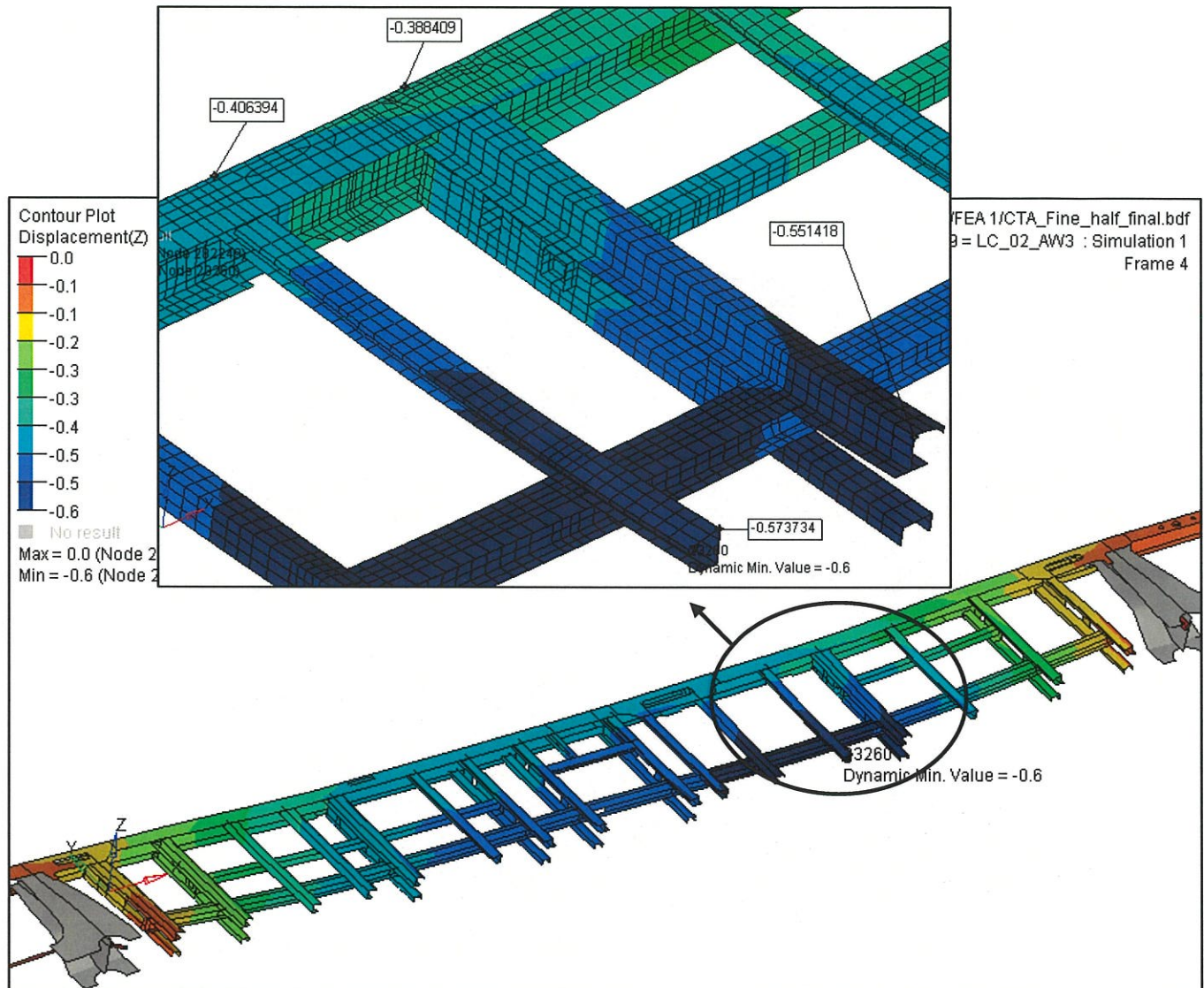


Figure 4.5.3: Cross Bearer maximum deflection for LC_02 (AW3)

Allowed cross beam deflection = span / 250 = 103 in / 250 = 0.412 in

Absolute FEA deflection of cross bearer web = -0.574 in

Absolute FEA deflection of the side sill in line with the cross beam web = -0.406 in

Relative deflection of the cross bearer = (-0.574) - (-0.406) = -0.17 in

The cross beam deflection (0.17 in) is a lot less than the allowed deflection of 0.412 in.

4.6 Main Air Duct:

The main air duct is the other main structural member of the central underframe. It has a limited structural role with respect to the main carbody structure (end-underframe, side sills ect...); however, it will be verified for stress concentrations since it will follow the general deflections of the structure with respect to the different load cases.

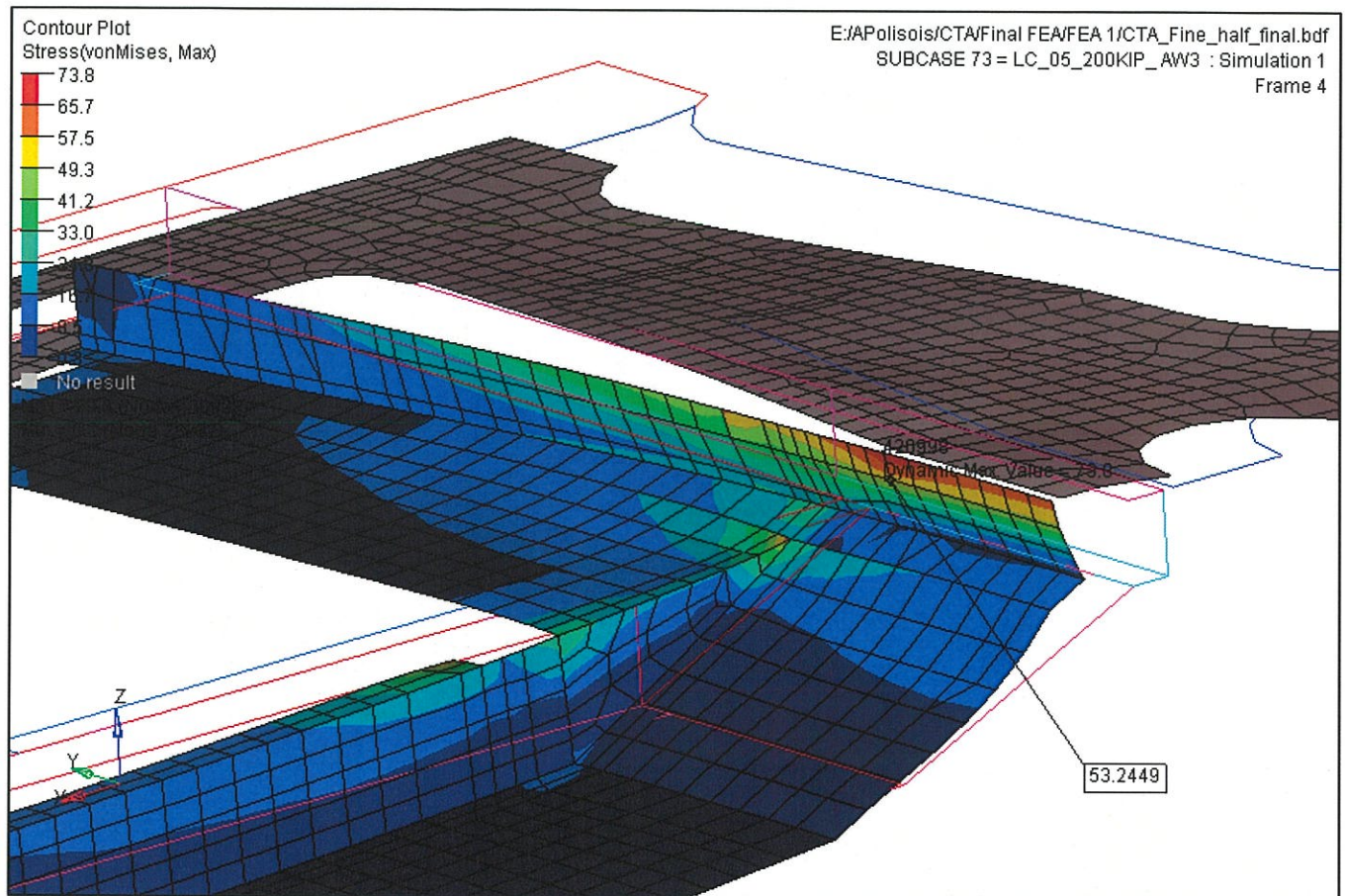


Figure 4.6.1: Main air duct maximum stress for LC_05 (200 kip + AW3)

Figure 4.6.1 shows the maximum Von Mises stress concentration at the air duct right behind the bolster top plate. The deformations are exaggerated in the plot to show the FEA secondary effect of having the main air duct connected to the bolster top plate through the plymetal. In reality the plymetal is not connected to the main air duct. The next closest node stress value of 53.3 ksi is more representative of a nominal stress in the region.

The allowable stress for the main air duct for LC_05 is 90% of yield = 62 ksi x 90% = 56 ksi

The calculated FEA maximum stress (figure 4.5.1) = 53.3 ksi

The main air duct minimum margin of safety for LC_05 = $(56 / 53.3) - 1 = 0.05$

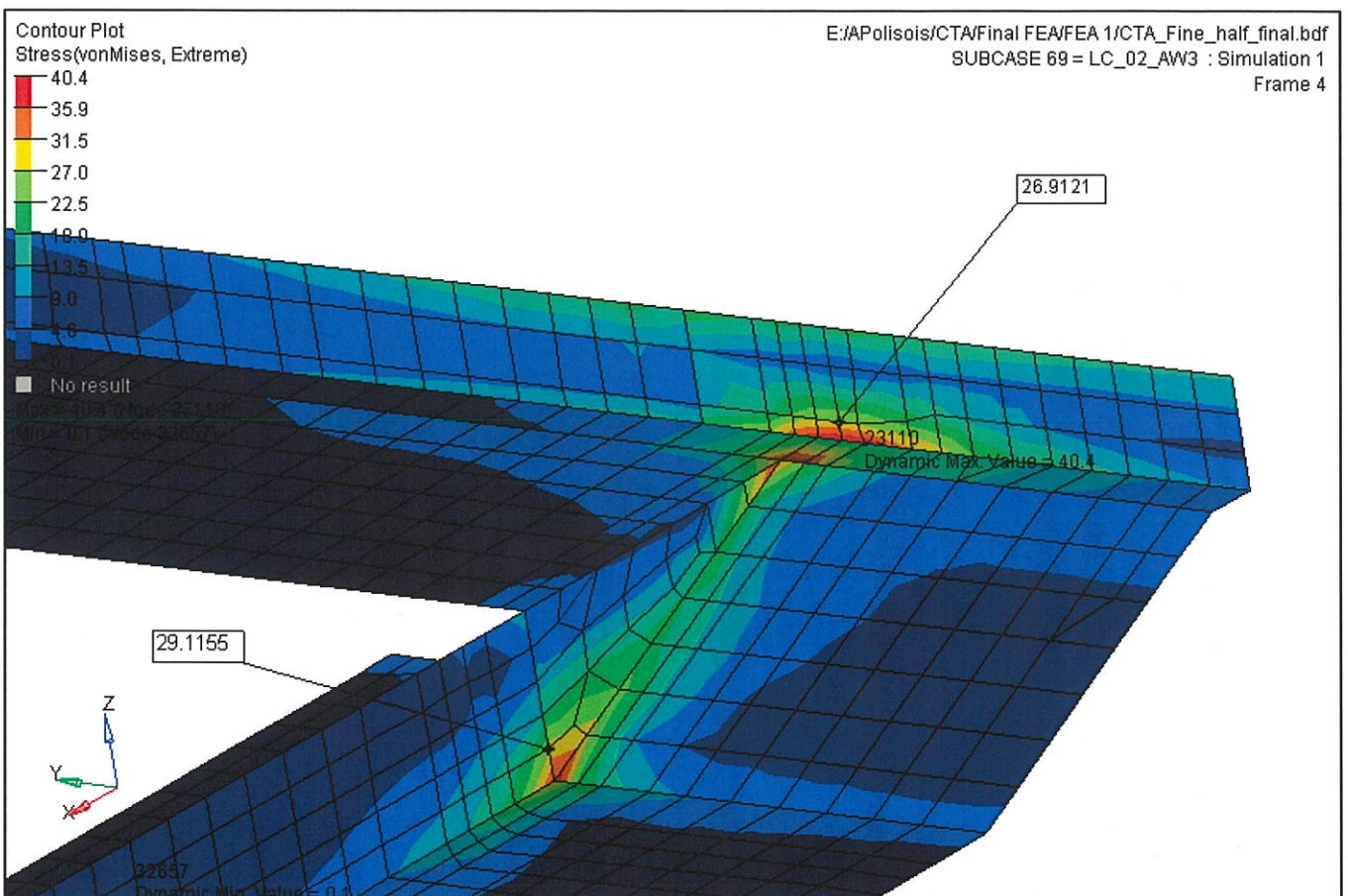


Figure 4.6.2 Main air duct maximum stress for LC_02 (AW3)

- Figure 4.6.2 shows a maximum Von Mises stress concentration of 40.4 ksi for LC_02 at the main air duct. The next closest node stress value of 29.1 ksi is more representative of a nominal stress in that area.

The allowable stress for the main air duct for LC_02 is 50% of yield = 62 ksi x 50% = 31 ksi

The calculated FEA maximum stress (figure 4.6.2) = 29.1 ksi

The main air duct minimum margin of safety for LC_02 = $(31 / 29.1) - 1 = 0.07$

4.7 Side Frame:

Von Mises stresses and main component stresses are reviewed for the side frame for all load cases. Results are presented for LC_02 'Vertical load at AW3', LC_05 'Compressive end load of 200 kip at AW3' and LC_10, 'Jacking for rerailing'. The allowable stresses for these load cases are 50% of yield for LC_02, and 90% of yield for LC_05 and yield for LC_10.

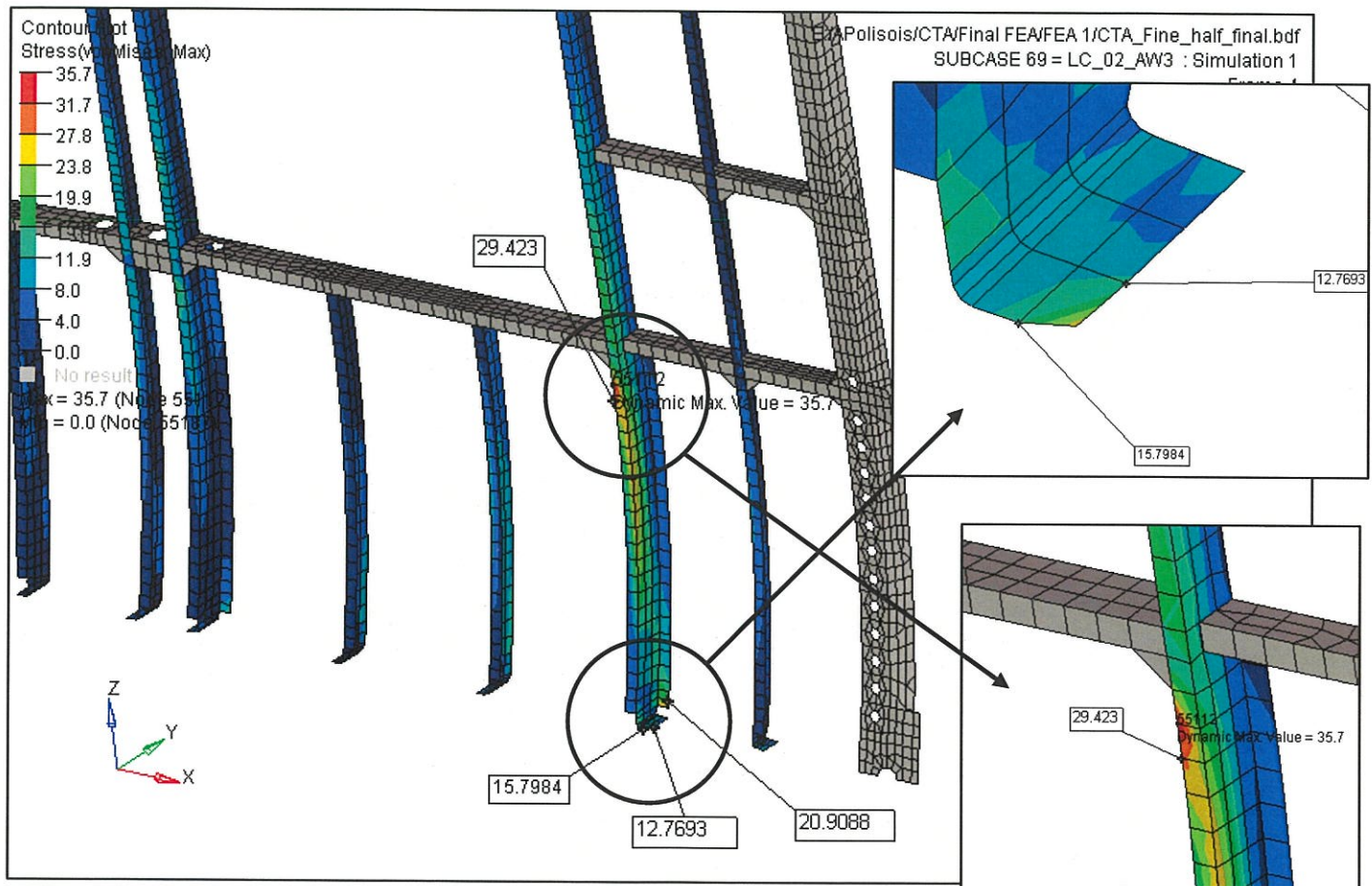


Figure 4.7.1:Side frame (posts) maximum stress for LC_02 (AW3)

Figure 4.7.1 shows the maximum Von Mises stress of 29.4 ksi at the second post behind the door frame. The close up also shows the stresses at the post clip connection with the side sill with a stress around 15.8 ksi.

The allowable stress for the post for LC_02 is 50% of yield = 62 ksi x 50% = 31 ksi

The calculated FEA maximum stress (figure 4.7.1) = 29.4 ksi

The side post minimum margin of safety for LC_02 = $(31 / 29.4) - 1 = 0.05$

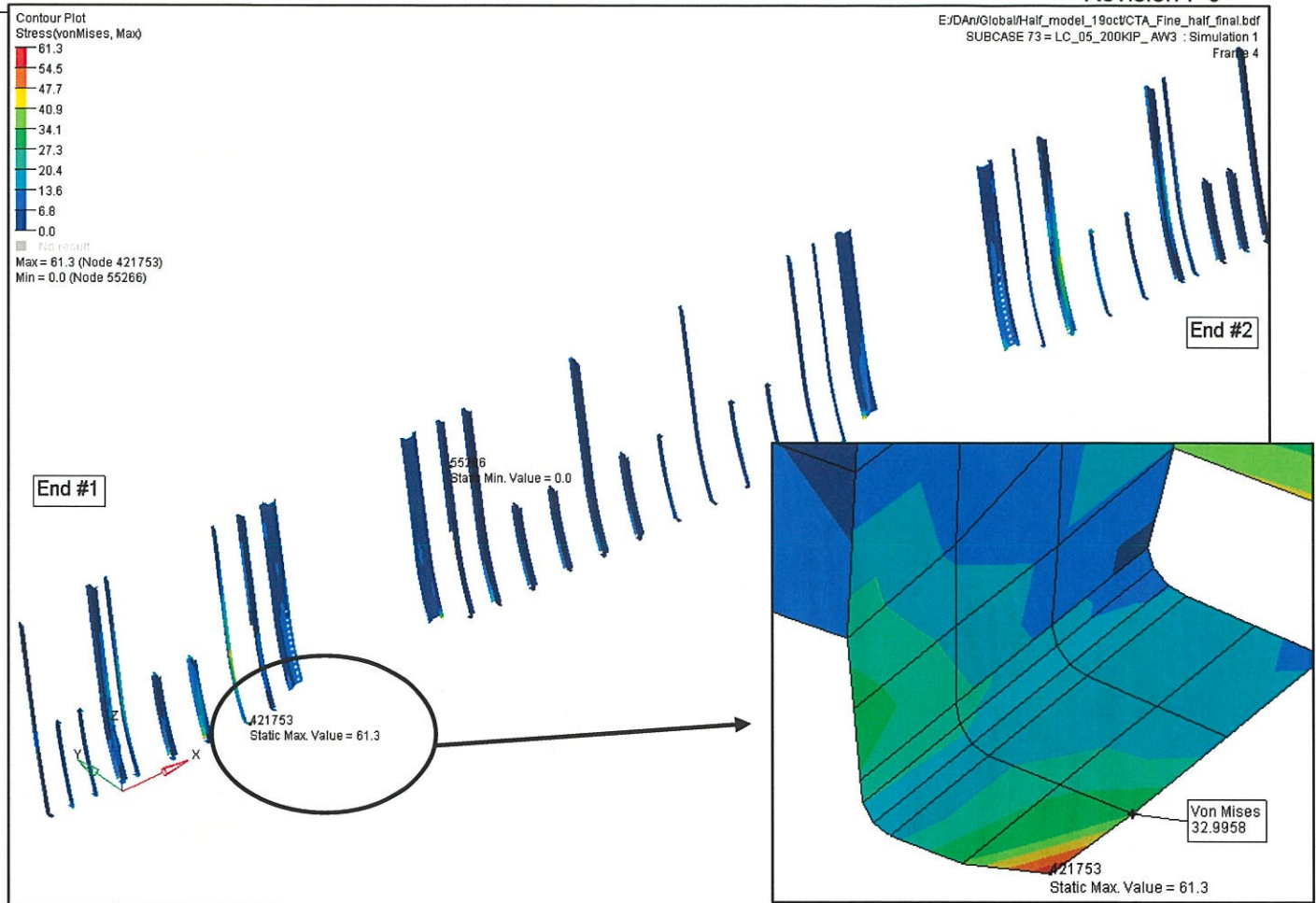


Figure 4.7.2:Side frame (posts) maximum stress for LC_05 (200 kip + AW3)

Figure 4.7.2 shows the maximum Von Mises stress of 33 ksi at the bottom clip (0.125 in thick, SS201 ¼ hard) of the second post behind the door frame.

The allowable stress for the post clip for LC_05 is 90% of yield = 62 ksi x 90% = 56 ksi

The calculated FEA maximum stress (figure 4.7.2) = 33 ksi

The side post minimum margin of safety for LC_05 = $(56 / 33) - 1 = 0.7$

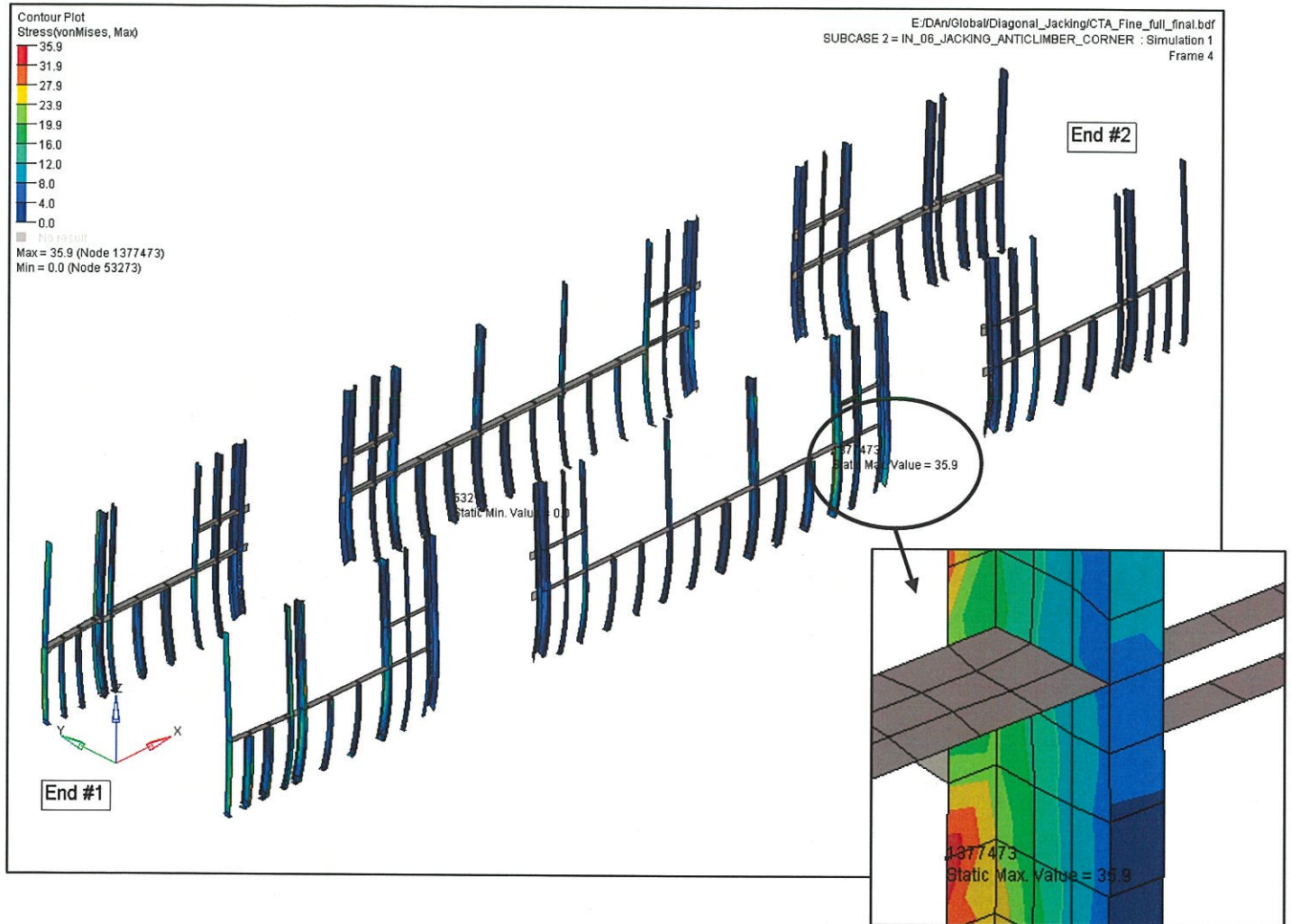


Figure 4.7.3:Side frame (posts) maximum stress for LC_10 (jacking for re-railing)

Figure 4.7.3 shows the maximum Von Mises stress of 35.9 ksi.

The allowable stress for the post clip for LC_10 is yield = 62 ksi.

The calculated FEA maximum stress (figure 4.7.3) = 35.9 ksi

The side post minimum margin of safety for LC_10 = $(62 / 35.9) - 1 = 0.72$.

4.8 Side Sheets & Side Corrugation:

Von Mises stresses and main component stresses are reviewed for the side sheets & side corrugation for all load cases. Results are presented for LC_02 'Vertical load at AW3', LC_05 'Compressive end load of 200 kip at AW3' and LC_10, 'Jacking for re-railing'. The allowable stresses for these load cases are 50% of yield for LC_02, and 90% of yield for LC_05 and yield for LC_10.

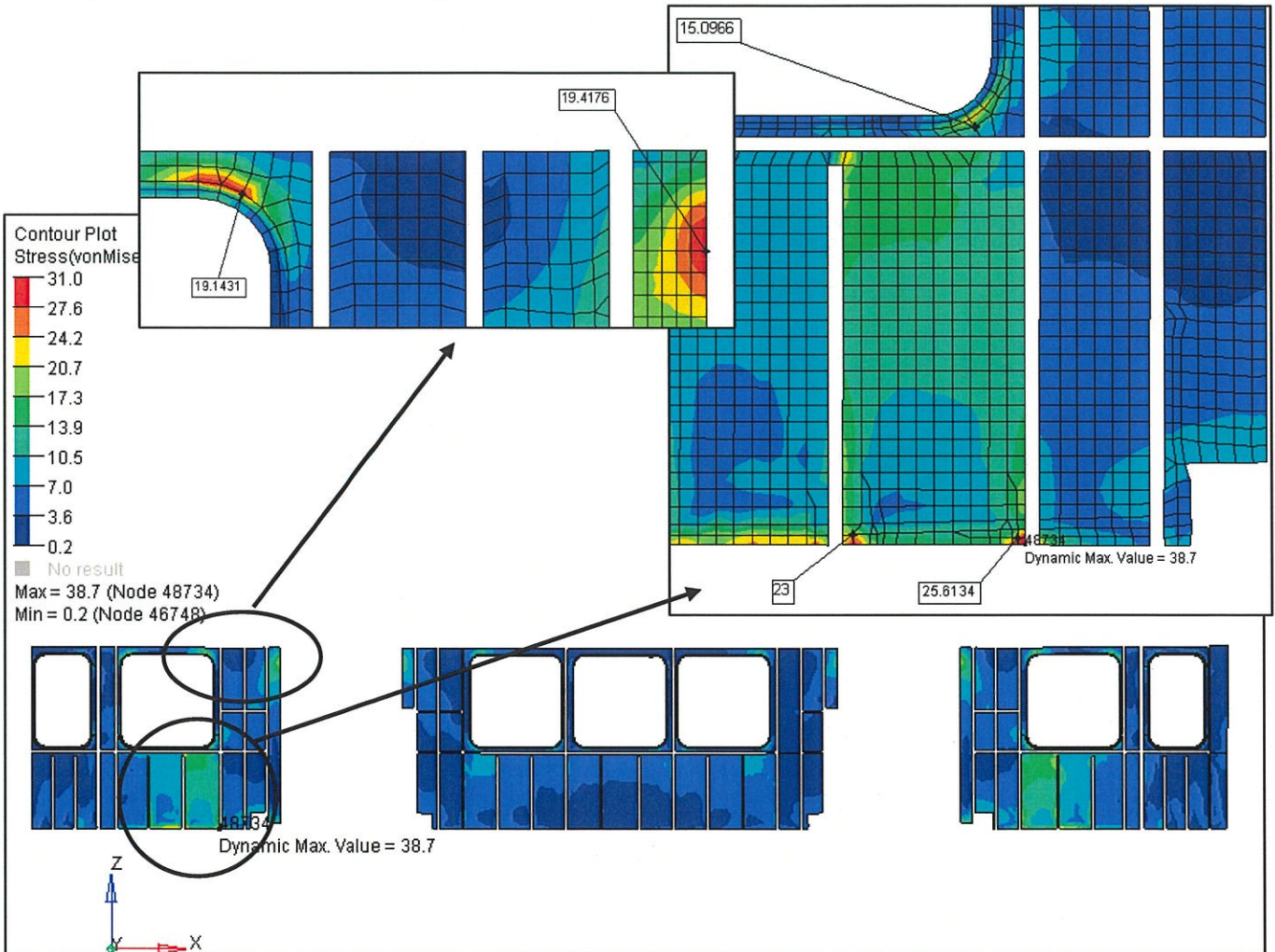


Figure 4.8.1: Side sheets & corrugation maximum stress for LC_02 (AW3)

Figure 4.8.1 shows a maximum Von Mises stress concentration of 38.7 ksi for LC_02 at the side corrugation. The next closest node stress value of 25.6 ksi is more representative of a nominal stress at that corner. The max. stress for the deadlight top skin is 19.4 ksi.

The allowable stress for the corrugation for LC_02 is 50% of yield = 62 ksi x 50% = 31 ksi

The allowable stress for the deadlight skin for LC_02 is 50% of yield = 50 ksi x 50% = 25 ksi

The calculated FEA maximum stress (figure 4.8.1) = 25.6 ksi

The side skin minimum margin of safety for LC_02 = $(31 / 25.6) - 1 = 0.21$

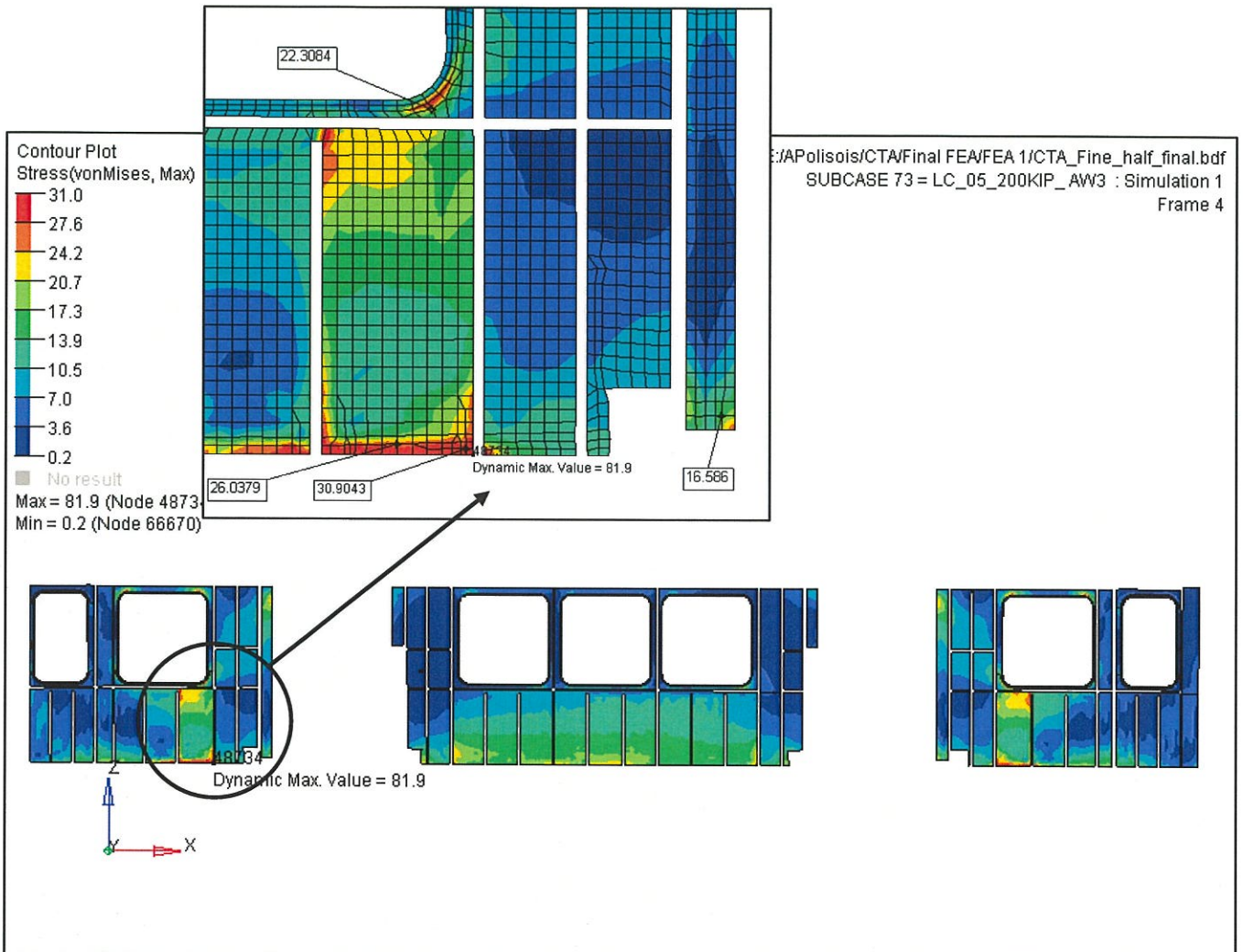


Figure 4.8.2: Side skin & corrugation maximum stress for LC_05 (200 kip + AW3)

Figure 4.8.2 shows the maximum Von Mises stress of 30.9 ksi at the bottom of the corrugation close to the second post behind the door frame.

The allowable stress for LC_05 is 90% of yield = 62 ksi x 90% = 56 ksi

The calculated FFA maximum stress (figure 4.8.2) = 30.9 ksi

The side skin minimum margin of safety for LC_05 = $(56 / 30.9) - 1 = 0.8$.

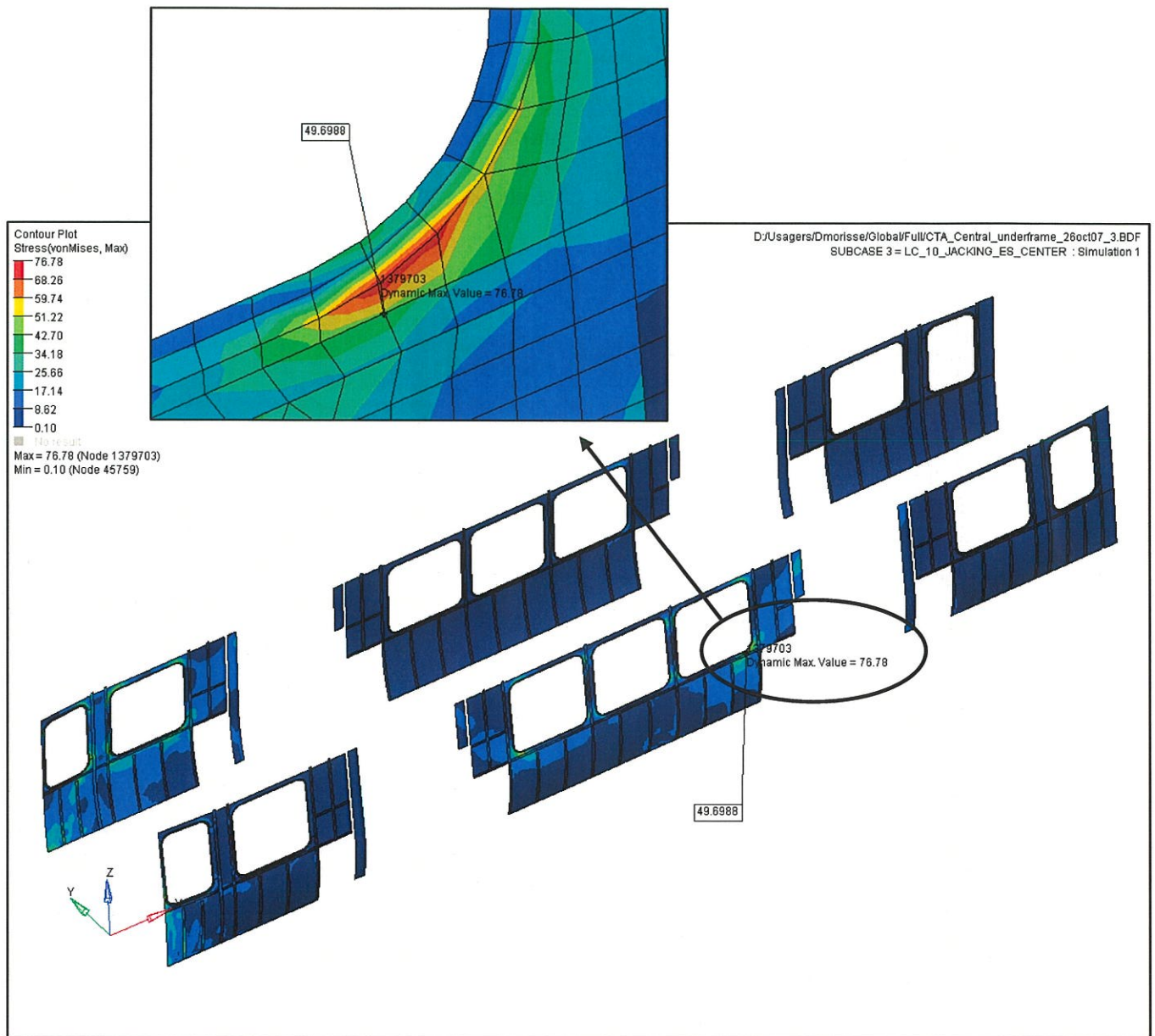


Figure 4.8.3: Side skin & corrugation maximum stress for LC_10 (jacking for re-railing)

Figure 4.8.3 shows the maximum Von Mises stress of 49.7 ksi at the window corner.

The allowable stress for the skin at the window frame for LC_10 is yield (deadlight) = 50 ksi

The calculated FEA maximum stress (figure 4.8.3) = 49.7 ksi

The side skin minimum margin of safety for LC_10 = $(50 / 49.7) - 1 = 0.01$

4.9 Door Frame:

Von Mises stresses and main component stresses are reviewed for the door posts and door mask for all load cases. Results are presented for LC_02 'Vertical load at AW3', LC_05 'Compressive end load of 200 kip at AW3' and LC_03, 'Vertical Fatigue'. The allowable stresses for these load cases are 50% of yield for LC_02, and 90% of yield for LC_05 Fatigue stresses for the door frame LC_03 will be reviewed as per AWS (ref. 3) in section 4.13.

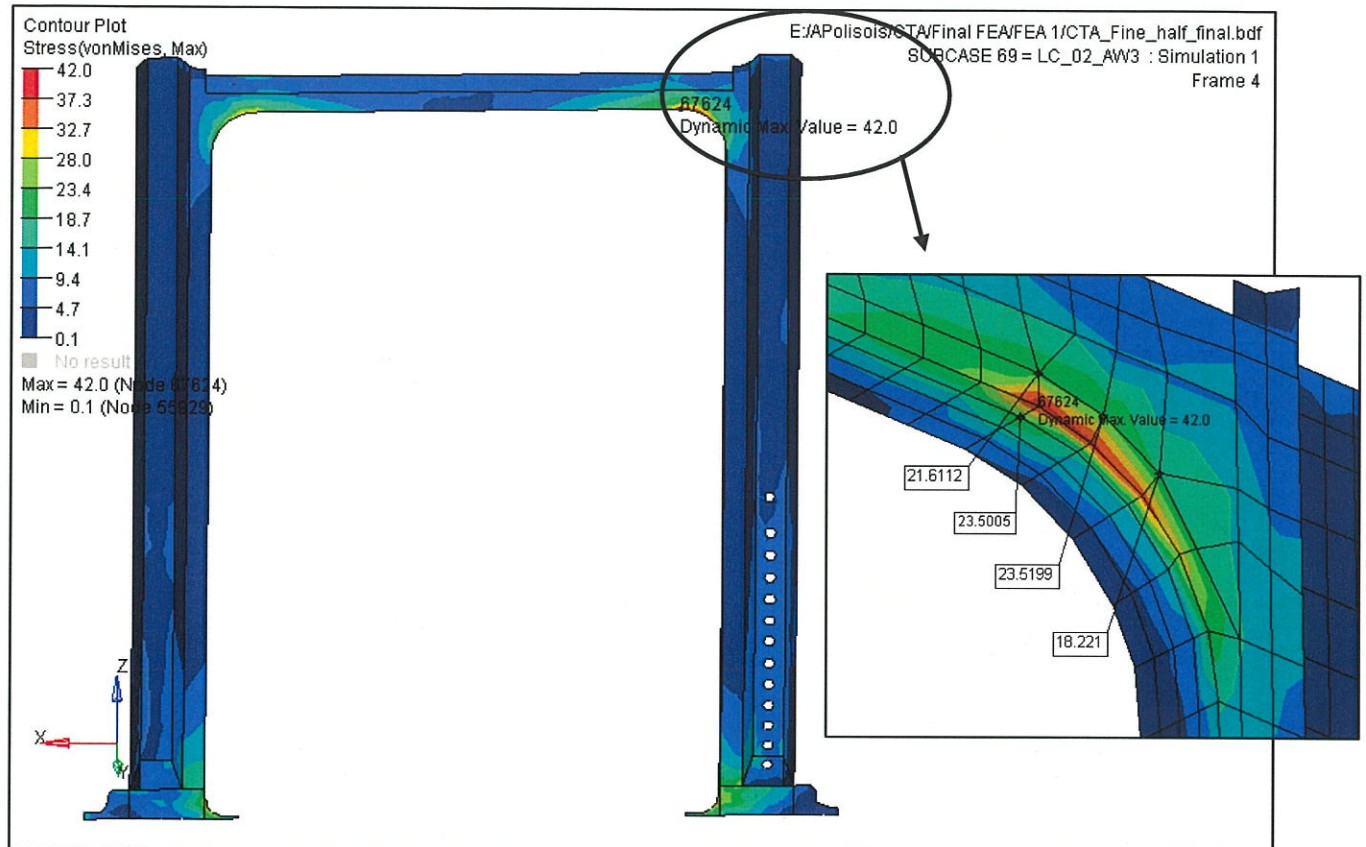


Figure 4.9.1: Door frame & door mask maximum stress for LC_02 (AW3)

Figure 4.9.1 shows a maximum Von Mises stress concentration of 42 ksi for LC_02 at the upper corner of the door mask. In the FEA there is a sharp corner which creates a high stress concentration, in reality there is a radius formed at this region. The next closest node stress value of 23.5 ksi is more representative of a nominal stress in that region.

The allowable stress for LC_02 is 50% of yield = 62 ksi x 50% = 31 ksi

The calculated FEA maximum stress (figure 4.9.1) = 23.5 ksi

The minimum margin of safety for LC_02 = $(31 / 23.5) - 1 = 0.32$

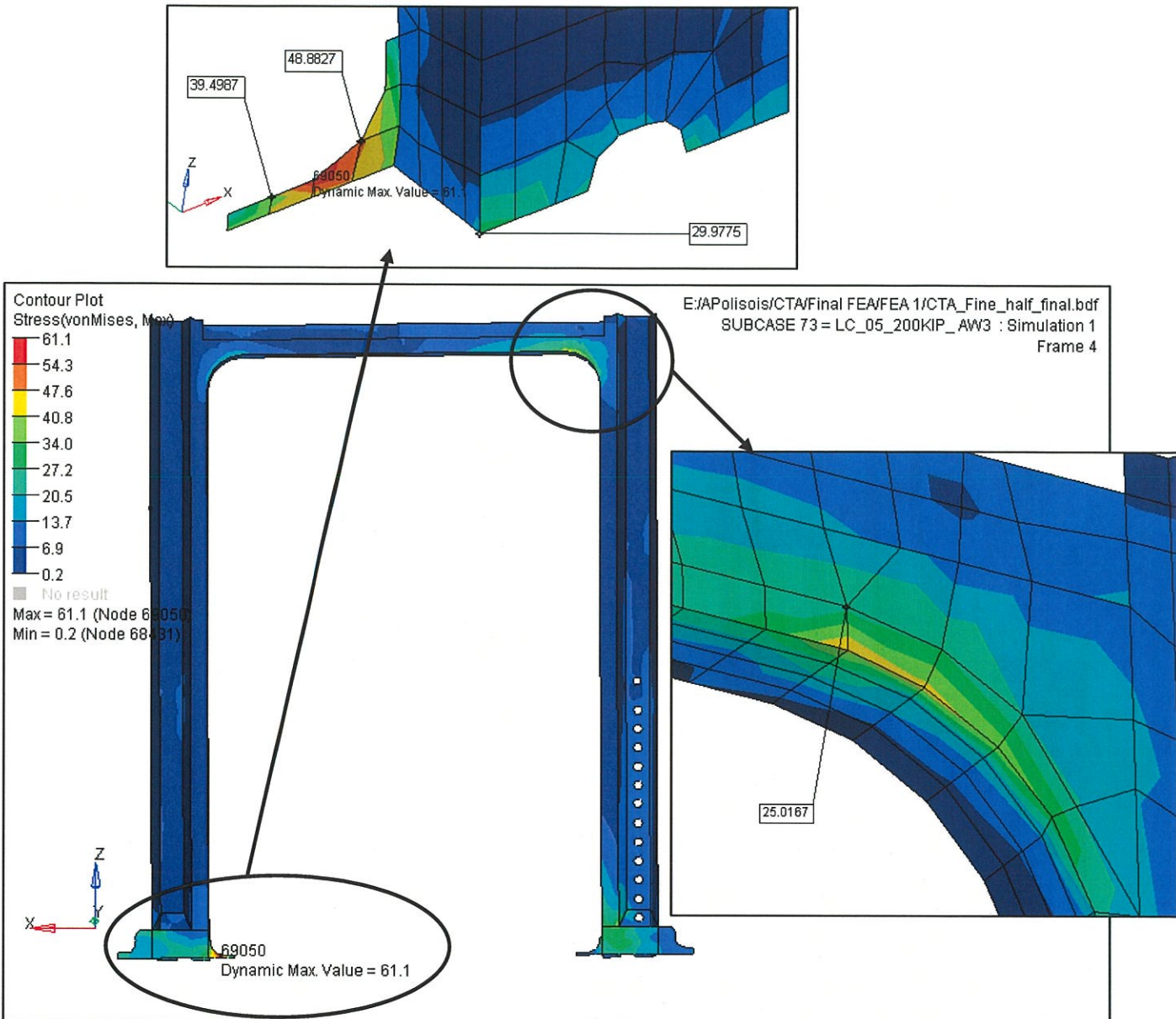


Figure 4.9.2: Door frame & door mask maximum stress for LC_05 (200 kip + AW3)

Figure 4.9.2 shows a maximum Von Mises localized stress concentration of 61.1 ksi for LC_05 at the door frame lower corner/door mask connection with the side. The next closest node stress value of 48.9 ksi is more representative of the stress in that region. The max. stress at the upper corner is around 25.1 ksi which is quite lower than the allowable.

The allowable stress for LC_05 is 90% of yield = 62 ksi x 90% = 56 ksi

The calculated FEA maximum stress (figure 4.9.2) = 48.9 ksi

The minimum margin of safety for LC_05 = $(56 / 48.9) - 1 = 0.15$.

4.10 Belt Rail:

Von Mises stresses are reviewed for the belt rail and horizontal stiffeners for all load cases. Results are presented for LC_02 'Vertical load at AW3', LC_05 'Compressive end load of 200 kip at AW3' and LC_10, 'Jacking for re-railing'. The allowable stresses for these load cases are 50% of yield for LC_02, and 90% of yield for LC_05 and yield for LC_10.

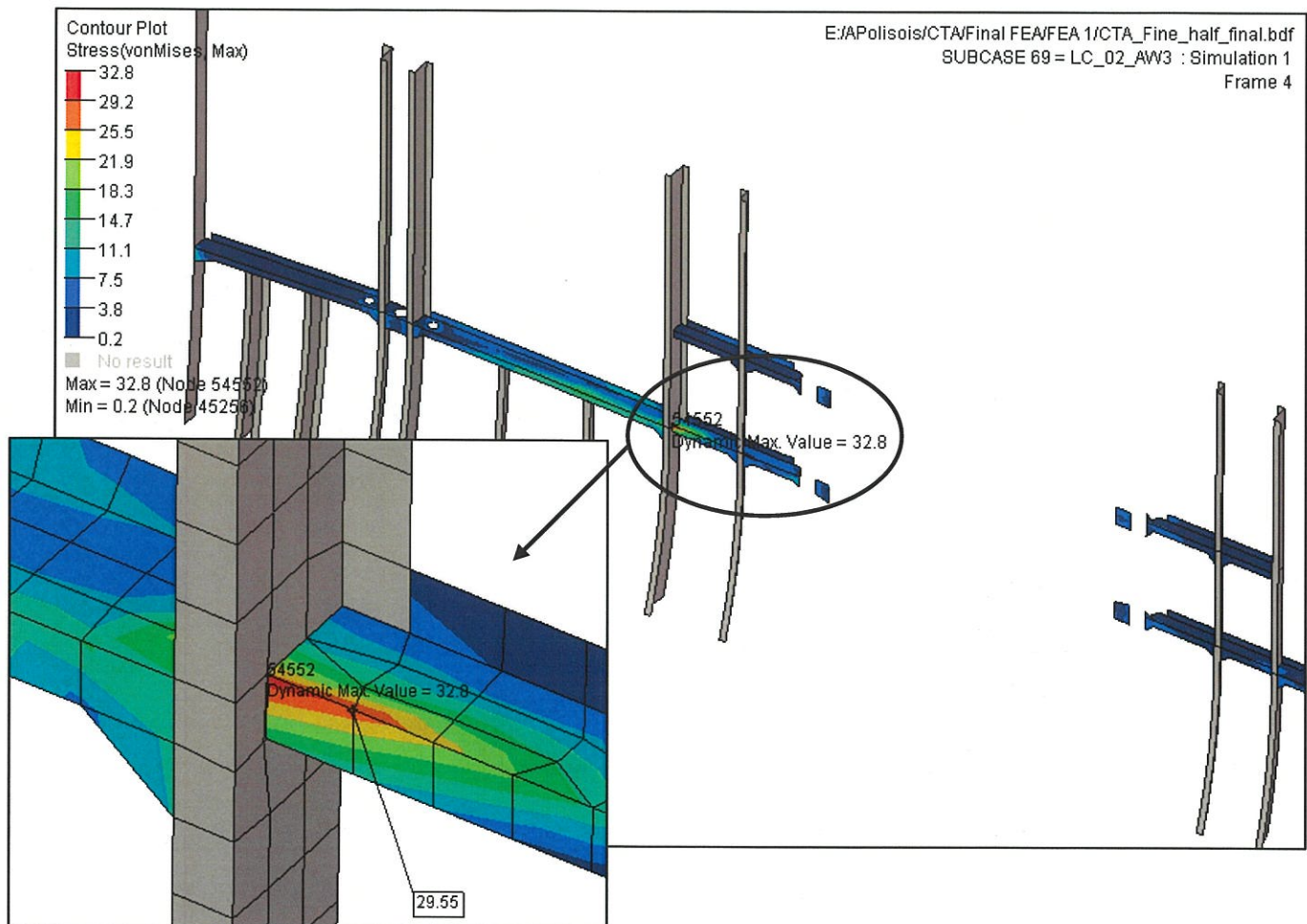


Figure 4.10.1: Belt rail maximum stress for LC_02 (AW3)

Figure 4.10.1 shows a maximum Von Mises stress concentration of 32.8 ksi due to the discontinuity with the rest of the belt rail. This discontinuity is due to the ventilation duct. The next closest node stress value of 29.6 ksi is more representative of a nominal stress in that region.

The allowable stress for LC_02 is 50% of yield = 62 ksi x 50% = 31 ksi

The calculated FEA maximum stress (figure 4.10.1) = 29.6 ksi

The belt rail minimum margin of safety for LC_02 = $(31 / 29.6) - 1 = 0.05$

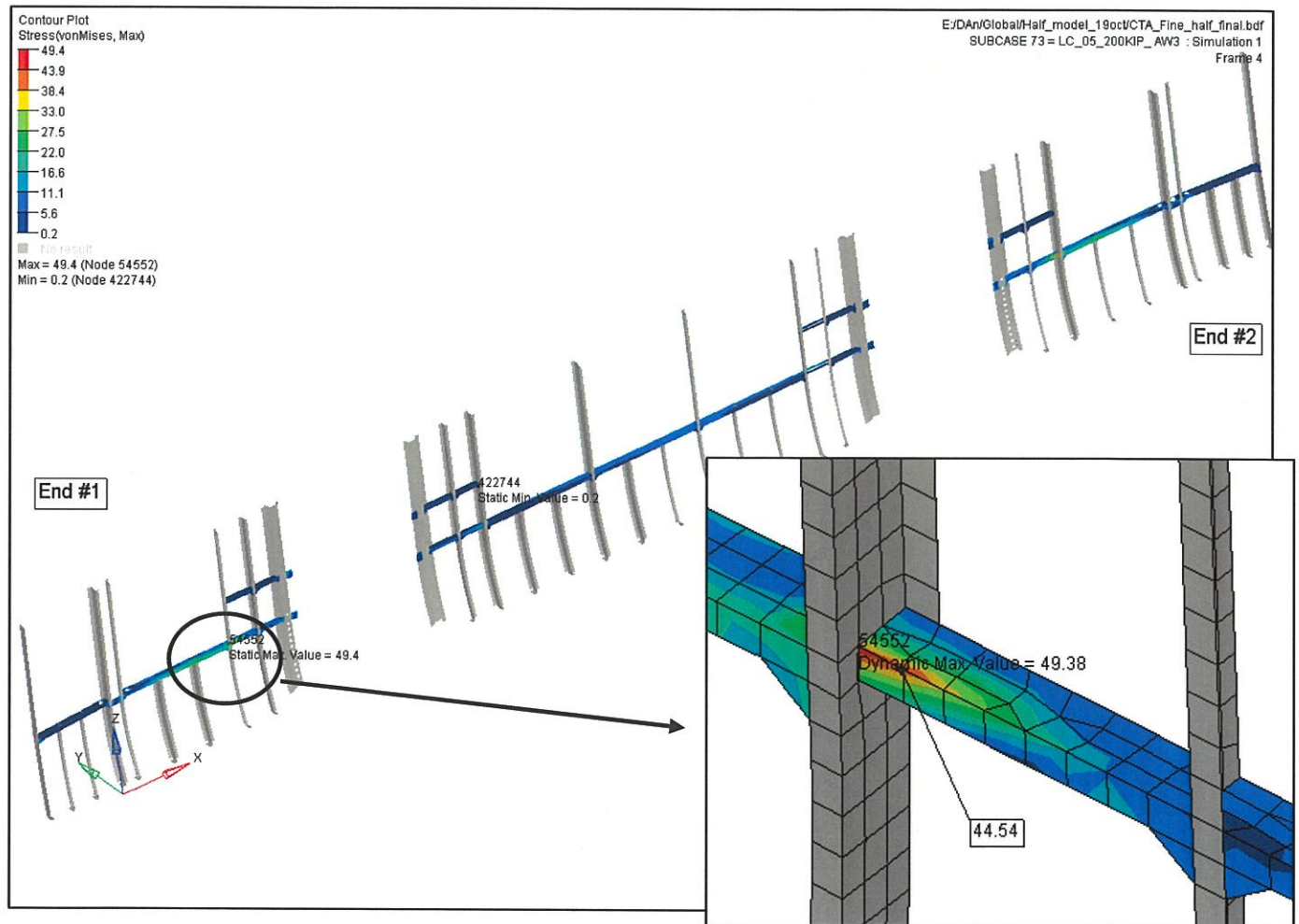


Figure 4.10.2: Belt rail maximum stress for LC_05 (200 kip + AW3)

Figure 4.10.2 shows a maximum Von Mises stress of 44.5 ksi for LC_05 at the smaller belt rail area due to the ventilation duct which is lower than the allowable.

The allowable stress for LC_05 is 90% of yield = 62 ksi x 90% = 56 ksi

The calculated FEA maximum stress (figure 4.10.2) = 44.5 ksi

The belt rail minimum margin of safety for LC_05 = $(56 / 44.5) - 1 = 0.26$

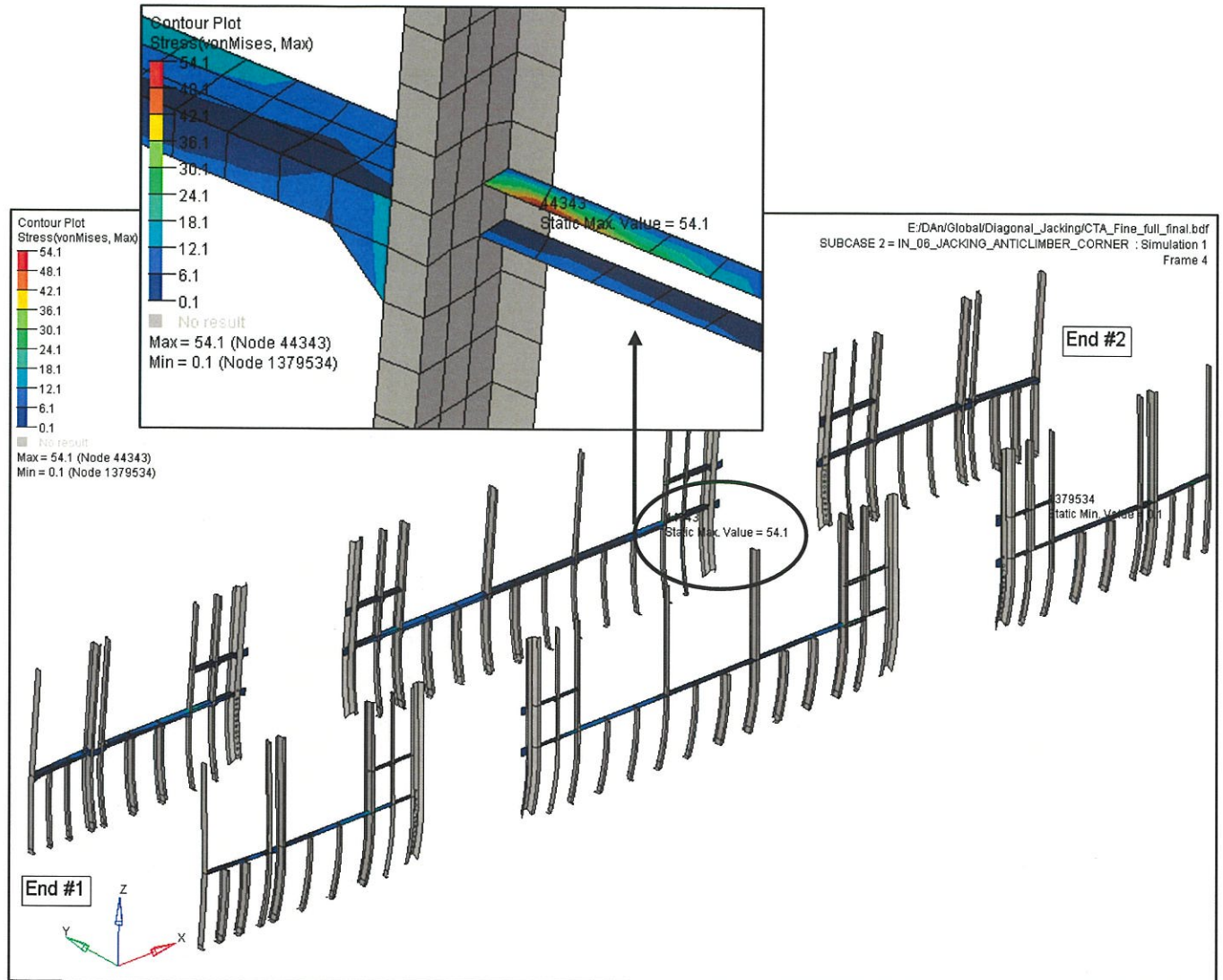


Figure 4.10.3: Belt rail maximum stress for LC_10 (jacking for re-railing)

Figure 4.10.3 shows the maximum Von Mises stress of 54.1 ksi at the small window rail behind the ventilation duct.

The allowable stress for the post clip for LC_10 is yield = 62 ksi

The calculated FEA maximum stress (figure 4.10.3) = 54.1 ksi

The minimum margin of safety for LC_10 = $(62 / 54.1) - 1 = 0.15$

4.11 Roof Rail & AT plate:

Von Mises stresses are reviewed for the roof rail and AT plate for all load cases. Results are presented for LC_02 'Vertical load at AW3', LC_05 'Compressive end load of 200 kip at AW3' and LC_10, 'Jacking for re-railing'. The allowable stresses for these load cases are 50% of yield for LC_02, and 90% of yield for LC_05 and yield for LC_10.

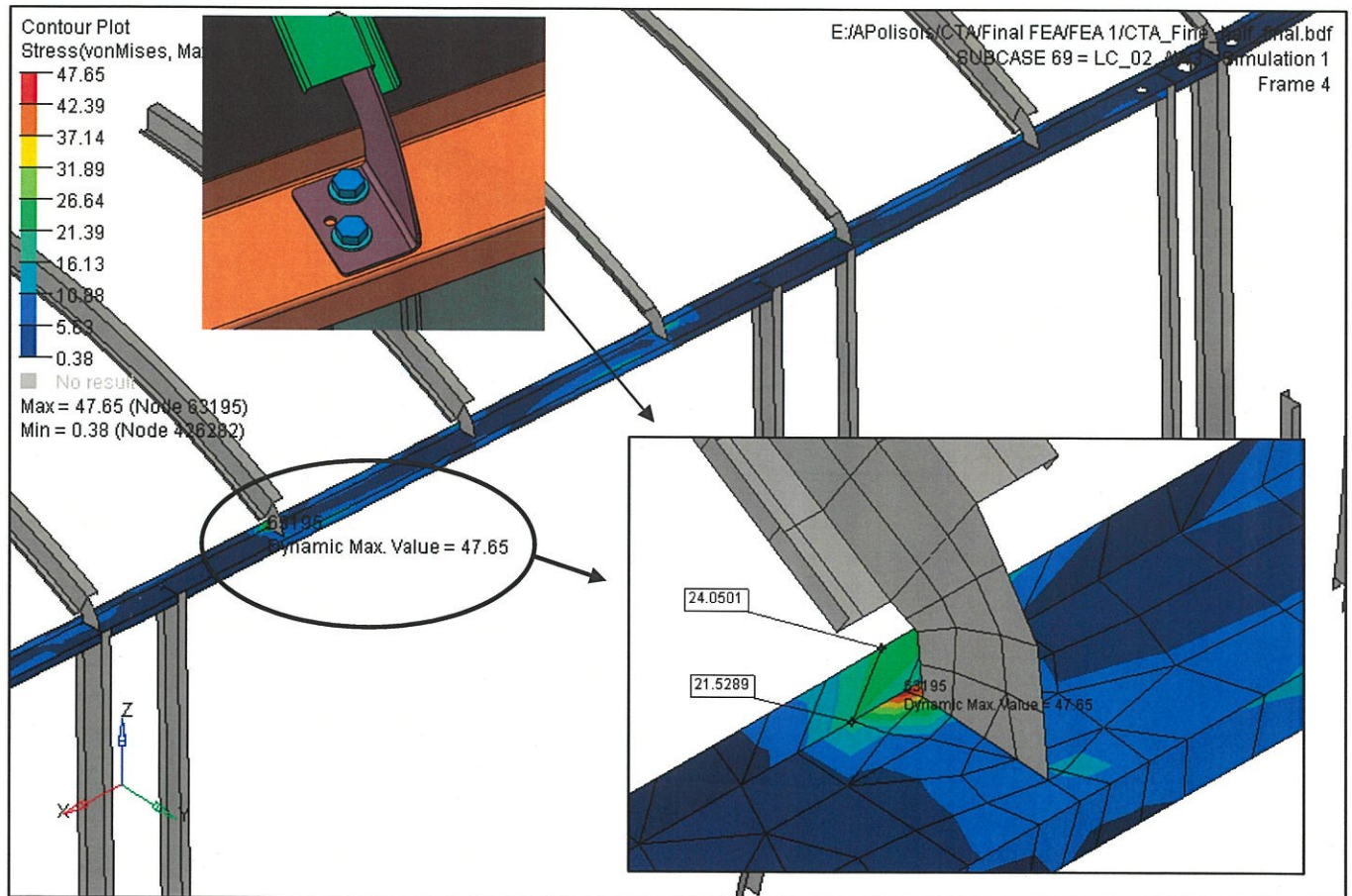


Figure 4.11.1:Roof rail maximum stress for LC_02 (AW3)

Figure 4.11.1 shows a maximum stress of 47.65 ksi in the roof rail. This high stress is principally attributed to high local bending which is due to modeling approximation. for simplicity. In the model, the carline webs are modeled as if they are welded in a T-joint with the roof rail.. In reality, the carline's L-shaped clips are bolted to the roof rail's web (see 3dxml image above). The bolted connection permits more bending flexibility, thus much lower local bending stresses. The next highest stress in the nodes closest to the carline-roof rail junction is 24.1 ksi; this stress value is also affected by local high bending in the region.

The allowable stress for LC_02 is 50% of yield = 62 ksi x 50% = 31 ksi

The calculated FEA maximum stress (figure 4.11.1) = 24.1 ksi

The roof rail minimum margin of safety for LC_02 = $(31 / 24.1) - 1 = 0.28$

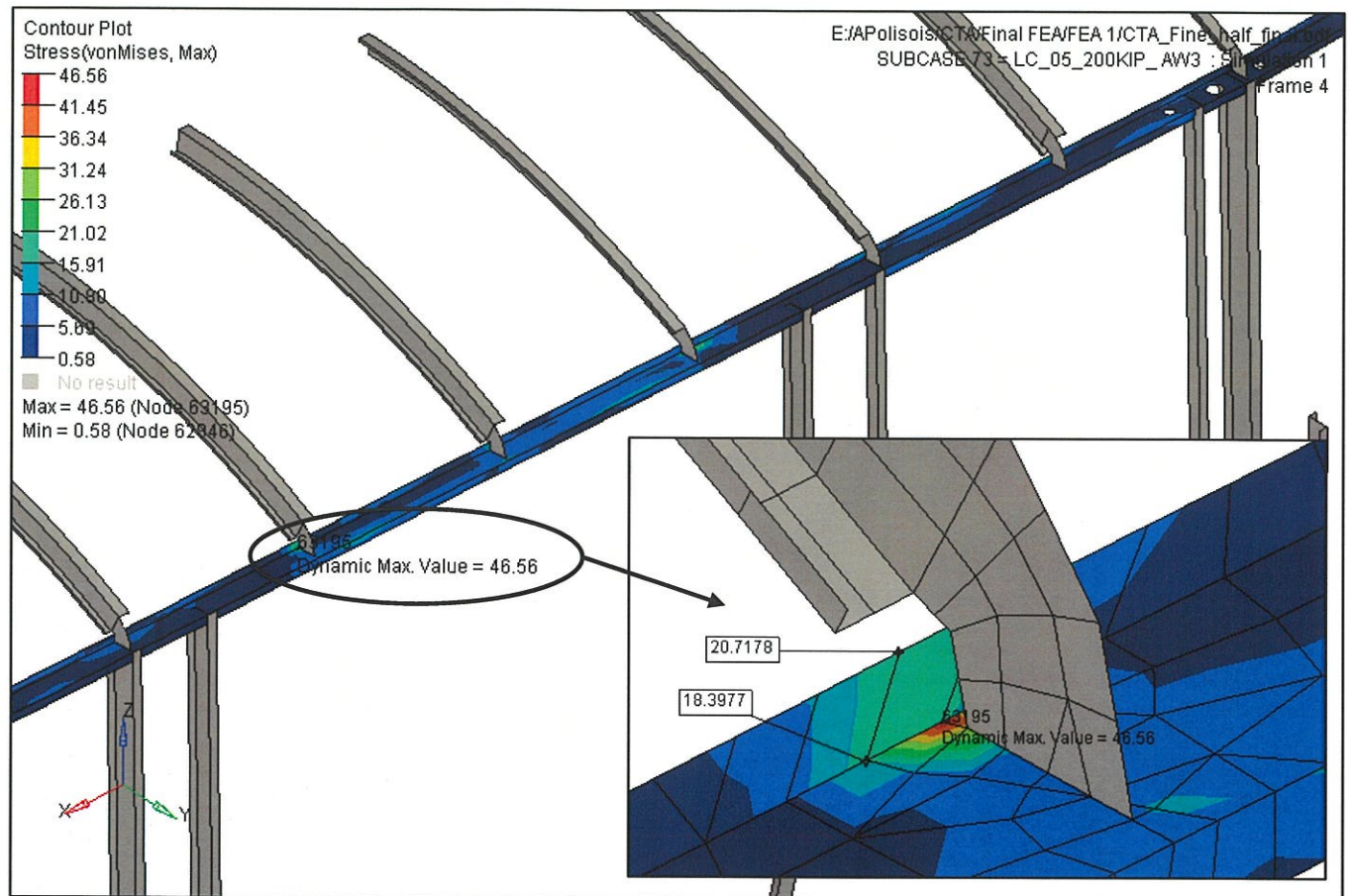


Figure 4.11.2: Roof rail maximum stress for LC_05 (200 kip + AW3)

Figure 4.11.2 shows a maximum Von Mises stress concentration of 46.6 ksi for LC_05 which is already lower than the allowable of 56 ksi. See justification of figure 4.11.1.

The allowable stress for LC_05 is 90% of yield = 62 ksi x 90% = 56 ksi

The calculated FEA maximum stress (figure 4.11.2) = 20.7 ksi

The roof rail minimum margin of safety for LC_05 = $(56 / 20.7) - 1 = 0.7$

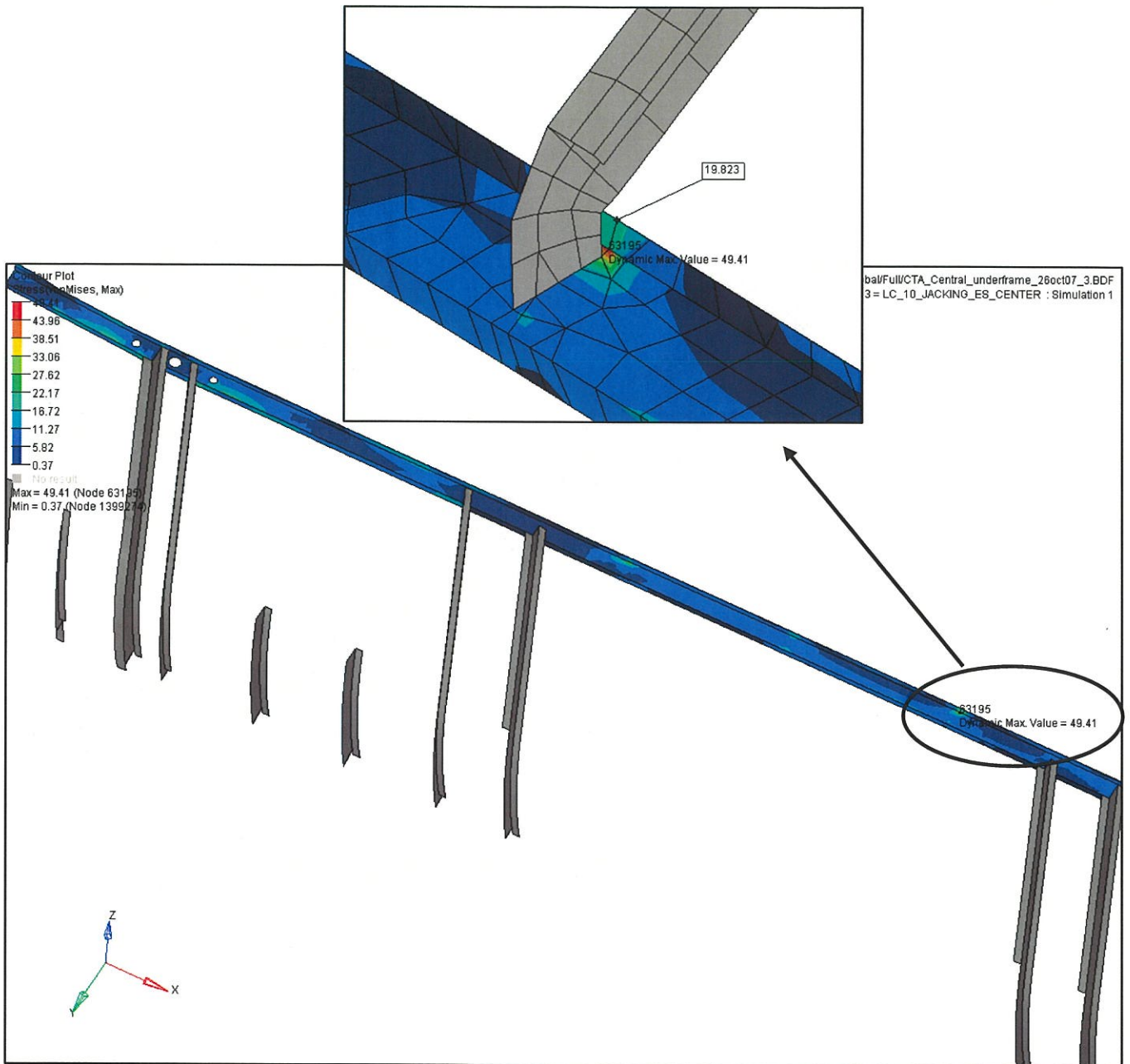


Figure 4.11.3:Roof rail maximum stress for LC_10 (jacking for re-railing)

Figure 4.11.3 shows a Von Mises stress of 19.8 ksi at the roof rail which is much lower than the yield allowable of 62 ksi. See justification of figure 4.11.1.

AT plate:

The AT plate is verified for all load cases. The highest stress is shown for LC_10 (jacking for re-railing).

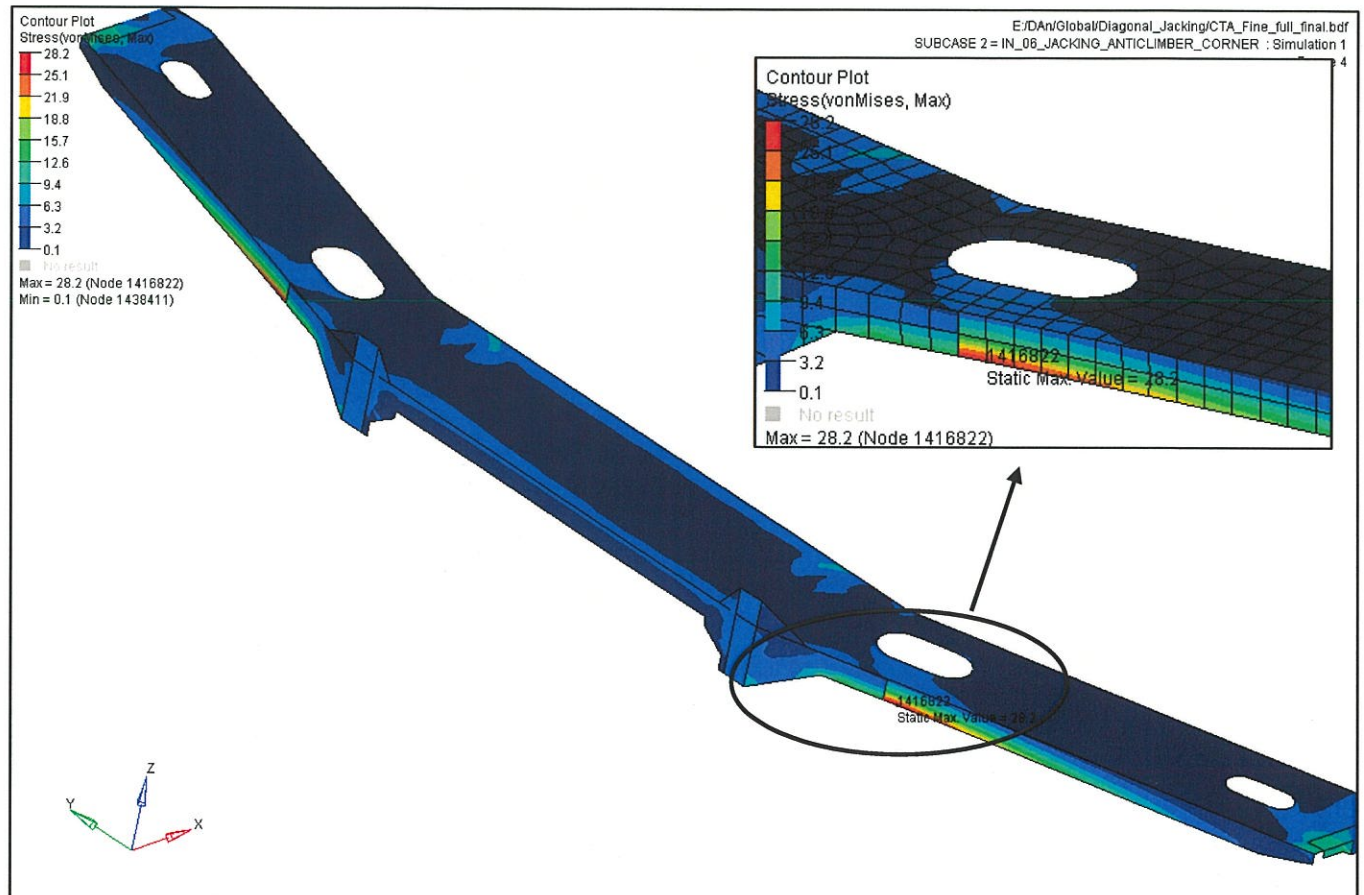


Figure 4.11.4: Roof rail maximum stress for LC_10 (jacking for re-railing)

Figure 4.11.4 shows the maximum Von Mises stress of 28.2 ksi which is lower than the yield allowable of 62 ksi.

The allowable stress for LC10 is yield = 62 ksi

The calculated FEA maximum stress (figure 4.11.4) = 28.2 ksi

The AT plate margin of safety for LC_10 = $(62 / 28.2) - 1 = 1.2$

4.12 Carlines, Roof Gutter and Purlines:

Von Mises stresses are reviewed for the carlines and purlines for all load cases. Results are presented for LC_02 'Vertical load at AW3', LC_05 'Compressive end load of 200 kip at AW3' and LC_10, 'Jacking for re-railing'. The allowable stresses for these load cases are 50% of yield for LC_02, and 90% of yield for LC_05 and yield for LC_10.

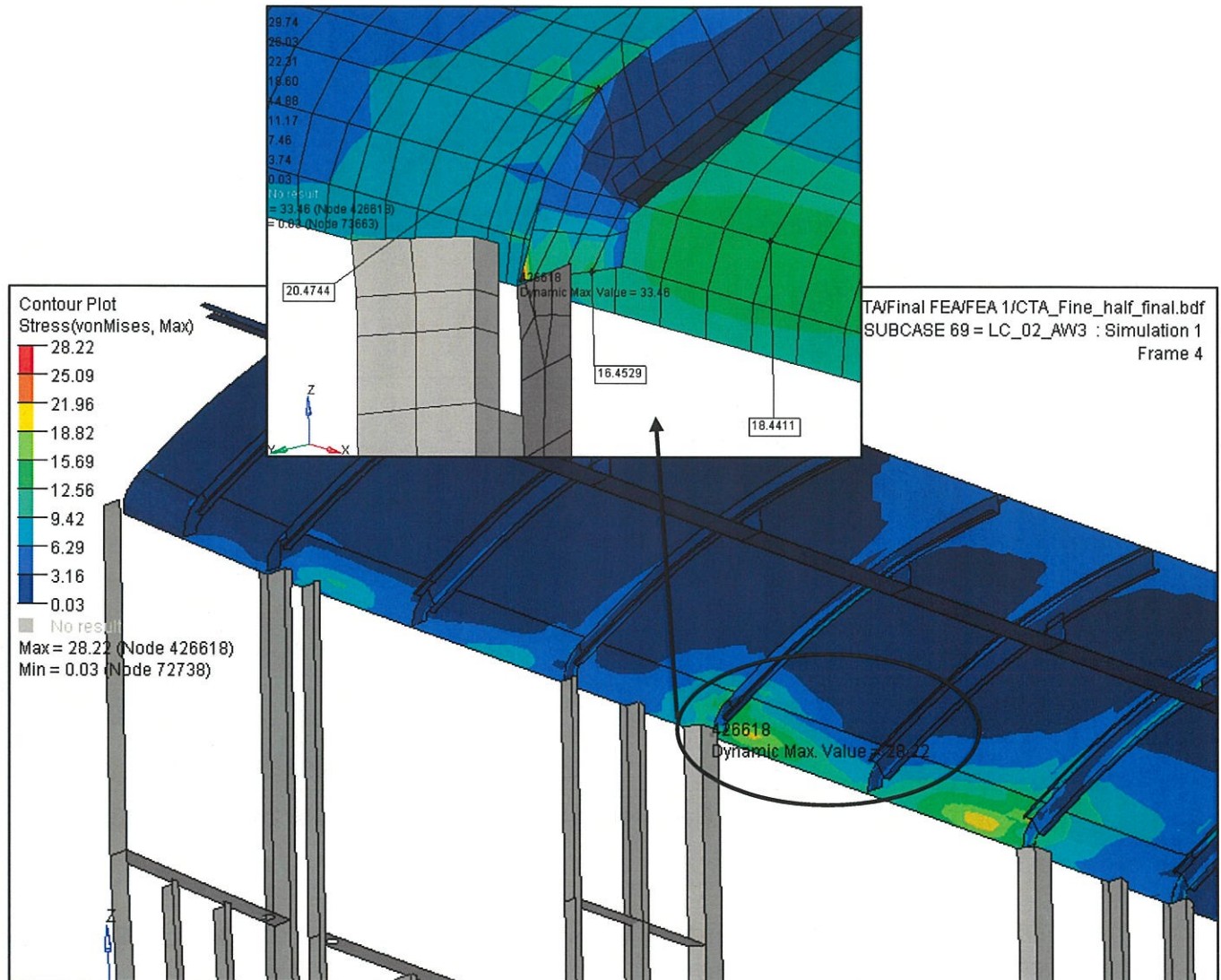


Figure 4.12.1: Carlines clip, roof gutter and roof maximum stress for LC_02 (AW3)

Figure 4.12.1 shows a maximum Von Mises stress concentration of 28.22 ksi which is due to the modeling intersection between the door posts and the clip (See justification of figure 4.11.1). The next closest node stress value of 16.5 ksi is more representative of a nominal stress in that region. The max. stress on the corrugated roof is 20.5 ksi and on the roof gutter is around 20 ksi.

The allowable stress for LC_02 is 50% of yield = 62 ksi x 50% = 31 ksi

The carline minimum margin of safety for LC_02 = $(31 / 16.5) - 1 = 0.8$

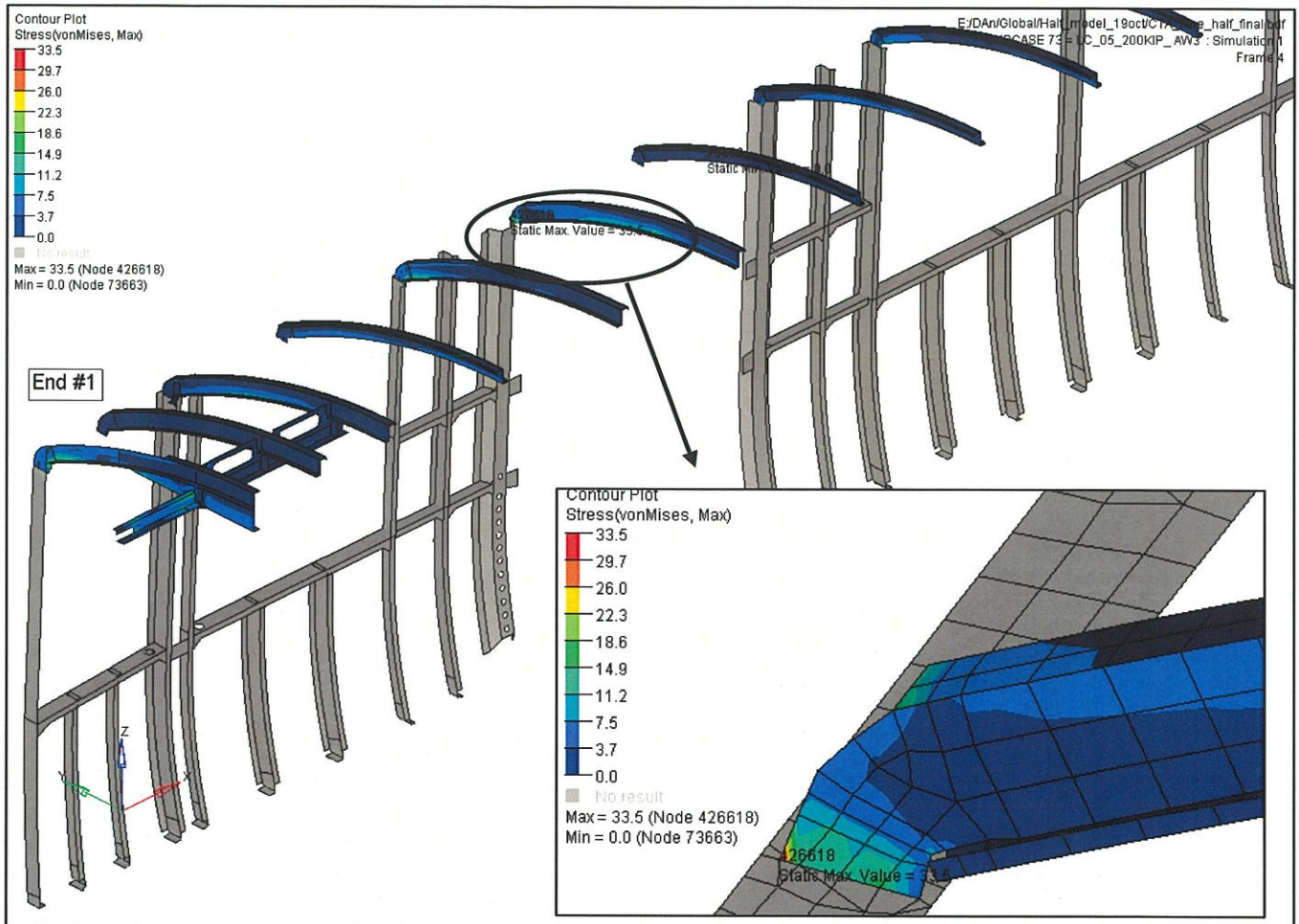


Figure 4.12.2: Carlines maximum stress for LC_05 (200 kip + AW3)

Figure 4.12.2 shows a maximum Von Mises stress concentration of 33.5 ksi for LC_05 which is lower than the allowable of 56 ksi.

The allowable stress for LC_05 is 90% of yield = 62 ksi x 90% = 56 ksi

The carline minimum margin of safety for LC_05 = $(56 / 33.5) - 1 = 0.67$

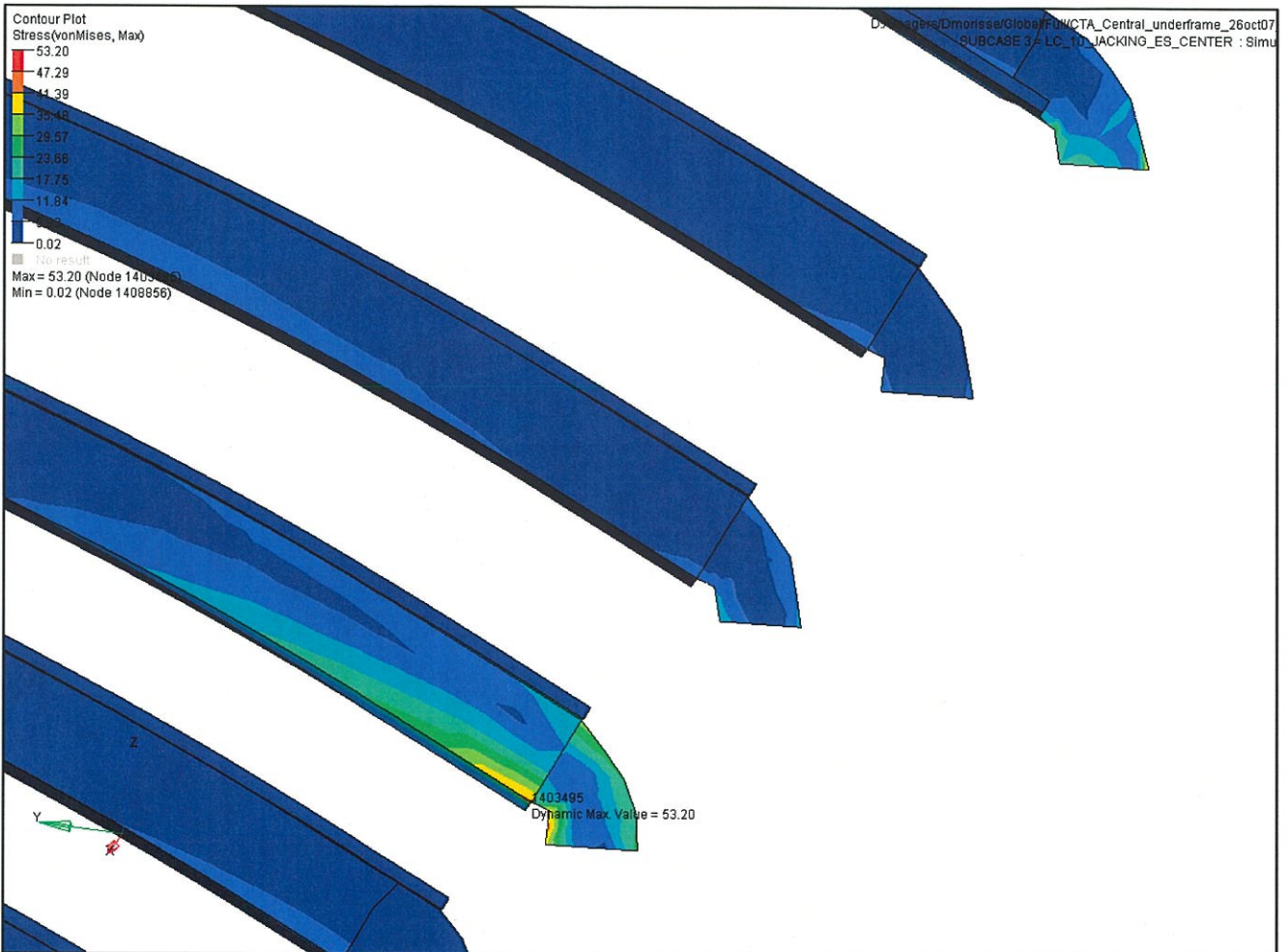


Figure 4.12.3:Carlines maximum stress for LC_10 (jacking for re-railing)

Figure 4.12.3 shows a maximum Von Mises stress concentration of 53.2 ksi for LC_10 which is lower than the allowable of 62 ksi.

The calculated FEA maximum stress (figure 4.12.3) = 53.2 ksi

The minimum margin of safety for LC_10 = $(62 / 53.2) - 1 = 0.17$

The purlines are verified for all load cases. The highest stress is shown for LC_10 (jacking for re-railing).

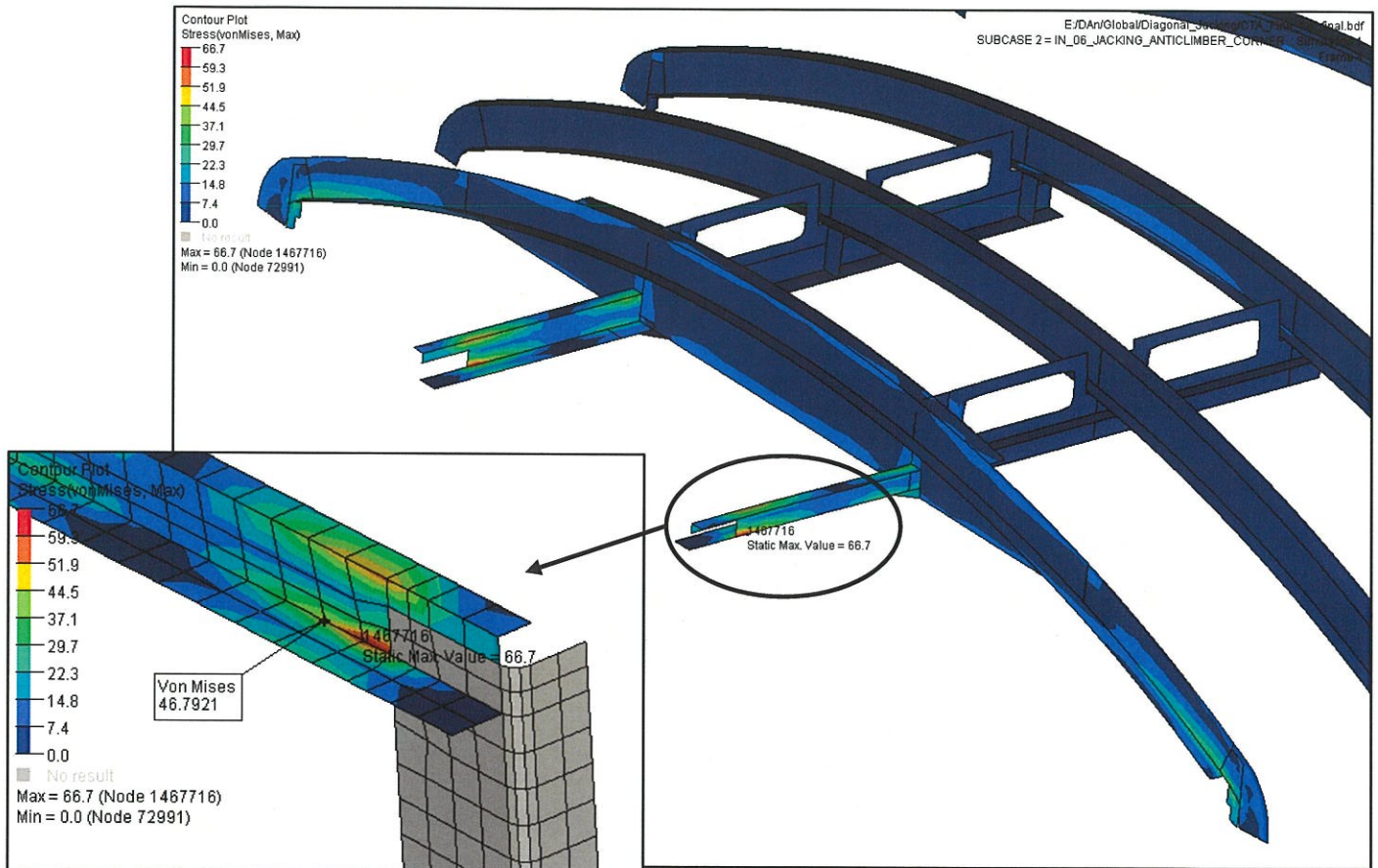


Figure 4.12.4: Purlines maximum stress for LC_10 (jacking for re-railing)

Figure 4.12.4 shows the maximum Von Mises stress of 46.8 ksi which is lower than the yield limit of 75 ksi (in tension).

The allowable stress for LC_10 is yield = 62 ksi.

The purline minimum margin of safety for LC_10 = $(62 / 46.8) - 1 = 0.32$

4.13 Fatigue Considerations:

Weld fatigue is verified for the main structural components that are sensitive to the vertical fatigue load of $\pm 0.15 g$ with 100 passengers in the car as described in LC_03 of ref. 1, hence the stress range is equal to 0.3 times the car weight with 100 passengers (52000 lb).

These components are the bolster, the side sill and the door frame.

Component or principal stresses are verified in the direction or perpendicular to the weld detail depending on the stress and or the weld direction.

Weld fatigue is verified for 10 million cycles as per the American Welding Society recommendations (ref. 2). Depending on the weld detail category the allowable stress range will vary from 24 ksi for a category 'A' to 4.5 ksi for a category 'E' weld (see table 3.1, the table was copied below for convenience).

Weld Category	Weld category summary description	Allowable Stress range (ksi)
A	Base metal	24
B	Continuous CJP or built up fillet welds	16
C	Continuous fillet weld or discontinuity in CJP weld	10
E	Discontinuity in fillet weld or plug welds	4.5
F	Shear in throat of weld	8

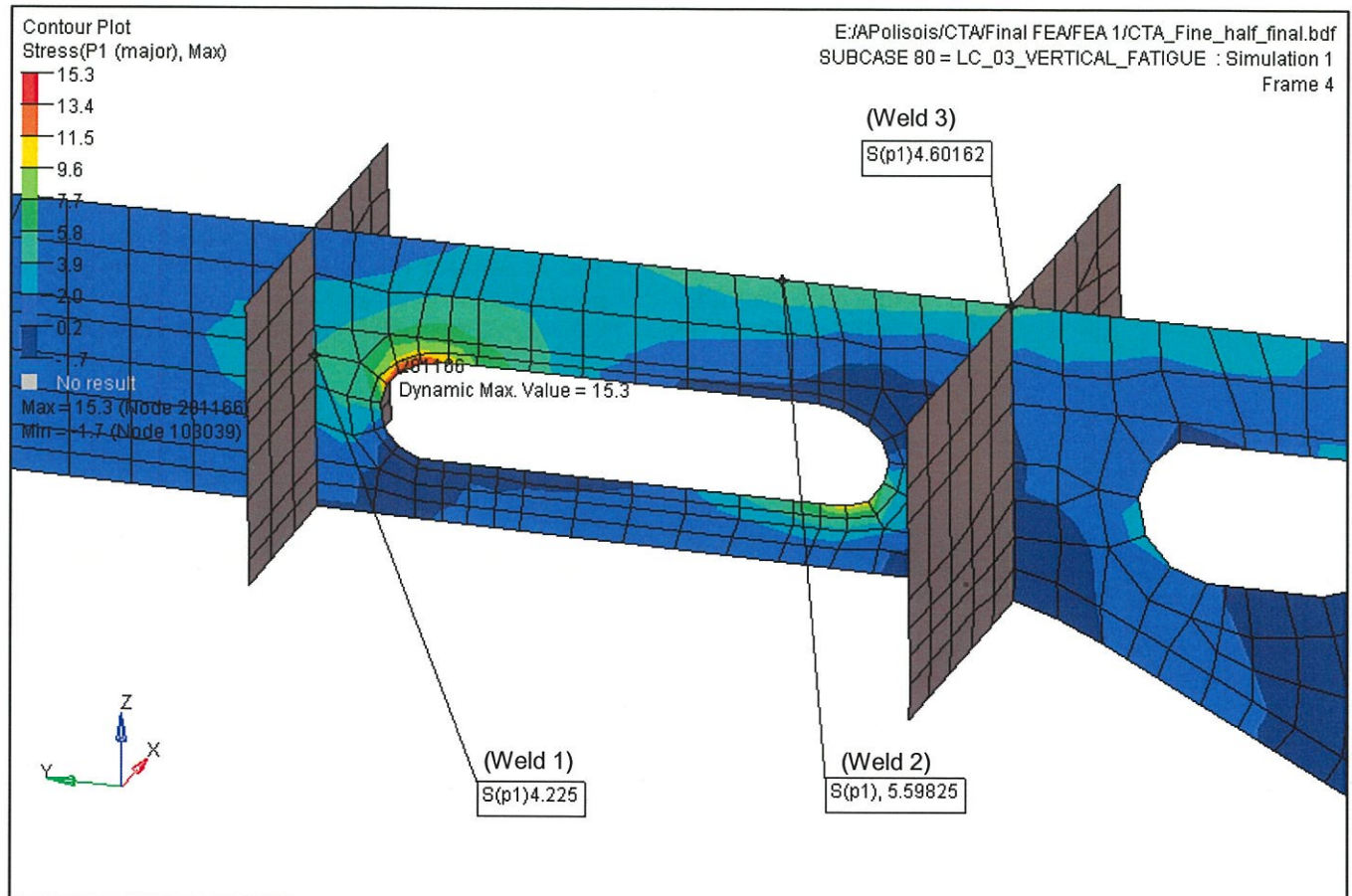
Bolster:

Figure 4.13.1 Bolster web principal (p1) stress range for LC_03

- Figure 4.13.1 shows the main principal stress of the bolster web. The maximum stress is at the hole opening. This is considered as a class “A” weld with an allowable stress range of 24 ksi.
- Welds 1 and 3 are considered as class “C” welds with an allowable stress range of 10 ksi.
- Weld 2 is considered as a class “B” weld with an allowable stress range of 16 ksi.

The smallest margin of safety (weld 3) = $(10 / 4.6) - 1 = 1.17$

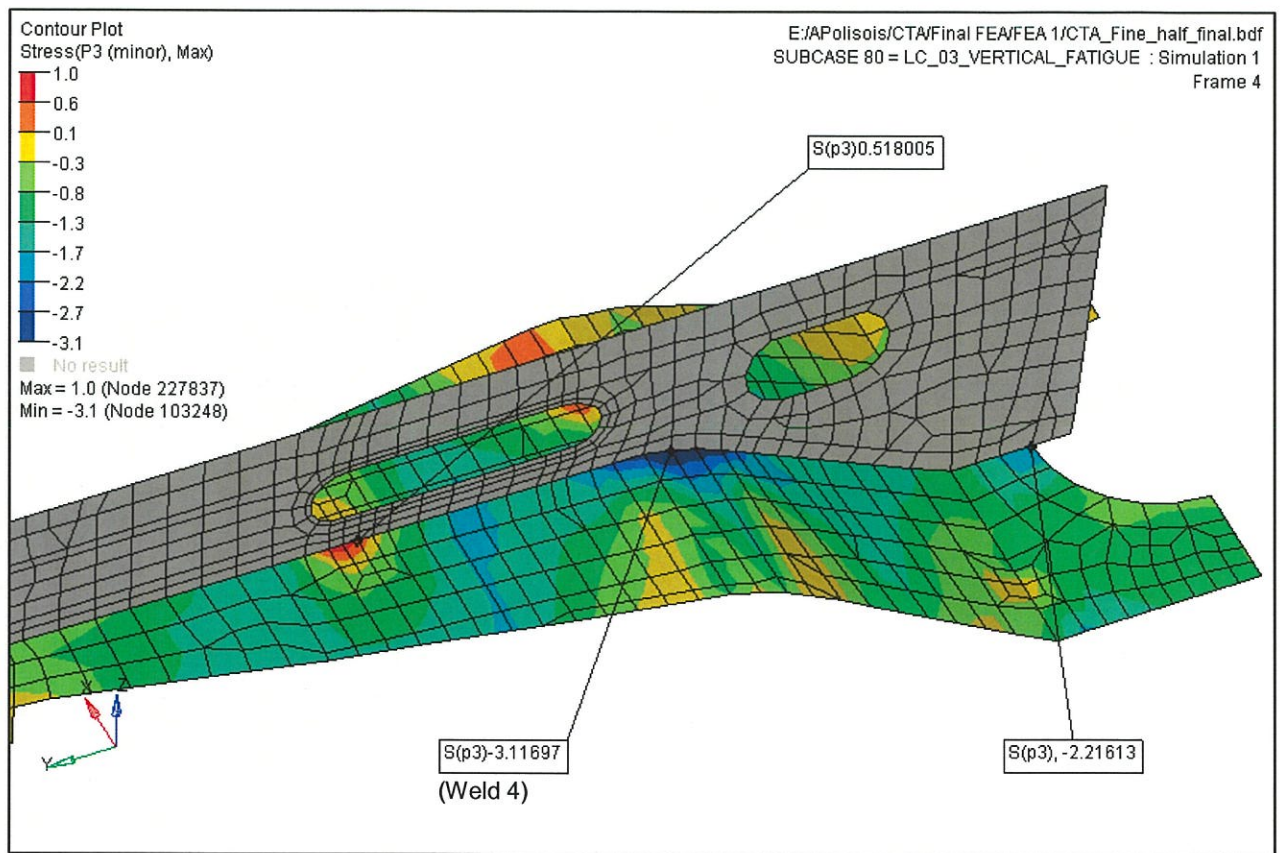


Figure 4.13.2 Bolster bottom plate minimum (p3) stress range for LC_03

- Figure 4.13.2 shows the minimum stress of the bolster bottom plate which is only -3.12 ksi. .
- Weld 4 is considered as a class “C” weld with an allowable stress range of 10 ksi.

The smallest margin of safety (weld 4) = $(10 / 3.1) - 1 = 2.2$

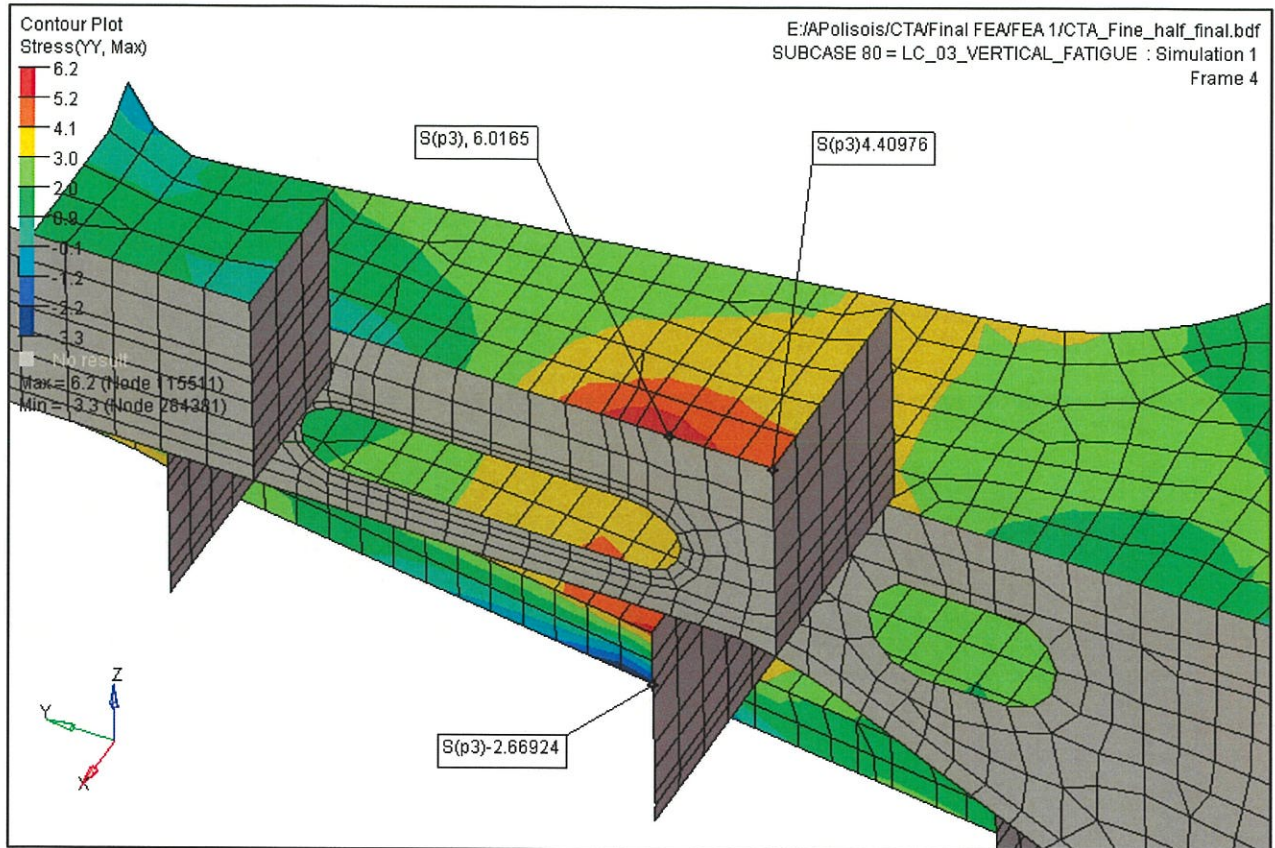


Figure 4.13.3 Bolster top plate component (Y) stress range for LC_03

Figure 4.13.3 shows a maximum component 'Y' stress of 6 ksi on the bolster top plate. This is considered as a class "B" weld with an allowable stress range of 16 ksi.

At the stiffener we have a stress of 4.4 ksi for a class "C" weld (all. 10 ksi) hence:

The margin of safety for the bolster top plate weld = $(10 / 4.4) - 1 = 1.2$

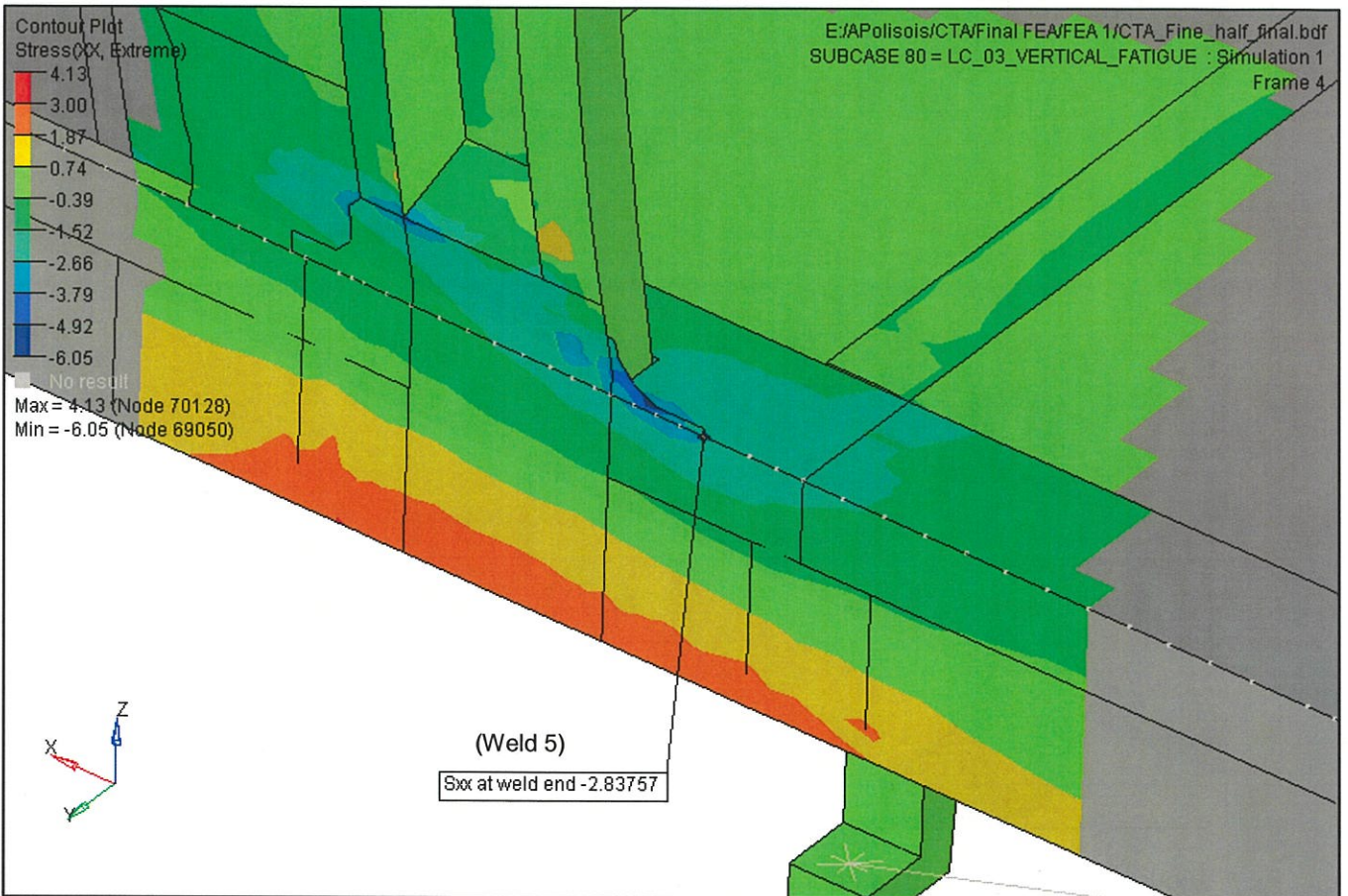
Side sill and door frame:

Figure 4.13.4 Side sill and door gusset component (X) stress range for LC_03

- Figure 4.13.4 shows the main stress (X) on the side sill at the end of the door gusset Weld 5 is considered as a class "E" weld with an allowable stress range of 4.5 ksi.

The margin of safety for weld 5 = $(4.5 / 2.8) - 1 = 0.6$

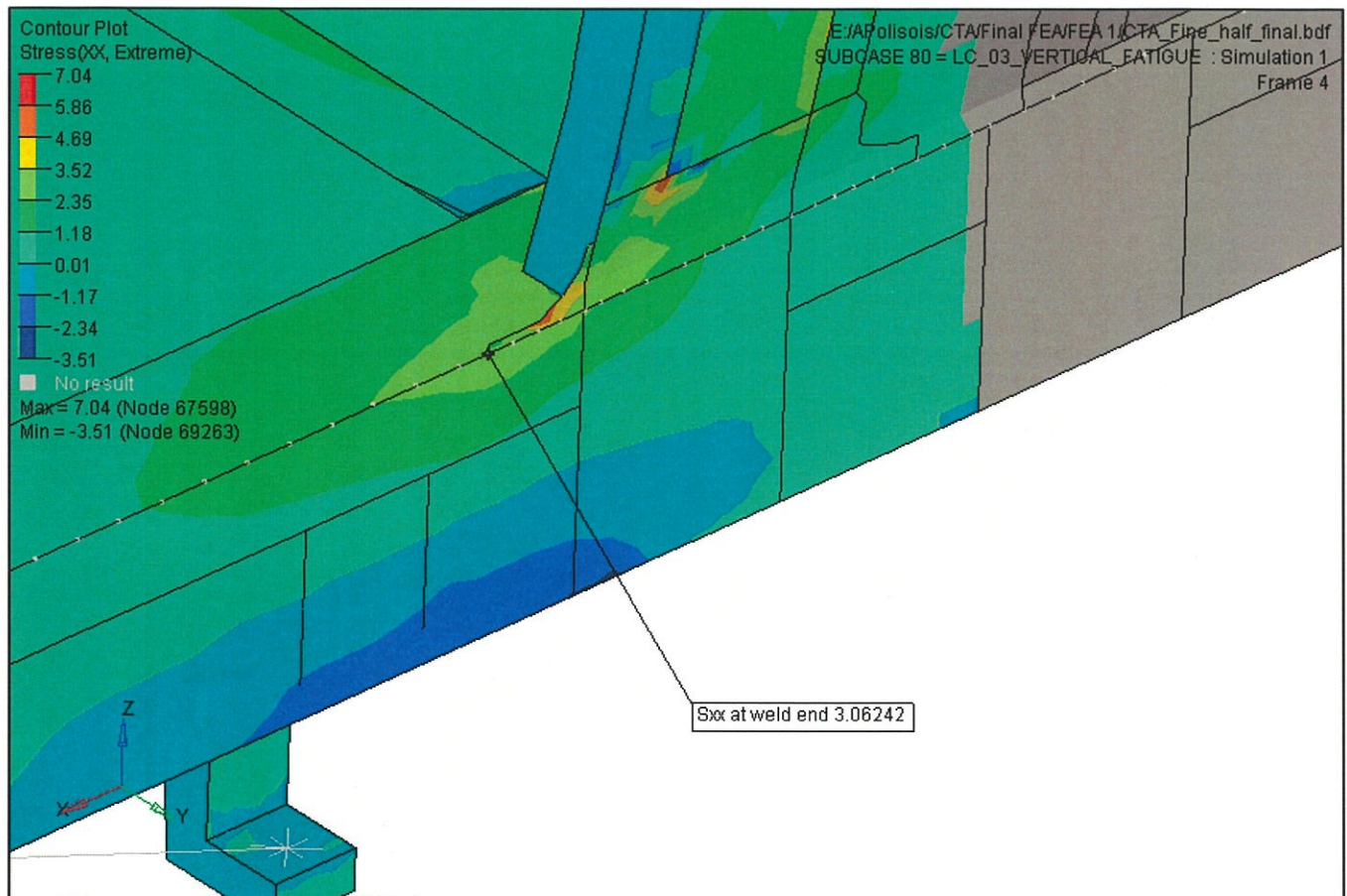


Figure 4.13.5 Side sill and door gusset component (X) stress range at the other side for LC_03.

- Figure 4.13.5 shows the main stress (X) on the side sill at the end of the door gusset. This weld detail is considered as a class “E” weld with an allowable stress range of 4.5 ksi.

The margin of safety for weld 5 at the other side of door = $(4.5 / 3.1) - 1 = 0.45$

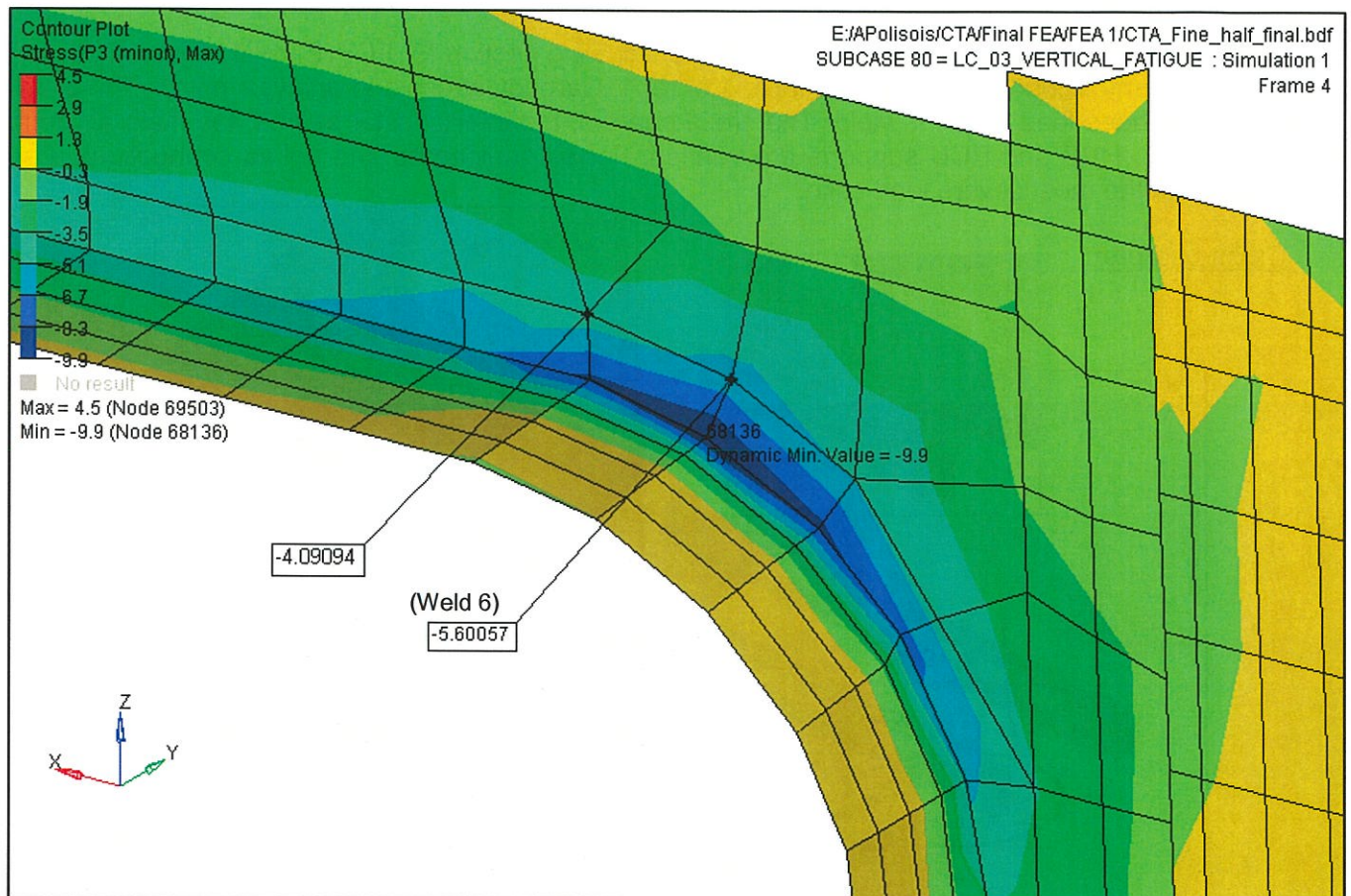


Figure 4.13.6 Top of door frame minimum (p3) stress range for LC_03

- Figure 4.13.6 shows the minimum stress at the top of the door frame which is only -5.6 ksi. .
- Weld 6 is considered as a class “B” weld with an allowable stress range of 16 ksi.

The margin of safety = $(16 / 5.6) - 1 = 1.8$

4.14 Equipment support structures:

Equipment support structures are verified in the following section for LC_12 (ref.1, 5g longitudinal load and a 1g vertical load at AW0 as per table 1 of ref.1, Carbody stress and analysis plan). The allowable stress for these load cases is yield. The cross bearers, the inter coastal beams, the main air duct, the HVAC,APS, HVB and PCU supports are verified. For all equipemnet the bolted connections are also verified for the most severe load case.

Cross-bearers:

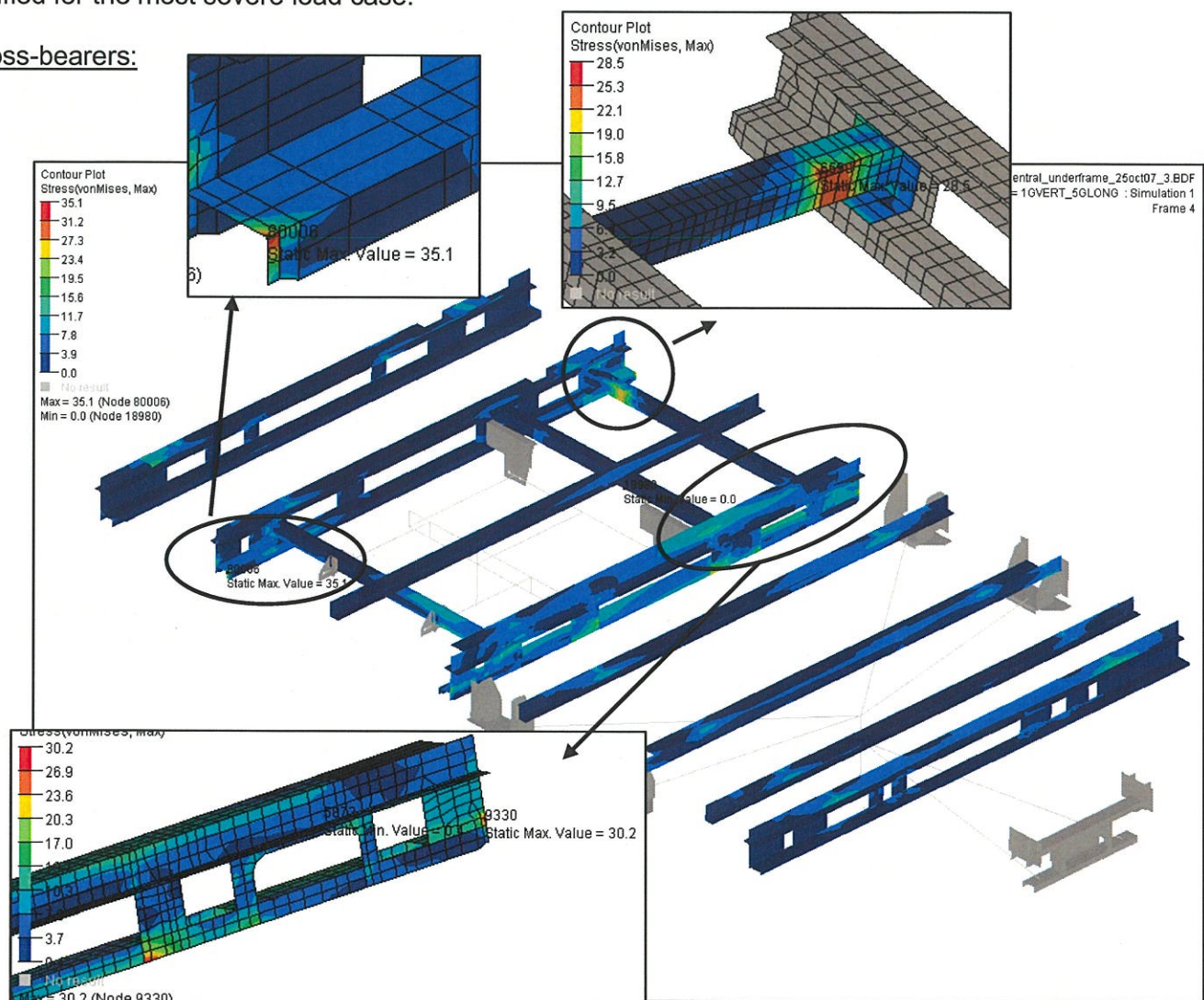


Figure 4.14.1: Cross-bearer and inter coastal beams maximum stress for LC_12 at AW0.

Figure 4.14.1 shows a maximum Von Mises stress concentration of 35.1 ksi for the cross bearers and inter coastal beams which in all cases are much lower than the yield. The allowable stress for LC_12 is yield = 62 ksi.

The cross-bearer minimum margin of safety for LC_12 = $(62 / 35.1) - 1 = 0.76$.

The inter coastal beam minimum margin of safety for LC_12 = $(62 / 28.5) - 1 = 1.7$.

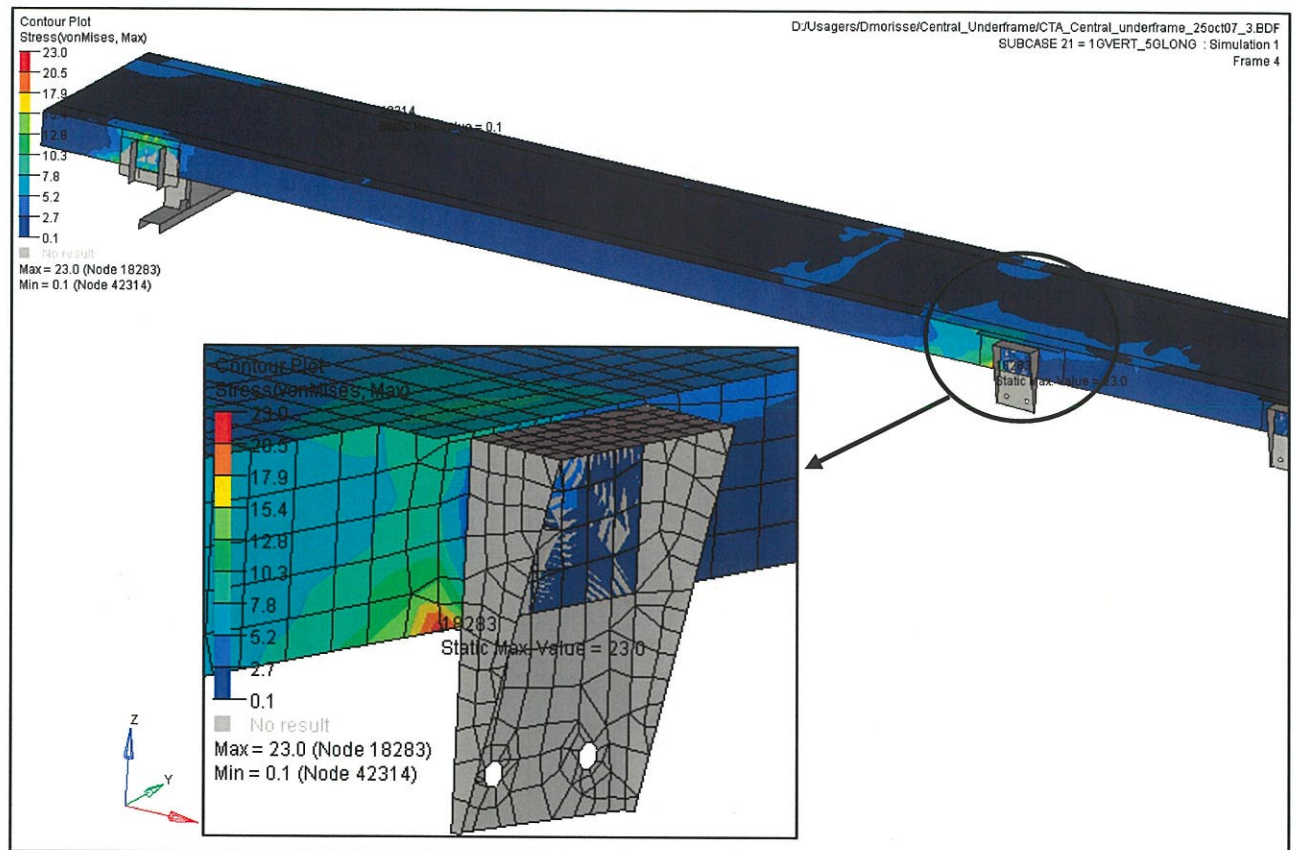
Main air duct:

Figure 4.14.2: Main air duct at the APS support maximum stress for LC_12 at AW0.

Figure 4.14.2 shows a maximum Von Mises stress concentration of 23 ksi on the main air duct support where connected to the APS support (shown in grey).

The allowable stress for LC_12 is yield = 62 ksi.

The main air duct minimum margin of safety for LC_12 = $(62 / 23) - 1 = 1.7$.

HVAC supports:

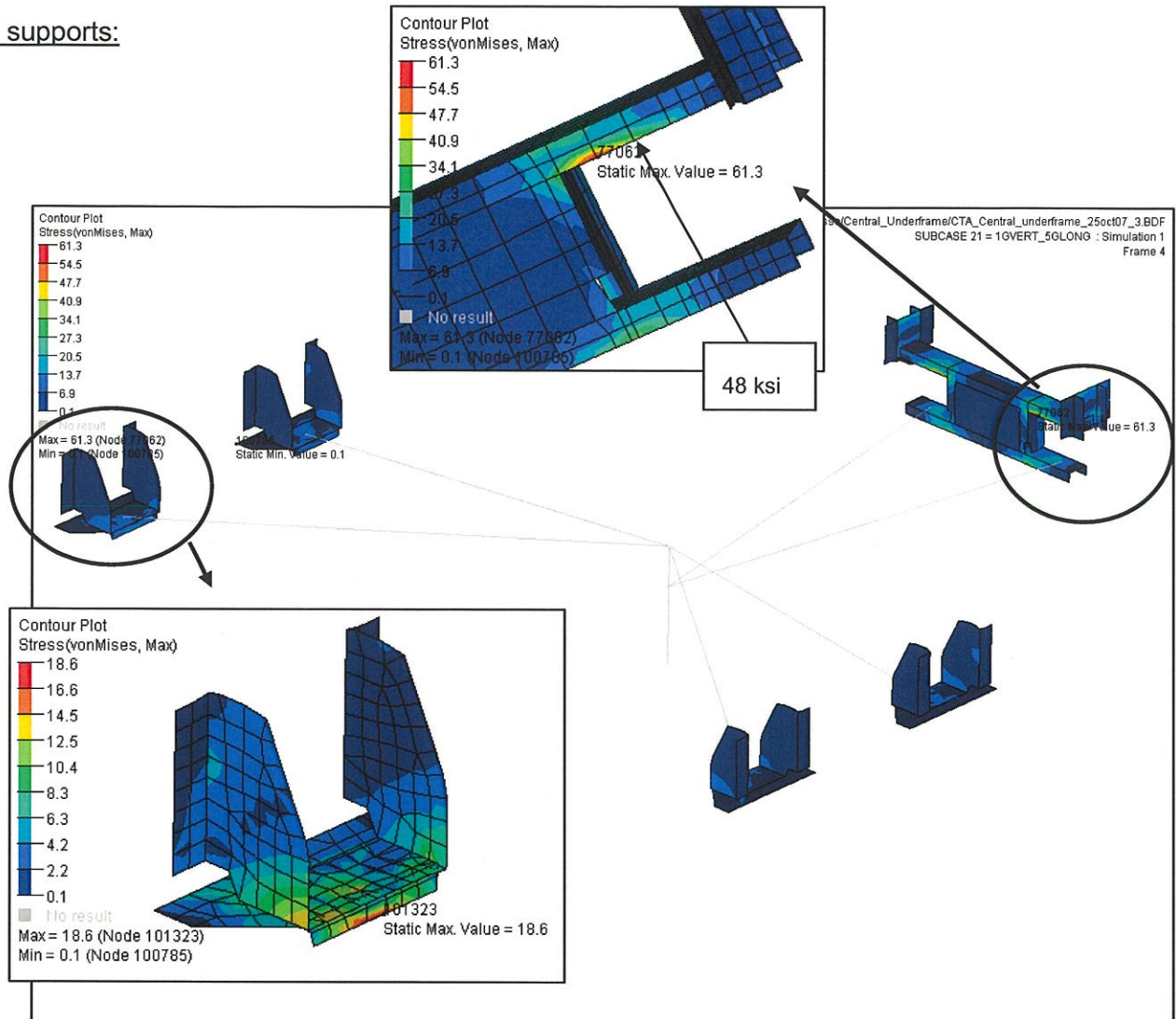


Figure 4.14.3:HVAC supports maximum Von Mises stresses for LC₁₂ at AW0.

Figure 4.14.3 shows a maximum Von Mises stress concentration of 61.3 ksi on the HVAC supports. The stress at the next closest node is around 48 ksi.

The allowable stress for LC₁₂ is yield = 62 ksi.

The HVAC support minimum margin of safety for LC₁₂ = $(62 / 48) - 1 = 0.3$.

HVAC support bolted connection:

The HVAC is bolted on the side sill support and the main air duct middle support. The equipment weight of the HVAC is 2136 lbs and is supported by $\frac{3}{4}$ " dia. bolts at six locations. From FEA analysis for the worst load case (LC_12), the resultant reactions are:

Node ID	X	Y	Z	Fx	Fy	Fz
76751	-11.75	10.01	30.95	0.01	0.07	0.98
76767	-11.75	-9.99	30.95	0.05	-0.07	0.98
100307	80.79	47.78	36.19	-3.15	-1.14	-0.90
100379	50.93	47.78	36.19	-2.30	0.94	1.00
100769	50.93	-47.78	36.19	-2.29	-0.89	0.99
100887	80.79	-47.78	36.19	-3.05	1.07	-0.90

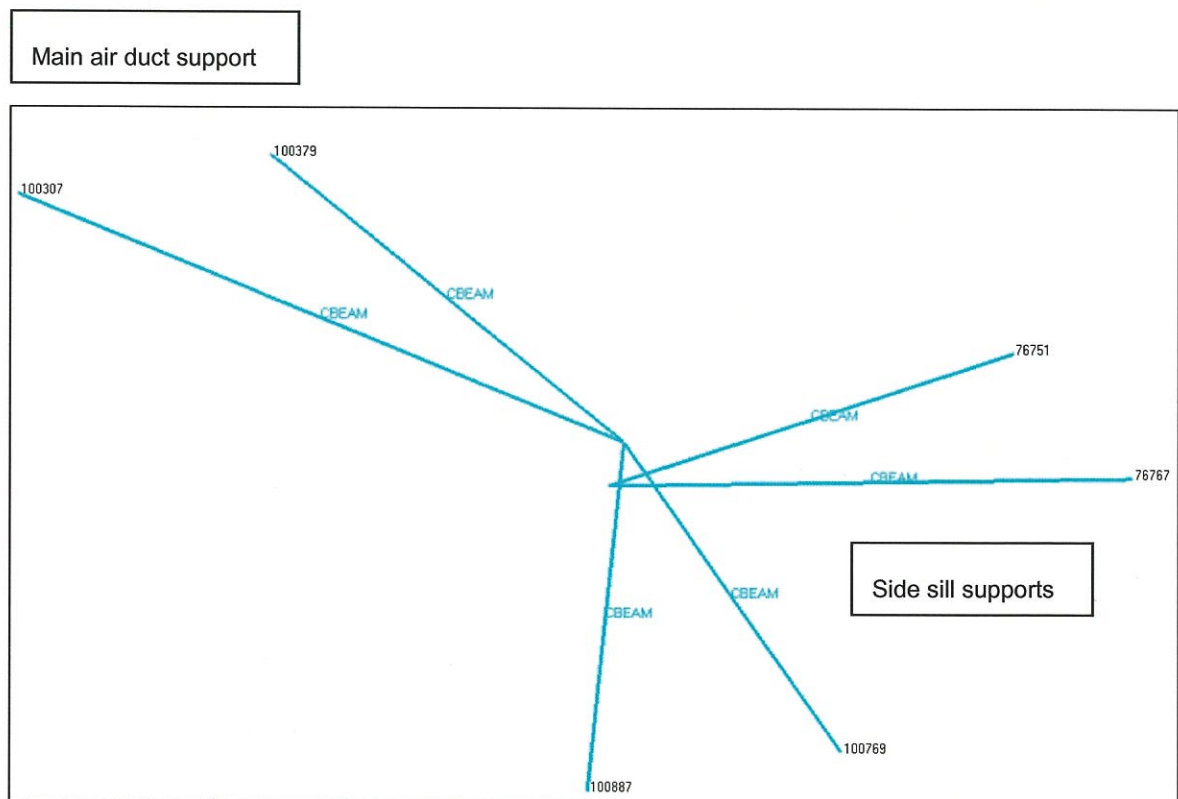


Figure 4.14.4:HVAC FEA spider support beams

Bolts at the Middle support (Main Air Duct):

Diameter	Dia	=	0.75	in
Pitch	P	=	10	threads per in
$At=0.7854(D-(0.9743/n))^2$	At	=	0.334	in ² (Tensile Area)
$As=0.7854(D-(1.3/n))^2$	At	=	0.302	in ² (Shear Area)

Force:

From node 100307	Fx	=	3.15	Kip
	Fy	=	1.14	Kip
	Fz	=	0.9	Kip
Radial Force	Fr	=	3.35	Kip
Tension Force	Ft	=	0.90	Kip

Stress Calculation:

σ_t	σ_t	=	2.69	ksi
	r	=	10.02	ksi
$\sigma_E = (\sigma^2 + 3t^2)^{1/2}$	σ_{ev}	=	17.56	ksi
Yield bolt	σ_y	=	92	Ksi
Safety Marge = $1 - (\sigma/\sigma_y)$	M.S.	=	0.81	

Bolts on the side sill

Diameter	Dia	=	0.75	in
Pitch	P	=	10	threads per in
$At=0.7854(D-(0.9743/n))^2$	At	=	0.334	in ² (Tensile Area)
$As=0.7854(D-(1.3/n))^2$	At	=	0.302	in ² (Shear Area)

Force:

From node 100887	Fx	=	3.05	Kip
	Fy	=	1.07	Kip
	Fz	=	0.9	Kip
Radial Force	Fr	=	3.23	Kip
Tension Force	Ft	=	0.90	Kip

Stress Calculation:

σ_t	σ_t	=	2.69	ksi
	r	=	9.66	ksi
$\sigma_E = (\sigma^2 + 3t^2)^{1/2}$	σ_{ev}	=	16.95	ksi
Yield bolt	σ_y	=	92	Ksi
Safety Marge = $1 - (\sigma/\sigma_y)$	M.S.	=	0.82	

The HVAC bolt minimum margin of safety for LC_12 = 0.81.

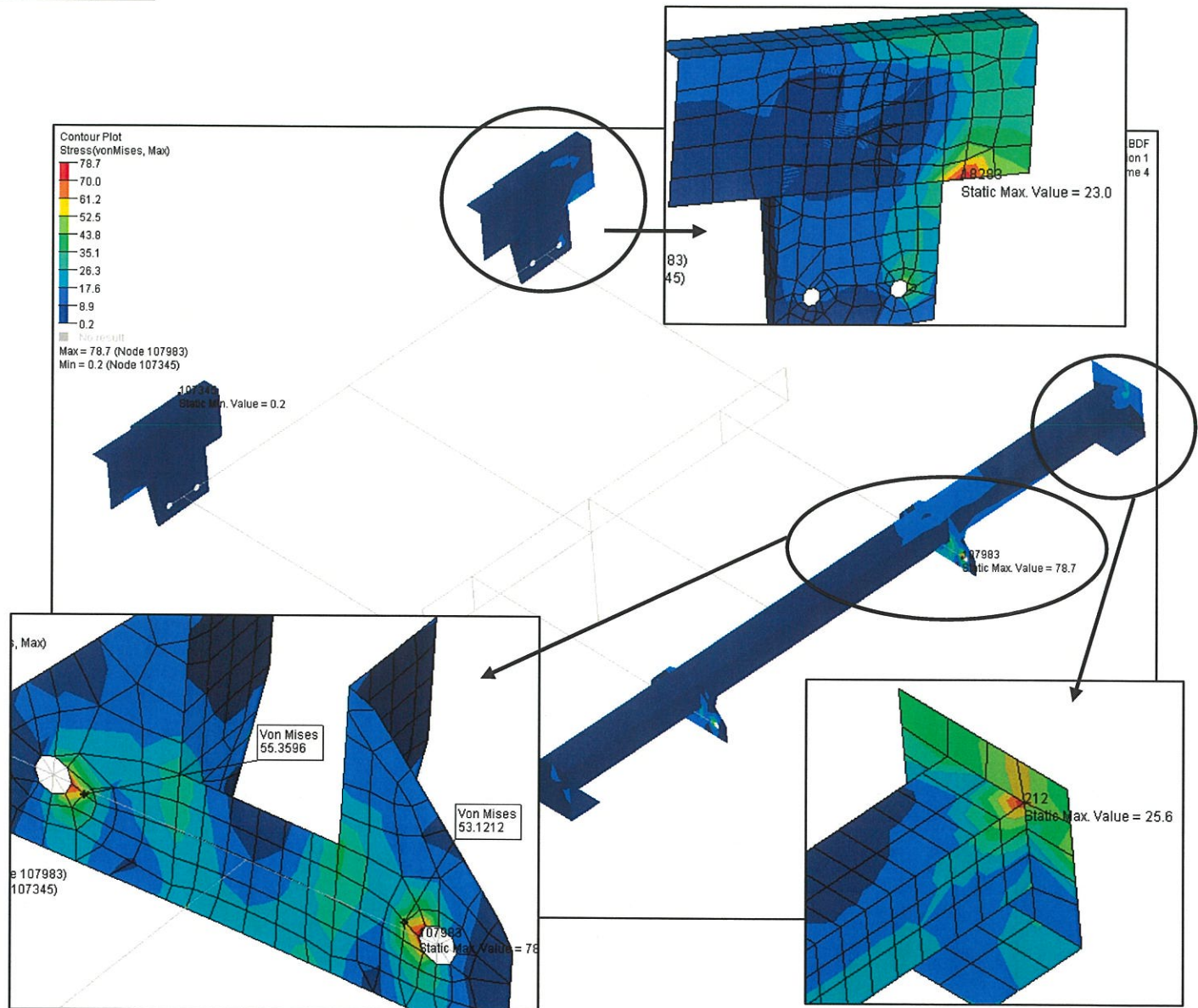
APS supports:

Figure 4.14.5:APS supports maximum Von Mises stresses for LC_12 at AW0.

Figure 4.14.4 shows maximum Von Mises stresses concentration of 78.8 ksi at the hole where spiders are connected to simulate the bolted connection. The stress at the next closest node is around 55.5 ksi. For all other APS supports the stresses are low.

The allowable stress for LC_12 is yield = 62 ksi.

The APS support minimum margin of safety for LC_12 = $(62 / 55.5) - 1 = 0.12$.

APS Bolts Calculation:

The APS is bolted on the inter-coastal support and the main air duct support. The equipment weight of the APS is 1290 lbs and is supported by eight 1/2" dia. bolts.

Reactions from FEA analysis for the worst load case (LC_12):

Node ID	X	Y	Z	Fx	Fy	Fz
108792	138.09	31.65	37.74	-0.52	-0.33	-0.46
108794	112.79	31.65	37.74	-0.86	0.61	0.28
108795	112.79	37.40	37.74	-1.16	-0.50	0.89
108796	144.50	-13.54	34.51	-0.75	0.16	-0.09
108797	141.75	-13.54	34.52	-0.71	0.07	-0.73
108798	107.50	-13.54	34.51	-0.86	-0.03	-0.04
108799	104.75	-13.54	34.52	-0.89	-0.19	1.53
108800	138.09	37.40	37.73	-0.74	0.22	-0.08

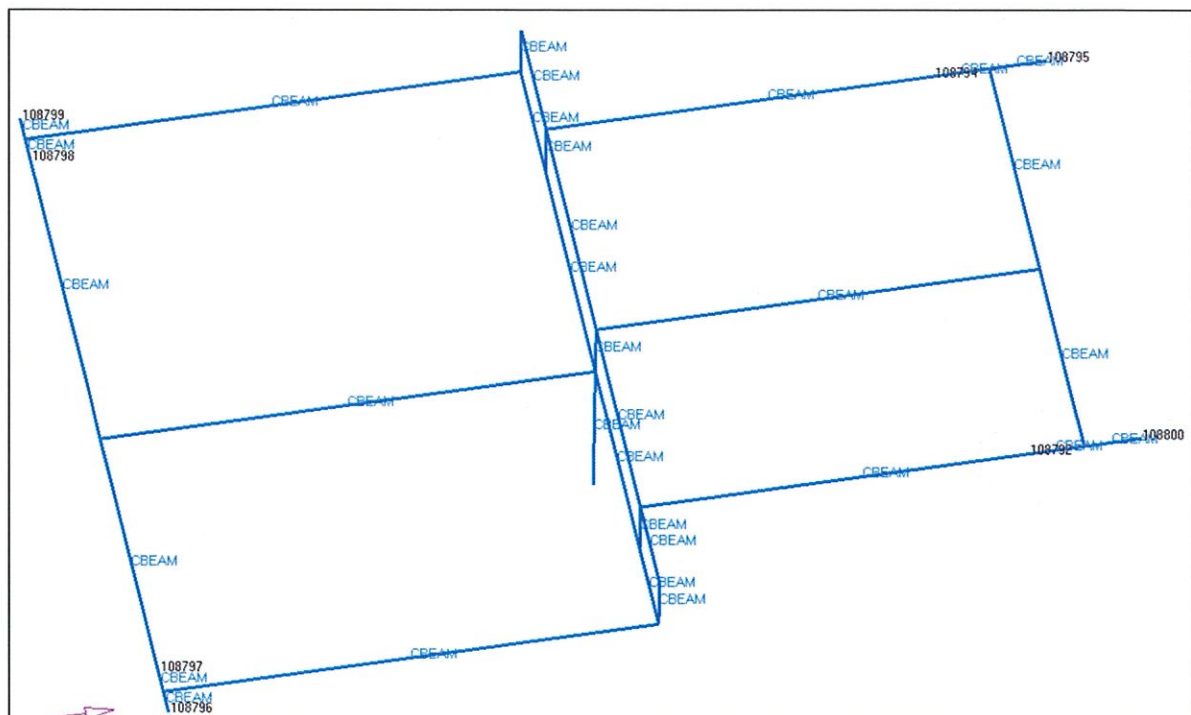


Figure 4.14.6:APS FEA spider support beams

Bolts on inter-coastal beam:

Diameter	Dia	=	0.5	in
Pitch	P	=	13	threads per in
$At=0.7854(D-(0.9743/n))^2$	At	=	0.142	in ² (Tensile Area)
$As=0.7854(D-(1.3/n))^2$	At	=	0.126	in ² (Shear Area)

Force:

From node 108795	Fx	=	1.16	Kip
	Fy	=	0.5	Kip
	Fz	=	0.89	Kip

Radial Force	Fr	=	1.26	Kip
Tension Force	Ft	=	0.89	Kip

Stress Calculation:

σ_t	σ_t	=	6.27	ksi
	τ	=	8.90	ksi
$\sigma_E = (\sigma^2 + 3\tau^2)^{1/2}$	σ_{ev}	=	16.65	ksi
Yield bolt	σ_y	=	92	Ksi
Safety Marge = $1 - (\sigma/\sigma_y)$	M.S.	=	0.82	

Bolts Main Air Duct:

Diameter	Dia	=	0.5	in
Pitch	P	=	13	threads per in
$At=0.7854(D-(0.9743/n))^2$	At	=	0.142	in ² (Tensile Area)
$As=0.7854(D-(1.3/n))^2$	At	=	0.126	in ² (Shear Area)

Force:

From node 108799	Fx	=	0.89	Kip
	Fy	=	0.19	Kip
	Fz	=	1.53	Kip

Radial Force	Fr	=	0.91	Kip
Tension Force	Ft	=	1.53	Kip

Stress Calculation:

σ_t	σ_t	=	10.78	ksi
	τ	=	6.41	ksi
$\sigma_E = (\sigma^2 + 3\tau^2)^{1/2}$	σ_{ev}	=	15.48	ksi
Yield bolt	σ_y	=	92	Ksi
Safety Marge = $1 - (\sigma/\sigma_y)$	M.S.	=	0.83	

The APS bolt connection minimum margin of safety for LC_12 = 0.82.

HVB supports :

The HVB supports are located on the side sill and on the inter-coastal beam. There are two supports connected with the side sill. The equipment weight of the HVB is 600 lbs. The most severe load case is the -5g longitudinal+1g vertical LC_12.

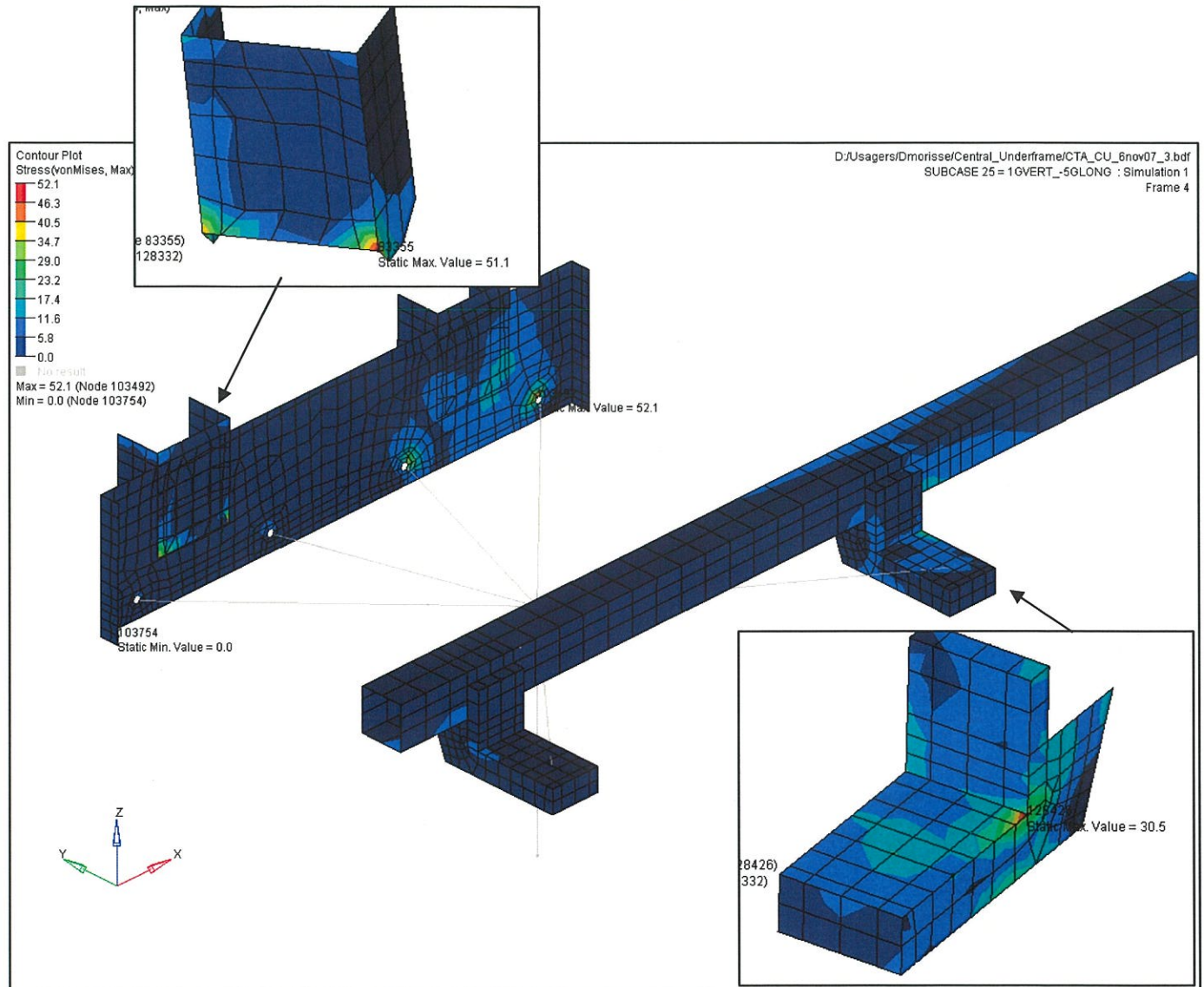


Figure 4.14.7:HVB supports max. Von Mises stress (LC_12)

Figure 4.14.7 shows maximum Von Mises peak stress of 52.1 ksi at the hole where spiders are connected to simulate the bolted connection. The stress at the support to the side sill is 51.1 ksi.

The allowable stress for LC_12 is yield = 62 ksi.

The HVB support minimum margin of safety for LC_12 = $(62 / 51.1) - 1 = 0.213$.

HVB Bolts Calculation:

The HVB is bolted on an attaching plate attached on two supports connected on the side sill and the inter-coastal supports. The equipment weight is 600 lbs and is supported by 3/8" dia. bolts at six locations. From FEA analysis for the worst load case, these are the reactions:

Node ID	X	Y	Z	Fx	Fy	Fz
128214	-82.59	49.06	35.22	0.37	-0.02	-0.87
128215	-74.34	49.06	35.22	0.76	0.01	-0.59
128216	-66.09	49.06	35.22	0.81	0.10	0.74
128217	-57.84	49.06	35.22	0.24	0.14	0.96
128254	-58.03	23.69	37.31	0.66	0.72	0.39
128255	-82.53	23.69	37.31	0.17	-0.95	-0.04

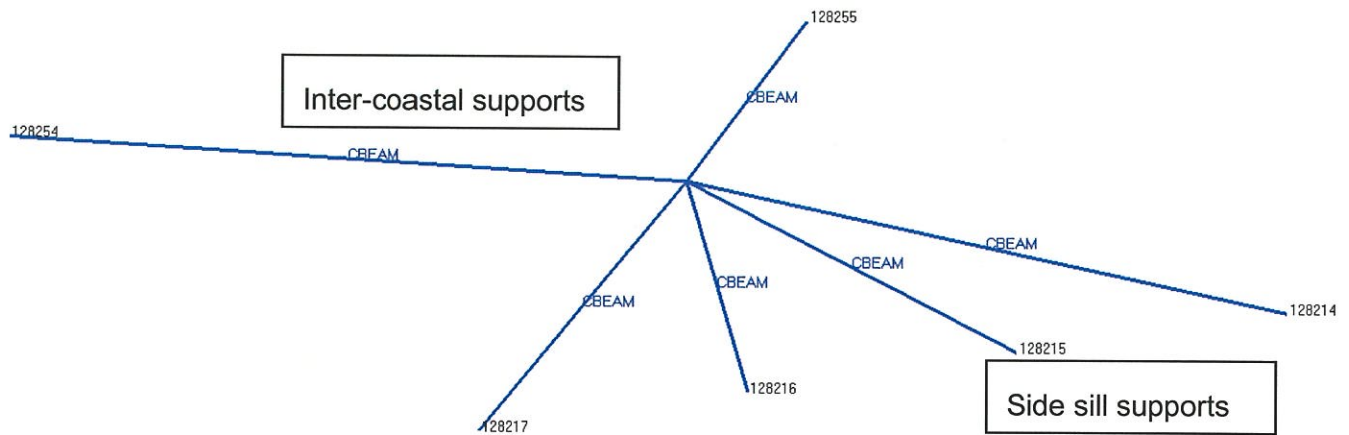


Figure 4.14.8:HCB FEA spider support beams.

Bolts on the side sill			
Diameter	Dia	=	0.375 in
Pitch	P	=	16 threads per in
$At=0.7854(D-(0.9743/n))^2$	At	=	0.077 in ² (Tensile Area)
$As=0.7854(D-(1.3/n))^2$	As	=	0.068 in ² (Shear Area)
Force:			
From node 128216	Fx	=	0.81 Kip
	Fy	=	0.1 Kip
	Fz	=	0.74 Kip
Radial Force	Fr	=	0.82 Kip
Tension Force	Ft	=	0.74 Kip
$\sigma_E = (\sigma^2 + 3t^2)^{1/2}$	σ_t	=	9.55 ksi
r	r	=	10.53 ksi
$\sigma_{ev} = ?(\sigma^2 + 3T^2)$	σ_{ev}	=	20.59 ksi
Yield bolt	σ_y	=	92 Ksi
Safety Marge = 1- (σ/σ_y)	M.S.	=	0.78

<u>Bolts at the Inter-coastal support:</u>			
Diameter	Dia	=	0.375 in
Pitch	P	=	16 threads per in
$At=0.7854(D-(0.9743/n))^2$	At	=	0.077 in^2 (Tensile Area)
$As=0.7854(D-(1.3/n))^2$	As	=	0.068 in^2 (Shear Area)
<u>Force:</u>			
From node 128254	Fx	=	0.66 Kip
	Fy	=	0.72 Kip
	Fz	=	0.39 Kip
Radial Force	Fr	=	0.98 Kip
Tension Force	Ft	=	0.39 Kip
<u>Stress Calculation:</u>			
σ_t	σ_t	=	5.03 ksi
τ	τ	=	12.60 ksi
$\sigma_E = (\sigma^2 + 3\tau^2)^{1/2}$	σ_{ev}	=	22.40 ksi
	σ_y	=	92 Ksi
Safety Marge = $1 - (\sigma/\sigma_y)$	M.S.	=	0.76

The HVB bolt connection minimum margin of safety for LC_12 = 0.76.

PCU supports:

The PCU supports are connected on the equipment beams. There are two supports per equipment beams. The equipment weight of the PCU is 919 lbs. The most severe load case is LC_12 (-5g longitudinal+1g vertical).

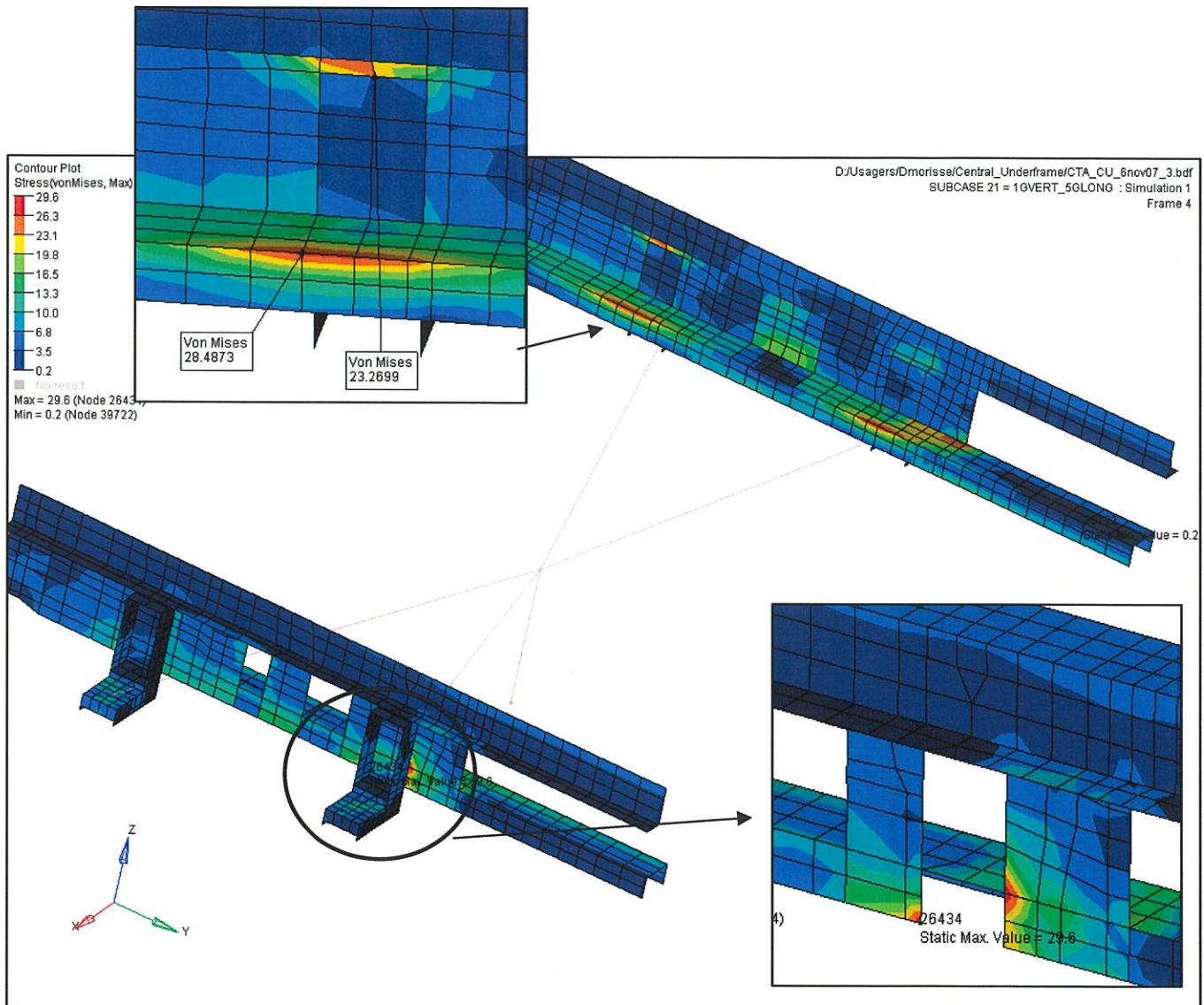


Figure 4.14.9:PCU supports max. Von Mises stress (LC_12)

Figure 4.14.9 shows a maximum Von Mises stress concentration of 29.6 ksi on the web near the support.

The allowable stress for LC_12 is yield = 62 ksi.

The PCU support minimum margin of safety for LC_12 = $(62 / 29.6) - 1 = 1.09$.

PCU Bolts Calculation:

The PCU is bolted at four supports on the equipment beam. The equipment weight is 919 lbs and is supported by 1/2" dia. bolts at four locations. From FEA analysis for the worst load case, these are the reactions:

Node ID	X	Y	Z	Fx	Fy	Fz
63029	-92.47	-39.32	35.20	1.55	-0.22	0.12
63040	-92.47	-19.13	35.20	2.11	0.29	-0.32
63053	-12.72	-39.32	35.20	0.56	0.10	0.25
63064	-12.72	-19.13	35.20	0.40	-0.18	0.88

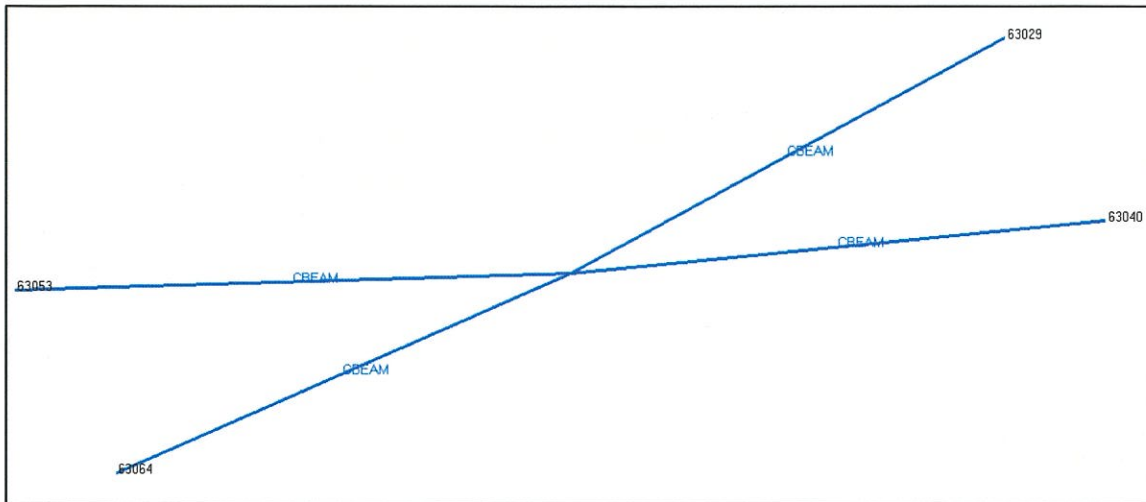


Figure 4.14.10:PCU FEA spider support beams.

Bolts:

Diameter	Dia	=	0.5	in
Pitch	P	=	13	threads per in
$At=0.7854(D-(0.9743/n))^2$	At	=	0.142	in^2 (Tensile Area)
$As=0.7854(D-(1.3/n))^2$	As	=	0.126	in^2 (Shear Area)

Force:

From node 63040	Fx	=	2.11	Kip
	Fy	=	0.29	Kip
	Fz	=	0.32	Kip
Radial Force	Fr	=	2.13	Kip
Tension Force	Ft	=	0.32	Kip

Stress Calculation:

σ_t	σ_t	=	2.26	ksi
	τ	=	15.01	ksi
$\sigma_E = (\sigma^2 + 3\tau^2)^{1/2}$	σ_{ev}	=	26.09	ksi
yield point	σ_y	=	92	Ksi
Safety Margn = $1 - (\sigma/\sigma_y)$	M.S.	=	0.72	

The PCU bolt connection minimum margin of safety for LC_12 = 0.72.

4.15 Jacking and pushing in the shop considerations:

Von Mises stresses are reviewed for the jacking at side sill (LC_08), jacking at end sill (LC_09), jacking for re-railing operation (LC_10 torsion load) and pushing in the shop (LC_11 as per table 1 of ref.1, Carbody stress and analysis plan). The allowable stress for all these load cases is yield.

Jacking at side sill (LC_08):

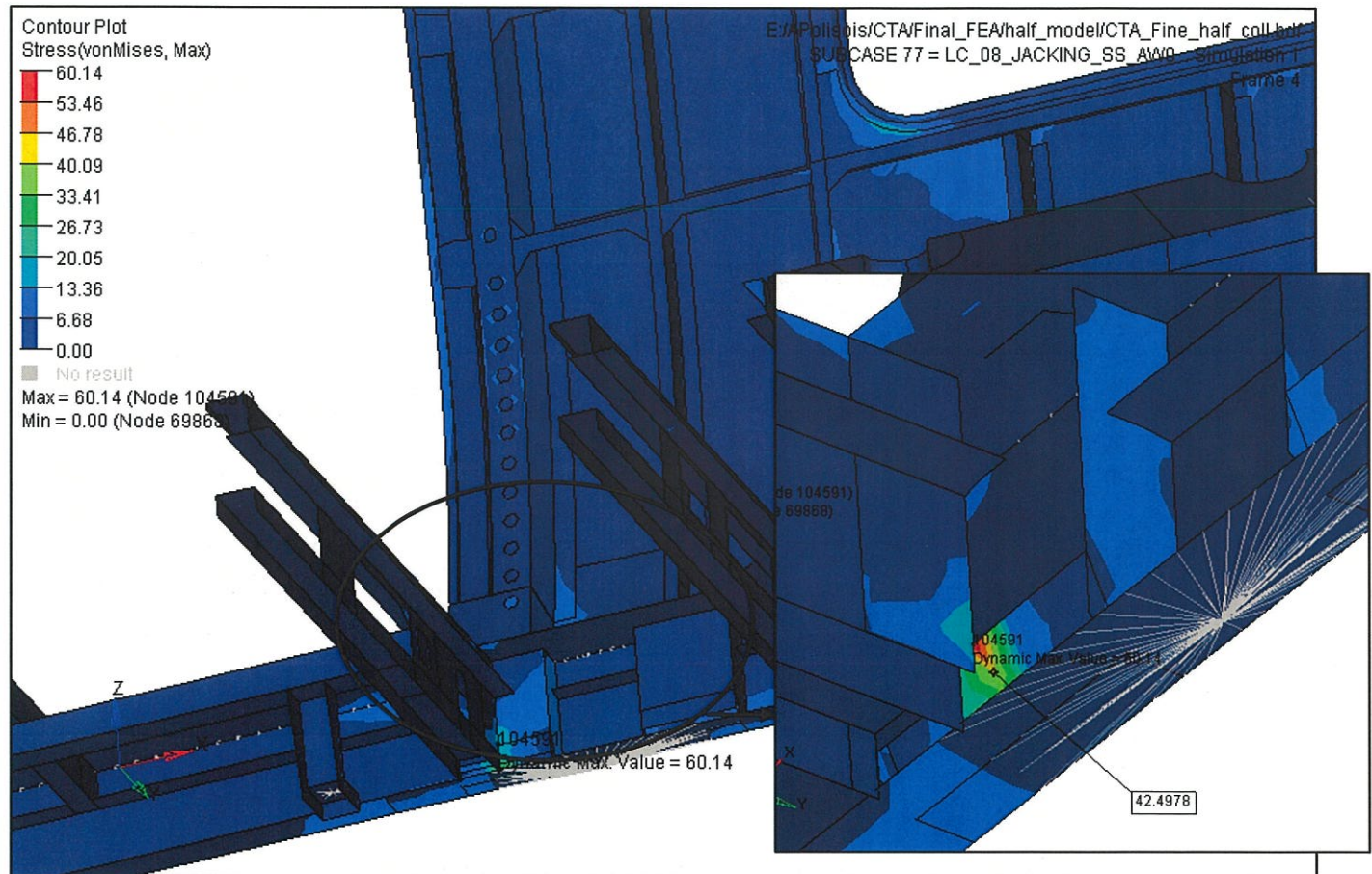


Figure 4.15.1: LC_08 Max. stress concentration of 42.5 ksi at jacking support (allow. yield = 62 ksi).

Figure 4.15.1 shows a maximum Von Mises stress concentration of 60.14 ksi which is due to the proximity of the rigid beams used to model the jacking lift. The next closest node stress value of 42.5 ksi is more representative of a nominal stress in that region.

The allowable stress for LC_18 is yield = 42.5 ksi.

The jacking pad support minimum margin of safety for LC_08 = $(62 / 42.5) - 1 = 0.45$

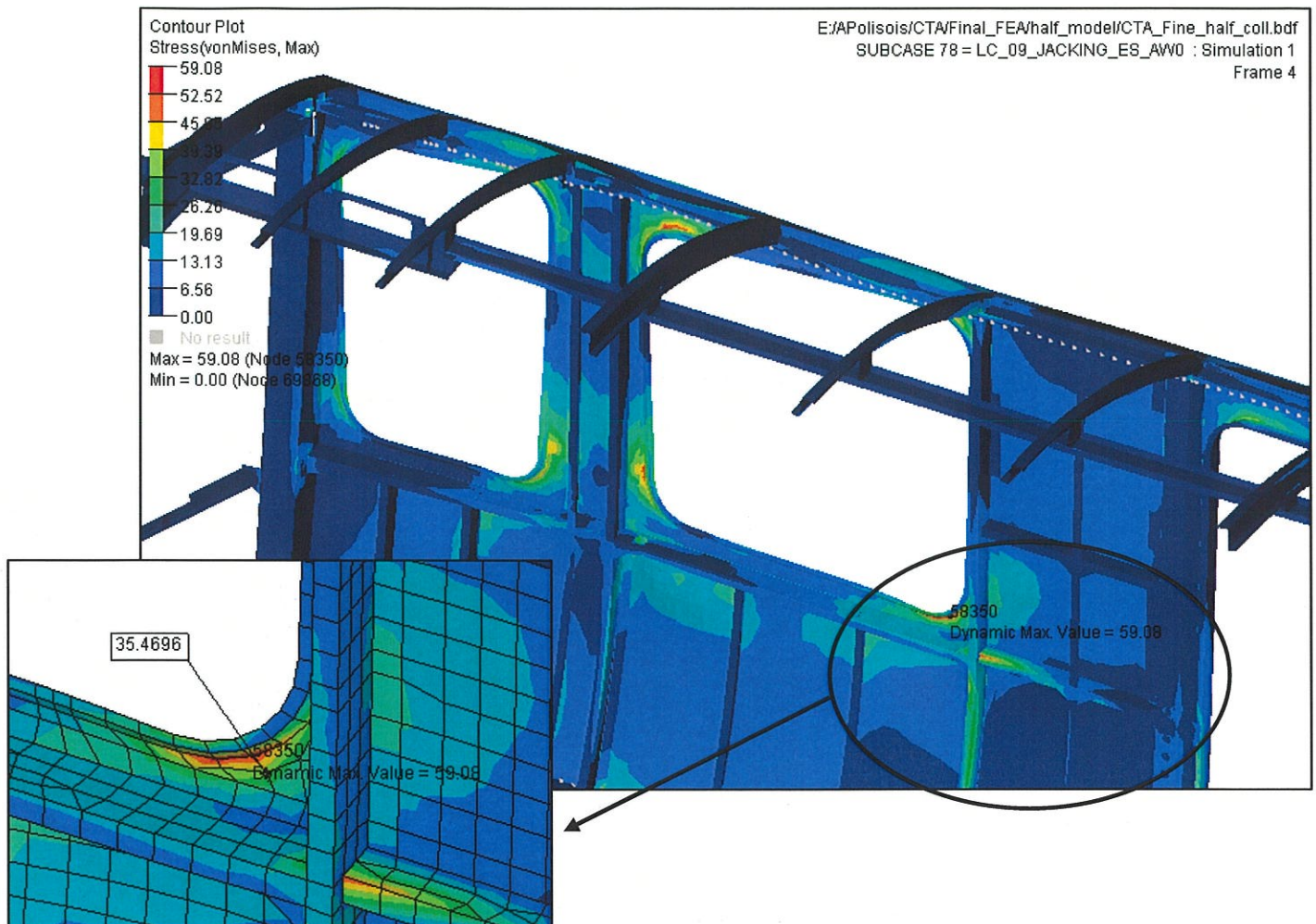
Jacking at end sill (LC 09):

Figure 4.15.2: LC_09 Max. stress of 35.5 ksi at window corner (allowable is yield = 62 ksi)..

Figure 4.15.2 shows a maximum Von Mises stress concentration of 59.1 ksi which is due to the window corner. The next closest node stress value of 35.5 ksi is more representative of a nominal stress in that region.

The allowable stress for LC_09 is yield = 35.5 ksi.

The window corner minimum margin of safety for LC_09 = $(62 / 35.5) - 1 = 0.75$

Jacking at end sill for re-railing (LC 10):

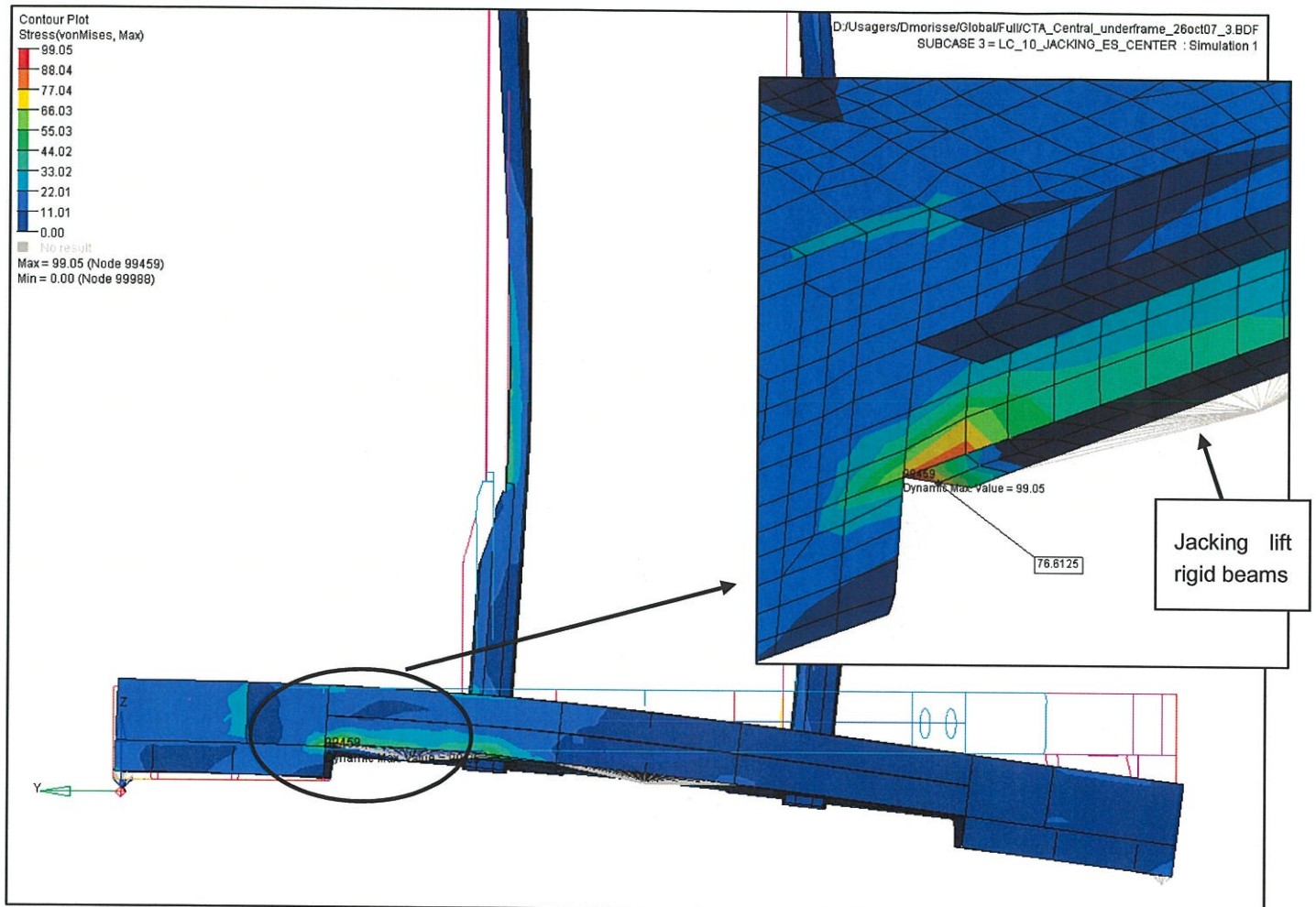


Figure 4.15.3:End sill maximum Von Mises stress (exaggerated deformations) for LC_10

Figure 4.15.3 shows a maximum Von Mises stress concentration of 99 ksi which is due to the proximity of the rigid beams used to model the jacking lift. The next closest node stress value of 76.6 ksi is more representative of a nominal stress in that region.

The allowable stress for LC_10 is yield = 80 ksi.

The end sill minimum margin of safety for LC_10 = $(80 / 76.6) - 1 = 0.04$

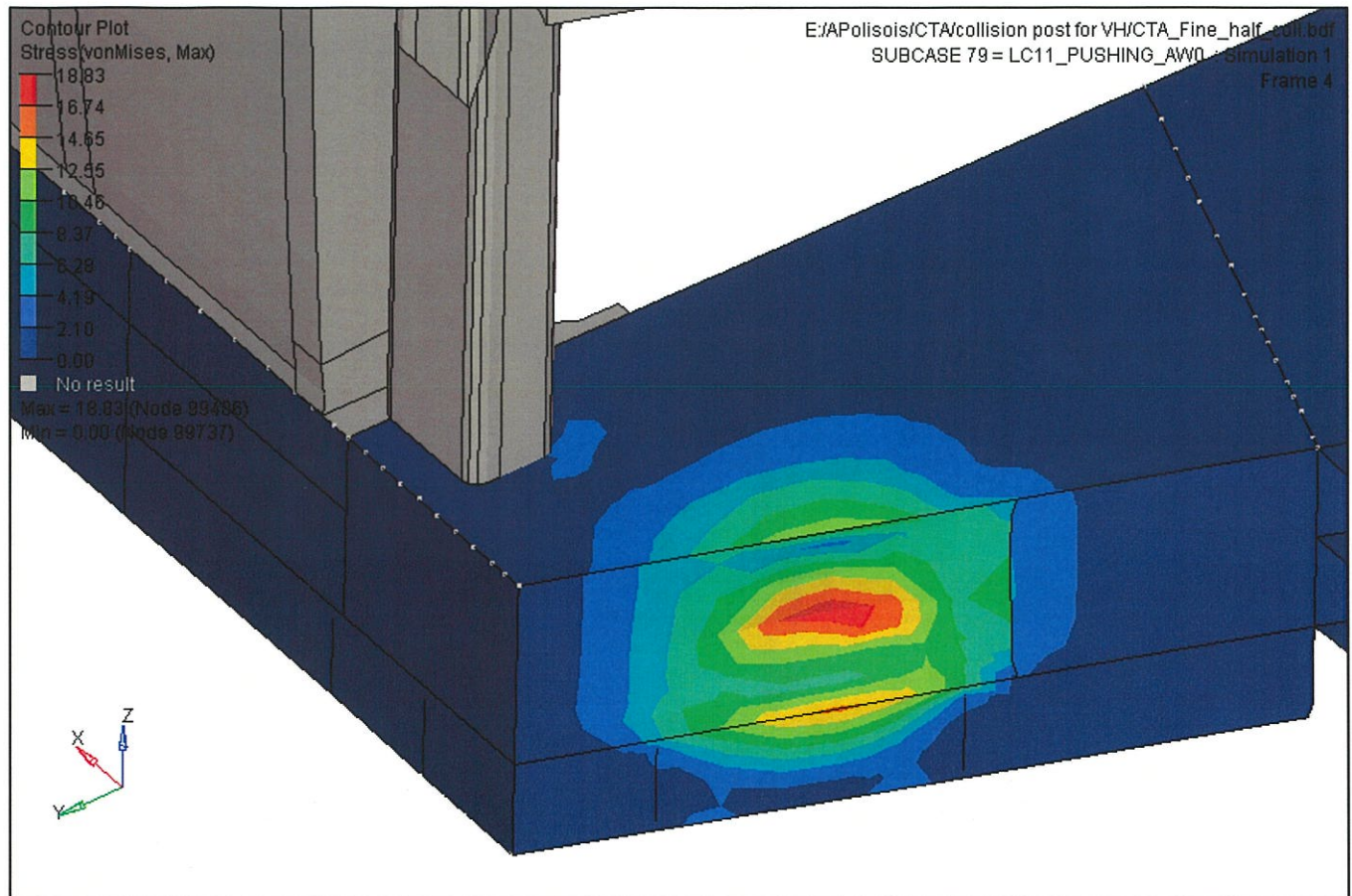
Pushing in the shop at AW0 (LC 11):

Figure 4.15.4:End sill Von Mises stress and exaggerated deformations for LC_11

Figure 4.15.4 shows a maximum Von Mises stress of 18.8 ksi due to the pushing in the shop with a force of 1000 lb (1 kip). This force is a load equal to a 4% grade push (500 lb) at AW0 with a factor of safety of two. The allowable stress for LC_10 is yield = 80 ksi.

The end sill minimum margin of safety for LC_11 = $(80 / 18.8) - 1 \gg 2$

4.16 Progressive Strength Distribution:

The strength distribution in the longitudinal direction between bolsters shall be 40% higher than the end sill. The strength shall also be 20% higher between the coupler anchor and the bolster than the end sill (ref. 1, table 1, LC_04 as per ref. 6 CTA specs section 3.02.a). The above requirement is verified with a transient dynamic crash analysis (ref. 8, 'Carbody Crash Analysis Report'). Figure 4.16.1 also shows that in static mode, the above requirement holds as well (Sxx as shown represents the longitudinal nominal stress distribution of the end underframe).

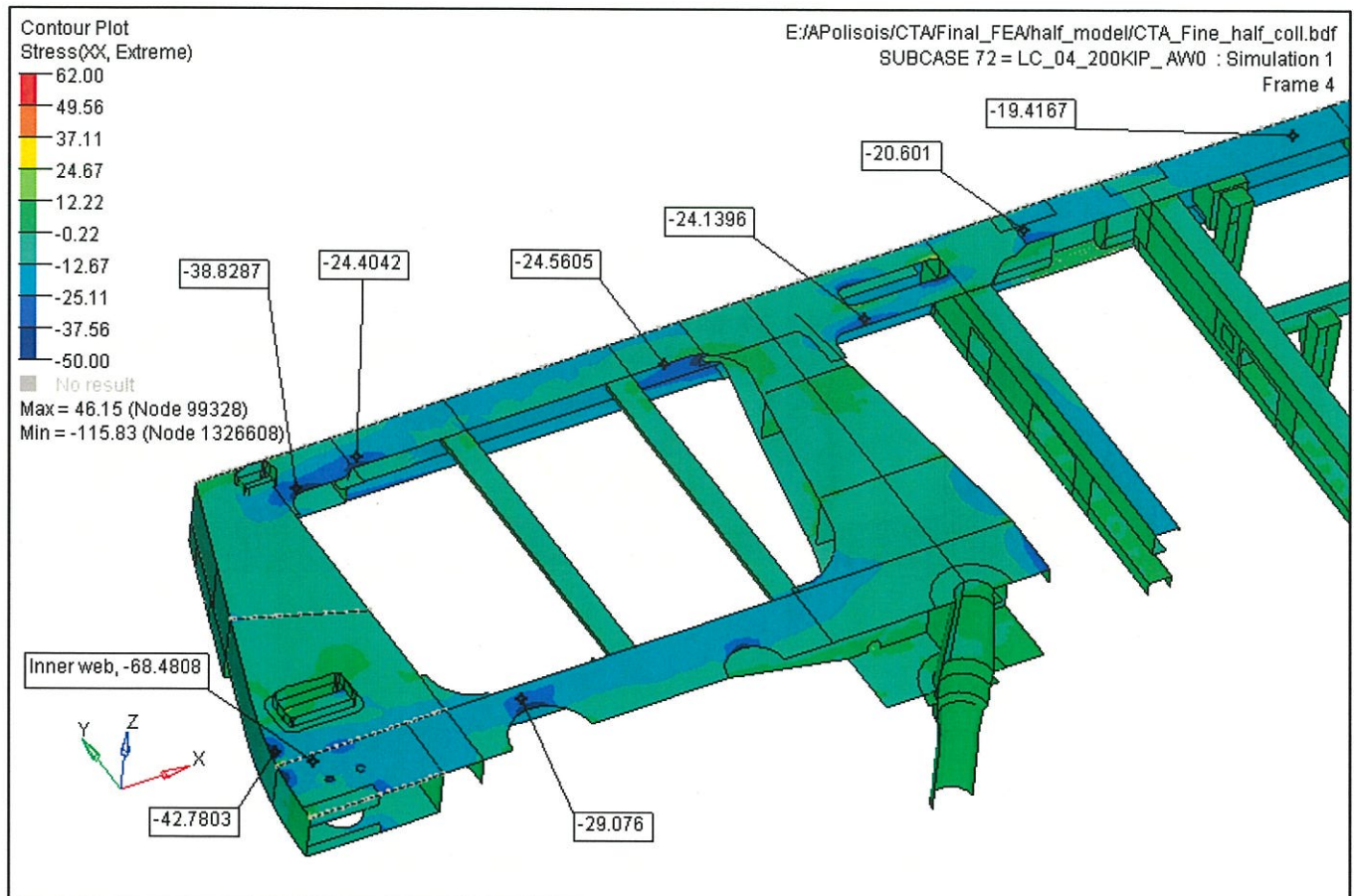


Figure 4.16.1: End underframe nominal longitudinal (Sxx) stress for LC_04

Figure 4.16.1 shows a general view of Sxx in the longitudinal direction. The above shows that the stress level in the end sill (-68 ksi) is much higher than between the coupler and bolster (-25 ksi) which is in turn higher than between the bolsters (-20 ksi).

The above figure and the crash analysis results show that the progressive strength distribution requirement is acceptable.

4.17 FEA Calculations of Natural frequencies:

Natural frequencies FEA calculations are done at AW0 to verify that the first torsion and bending modes of the carbody are high enough to ensure good vehicle ride quality. As shown in figure 4.17.1 the first predicted mode is the first torsion mode at 8.48 Hz (figure 4.17.1). The next mode is the first bending mode at 9.68 Hz (figure 4.17.2).

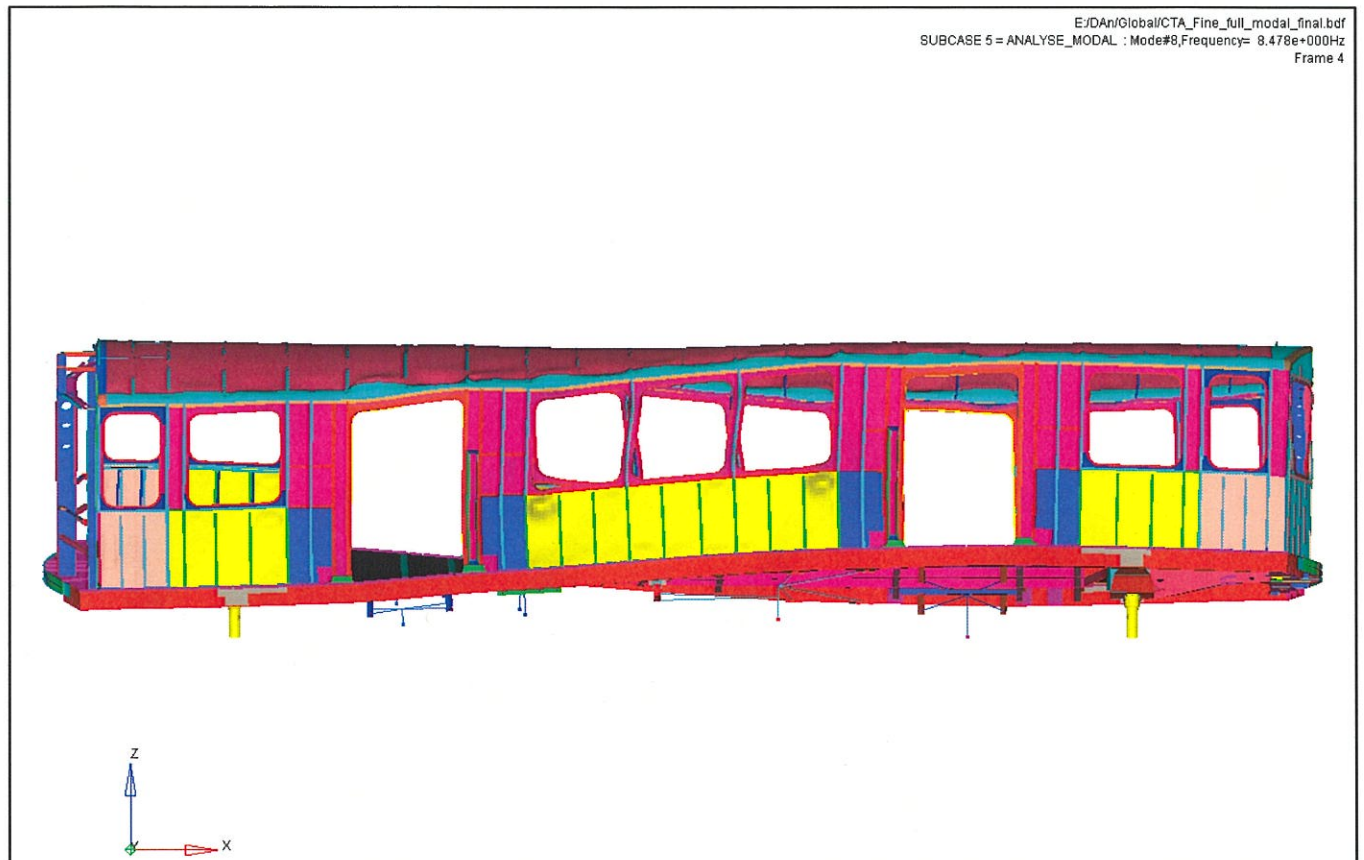


Figure 4.17.1 First Torsion mode ($f_n = 8.48$ Hz) at AW0.

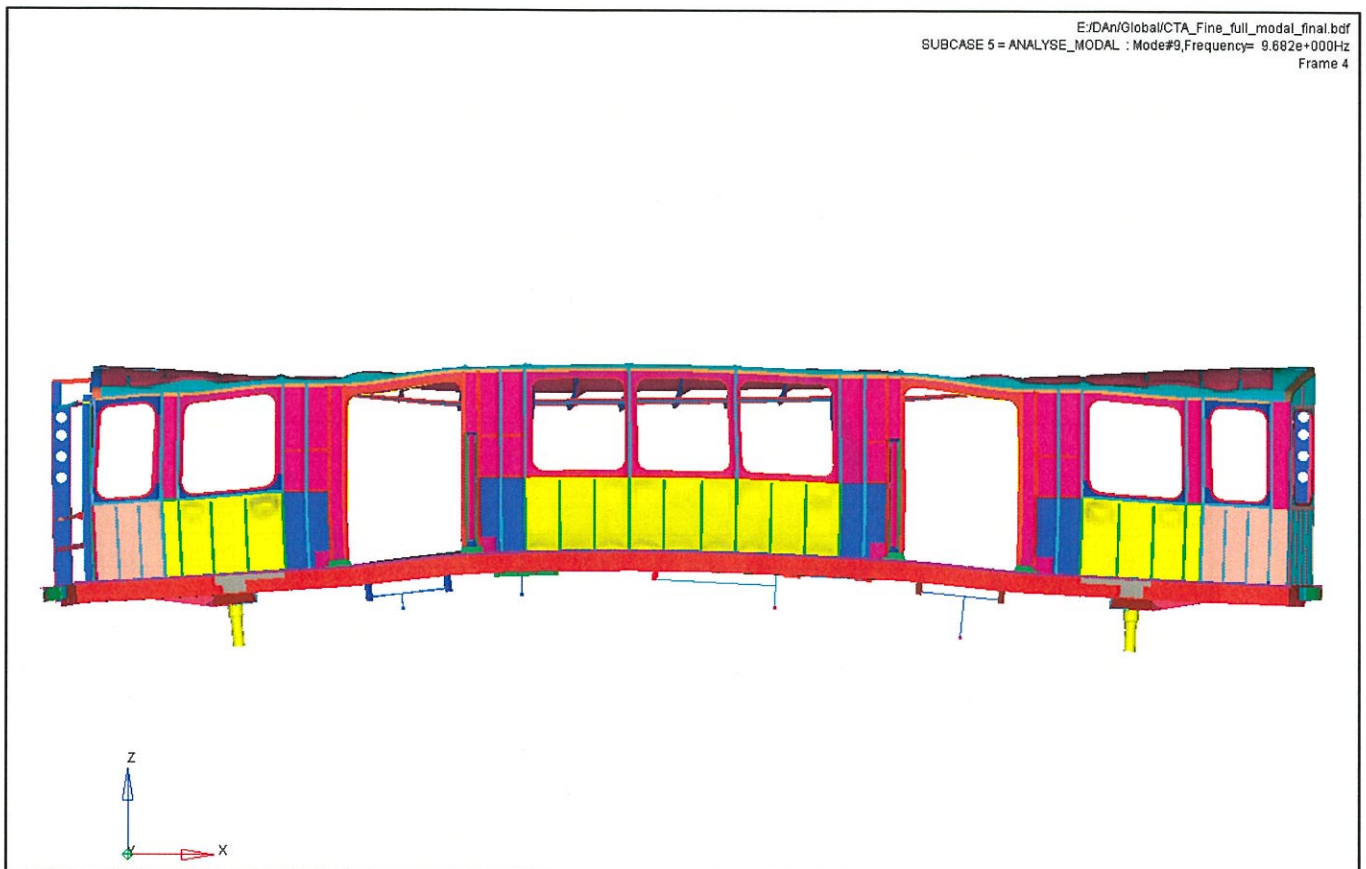


Figure 4.17.2 First vertical bending mode of ($f_n = 9.68$ Hz) at AW0.

5 Discussions and Conclusions

In view of the detailed FEA models that were produced for this report and the inherent analysis which also includes manual calculations, it can be concluded that all the principal carbody components have sufficient strength and comply with the requirements of the CTA specification (ref. 6).

The minimum margins of safety (MS) is 0.01 for the end sill main rib during the 200 kip compressive end load.

The summary table of margins of safety of section 1 is repeated here for convenience. Other requirements were also verified in the report, they are:

- End post connections, vertical loads and minimum sections moduli (section 3.2).
- Side sill to end sill and side sill to bolster connections (section 3.5).
- Bolster and it's connections for 50kip vert. & 150kip hor. Loads (sections 4.5 and 4.3).
- Welds verification for fatigue loads (section 4.13).
- Equipment supports and their connections (section 4.14).
- Progressive strength distribution (section 4.16 and ref. 8).
- Carbody natural frequencies (section 4.17).

COMPONENTS (MT)**	LOAD CONDITIONS								
	Vert. load @AW3(LC_02)		Comp @AW3(LC_05)		Torsion at AW0 (LC_10)		Other load cases		
	Max. Stress(ksi)	MS *	Max. Stress(ksi)	MS *	Max. Stress(ksi)	MS *	Max. Stress(ksi)	MS *	LC# ***
Anticlimber(HSLA80)							77.70	0.03	LC6, LC7
End sill (HSLA80)			71.30	0.01			76.60	0.04	LC10
Collision post (MT)								1.10	LC14
Corner post (MT)								0.03	LC15
Draft sill (HSLA 80)			55.80	0.29					
Bolster (HSLA 80)	38.30	0.04	49.40	0.45			6.00	0.60	LC3
Side sill			47.00	0.19			-3.10	0.45	LC3
Cross bearer (MT)	18.10	0.70	49.50	0.13			35.10	0.76	LC12
Main air duct (MT)	29.10	0.07	53.30	0.05			23.00	1.70	LC12
Side frame (MT)	29.40	0.05	33.00	0.70	35.90	0.72			
Side sheets (DLT)	25.60	0.21	30.90	0.80	49.70	0.01			
Door frame (MT)	23.50	0.32	48.90	0.15			-5.60	0.70	LC3
Belt rail (MT)	29.60	0.05	44.50	0.26	54.10	0.15			
Roof rail (MT)	24.10	0.28	20.70	0.70	19.80	>2			
AT plate (MT)					28.20	>2		0.54	LC17
Carlines (MT)	16.50	0.80	33.50	0.67	53.20	0.17	-43.20	0.43	LC19
Purlines (MT)					46.80	0.32			
Roof corrugation(MT)							-36.00	0.60	LC19
Equip. support HVAC							48.00	0.30	LC12
Equip. support APS							55.50	0.12	LC12
Equip. support HVB							51.10	0.21	LC12
Equip. support PCU							29.60	0.72****	LC12

NOTES: * MS = Margin of safety as calculated in section 2.4

** Material nomenclature as per table 2 of ref. 1

*** Load cases are described in table 1 of ref. 1 (Carbody Stress Analysis and Test Plan)

**** Bolted connection MS.

Copy of table 1.1 Summary of maximum stresses and minimum margins of safety for the carbody.

6 References

- 1) 076-PLA-0012, 'Carbody Stress Analysis and Test Plan', rev. 0'.
- 2) AWS, American Welding Society, AWS D1.1/D1.1M:2004.
- 3) 076-PLA-0013, 'Carbody Crash Analysis Report', rev. 0'.
- 4) WATTER and LINCOLN, *Strength of Stainless Steel Structural Members as Function of Design*, Allegheny Ludlum Steel Corporation, First Edition, Pittsburgh, Pa, 1950.
- 5) BRUHN, *Analysis & Design of Flight Vehicle Structures*, Jacobs Publishing, Inc., 1973.
- 6) CTA-6900-04 Rapid Transit Passenger Cars Technical Specification
- 7) Bombardier BAFO Technical Proposal for CTA, dated February 21, 2006.
- 8) 076-BRA-0017, 'Carbody Crash Analysis Report', rev. 0'.

Appendix A: Manual Calculations References

A.1 Applied formulas and tables for buckling calculations

1) The buckling capacity in compression of a panel is calculated as follows:

$$\sigma = \frac{\pi^2 K_c E_r}{12(1-\nu^2)} \left(\frac{t}{b}\right)^2$$

Where

K_c = compressive buckling coefficient (Ref. 5, see Figure A.1.1)

E_r = reduced modulus for stainless steel from Watter and Lincoln (Ref. 4, see Figure A.1.2)

ν = Poisson ratio

b = short dimension or loaded edge

t = thickness of the plate

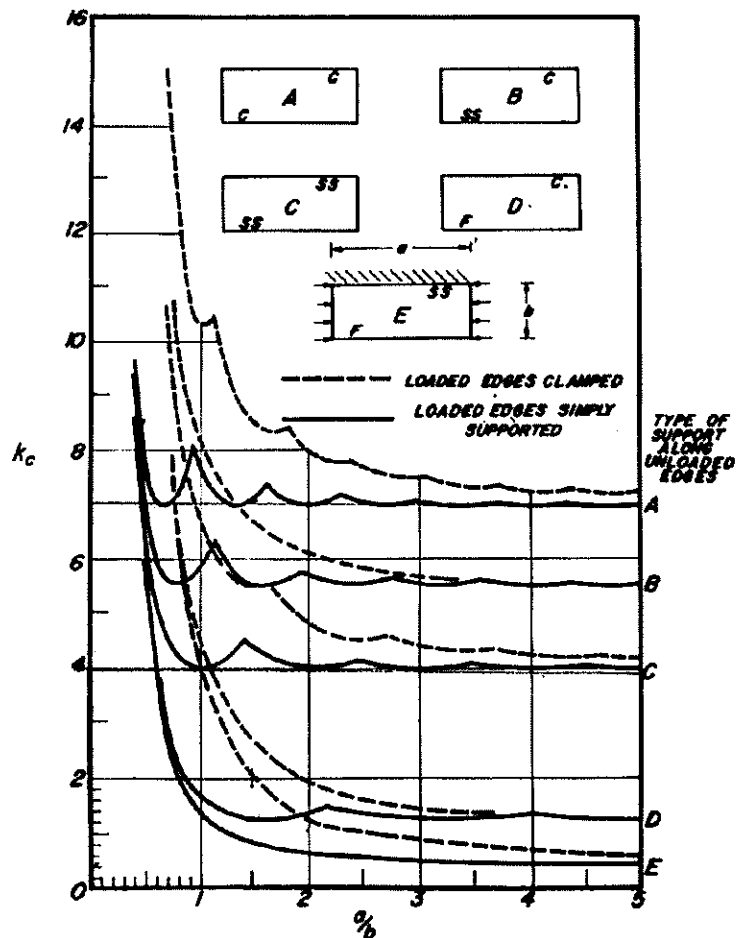


Figure A.1.1: Compressive Buckling coefficient (Ref. 5, Bruhn, and Fig.C5.2)

The data used for the reduced modulus are from Watter and Lincoln (ref. 4, Figure 45, Longitudinal Reduced Compression Modulus).

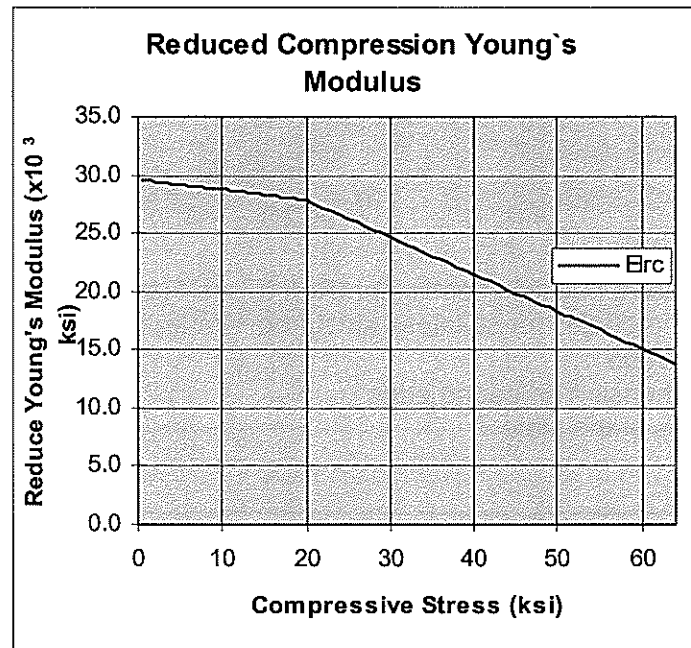


Figure A.1.2: Reduced Young's Modulus (Ref. 4: Watter & Lincoln)

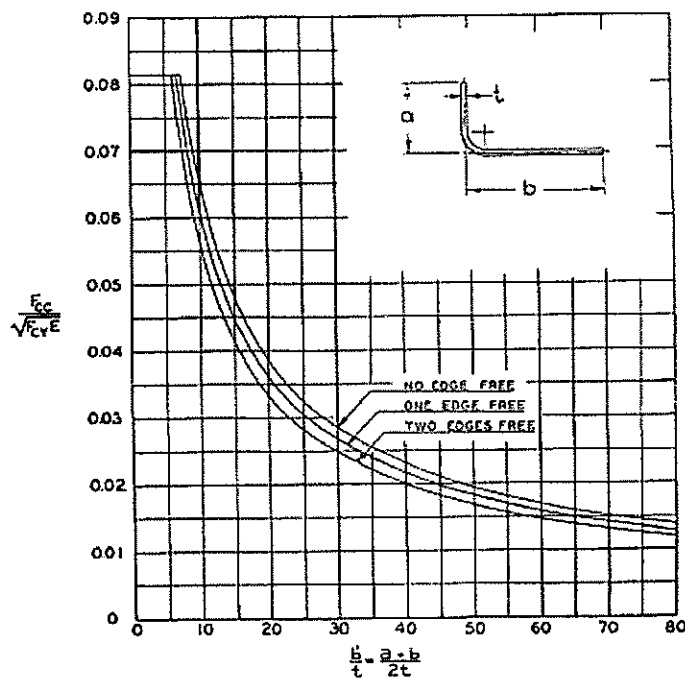
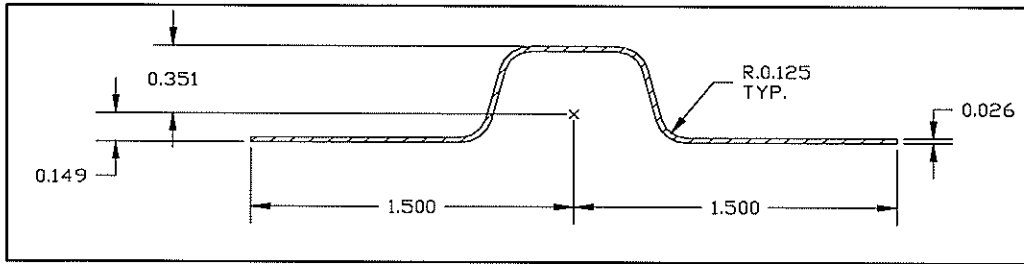


Figure A.1.3: Compressive Buckling coefficient for an angle (Ref. 5, Bruhn, and Fig.C7.3)

A.2 Corrugated roof properties calculations:



Roof Corrugated sheet geometry

Sheet thickness: $t_s =$	0.026 in.	Area =	0.0966 in ²
Corrugation height: $h =$	0.500 in	$I_{xx} =$	0.0033 in ⁴
Corrugation pitch: $p =$	3.000 in.	$I_{yy} =$	0.0610 in ⁴
Young Modulus : $E =$	28000 ksi	$z_c =$	0.1490 in
		$L =$	12.0 in

$t =$	0.032	in.	Shell effective thickness
RMI =	13882.6		Ratio for the bending moment of inertia (stiffness) $RMI = (I_{yy}) / (p \cdot TK^3 / 12)$
CTOP =	0.351	in.	Distance from center to top
CBOT =	0.149	in.	Distance from center to bottom

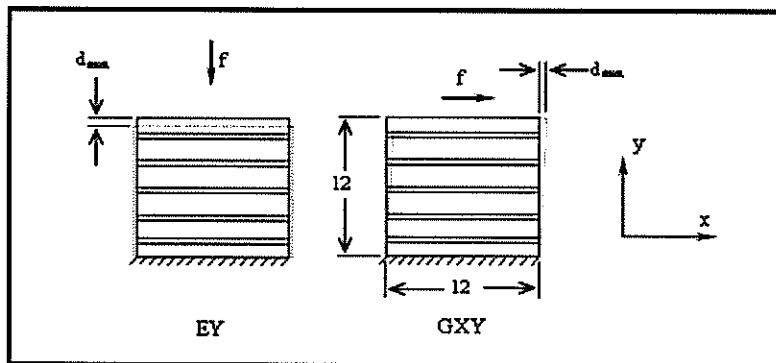
Material Properties

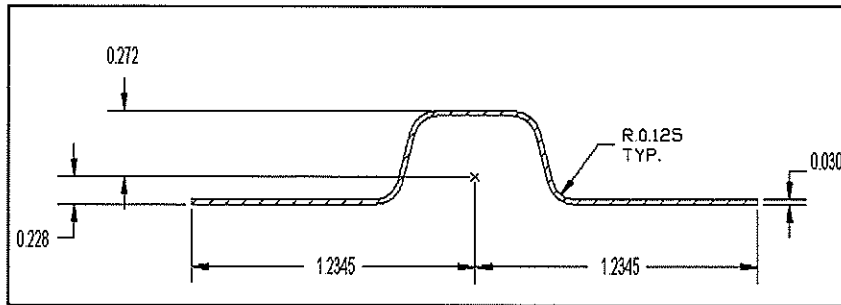
EX =	34684	ksi	Young modulus for Stainless steel $E_x = E \cdot (TK / t_s)$
EY =	24642	ksi	Calculated Young modulus
EZ =	34684	ksi	Young modulus for Stainless steel
GXY =	3759	ksi	Calculated shear modulus for corrugated sheet
GYZ =	13340	ksi	Shear modulus for Stainless steel $G_{yz} = (E / 2 \cdot (1 + \nu_{yz})) \cdot (TK / t_s)$
GXZ =	13340	ksi	Shear modulus for Stainless steel
NUXY =	0.3		Effective Poisson ratio

Calculation of Modulus (from FE model displacements)

F =	1000 lb	force applied on the FE model
A = L * TK	0.39 in ²	effective section area of the sheet model
S = F/A	2587.5 psi	nominal stress of the sheet

$d_{max} =$	$\frac{F}{EY}$	$\frac{GXY}{EY}$	
	1.26E-03	8.26E-03	in
	1.05E-04	6.88E-04	%
	24642.4	3759	ksi
			Roof modulus used in FEA



A.3 Corrugated side sheet properties calculations:**Corrugated side sheet geometry**

Sheet thickness:	ts=	0.030 in.	Area=	0.0960 in ²
Corrugation height:	h=	0.500 in	I _{xx} =	0.0041 in ⁴
Corrugation pitch:	p=	2.469 in.	I _{yy} =	0.0441 in ⁴
Young Modulus :	E=	28000 ksi	z _c =	0.1490 in
			L=	9.876 in

TK =	0.039	in.	Shell effective thickness
RMI =	7933.0		Ratio for the bending moment of inertia (stiffness) RMI = (I _{yy}) / (p*TK ³ /12)
CTOP =	0.351	in.	Distance from center to top
CBOT =	0.149	in.	Distance from center to bottom

Material Properties

EX =	36290	ksi	Young modulus for Stainless steel Ex = E * (TK / ts)
EY =	24730	ksi	Calculated Young modulus
EZ =	36290	ksi	Young modulus for Stainless steel
GXY =	3755	ksi	Calculated shear modulus for corrugated sheet
GYZ =	13958	ksi	Shear modulus for Stainless steel Gyz = (E / 2*(1+NUyz))* (TK/ts)
GXZ =	13958	ksi	Shear modulus for Stainless steel
NUXY =	0.3		Effective Poisson ratio

Calculation of Modulus (from FE model displacements)

F=	1000 lb	force applied on the FE model
A = L*TK	0.38 in ²	effective section area of the sheet model
S = F/A	2604.2 psi	nominal stress of the sheet

d _{max} =	EY	GXY		
	1.04E-03	6.85E-03	in	displacement from the model
	1.05E-04	6.94E-04	%	resultant strain
	24729.6	3755	ksi	modulus used in FEA model

A.4 Plymetal properties calculations:

Section Moment of inertia are:

$$I_{ply} = \frac{d^3}{12} \quad ; I_{ply} \text{ (in}^4\text{)} = 0.03515625$$

$$I_{skin} = \frac{(d^3 - h^3)}{12} \quad ; I_{skin} \text{ (in}^4\text{)} = 0.004310731$$

$$I_{core} = \frac{h^3}{12} \quad ; I_{core} \text{ (in}^4\text{)} = 0.030845519$$

Where d is the panel thickness (in) = 0.75
 h is the plywood (core) thickness (in) = $d - 2t$ = 0.718
 t is the skins thickness (in) = 0.016

The equivalent Young's Modulus (E_{ply}) of the floor panel is calculated with the following equation from Gere & Timoshenko, Mechanics of Materials, Eq 5.9 & 5.45:

For a symmetric beam containing isotropic layers, the effective bending stiffness becomes

$$(EI)_b = \sum E_i I_i$$

Therefore

$$E_{ply} = \frac{E_{skin} \cdot I_{skin} + E_{core} \cdot I_{core}}{I_{ply}}$$

Where E_{skin} is Stainless Steel Young's Modulus (ksi) = 28000
 E_{core} is the plywood Young's Modulus (ksi) = 1500
 (Ref: APA - The Engineered Wood Association)
 I_{skin} is the Moment of inertia of the Outer skins (in⁴)
 I_{core} is the Moment of inertia of the core (plywood) (in⁴)
 I_{ply} is the Moment of inertia of the plymetal panel (in⁴)

$$E_{ply} = 4749 \text{ ksi}$$

Plymetal properties calculations (cont.):**Plymetal Density & Mass**

Plywood density from APA Plywood Design Specification

Mass/Area	2.2 Lbs/ft ²
Mass/Area	0.0153 Lbs/in ²
Density	0.0204 Lbs/in ³

Stainless Steel density

Density	0.2859 Lbs/in ³
---------	----------------------------

Plymetal density

$$\rho_{plymetal} = \frac{(\rho_{wood} \times t_{wood}) + (\rho_{sstl} \times t_{sstl})}{(t_{wood} + t_{sstl})}$$

$$d_{plymetal} = 0.0317 \text{ Lbs/in}^3$$

FEM Floor Panel Material Properties

FEM Young's Modulus =	28000 ksi
FEM panel thickness =	0.032 in.
I_{model} =	2.73067E-06 in ⁴
d_{FEM} =	0.743 Lbs/in ³
E_{ply} =	4749 ksi

Plymetal modulus used in FEA

Rmi (12I/T3)

$$RMI = \frac{(E_{ply} \times I_{ply})}{E_{mod\ el} \times I_{mod\ el}}$$

$$Rmi = 2183.78$$

A.5 Sub-floor properties calculations:

First the actual sub-floor buckling capacity was calculated. Then with the FEA model Young's modulus was adjusted to achieve approximately the limit value of the subfloor buckling stress. The process is iterative and reduces the properties of the subfloor material which is 201LN-LT (annealed).

The buckling calculation method of section A.1 is used, Shear buckling is treated with figure A.5.1:

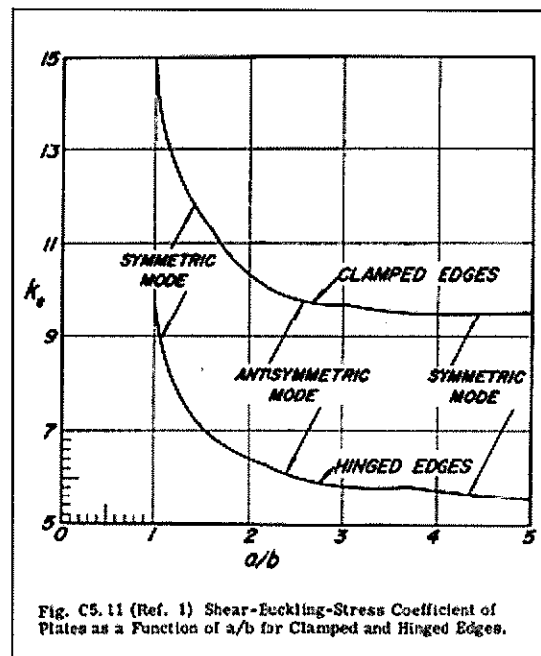


Figure A.5.1 (Ref. 5) Shear Buckling Stress Coefficient of plates

$$\sigma = \frac{\pi^2 K_c E_r}{12(1-\nu^2)} \left(\frac{t}{b}\right)^2$$

Where

K_c = Compressive or shear Buckling coefficient

E_r = reduced modulus from Walter and Lincoln

ν = Poisson ratio

b = short dimension loaded edge

t = thickness of the plate

Sub-floor properties calculations (cont.):

$$\sigma = \frac{\pi^2 Kc Er}{12(1-\nu^2)} \left(\frac{t}{b}\right)^2$$

Compressive buckling along 'X' axis:

Where

a = 12 "

b = 20 "

Kc = 11.2 (Ref. 5, see Figure A.1.1)

Er = 29000 ksi

ν = 0.3

t = 0.02"

$$\sigma_{CR} \text{ (X axis)} = -0.30 \text{ ksi}$$

Compressive buckling along 'Y' axis:

Where

a = 20 "

b = 12 "

Kc = 6.4 (Ref. 5, see Figure A.1.1)

Er = 29000 ksi

ν = 0.3

t = 0.02"

$$\sigma_{CR} \text{ (Y axis)} = -0.47 \text{ ksi}$$

Shear buckling along 'XY' plane:

Where

a = 20 "

b = 12 "

Kc = 9.0 (Ref. 5, see Figure A.5.1)

Er = 29000 ksi

ν = 0.3

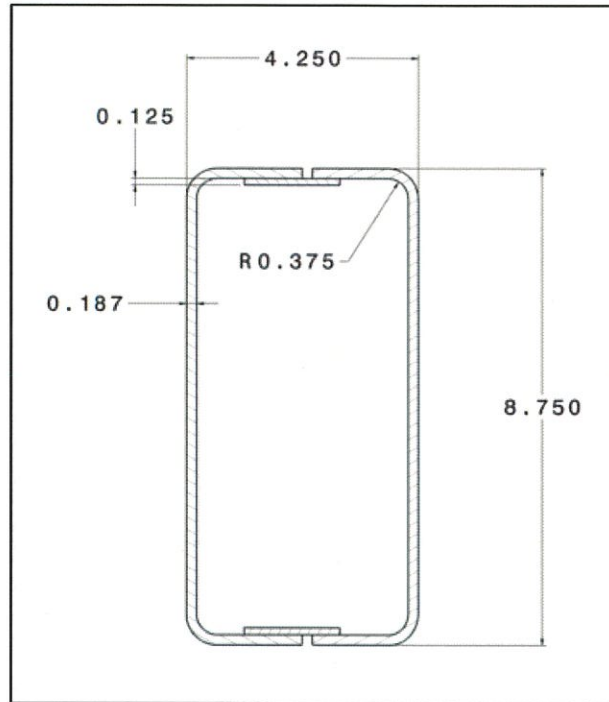
t = 0.02"

$$\tau_{CR} \text{ (XY plane)} = 0.63 \text{ ksi}$$

After many FEA iterations to achieve the above 0.63 ksi average stress in the subfloor, the subfloor reduced Young's modulus was adjusted to 1000 ksi.

$$E_{\text{sub-floor (reduced)}} = 1000 \text{ ksi for a thickness of 0.02 in}$$

A.6 Collision post properties calculations:

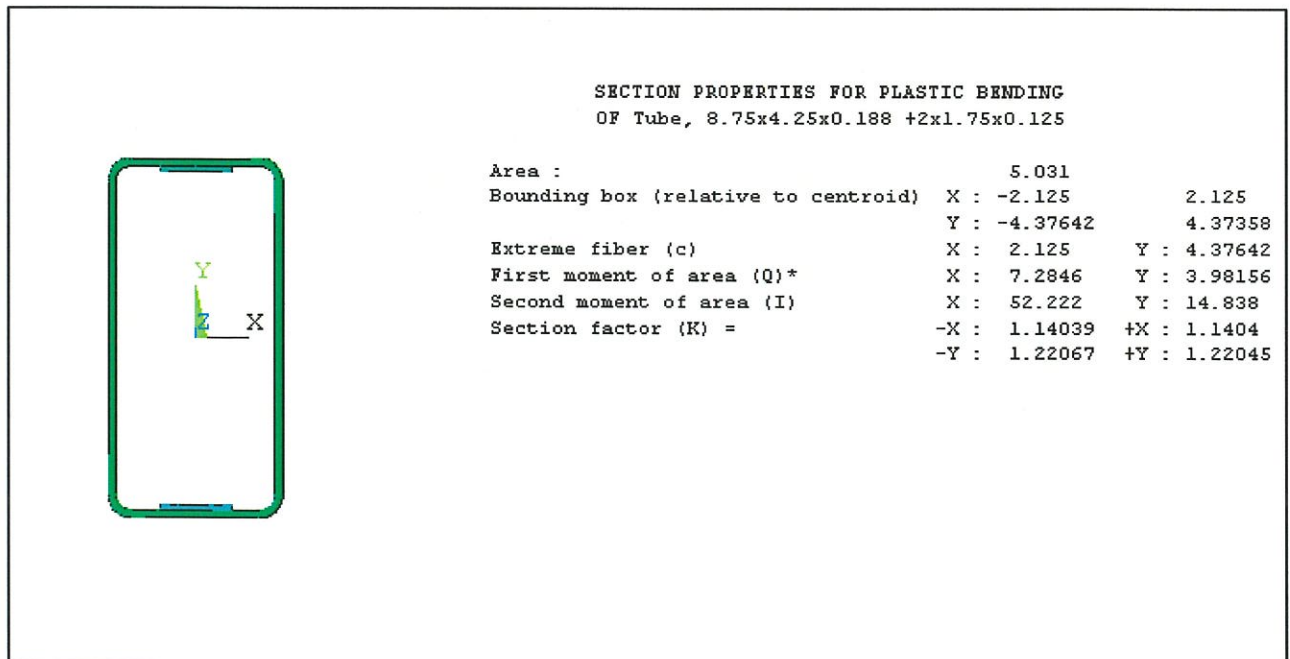


$$\text{Area} = 5 \text{ in}^2$$

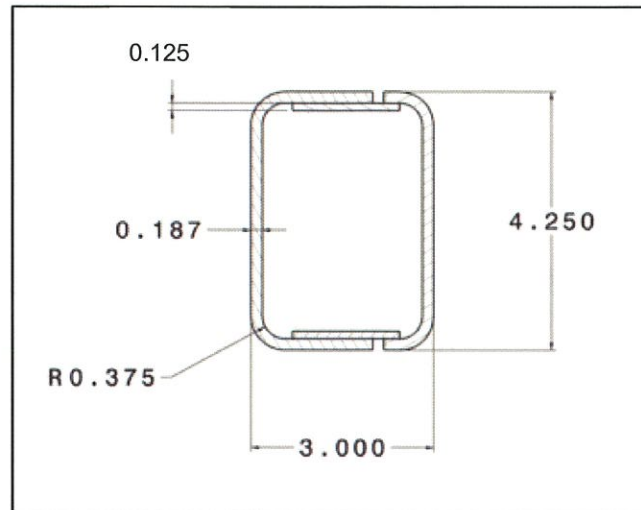
$$c = 4.375 \text{ in}$$

$$I_{XX} = 52.22 \text{ in}^4$$

$$S_{XX} = 52.22 / 4.375 = 11.94 \text{ in}^3$$



A.7 Corner post properties calculations:

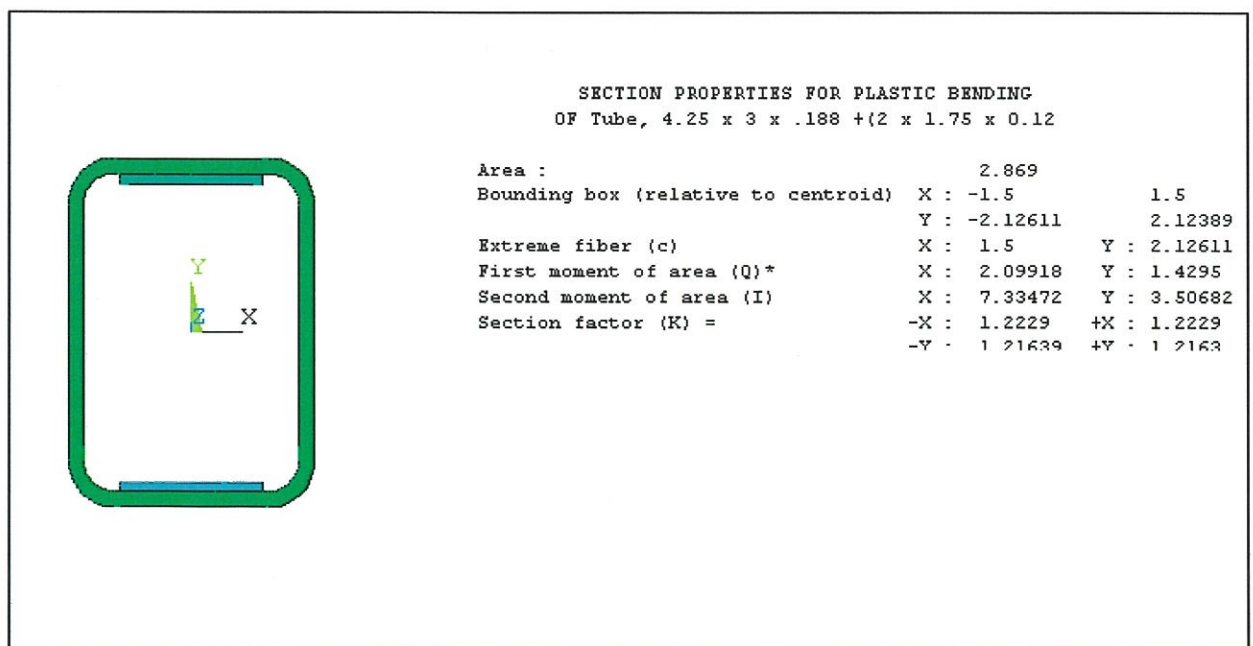


$$\text{Area} = 2.8 \text{ in}^2$$

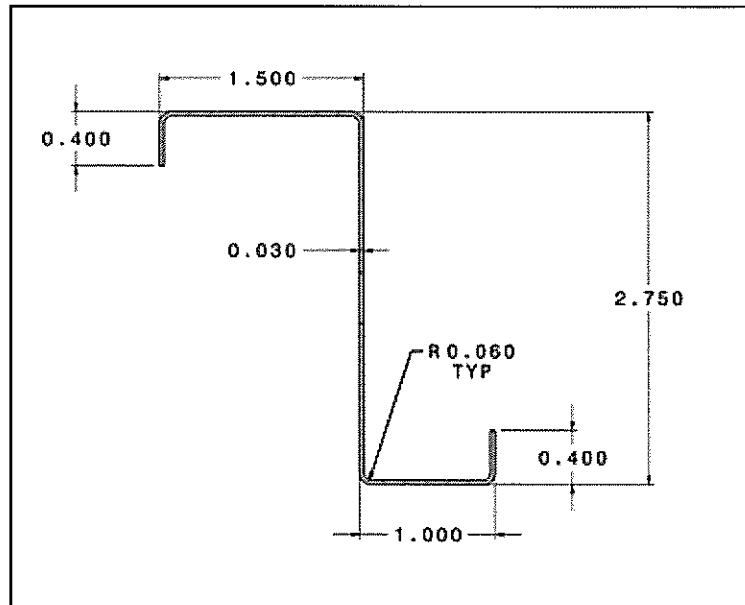
$$c = 2.125 \text{ in}$$

$$I_{XX} = 7.34 \text{ in}^4$$

$$S_{XX} = 7.34 / 2.125 = 3.45 \text{ in}^3$$



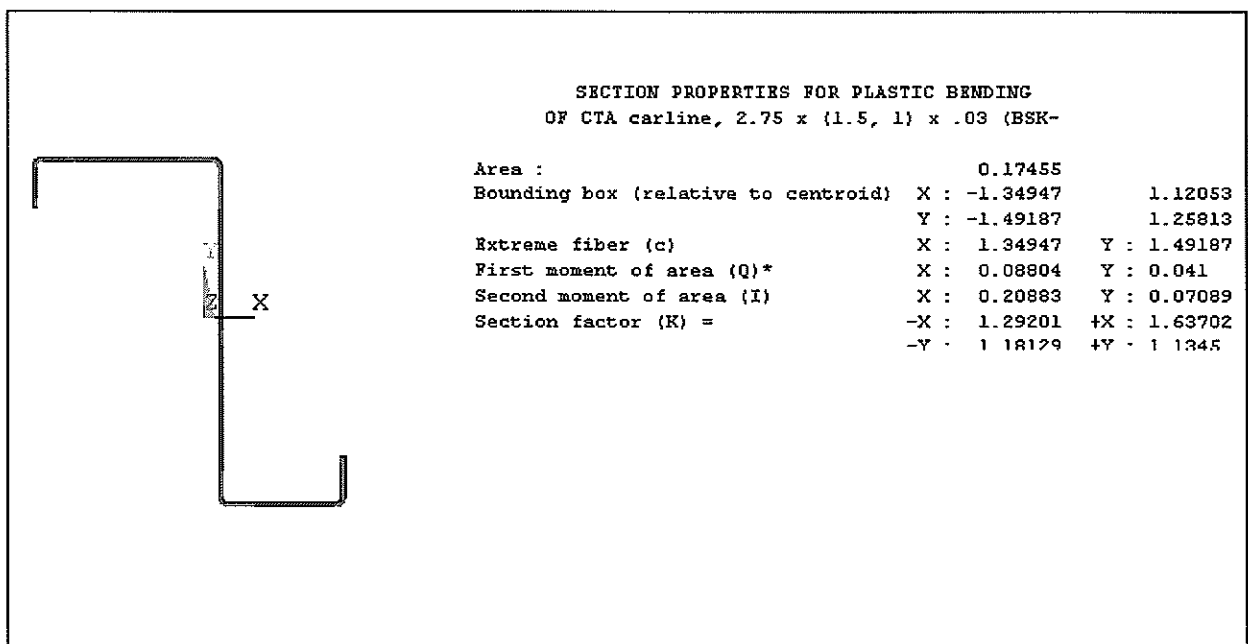
A.8 Carline properties calculations:



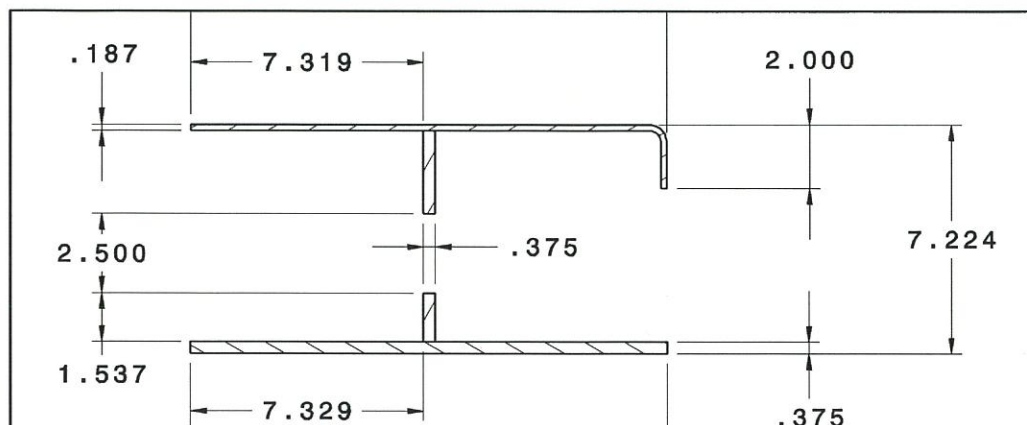
$$\text{Area} = 0.175 \text{ in}^2$$

$$c = (2.75 - 1.5) = 1.25 \text{ in (with respect to top flange)}$$

$$I_{XX} = 0.29 \text{ in}^4$$



A.9 Bolster properties calculations at $y = 25.5$ in:

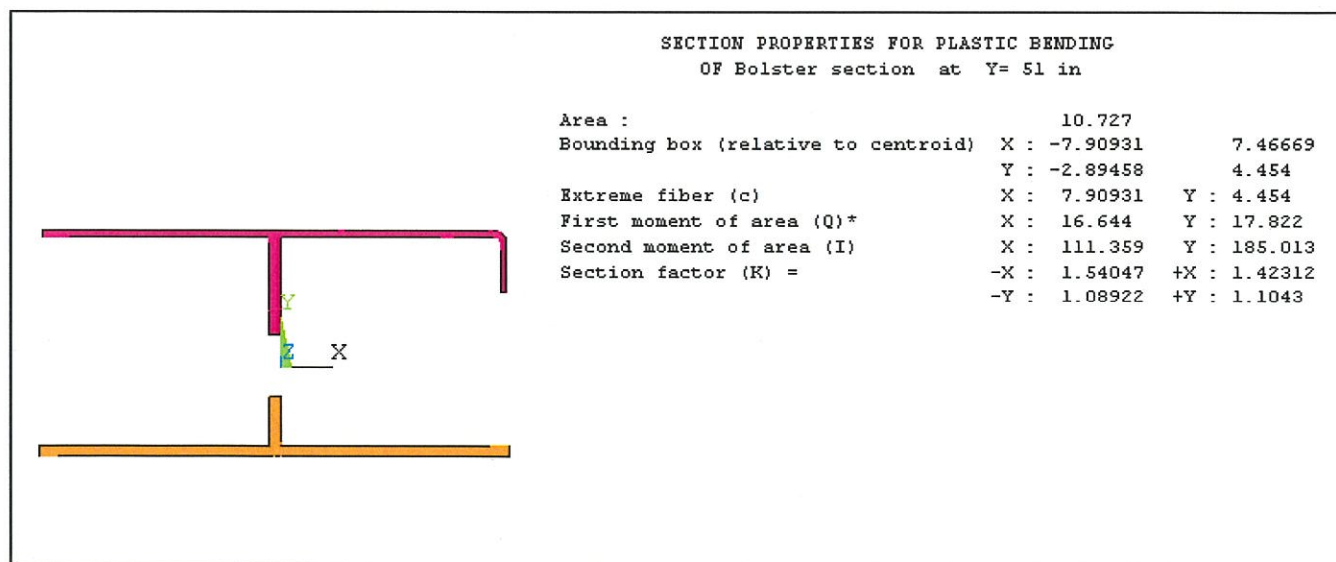


$$\text{Area} = 10.7 \text{ in}^2$$

$$c = 4.45 \text{ in (with respect to top plate)}$$

$$I_{XX} = 111.4 \text{ in}^4$$

$$S_{XX} = 111.4 / 4.45 = 25 \text{ in}^3$$



Appendix B: FEA Models and Load Cases Description Plots

B.1 FEA modeling assumptions:

The Finite Element Models were created on the basis of the carbody CAD Catia model using Hypermesh 8.0 preprocessing software. Model computation is performed by MSC NASTRAN 5.0 Finite Element Analysis software developed by MSC Software Corporation. This model uses plate, beam and mass elements, properly located to represent the geometry of the structural assemblies. Each component is characterized by its material property, physical property, element type and coordinate system. Three models were used for the analysis:

- 1) Half a full carbody model for all symmetric load cases
 - 2) Full carbody model for the torsion (LC_10) and for modal analysis.
 - 3) Central underframe model with the undercar equipment support details.
- Modeling Assumptions:
 - The global coordinate system has been chosen for all models to comply with the coordinates of the drawings with the following system :
 - * X axis is along the longitudinal direction, with its origin located at the car center, between the two bolsters as defined on NJT drawings. (X+ = B-End)
 - * Y axis runs along the car transverse direction with its origin centered between the two rails. (Y+ = right side)
 - * Z axis is vertically upward with the top of rail defined as the datum.
 - *
 - Quadrilateral plate elements are used for all the shell elements; in the fine carbody models triangular elements are only to be used when inevitable.
 - Beam elements are not entered to represent any hardware, they have no weight. The main purpose of the beam is to connect equipment CG locations or to transfer loads from the truck, coupler or jacking systems to the structure.
 - Mass elements are used to simulate the weight of the equipment or of the distributed weight of elements in the carbody.
 - The shell elements representing the corrugated sheet of the roof, the corrugated sheet of the skin, the plymetal or the subfloor have special properties as calculated and defined in Appendix A.

B.2 FEA model Plots:

The following plots show the three models. Components plate thickness and material are not described in the plots but are in line with the CATIA model and dwg. A-399-0007 Rev." " Carbody Assy "A".

The boundary conditions are shown for the main load cases only.

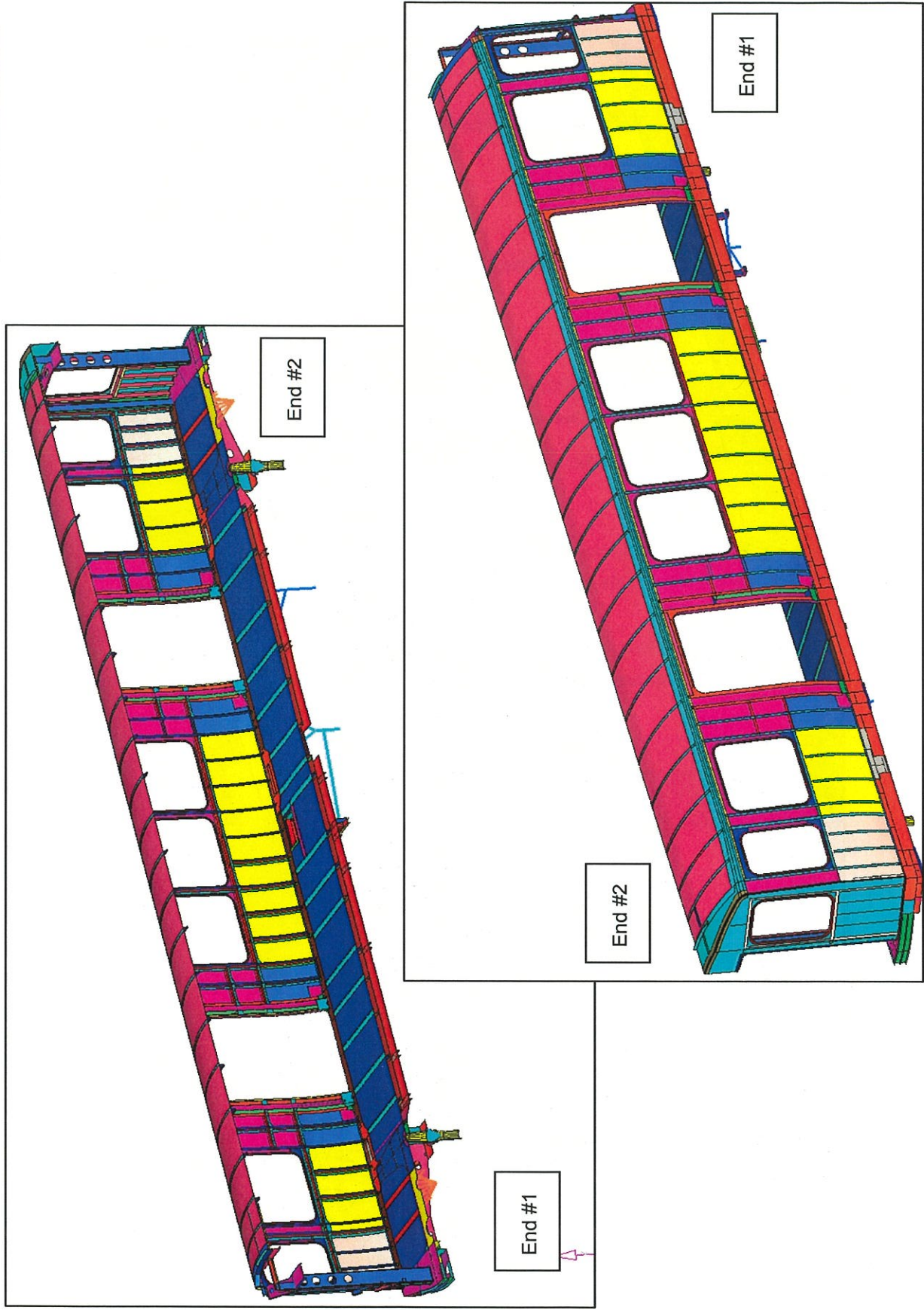


Figure B.1 FEA half model inside & outside view.

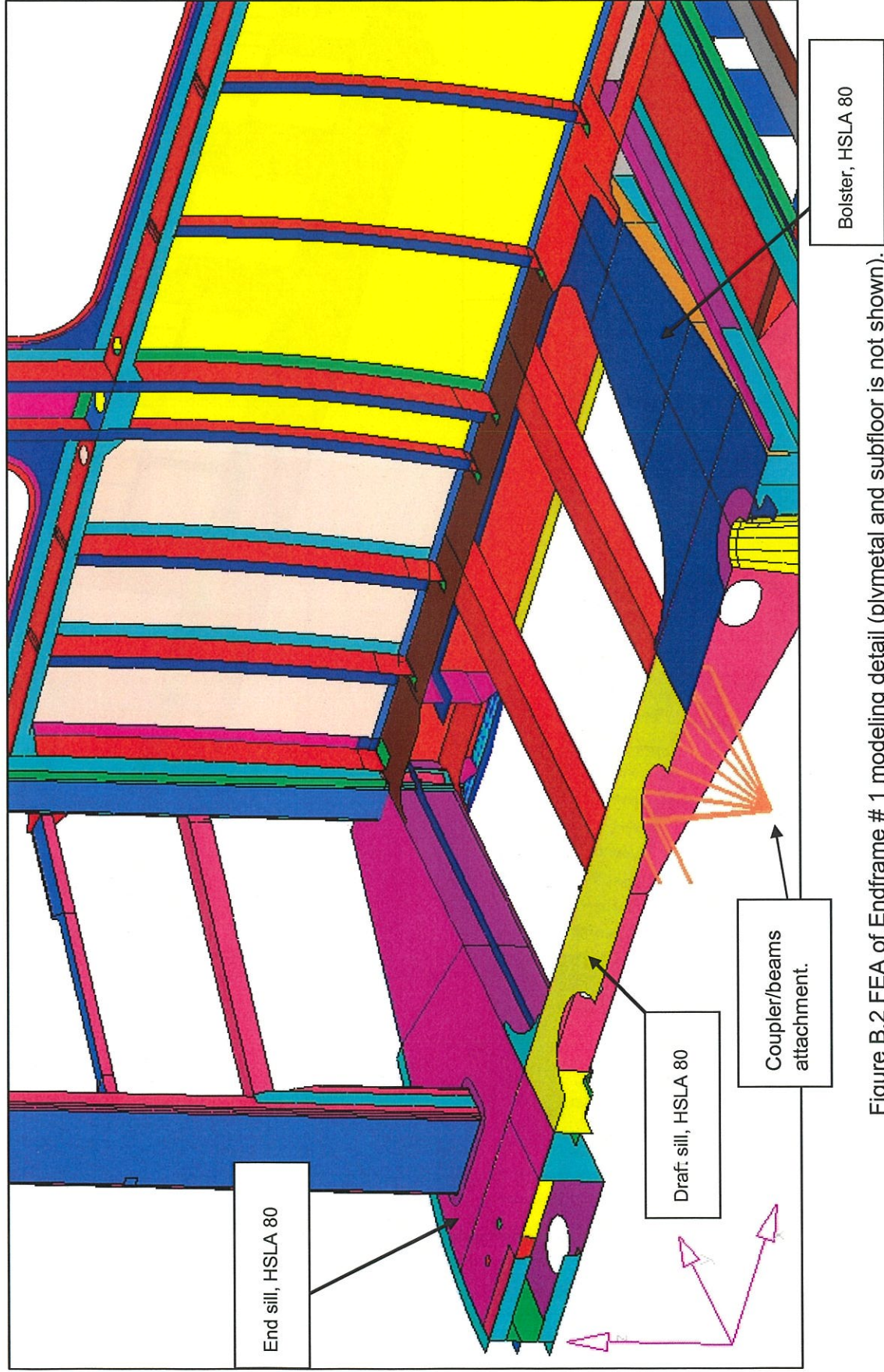


Figure B.2 FEA of Endframe # 1 modeling detail (plymetal and subfloor is not shown).

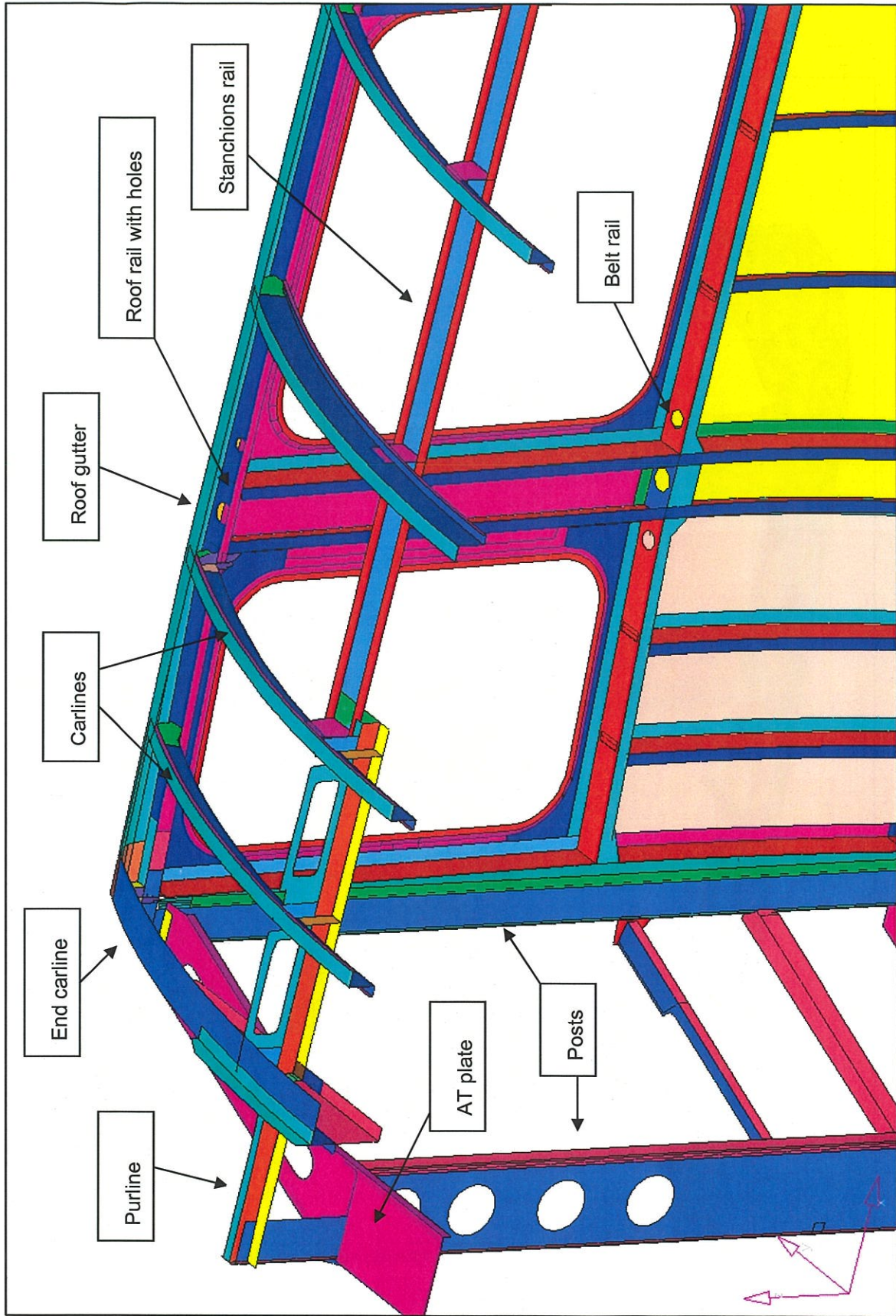


Figure B.3 FEA of Endframe # 1 modeling detail of roof (roof corrugation is not shown).

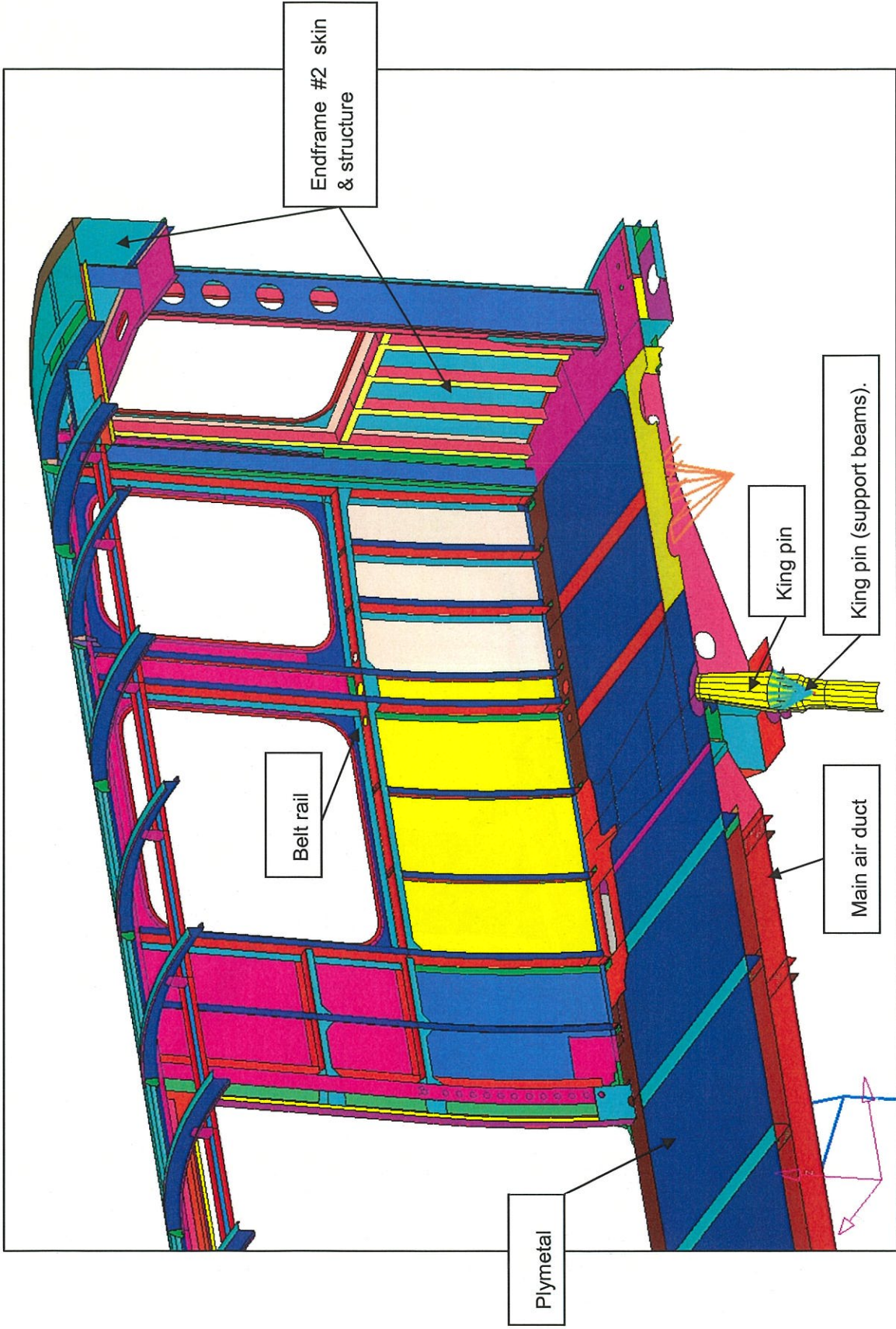


Figure B.4 FEA of Endframe # 2 (roof corrugation is not shown).

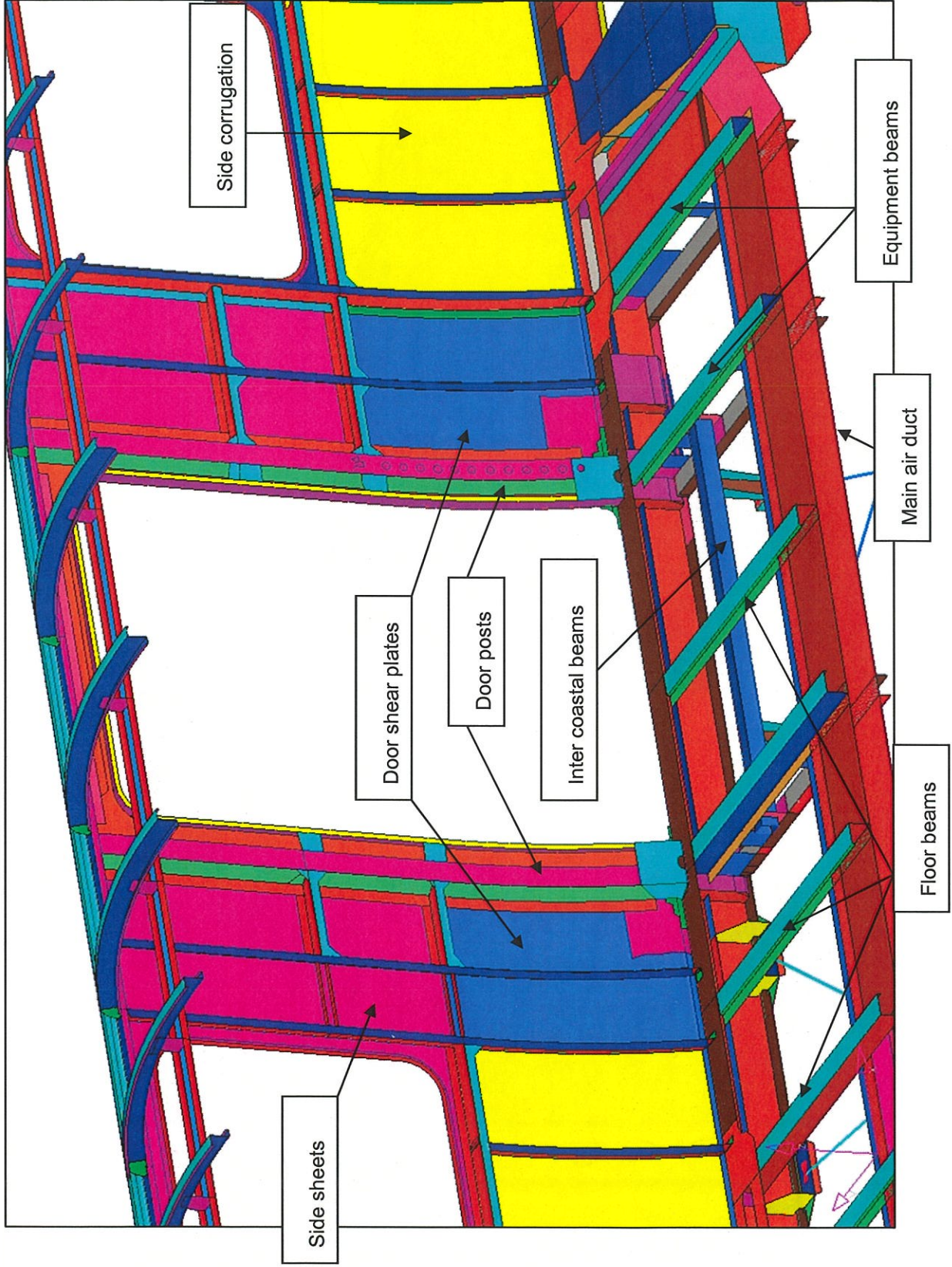


Figure B.5 FEA of Door area and underframe details (plymetal and subfloor not shown).

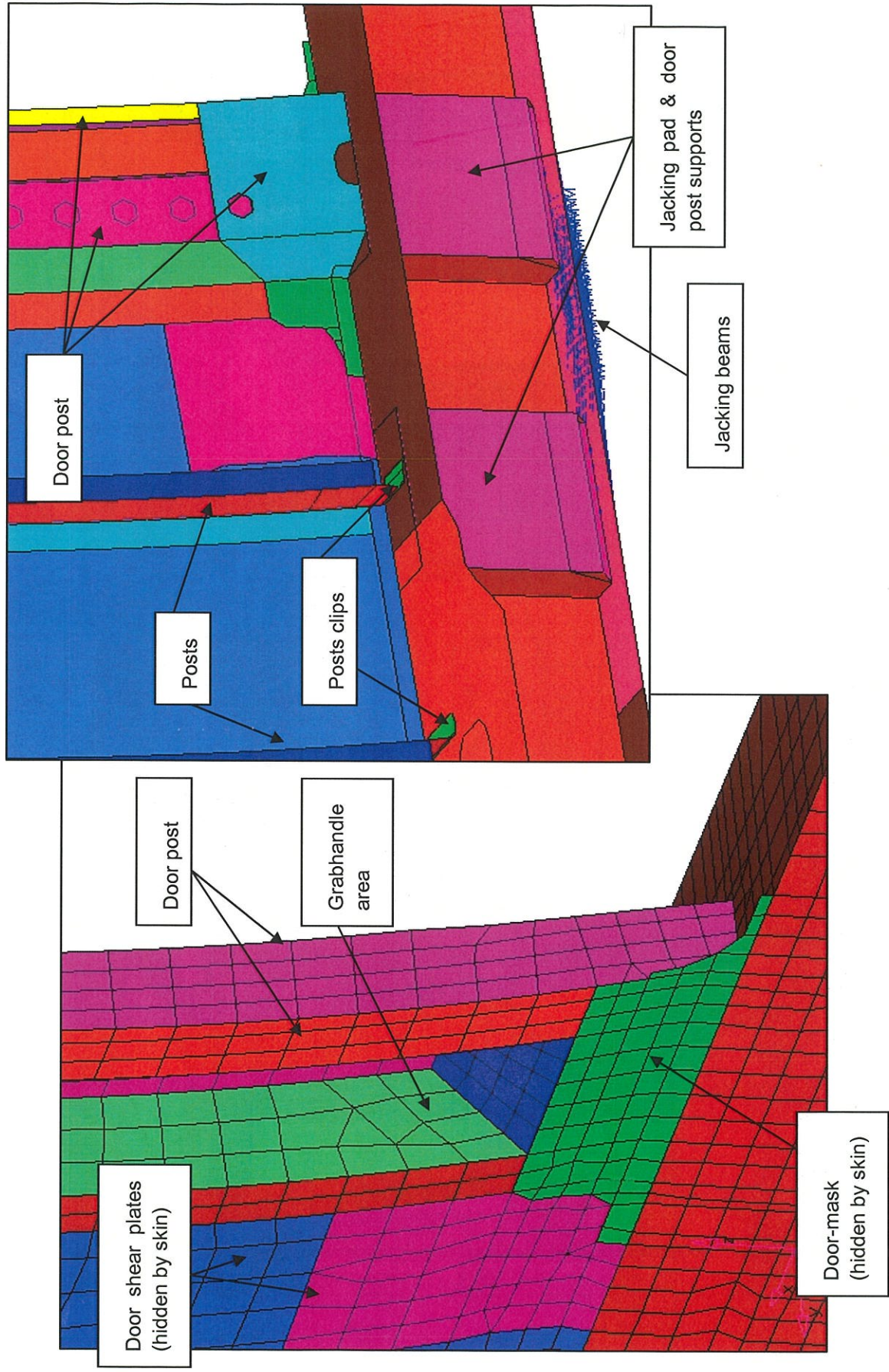


Figure B.6. FEA of Door post, grab handle and jacking supports..